

5-2021

Endogenous Mechanisms Regulating Myeloid Cell Mediated Inflammation During Acute Lung Injuries

Nathaniel Berg

Follow this and additional works at: https://digitalcommons.library.tmc.edu/utgsbs_dissertations

 Part of the [Biological Phenomena, Cell Phenomena, and Immunity Commons](#), and the [Circulatory and Respiratory Physiology Commons](#)

Recommended Citation

Berg, Nathaniel, "Endogenous Mechanisms Regulating Myeloid Cell Mediated Inflammation During Acute Lung Injuries" (2021). *The University of Texas MD Anderson Cancer Center UTHealth Graduate School of Biomedical Sciences Dissertations and Theses (Open Access)*. 1077.
https://digitalcommons.library.tmc.edu/utgsbs_dissertations/1077

This Dissertation (PhD) is brought to you for free and open access by the The University of Texas MD Anderson Cancer Center UTHealth Graduate School of Biomedical Sciences at DigitalCommons@TMC. It has been accepted for inclusion in The University of Texas MD Anderson Cancer Center UTHealth Graduate School of Biomedical Sciences Dissertations and Theses (Open Access) by an authorized administrator of DigitalCommons@TMC. For more information, please contact digitalcommons@library.tmc.edu.

Endogenous Mechanisms Regulating Myeloid Cell Mediated Inflammation During

Acute Lung Injuries

by

Nathaniel Karl Berg

APPROVED:

Holger Eltzschig, M.D., Ph.D.
Advisory Professor

Farrah Kheradmand, M.D.

Cynthia Ju, Ph.D.

Harry Karmouty-Quintana, Ph.D.

Edgar T. Walters, Ph.D.

APPROVED:

Michael Blackburn, Ph.D.
Dean, The University of Texas
MD Anderson Cancer Center UTHealth Graduate School of Biomedical Sciences

**Endogenous Mechanisms Regulating Myeloid Cell Mediated Inflammation
During Acute Lung Injuries**

A Dissertation

Presented to the Faculty of

The University of Texas

MD Anderson Cancer Center UTHealth

Graduate School of Biomedical Sciences

in Partial Fulfillment

of the Requirements

for the Degree of

Doctor of Philosophy

by

Nathaniel Karl Berg

Houston, Texas

May, 2021

To my father.

You always told me that you had forgotten more than I will ever learn.

Your challenge has brought me here.

Acknowledgments:

Training for my PhD degree has been the single most challenging thing I have done in my life. Graduate training is accompanied with its nearly universal uncertainties, demands that we follow data into the unknown, and requires students to develop a strong sense of confidence in their mental and physical abilities. Paramount to accomplishing such arduous tasks and achieving eventual graduation are the people who help us along the way. Unlike many educational experiences I have participated in, there is no book, curriculum, study guide, or secret-sauce podcast that will get you to the end. Mentors, colleagues, friends, and family make the graduate student. I have such a tremendous list of individuals that need to be mentioned here. I will do my best, but I will ultimately never be able to do this proper justice.

Foremost I would like to thank my mentors Holger Eltzhig and Xiaoyi Yuan, who were both instrumental in my academic growth, providers for all my research necessities, and who supported my pursuit for new ideas. You were both generously patient and kind while helping me stay the course towards success. It has been the greatest pleasure to work under your combined guidance.

I also acknowledge my advisory committee members, Cynthia Ju, Farrah Kheradmand, Harry Karmouty-Quintana, Edgar T. Walters, and Russell Broaddus. While writing this dissertation, I revisited the first PowerPoint presentation I ever delivered to you all. Wow, was it confusing and disorganized. Though embarrassing it is to recall how novice I must have come across, I can proudly reflect on the tremendous growth I've made as a scientist. Thank you all for your experimental suggestions, constructive scrutiny, valuable time, and focused attention, all of which were critical for my progress.

To my dear lab members and departmental friends (former and current): Jiwen Li, Boyun Kim, Xiangyun Li, Yanyu Wang, Jae Woong Lee, Wei Ruan, Frank Chen, Jessica Bowser, Cathi Conrad, Agnieszka Czopik, Pooja Shivshankar, Busra Cekmecelioglu,

Seungwon Choi, Synthea Horton, Victor Guaregua and all of the students, residents, administrators, and visiting scientists, thank you for your kind friendship, constant assistance, helping me to complete my work, and doing inspirational science. It was such a great experience to have learned from you all!

Much like the steps of a pyramid, education is a construct of accumulated knowledge that is highly dependent on its foundation. I would be remiss to not recognize the tremendous impact my primary and secondary teachers have had on my academic career thus far. I really enjoyed school growing up and I would gladly re-experience any moment of it. At times, school was even therapeutic and helped me overcome personal hardship. If you are reading this and were ever one of my teachers in any capacity, whether it was at Tiffany Elementary, Bonita Vista Middle and High Schools, or the University of Michigan, thank you!

I'd like to acknowledge the support of faculty and staff at the MD Anderson UTHealth MSTP and GSBS programs. The attention and care that is provided for students was consistently top-notch. In addition, the friends and colleagues I made along the way comprised a community that has been a pillar of support during the universal challenges of graduate studies. I have met brilliant classmates that have consistently impressed me. Thank you all for being there to share our experiences with one another and inspiring me to be a better scientist.

To the friends I have made along the way, thank you for the great times we have had. Getting through a rigorous curriculum and education requirements is impossible without having people around who care about you and for this reason I am indebted to you all. From my high school friends, the ones I made in Michigan (big shout out to the wine crew), and the ones I made during medical school, I would like to extend my greatest appreciation. You have all made life during graduate school more fun and exciting, which is an essential role to fulfill!

I'd like to recognize a number of family members have committed themselves to my success. To my mother, thank you for the dedication and nourishment you provided for my

entire life. All the while you maintained a successful professional career as a dentist. You were more than a parent, you were a role model. To my brother, Evan, you have taught me more along the way than you likely realize. Being happy is more important than anything else. Do what you like, be weird, and invest in your hobbies. I'm beyond proud of you and your recent accomplishments, as well. Keep it up! My grandparents, Lorraine and Norman Bercoon, were instrumental in my success. While in college, Chicago was a home away from home. They have been extremely generous in many ways. My grandfather gifted me his old car that I still rely on for getting anywhere. I literally wouldn't be here today if it weren't for them (I drove said car down from Michigan).

Lastly, I have to thank my significant other / best friend / guardian, Alyssa. You probably didn't sign up for all this when we started dating, but I don't think I would have made it through without you. You have cared about me in ways I neglected to care about myself when times were at their most challenging, normalized the amount of ice cream I consume, brought me into your family (shout out to all the Kahls!), and been a living reminder that I have every reason to be happy and hopeful. I also want to thank my dog, Jessie. Though you'll never fully appreciate the sentiment, thanks for your loyalty, motivating me to walk more, and sitting next to me on the couch while I wrote this dissertation.

To anyone that I forgot to mention, whether you let me sleep on your couch or spare bed while I moved or was flooded out of my apartment, invited me to your family's gatherings, shared the burden of life, bought me a beer, sent me a funny picture, stopped for a chat in the hallway, or literally anything else that counts as human interaction, thank you. All the little things amount to so much more than you can imagine.

Endogenous Mechanisms Regulating Myeloid Cell Mediated Inflammation During Acute Lung Injuries

Nathaniel Karl Berg, B.S.E.

Advisory Professor: Holger Eltzschig, M.D, Ph.D.

Acute lung injuries (ALI) can result from both direct insults (e.g. pneumonia or inhalation injury), or systemic conditions such as sepsis or trauma. Current treatment options for patients are limited to supportive care and novel approaches are urgently needed. Appreciating the role of excessive inflammation that underlies the pathophysiology of ALI, we sought to identify endogenous mechanisms that dampen inflammation. Here we investigated two pathways that worked to limit excessive pulmonary inflammation in myeloid cells using a mouse model of sepsis-associated ALI. In the first approach we screened for microRNAs during the recovery phase of ALI that could potentially regulate inflammation. We found that miR-147 is highly expressed during the recovery phase of ALI and worked to dampen inflammation by targeting the mitochondrial subunit, NDUFA4, which resulted in an accumulation of succinate in macrophages. Succinate in turn inhibited the demethylation of Histone H3 to silence the expression of inflammatory cytokines. In the second approach, we demonstrate that the neuronal guidance protein, Netrin-1, is highly expressed in infiltrating alveolar macrophages after the onset of ALI. Netrin-1 deletion in the myeloid compartment resulted in exacerbated ALI and increased NK cell recruitment, which was dependent on the upregulation of the chemokine, CCL2, in the alveolar space. Together, the studies described in this dissertation point to two previously unappreciated mechanisms that serve to limit the pro-inflammatory processes of macrophages and limit tissue damage during ALI. Future work focused on leveraging these processes have great potential to guide the development of novel treatments for ALI.

Table of Contents:

Dedication iii

Acknowledgments: iv

Abstract: vii

Table of Contents: viii

List of Figures: x

List of Tables: xii

Abbreviations: xiii

Chapter 1: An introduction to the acute respiratory distress syndrome (ARDS) 1

 1.1 The historical context and definition of ARDS 1

 1.2 Epidemiology of ARDS 2

 1.3 Etiologies and pathobiology of ARDS 3

 1.4 ARDS in Coronavirus disease 2019 (COVID-19) 6

 1.5 Current treatment and management approaches for ARDS 9

 1.5.1 Harnessing heterogeneity in ARDS to personalize therapy 24

 1.6 Conclusion: The urgent need for novel ARDS treatment 26

Chapter 2: Pre-clinical insights into ARDS 28

 2.1 Modeling ARDS in the laboratory: acute lung injury 28

 2.1.1 Cell culture systems for studying ALI 29

 2.1.2 Animal models of ALI 31

 2.2 The underlying role of dysregulated inflammation in ALI 36

2.2.1 Endogenous mechanisms for the regulation of inflammation and their potential as treatments for ALI.....	40
2.2.1.1 The role of Hypoxia Inducible Factors	40
2.2.1.2 The role of adenosine signaling	46
2.2.1.3 The role of microRNAs.....	50
2.3 Conclusion: The therapeutic potential for regulating inflammation of ARDS	52
General methods and materials	53
Chapter 3: The role of miR-147 in the regulation of inflammation during ALI	59
3.1 Introduction.....	59
3.2 Materials and Methods.....	61
3.3 Results.....	71
3.4 Conclusions and Significance	108
Chapter 4: The role of netrin-1 in the regulation of inflammation during ALI	115
4.1 Introduction.....	115
4.2 Materials and Methods.....	117
4.3 Results.....	128
4.4 Conclusions and Significance	147
Chapter 5: Conclusion of dissertation.....	152
Bibliography:	154
Vita.....	229

List of Figures:

Figure 1: Pathophysiology of Acute Respiratory Distress Syndrome (ARDS) in Coronaviruas Disease 2019 (COVID-19).....	4
Figure 2: A summary of 25 years of Acute Respiratory Distress Snyderome (ARDS) intervention trials.	10
Figure 3: Venovenous (V-V) Extracorporeal Membrane Oxygenation (ECMO).....	22
Figure 4: Hypoxia Inducible Factor (HIF)- α stabilization in the Acute Respiratory Distress Syndrome (ARDS) lung.....	44
Figure 5: Adenosine signaling during inflammation.....	48
Figure 6: MicroRNA-147 is highly upregulated in lungs after the onset of ALI.	73
Figure 7: Pharmacologic inhibition or genetic deletion of miR-147 exacerbates ALI	77
Figure 8: Liposomal miR-147-mimic treatment promotes resolution of ALI	80
Figure 9: Myeloid-specific deletion of miR-147 phenocopies whole-body deletion.....	83
Figure 10: <i>miR147^{loxp/loxp}</i> LysM Cre mice have higher levels of inflammation during ALI	87
Figure 11: miR-147 is induced during ALI in a Hif1 α -dependent manner.	90
Figure 12: miR-147 targets the mitochondrial complex IV subunit, NDUFA4	94
Figure 13: NDUFA4 deletion dampens inflammatory gene expression independent of LPS-TLR4 signaling	97
Figure 14: NDUFA4 deletion leads to succinate accumulation via dampening the electron transport chain	101
Figure 15: Succinate accumulation in NDUFA4 knockout cells epigenetically regulates inflammation.....	106
Figure 16: Proposed mechanism for miR-147-mediated regulation of inflammation during ALI	114
Figure 17: Lack of significant sex differences in <i>Hif1a^{loxp/loxp}</i> LysM Cre Mice.	119
Figure 18: Confirmation of <i>Ntn1</i> knockout in <i>Ntn1^{loxp/loxp}</i> LysM Cre mice.	121

Figure 19: Netrin-1 is significantly upregulated in endotoxin treated myeloid cells..... 130

Figure 20: Myeloid cells recruited during endotoxin-induced lung injury have high levels of netrin-1..... 132

Figure 21: LPS-induced netrin-1 expression in myeloid cells is regulated by HIF-1 α 135

Figure 22: Netrin-1 deletion in myeloid cells exacerbates LPS-induced lung injury..... 138

Figure 23: *Ntn1*^{loxp/loxp} LysM Cre mice display increased natural killer (NK) cell infiltration in the airway during LPS-induced lung injury. 142

Figure 24: C-C motif chemokine ligand 2 (CCL2) neutralization in *Ntn1*loxp/loxp LysM Cre mice reduces natural killer (NK) cell infiltration in the airway and improves LPS-induced lung injury. 145

Figure 25: Proposed mechanism for myeloid cell-derived Netrin-1 during LPS-induced acute lung injury..... 151

List of Tables:

Table 1: PCR probes used for Chapter 3.....	63
Table 2: Antibodies used in Chapter 3.....	65
Table 3: Mouse strain details for chapter 4.....	118
Table 4: Reagents for chapter 4	123
Table 5: Antibodies used in chapter 4.	125

Abbreviations:

A₂AAR/A₂BAR: A₂A/A₂B adenosine receptor

ACE2: angiotensin converting enzyme 2

AEC: alveolar epithelial cells

AECC: American-European Consensus Conference

ALI: Acute lung injury

AlvMΦ: alveolar macrophages

ANOVA: analysis of variance

AOC: area under the curve

ARDS: Acute respiratory distress syndrome

ATII: alveolar type II cell

ATP/ADP/AMP: adenosine tri-, bi- or mono-phosphate

BAL: bronchoalveolar lavage

BALF: bronchoalveolar lavage fluid

BMDM: Bone marrow-derived macrophage

CCL2: C-C Motif Chemokine Ligand 2

ChIP: chromatin immunoprecipitation

CLP: cecal ligation and puncture

CMV: cytomegalovirus

COVID-19: Coronavirus disease 2019

Cre: Recombinase

CRISPR: clustered regularly interspaced short palindromic repeats

CT: computed tomography

CTRL: control

CVP: central venous pressure

DAD: diffuse alveolar damage

DAMP: damage-associated molecular pattern

DIC: diffuse intravascular coagulation

DOPC: di-oleoyl-phosphatidylcholine

ECMO: extra corporeal membrane oxygenation

ELISA: enzyme-linked immunosorbent assays

ENT1/2: equilibrative nucleoside transporters 1 and 2

ETC: electron transport chain

EZH2: enhancer of zeste homolog 2

FACS: Fluorescence activated cell sorting

FCCP: Carbonyl cyanide-4-(trifluoromethoxy)phenylhydrazine

FCS: fetal calf serum

FDR: False discovery rate

FiO₂: inspired oxygen fraction

GLUT1: glucose transporter 1

GM-CSF: granulocyte-macrophage colony-stimulating factor

H3K4/9/27me3: tri-methylated histone-3 lysine-4/9/27

HIF: Hypoxia inducible factor

hMDM: human monocyte derived macrophages

HRE: hypoxia response element

HRMS: high-resolution mass spectrometry

i.p.: Intra-peritoneal

i.t.: Intra-tracheal

i.v.: intravenous

IC: ion chromatography

ICAM-1: intercellular adhesion molecule-1

ICE: Inference of CRISPR Edits

ICU: Intensive care unit

IgG: Immunoglobulin G

IL: interleukin

iNO: inhaled nitric oxide

iNOS: inducible nitric synthase

IRAK: IL-1 associated kinase

IRDS: infant respiratory distress syndrome

IRF: interferon regulatory factors

IRG1: immune responsive gene

JMJD3: jumonji domain containing-3

KDM: lysine-specific demethylase

kg_{PBW}: kg of predicted body weight

LC: liquid chromatography

LNA: locked nucleic acids

LPS: lipopolysaccharide

LRM: Lung recruitment maneuvers

LysM: lysozyme M

M-CSF: macrophage colony-stimulating factor

miRNA or miR: microRNA

MMP: metalloproteinase

MPB: Mobile phase B

mRNA: messenger RNA

MΦs: macrophages

NDUFA4: NADH dehydrogenase (ubiquinone) 1 alpha subcomplex 4

NF-κB: nuclear factor kappa-light-chain-enhancer of activated B cells

NGP: Neuronal guidance peptides

NGP: neuronal guidance protein

NHLBI: National Heart, Lung, and Blood Institute

NIS: National Inpatient Survey

NIV: non-invasive ventilation

NK cell: Natural killer cell

NLRP3: NOD-, LRR- and pyrin domain-containing protein 3

NMES1: normal mucosa of esophagus specific 1

NTN1: netrin-1

OCR: oxygen consumption rate

ODD: oxygen dependent domain
 PAMP: pathogen-associated molecular pattern
 PaO₂: arterial oxygen tension (in mmHg)
 PARP-1: poly(adenosine diphosphate-ribose) polymerase-1
 PBMCs: peripheral blood mononuclear cells
 PBS: phosphate buffered saline
 PCR: polymerase chain reaction
 PDK1: pyruvate dehydrogenase kinase 1
 PEEP: Positive End Expiratory Pressure
 PETAL Network: Prevention and Early Treatment of Acute Lung Injury Network
 PHD: prolyl hydroxylase domain proteins
 PIMs: pulmonary intravascular macrophages
 PMA: phorbol 12-myristate 13-acetate
 PMN: polymorphonuclear leukocytes
 qPCR: quantitative polymerase chain reaction
 RAF: TNF associated factor
 RecMΦ: recruited macrophages
 RFU: relative fluorescence units
 ROS: reactive oxygen species
 Rot/AA: rotenone and actinomycin A
 SARS-CoV-2: Severe Acute Respiratory Syndrome Coronavirus-2
 SCR: scrambled
 SD: standard deviation
 SDH: succinate dehydrogenase
 SEAP: secreted alkaline phosphatase
 Seq: sequencing
 SOCS-1: suppressor of cytokine signaling-1
 SpO₂: hemoglobin oxygen saturation
 sRAGE: soluble receptor for advanced glycation end products
 STEMI: ST-elevation myocardial infarction
 SUNCR1: succinate receptor 1
 TAC: Transcriptome Analysis Console
 TBP: tata-box binding protein
 TCA: tricarboxylic acid cycle
 TLR: toll-like receptors
 TNF: tumor necrosis factor
 TSS: transcription start site
 UTR: untranslated region
 VFD: Ventilator-free days
 VHL: Von-Hippel Lindau
 VILI: ventilator induced lung injury
 V-V ECMO: Venovenous extra corporeal membrane oxygenation
 WT: wild type
 αCCL2: neutralizing CCL2 antibodies
 α-KG: alpha-ketoglutarate

Chapter 1: An introduction to the acute respiratory distress syndrome (ARDS)

Some sections of this chapter were previously published in:

George W. Williams*, Nathaniel K. Berg*, Alexander Reskallah, Xiaoyi Yuan, Holger K. Eitzschig; Acute Respiratory Distress Syndrome: Contemporary Management and Novel Approaches during COVID-19. *Anesthesiology* 2021; 134:270–282

*Denotes co-first authorship

Re-use of these materials for this dissertation were allowed with permission from the publisher.

1.1 The historical context and definition of ARDS

In 1821 René Laennec, inventor of the stethoscope, described the gross edematous pathology of lungs from patients with severe shortness of breath and cyanosis.¹ In his account, he noted the pulmonary edema was not explained by heart failure and termed the finding as idiopathic anascara of the lungs. At these times, the constellation of idiopathic anascara of the lungs, shortness of breath and cyanosis was widely fatal. The descriptions from Laennec are perhaps the earliest account of what we now recognize as the acute respiratory distress syndrome (ARDS). In 1967, a seminal report by Ashbaugh et al. described cases of respiratory distress in adults that closely resembled that seen in premature babies with infant respiratory distress syndrome (IRDS), eventually referring to it as “adult” respiratory distress syndrome.² Then in 1994 the American-European Consensus Conference (AECC) agreed that the term “acute lung injury” be used and that “acute respiratory distress syndrome” be saved for patients with a ratio of arterial oxygen tension (PaO₂) to inspired oxygen fraction (FiO₂) of 200 or lower.³ The term “adult” was replaced with “acute” because, unlike IRDS, ARDS does not respond to surfactant

replacement. In order to make the syndrome easier to describe more precisely and to aid the classification of disease severity for clinical trial and research pursuits, the Berlin definition of ARDS was published in 2012, which dropped the term “acute lung injury” for ARDS and allowed for stratification of severity based on the degree of hypoxemia.⁴ Nonetheless, the term “acute lung injury” is still used to describe experimental studies of ARDS in animal models.

According to the 2012 Berlin definition, ARDS is a clinical condition characterized by an acute lung injury that leads to the onset of non-cardiogenic pulmonary edema and decreased capacity for gas exchange that results in hypoxemia.⁴⁻⁶ The diagnosis of ARDS is confirmed by radiographic evidence of pulmonary edema and a blood gas analysis demonstrating hypoxemia defined by a ratio of arterial oxygen tension to fraction of inspired oxygen (PaO₂:FiO₂ ratio) less than 300. ARDS is further stratified based on severity of hypoxemia, with PaO₂:FiO₂ ratios of less than 300, 200, or 100 acting as cutoffs for mild, moderate or severe disease, respectively.⁴ ARDS commonly afflicts critically ill and high-risk surgical patients and is associated with a devastatingly large mortality rate (typically between 35% and 45%).^{1, 7}

1.2 Epidemiology of ARDS

Between April 1999 and July 2000, Rubenfeld and colleagues performed a prospective study in Kings County, Washington aimed at measuring the incidence of ARDS in the United States by identifying patients with bilateral opacities on chest radiography and a PaO₂/FiO₂ < 300 mmHg.⁸ The investigators estimated that there were 190,000 annual cases in the US, with an associated mortality rate of 38.5%.⁸ A subsequent retrospective analysis of ARDS patients identified in the National Inpatient Survey (NIS) between 2006 and 2014 suggested that the incidence of ARDS is slightly increasing and mortality rates are declining.⁹ However, the LUNG-SAFE study, a 2014, 50 center, multinational prospective cohort, reported that ARDS has an incidence of 10.4% across all ICU patients and 23.4% in all patients requiring mechanical ventilation, indicating that ARDS is still a prevalent problem in the critically ill.¹⁰ Multiplying the

LUNG-SAFE-reported incidence of 0.46 cases of ARDS per ICU bed per 4 weeks in North America with 94,837 ICU beds in the United States (provided by American Hospital Association 2015 annual statistics) and adjusting for 52 weeks in one year, results in an updated estimate of 567,000 ARDS cases per year in the United States.^{10, 11} Furthermore, the LUNG-SAFE study demonstrated that ARDS mortality rates remain between 35% and 45%.¹⁰ Using an estimate of 40% mortality, this would result in over 226,000 ARDS-associated deaths per year. Perhaps the most worrisome trend is that reported mortality rates between 2000 and the 2014 LUNG-SAFE study have largely remained unchanged, indicating an urgent need for the advancement of recognition, prevention, and therapeutics for ARDS.

1.3 Etiologies and pathobiology of ARDS

Etiologic risk factors for ARDS encompass both direct- and indirect-lung injuries including, but not limited to pneumonia, sepsis, non-cardiogenic shock, aspiration, trauma, contusion, transfusion, inhalation injuries, gastroesophageal reflux, and ventilator induced lung injury. Importantly, there are a number of clinical “mimics” of ARDS, such as interstitial lung disease and vasculitis that can obfuscate proper diagnosis.¹² The activation of resident lung macrophages through recognition of pathogen- and damage-associated molecular patterns (PAMPS/DAMPS) plays a critical role in initiating and/or perpetuating ARDS by stimulating the release of cytokines and recruitment of inflammatory monocytes and neutrophils.^{13, 14} Immune-cell effector molecules, such as cytokines and proteolytic enzymes, contribute to the activation and loss of barrier function of endothelial cells. Additionally, alveolar epithelial cell inflammation and death results from both direct (e.g. bacterial toxins, viruses, mechanical ventilation) or indirect (i.e. collateral inflammation imparted by dysregulated immune cell activity) causes.¹⁴ The loss of barrier function from epithelial and endothelial linings of the alveoli results in the accumulation of protein-rich edema into the airspace.¹⁵ The ultimate physiological consequence of alveolar fluid accumulation and alveolar inflammation is the impairment of essential gas exchange leading to hypoxemia (Figure 1).¹⁵

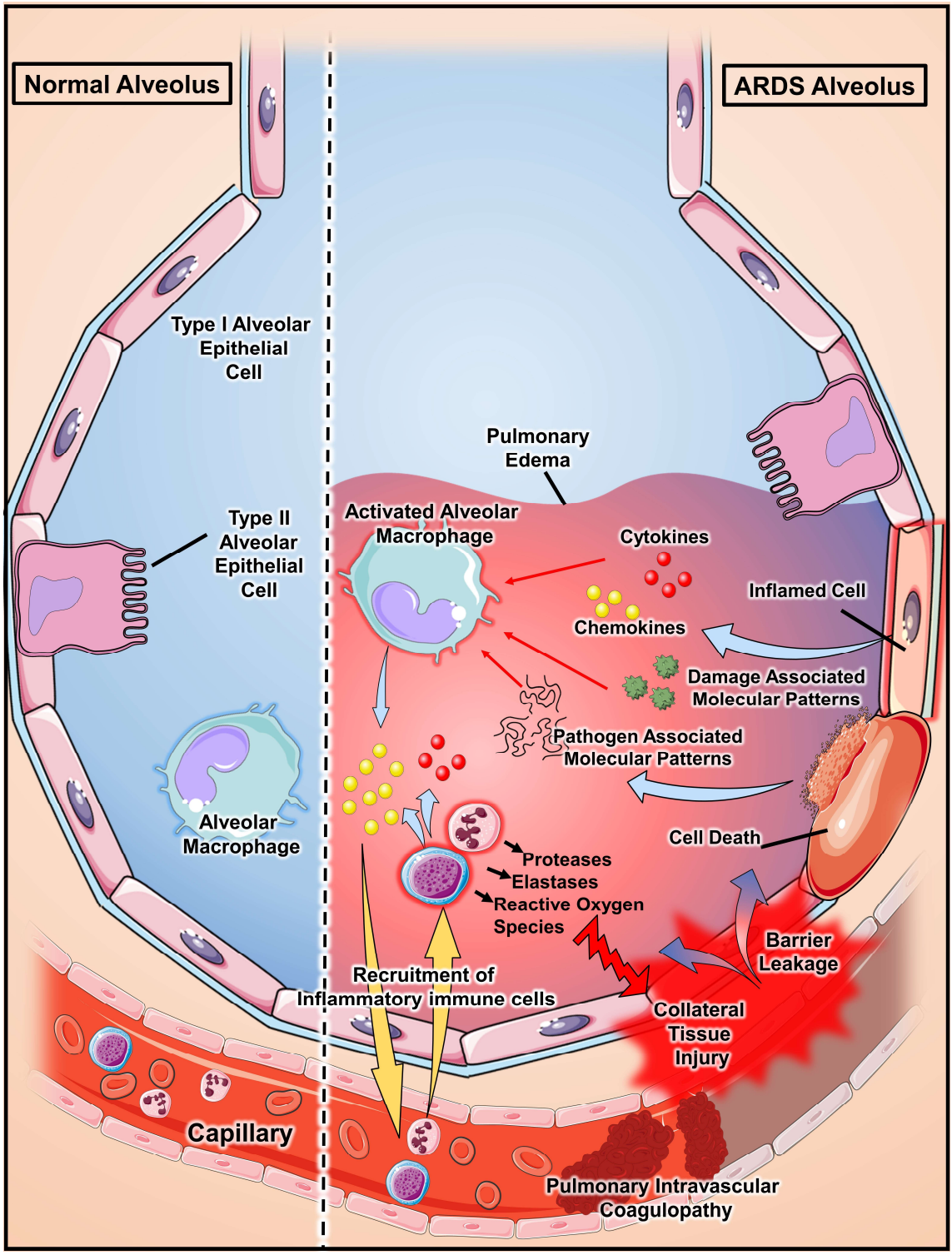


Figure 1: Pathophysiology of Acute Respiratory Distress Syndrome (ARDS) in Coronavirus Disease 2019 (COVID-19).

The activation of resident lung macrophages through recognition of pathogen- and damage-associated molecular patterns (PAMPS/DAMPS) plays a critical role in initiating and/or

Figure 1 (Continued):

perpetuating ARDS by stimulating the release of cytokines and recruitment of inflammatory monocytes and neutrophils.^{13, 14} Additionally, injury to epithelial and endothelial cells can also initiate and enhance inflammation. Cellular injury or infectious pathogens can result in the release of inflammatory Damage and Pathogen Associated Molecular Patterns (DAMPs/PAMPs). Recognition of PAMPs/DAMPs and cytokines activates alveolar macrophages and chemokines act to recruit inflammatory immune cells to the lung. Excessive immune cell release of antimicrobial effectors, such as metalloproteinases (MMPs), elastases, and reactive oxygen species (ROS), induce collateral tissue injury that results in loss of epithelial and endothelial barrier integrity and infiltration of proteinaceous fluid into the alveolar airspace.⁴⁰ Furthermore, ARDS can involve development of extensive pulmonary intravascular coagulopathy.⁴¹⁻⁴³

Histologically, ARDS is characterized by diffuse alveolar damage (DAD) that is hallmarked by hyaline membranes.¹⁶ The presence of DAD – as assessed by autopsy or open lung biopsy – is associated with ARDS mortality, which would make it a useful prognostic, but clinical parameters have not been identified that might predict DAD in ARDS patients.^{17, 18} Several co-morbidities and behavioral or environmental factors have also been correlated with increased risk for ARDS such as alcohol abuse¹⁹, cigarette smoking^{20, 21}, air pollution^{22, 23}, and low total serum protein.²⁴ Interestingly, obesity appears to be a risk factor for ARDS development but is protective against the mortality of ARDS, the so-called “obesity paradox”.^{25, 26} Some proposed explanations for this “obesity paradox” include altered inflammatory responses consisting of decreased levels of pro-inflammatory cytokines (IL-6 and IL-8) in obese ARDS patients,²⁷ a confounding role for optimized or aggressive medical management given the increased risk for co-morbidities in obese patients such as diabetes and heart disease,²⁸ and the potential role that obese patients may have increased energy stores to counteract the catabolic stress of critical illness. Although several reports suggest a role for diabetes in ARDS risk, data from large, prospective observations offered no association between ARDS development and outcomes in patients with diabetes.¹⁰

1.4 ARDS in Coronavirus disease 2019 (COVID-19)

Coronavirus disease-2019 (COVID-19) is caused by infection of the lower airway by Severe Acute Respiratory Syndrome Coronavirus-2 (SARS-CoV-2). SARS-CoV-2 emerged in December 2019 in Wuhan, Hubei province, central China where it is believed to have transmitted to humans at a seafood market.^{29, 30} Since then, it has spread globally and has resulted in the current COVID-19 pandemic. At the time of this writing (April 20, 2019), there are over 142 million confirmed cases globally and over 3 million deaths.³¹ The cases reported in the United States account for roughly 31 million positive cases and over 568,000 deaths.³¹

SARS-CoV-2 is a strain of coronavirus of zoonotic origins.²⁹ The virus infects the lower lung primarily through binding of Spike protein found on the surface of the virus to its receptor, angiotensin converting enzyme 2 (ACE2), found on the surface of alveolar epithelial cells (Figure 1).^{29, 32} After the entrance into cells via endocytosis, the virus releases its positive-stranded RNA genome, which relies on host translational machinery to produce viral proteins. One such protein is an RNA-dependent RNA polymerase (the drug target of Remdesivir) that replicates the viral genome, which becomes assembled within newly synthesized viral particles that are then released from the cell through exocytosis, completing the SARS-CoV-2 life cycle.³³ Virus infection by SARS-CoV-2 results in injury and destruction of cells as a result of its cytopathic life cycle. Cell death can occur through pyroptosis, which is a highly inflammatory mechanism of programmed cell death that results in the release of cytokines and Pathogen and Damage Associated Molecular patterns (PAMPs and DAMPs), such as RNA, DNA, and ATP. Recognition of PAMPs and DAMPs results in the recruitment and activation of immune cells, primarily monocytes, and lymphocytes in COVID-19.³⁴ In most cases, immune cell recruitment and inflammatory responses are sufficient to clear the invading virus, but then subsequently resolve to allow for a return to normal tissue homeostasis. However, in a subset of patients inflammation can become dysregulated leading to excess release of cytokines and recruitment of immune cells, resulting in widespread collateral lung injury³⁴. Dysregulated inflammation in COVID-19 patients is evident as increased levels of inflammatory cytokines were found in the serum of patients that required intensive care and patients that had relatively increased levels of serum IL-6, a potent inflammatory cytokine, were statistically more likely to not survive.^{35, 36} Furthermore, cell and animal models of SARS-CoV-2 infection, as well as serum samples from COVID-19 patients, demonstrate a diminished innate anti-viral response coupled with inappropriate cytokine expression.³⁷ Clinically, dysregulated and persistent lung inflammation in COVID-19 disease results in the development of ARDS with associated characteristic pathological features of diffuse alveolar damage and pulmonary edema.^{38, 39}

ARDS is highly prevalent in COVID-19 hospitalized patients, with reports indicating an incidence of 30-40%, and is associated with 70% of fatal cases.^{36, 45} ARDS in COVID-19 patients present with several unique characteristics that are not regularly described in non-COVID-19 associated ARDS. Among these characteristics is the significant development of microvascular thrombosis within the lung vasculature that contributes to the shunting of blood and right ventricular stress.^{36, 46, 47} In severe cases, patients develop disseminated intravascular coagulation (DIC). Tang et al. reported that DIC was present in 71.4% of fatal COVID-19 cases.⁴⁸ Though the cause for widespread activation of the coagulation cascade is not yet fully understood, dysregulated inflammation and direct injury to endothelial cells by SARS-CoV-2 contribute to the development of microthrombotic immunopathology.^{46, 47, 49} Additionally, endothelial cell damage in COVID-19 infection impairs pulmonary vasoconstriction that normally occurs in response to hypoxia to restrict blood flow to poorly ventilated areas of the lung. Disruption in this physiologic adaptation in COVID-19 patients results in a ventilation-perfusion mismatch. To this end, Gattioni et al. have described severely hypoxemic patients with well-preserved lung compliance in non-ARDS COVID-19 pneumonia.⁵⁰⁻⁵² There are also reports of non-ventilated SARS-CoV-2 patients who appear comfortable at oxygen saturation levels between 50 and 70%, a phenomenon of COVID-19 often referred to as 'happy hypoxia'.^{53, 54} Patients presenting in this early stage of the disease can benefit from limited PEEP (8–10 cmH₂O) and prone positioning due to improved distribution of pulmonary perfusion. Furthermore, early mechanical ventilation with sedation may prevent exacerbation of lung inflammation caused by potentially injurious transpulmonary pressure swings produced by strong respiratory drives.⁵⁵ However, in patients that present with or progress to ARDS (severe hypoxemia with *low* pulmonary compliance), a conventional lung-protective strategy utilizing low tidal volumes, prone positioning, and PEEP up to 14–15 cmH₂O is recommended.⁵⁶ On the other hand, an effort to prevent early mechanical ventilation through increased use of non-invasive ventilation (NIV) methods and proning have been suggested in order to minimize unnecessary invasive intubation and to preserve resources for patients who present with more

critical respiratory failure.⁵⁷ Indeed, a small trial reported by Sartini et al. demonstrated that NIV combined with proning in COVID-19 patients was feasible and resulted in improvements in respiratory rate and oxygenation.⁵⁸ However, it still remains to be determined whether NIV and proning can prevent or delay mechanical ventilation in randomized controlled study.

1.5 Current treatment and management approaches for ARDS

Nationally Organized Research Consortia to Study ARDS

In order to improve outcomes and develop treatment protocols for ARDS, the National Heart, Lung, and Blood Institute (NHLBI) of the NIH funded a series of multi-center clinical trials, which formed a research collaboration called the ARDS Network (<http://ardsnet.org>).⁵⁹ Beginning in 1994, the network studies enrolled over 5,500 patients, included 10 clinical trials and 1 observational study, led to the development of new clinical parameters such as ventilator free days (VFD)⁶⁰ and resulted in seminal advances that have helped to shape current ARDS management. NHLBI-funded clinical trials continue presently under the Prevention and Early Treatment of Acute Lung Injury (PETAL) Network (<http://petalnet.org>). In this section, we will discuss many of the ARDS management guidelines that were elucidated by these trial networks as well as ideas that are emerging from other rigorously-conducted clinical research (Figure 2).

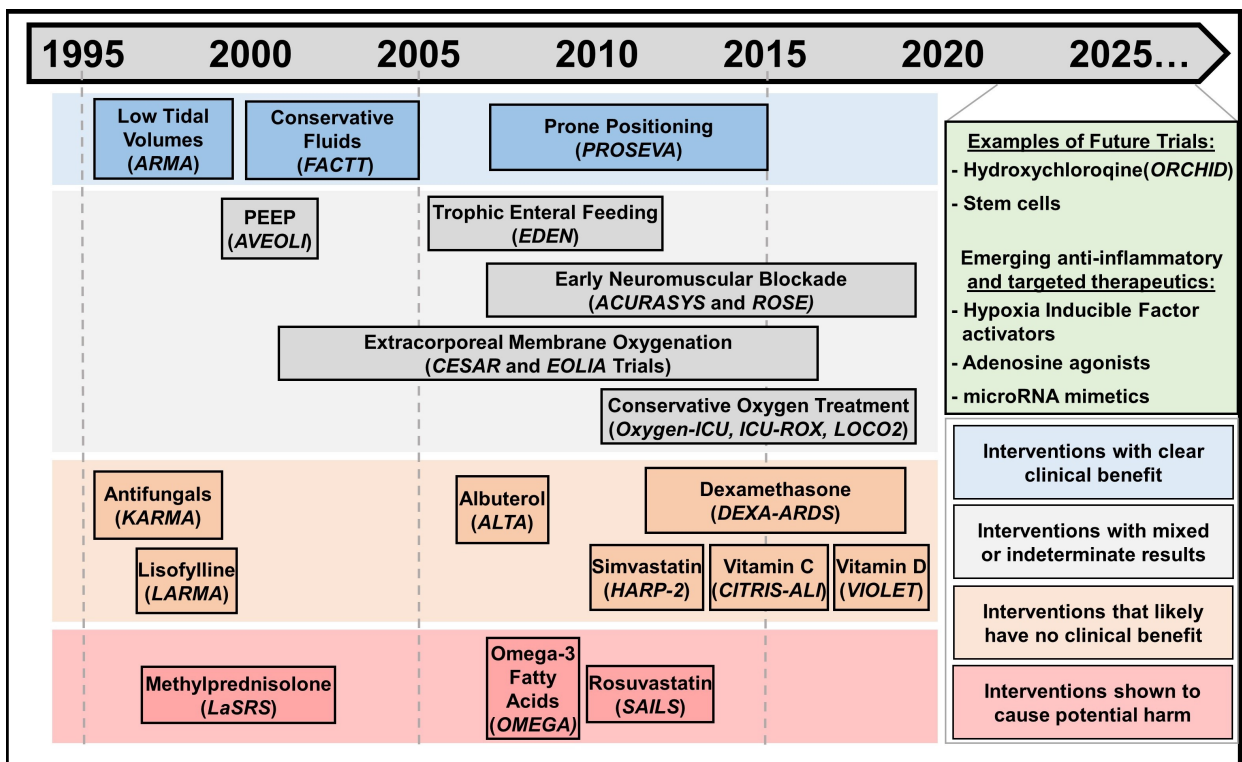


Figure 2: A summary of 25 years of Acute Respiratory Distress Syndrome (ARDS) intervention trials.

Interventions are chronologically displayed with corresponding clinical trials italicized underneath and color-coded to denote clinical efficacy. Interventions that have clear clinical efficacy, in *blue boxes*, include the use of small tidal volumes,⁶¹ prone positioning,⁶² and restrictive fluid administration,⁶³ which have demonstrated clear mortality or ventilator-free days benefits. Interventions in *grey boxes* include those that have mixed results from different trials, as is the case for conservative oxygen treatment⁶⁴⁻⁶⁶ and early neuromuscular blockade.^{67, 68} This category (*grey boxes*) also includes interventions with indeterminate results, such as the case for Positive End Expiratory Pressure (PEEP)⁶⁹ – itself is a component of lung-protective ventilation, but the appropriate amount to use is still contended – or those that have value in ARDS patients aside from improving ARDS outcomes, such as early trophic enteral nutrition to prevent gastric intolerance⁷⁰ and Extracorporeal Membrane Oxygenation (ECMO) as a rescue therapy.^{71, 72} In *orange boxes* are interventions that failed to demonstrate improvements in

Figure 2 (continued):

ARDS outcomes, such as antifungals, lisofylline, albuterol, simvastatin, vitamin C and vitamin D.⁷³⁻⁷⁹ Dexamethasone is also listed in this category given that the DEXA-ALI trial was conducted in an unblinded fashion⁸⁰ and prior randomized trials showed no clinical efficacy for steroid administration in ARDS. Methylprednisolone,⁸¹ rosuvastatin⁸⁰ and ω -3 Fatty Acids,⁸² listed in *red boxes*, have shown to cause potential harm in randomized controlled trials. Currently, ongoing or planned trials and emerging therapeutic targets are displayed in green.

Small tidal volumes

Amongst the best-established guidelines in managing ARDS patients is the use of small tidal volumes during mechanical ventilation (Figure 2). In 2000, Investigators from the ARDSNet Lower Tidal Volume Trial (ARMA) trial reported significantly decreased rates of mortality (31.0% vs. 39.8 %) in ARDS patients ventilated with 6ml/kg of predicted body weight (kg_{PBW}) tidal volumes versus those with 12 ml/ kg_{PBW} .⁶¹ While small tidal volume ventilation remains a tenant of lung-protective ventilation during ARDS, recent efforts have sought to determine whether small tidal volumes play a lung-protective role more broadly in all critically-ill ventilated patients. Though results of a meta-analysis suggested decreased development of lung injury and mortality through the use of small tidal volumes in non-ARDS patients⁸³, in 2018 the Protective Ventilation in Patients Without ARDS (PreVENT) trial demonstrated that ventilation with low tidal volumes may not be more effective than intermediate volumes in non-ARDS ICU patients.⁸⁴ The trial randomized 961 non-ARDS patients expected to receive more than 24 hours of mechanical ventilation to either receive low ($\leq 6 \text{ ml/kg}_{\text{PBW}}$) or intermediate tidal volumes ($\geq 10 \text{ ml/kg}_{\text{PBW}}$). The investigators reported no statistically significant changes in ventilator-free days or mortality between the two groups, however, by one day after randomization, 59% of patients allocated to the low tidal volume group received ventilation with pressure support ventilation resulting in tidal volumes in excess of 6 ml/ kg_{PBW} . Because the trial's ventilation targets were clearly not met, whether low tidal volumes improves outcomes in non ARDS critically ill patients remains to be evaluated in a randomized control trial.

Small tidal volumes in the operating room

Of particular interest to the practicing anesthesiologist is a growing body of evidence that suggests the application of lower tidal volumes plays a protective role in reducing the rate of postoperative pulmonary complications.⁸⁵ In a small (n=58) randomized clinical trial of open abdominal surgery patients who were randomized to a protective ventilation strategy (tidal

volumes of 7 ml/kg_{PBW}, 10 cm H₂O PEEP, and recruitment maneuvers) had improved respiratory function and decreased pulmonary infectious complications than those allocated to received mechanical ventilation with a standard strategy (tidal volume of 9 ml/kg_{PBW} and no PEEP).⁸⁶ Furthermore, a retrospective observational study of 4,694 cardiac surgery patients found that intraoperative lung protective ventilation (tidal volumes < 8 ml/kg_{PBW}, modified driving pressure [peak inspiratory pressure - PEEP] < 16 cm H₂O, and PEEP ≥ 5 cm H₂O) was associated with reduced pulmonary complications.⁸⁷ However, future large-scale prospective interventional studies will be required to establish whether such ventilation strategies should become part of guidelines and if they are indicated for all or just a subset of patients undergoing surgery.

Positive End Expiratory Pressure (PEEP) and Lung Recruitment Maneuvers (LRMs)

In their seminal 1967 report of ARDS cases, Ashbaugh et al reported that improvement of hypoxemia and atelectasis was achieved by the implementation of PEEP.² Since then, PEEP continues to be employed in ARDS management and remains the focus of many clinical research efforts. Conceptually, PEEP is administered in order to reduce atelectrauma (repetitive opening and closing of alveoli) by recruiting collapsed alveoli.⁸⁸ Much attention has been directed at the levels at which PEEP is applied, with clinical evidence yielding mixed results (Figure 2). Several trials that report protective benefits from higher versus lower targets of PEEP employed higher tidal volumes in their control (lower PEEP) groups, which perhaps introduced bias in their conclusions.^{89, 90} Trials that have controlled for low tidal volumes (6 ml/kg), including the 2004 ARDS Network ALVEOLI trial, have failed to demonstrate a survival benefit for higher PEEP, though there was some efficacy towards secondary endpoints such as hypoxemia and use of rescue therapies.^{69,91} A more recent systematic review of the clinical evidence supports the overall conclusion that higher versus lower levels of PEEP is not associated with improved hospital survival.⁹² Subgroup analysis does, however, suggest that higher PEEP is associated with improved survival among the subgroup of patients with ARDS

who objectively respond to increased PEEP (patients who show improved oxygenation in response to increased PEEP).⁹³ Still, it has yet to be demonstrated whether survival in selected patients improves with increased PEEP in large randomized trials. Furthermore, determination of an optimal PEEP level for an individual ARDS patient remains an important challenge. Currently, several methods, such as compliance-, FiO_2 -, and electrical impedance tomography-guided PEEP titration, are being investigated, but ARDS mortality outcome data from large randomized trials implementing these personalized techniques are still not available.^{94, 95}

Lung recruitment maneuvers (LRMs) are a set of techniques aimed at recruiting collapsed alveoli in order to increase the lung volume receptive to tidal ventilation. LRMs include methods that employ sustained increases in airway pressure to open collapsed alveoli (e.g. prolonged high continuous positive airway pressure (30–40 cm H_2O for 30-40 seconds), which are followed with sufficient PEEP that maintain the recruited lung volume.⁹⁶ Though some studies implementing lung recruitment maneuvers have shown promising results in managing ARDS, the confidence regarding these effects were confounded by the use of higher PEEP ventilation in LRM groups.⁹⁷ In 2017, the Writing Group for the Alveolar Recruitment for Acute Respiratory Distress Syndrome Trial (ART) Investigators reported the results of a trial in which 1010 ARDS patients were randomized to receive recruitment maneuvers with PEEP as high as 45 cm H_2O and peak airway pressures as high as 60 cm H_2O , followed by decremental PEEP to identify optimal lung compliance.⁹⁸ Patients receiving the lung recruitment protocol had significantly increased 28-day and 6-month mortality, providing strong evidence against the use of recruitment maneuvers in ARDS patients.

Prone positioning

Beneficial effects of prone positioning during mechanical ventilation of ARDS patients are considered in order to establish a more even distribution of gravitational force in pleural pressure allowing for improved ventilation of the dorsal lung space⁹⁹ and to limit over-distention of alveoli.¹⁰⁰ In 2013, Guérin and colleagues reported the results of the Prone Severe ARDS

Patients (PROSEVA) trial in which severe ARDS patients ($\text{PaO}_2/\text{FiO}_2$ less than 150 on FiO_2 of at least 0.6) were randomized to prone positioning for a minimum of 16 hours a day. Patients randomized to prone positioning had a 50% reduction in mortality (16% versus 32.8%) at 28 days (Figure 2).⁶² A recent meta-analysis corroborates these results and supports the survival benefits of prolonged prone positioning (greater than 12 hours) in patients with severe ARDS.¹⁰¹ Despite these encouraging results in reducing mortality with the use of prone positioning, data from a large, multinational prospective observational study indicate that the maneuver was employed in only 16.3% of severe ARDS patients.¹⁰ Possible reasons for this low implementation could be attributed to the relative complexity and logistic considerations of prone positioning (e.g. multiple persons required for the maneuver, increased workloads, management of secretions, and nutrition) or due to the inherent risks of the procedure such as endotracheal tube and vascular line displacement. Nonetheless, the use of prone positioning for more than 12 hours per day remains a strong recommendation for patients with severe ARDS.¹⁰²

Although the efficacy of prone positioning is almost exclusively suggested in patients with $\text{PaO}_2/\text{FiO}_2$ ratios of 150 or less, trials that failed to show efficacy in mild and moderate ARDS are largely underpowered and failed to administer prone positioning for recommended lengths of time.¹⁰³ As such, randomized trials implementing early prone positioning in mild to moderate cases of ARDS are necessary in order to determine any survival benefits and to make recommendations for clinical implementation.

Neuromuscular Blockade

Neuromuscular blockade is administered in order to reduce patient-ventilator dyssynchrony and the work of breathing in patients.¹⁰⁴ Investigators from the 2010 ARDS et Curarisation Systematique (ACURASYS) study sought whether two days of neuromuscular blockade early in the course of severe ARDS would improve outcomes (Figure 2).⁶⁷ Patients in the treatment

arm (bolus and infusion of cisatracurium for 48 hours) demonstrated improved 90-day survival and increase in ventilator-free days. Despite these positive results, early neuromuscular blockade was not widely adopted given concerns of long-term effects of paralysis, including ICU-acquired weakness. A 2019 follow-up study from the PETAL Network re-visited the findings with the Reevaluation of Systemic Early Neuromuscular Blockade (ROSE) trial (Figure 2).⁶⁸ The trial was stopped early for futility as there was no difference in 90 day mortality between patients randomized to receive early deep sedation and those randomized to the lighter sedation targets. Additionally, the results of the ROSE trial indicated that early neuromuscular blockade was associated with an increase in serious adverse cardiovascular events, which may be attributed to the deeper sedation targets in the intervention group. Nonetheless, the outcomes of the ROSE trial do not provide evidence for the systematic early administration of neuromuscular blockade. However, these results do not preclude the notion that early neuromuscular blockade might provide efficacy in patients with severe refractory hypoxemia or ventilator dyssynchrony.¹⁰⁵

Steroids

In the report of ARDS patients by Ashbaugh et al. in 1967, it was suggested that corticosteroids appeared to have clinical value in cases associated with fat emboli and viral pneumonia.² Randomized control trials conducted in the 1980s have since demonstrated that early administration of methylprednisolone did not result in improved ARDS survival.^{106, 107} However, in 1998 a prospective trial by Meduri and colleagues showed an improved outcome in ARDS patients treated with prolonged methylprednisolone.¹⁰⁸ The results of the study were subject to scrutiny due to the small sample size (n=8) of the control group, significant cross-over into the methylprednisolone group (all of which died) and a relatively large mortality rate of 60%. Subsequently, in 2006 the ARDS Network addressed the role of corticosteroid administration late in ARDS with the Late Steroid Rescue Study (LaSRS) in which 180 patients were randomized to methylprednisolone administration 7 to 28 days after diagnosis of ARDS.

Administration of methylprednisolone was associated with no significant reduction in mortality (Figure 2).⁸¹ Furthermore, patients who started steroid treatment after 14 days of diagnosis experienced increased mortality.

Based on the postulate that, compared to other corticosteroids, dexamethasone has an improved potency, lengthened duration of action, and weak mineralocorticoid effect, Villar and colleagues performed a prospective trial randomizing ARDS patients to receive either dexamethasone or placebo.⁸⁰ Compared to Patients in the control group, dexamethasone treatment group showed a reduced time on mechanical ventilation and 60-day mortality, however, drug allocation and data analysis were performed in an unblinded fashion, potentially leading to bias. Furthermore, 250 patients were excluded for already receiving steroids prior to randomization, indicating that participating physicians already favored the use of corticosteroids which might have influenced clinical decisions to modify mechanical ventilation duration. In summary, guidelines supporting routine glucocorticoid administration in ARDS based on rigorously performed RCTs are currently not supporting their use.

Steroids in COVID-19 ARDS

Recent data from the UK RECOVERY (Randomised Evaluation of COVid-19 thERapY) trial investigating the use of dexamethasone in hospitalized COVID-19 patients have demonstrated that dexamethasone is the first drug to improve mortality.¹⁰⁹ Mechanically ventilated patients that were randomized to receive 6 mg once per day for 10 days were found to have a reduction of mortality by one third when compared to patients who underwent usual care. Interestingly, this mortality benefit was not observed in patients who did not require respiratory support. In response to these findings, current COVID-19 treatment guidelines from the National Institutes of Health recommend its use in patients that are mechanically ventilated or require oxygen supplementation.¹¹⁰ Moreover, similar to ARDS and PETAL Network studies, the RECOVERY trial provides an example for the power of organized multicenter investigations for new treatment approaches in critically-ill patients, especially those with ARDS. Moving forward, data

from the dexamethasone arm are likely to reinvigorate studies for its use in non-COVID-19 ARDS patients that may support the open-label dexamethasone studies previously mentioned.⁸⁰

Fluid Management

Fluid management in ARDS patients requires physicians to carefully consider both the alveolar and intravascular compartments. A decreased barrier function in the lungs calls for limitation of fluid administration and promotion of renal excretion in order to mitigate pulmonary edema. Conversely, an excessive decrease in intravascular volume can have negative effects on under-perfused non-pulmonary organs (for example rates of acute kidney injury).¹¹¹ The 2006 ARDS Network Fluids and Catheters Treatment Trial (FACTT) sought to identify an optimal fluid strategy by randomizing patients to liberal (central venous pressure [CVP] of 10-14) or conservative (CVP <4) fluid management strategies (Figure 2).⁶³ The investigators reported no survival benefit in either strategy, though the conservative group was associated with increased ventilator-free days and a reduction in ICU length of stay. Interestingly, post hoc analysis of the FACCT trial found that non-Hispanic black patients had a mortality benefit when treated with conservative versus liberal fluid therapy indicating that race may play an important role in determining the efficacy of conservative fluid management.¹¹² Nonetheless, conservative fluid management in ARDS patients is preferred given its reported improvement in ventilator free days and ICU lengths of stay. Additionally, a 2018 retrospective study analyzing day 3 fluid balance in critically ill patients found that a negative fluid balance was associated with decreased mortality, further supporting the use of conservative fluid protocols in ARDS patients.¹¹³ The use of restrictive fluid administration for the resuscitation of sepsis patients who are at high risk for ARDS development is currently under investigation in the PETAL Network Crystalloid Liberal or Vasopressors Early Resuscitation in Sepsis (CLOVERS) trial (NCT03434028). Outcome measures for the trial include whether a restrictive fluid strategy will

reduce overall 90 day mortality or the incidence of ARDS (primary and secondary outcomes, respectively).

Nutritional pharmacology and management

Several vitamins and nutritional supplements have experimentally been shown to have anti-inflammatory and injury-reducing properties, but attempts to determine if these effects translate into disease-modifying clinical benefits have largely been unsuccessful (Figure 2). Large randomized controlled trials investigating the use of Vitamins C and D both failed to demonstrate therapeutic benefits in ARDS patients.^{114, 115} Similarly, ω -3 fatty acids, γ -linolenic acid, and antioxidants were associated with decreased ventilator-free days, decreased ICU free days, and non-statistically significant ($p=0.054$) increase in 60-day mortality.⁸² Collectively, these results provide strong evidence that the use of vitamin or fatty acid supplements is not supported as interventions to improve mortality or morbidity in ARDS patients.

ARDS patients have high energetic demands and require nutritional support in order to offset catabolic losses. When possible, a strategy using enteral feeding is preferred over parenteral nutrition as it is associated with decreased infectious morbidity.¹¹⁶ Additionally, attention has been placed on the amount of nutrition ARDS patients receive. In a 2012 ARDS Network clinical trial, a strategy using initial trophic enteral feeding (10-20 kcal/h) versus full enteral feeding (25 to 30 kcal/kg per day of non-protein calories and 1.2 to 1.6 g/kg per day of protein) for up to 6 days did not improve clinical endpoints but was associated with improved gastrointestinal tolerance (Figure 2).⁷⁰ Currently, recommendations support the use of initial trophic feeding of the first week of mechanical ventilation in ARDS before switching to full nutritional targets¹¹⁶.

Conservative Oxygenation

Among the most common therapies implemented in critically ill patients and nearly all ARDS patients is the supplemental provision of oxygen. Oxygen is frequently delivered generously in

order to increase PaO₂ and oftentimes patients become hyperoxic while attempting to reverse tissue hypoxia. However, evidence indicates that liberal oxygen use is associated with vasoconstriction, decreased cardiac output, absorption atelectasis, increased pro-inflammatory responses, and increased mortality.^{117, 118} As such, establishing a protocol of oxygen treatment that balances essential delivery to organs while preventing excessive harmful effects of hyperoxia has been an important subject of recent investigations (Figure 2). In a single-center randomized trial published in 2016, critically ill ICU patients with a length of stay of 3 days or longer who were assigned to receive conservative oxygen therapy (PaO₂ between 70 and 100 mm Hg) had lower mortality than those who received more conventional care (PaO₂ up to 150 mm Hg).⁶⁴ Two recently published multicenter trials aimed to further investigate the effects of conservative oxygen delivery in mechanically ventilated patients. In the first study, the 2019 Intensive Care Unit Randomized Trial Comparing Two Approaches to Oxygen Therapy (ICU-ROX), Mackle and colleagues randomized intensive care unit patients to usual (no upper limit on SpO₂ targets) or conservative oxygen (target SpO₂ between 90 and 97%). Patients assigned to conservative oxygen treatment spent a significantly higher time on atmospheric oxygen concentration (FiO₂ = 0.21) than the usual care arm, however, there were no reported differences in ventilator free days or survival.⁶⁵ The failure to detect changes in clinical outcomes in the two treatment groups may have resulted from the small differences between the targeted SpO₂ intervals compared with previous studies that used more distanced intervals.⁶⁴

In the second recently published study, the 2020 Liberal Oxygenation versus Conservative Oxygenation in Acute Respiratory Distress Syndrome (LOCO₂) trial, Barrot et al. recruited ARDS patients to conservative (SpO₂ between 88 and 92%) or liberal (SpO₂ greater than 96%) oxygen treatment arms. The trial was terminated early due to an associated increase in mortality at 28 days and five episodes of mesenteric ischemia in the conservative oxygen treatment group.⁶⁶ Worse outcomes in the LOCO₂ may be attributed to the deteriorated gas exchange in ARDS patients, making them more prone to hypoxemia in the conservative

oxygen treatment arm. Furthermore, the target oxygen levels in the LOCO₂ conservative group were significantly lower than in the ICU-ROX trial, thereby increasing the risk for detrimental hypoxemia. Going forward, trials will need to carefully assess how to determine target oxygenation levels (e.g. SpO₂ and PaO₂ targets, measurements from mixed venous blood, different targets for different organ injuries) to better answer how oxygen concentrations are selected. In the meantime, clinical guidelines recommending avoidance of excessive oxygen, such as restraining the use of supplemental oxygen when SpO₂ is greater than 96% (or even greater than 92-93% in some guidelines), are practical for current ARDS management^{119, 120}.

ECMO and inhaled nitric oxide rescue therapies

Extracorporeal membrane oxygenation (ECMO) is a rescue therapy that has been employed in ARDS patients that fail to improve on mechanical ventilation management and as a means to avoid potential injurious aspects of ventilator associated lung injury (Figure 3).

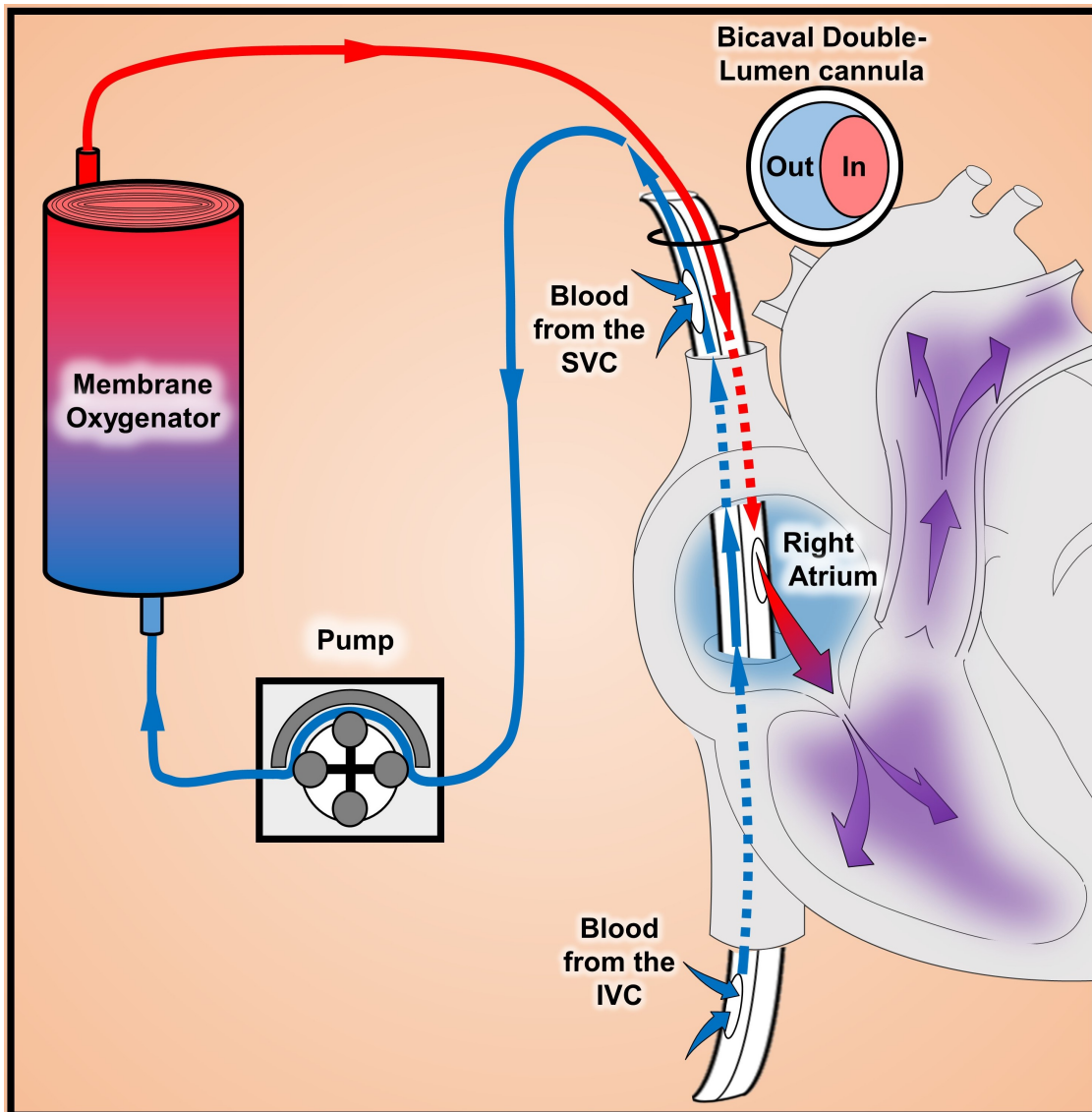


Figure 3: Venovenous (V-V) Extracorporeal Membrane Oxygenation (ECMO).

V-V ECMO is primarily employed to oxygenate blood and to remove carbon dioxide in the setting of compromised pulmonary gas exchange, as is the case in severe ARDS. Portrayed is a single cannula, double-lumen ECMO access whereby blood can be removed and returned to a large vein, typically the vena cava. Blood is pumped from the body through a membrane oxygenator that allows for gas exchange before being returned to the right atrium where it mixes with deoxygenated venous blood (depicted in purple). In V-V ECMO, blood is pumped by the heart into the systemic arterial vasculature.

Advances in ECMO delivery have been associated with an increase in the number of centers and cases using it, particularly since the 2009 H1N1 influenza pandemic.¹²¹ Investigators from the 2009 Conventional Ventilatory Support versus Extracorporeal Membrane Oxygenation for Severe Adult Respiratory Failure (CESAR) trial group sought to answer whether the use of ECMO during severe ARDS would provide a survival benefit when compared to conventional support by mechanical ventilation (Figure 2).⁷¹ The results of the trial indicated that there was a survival benefit in favor of patients being randomized to ECMO treatment, but this difference was not statistically significant. Furthermore, the study was impaired by the use of heterogeneous mechanical ventilation strategies in the control group (including the use of large tidal volumes). Additionally, a large percentage of patients in the ECMO group who were transferred to ECMO-capable hospitals never received ECMO, allowing for the potential confounding effects attributed to the fact that ECMO-capable hospitals may attain enhanced ARDS survival regardless of whether patients actually received ECMO.

A subsequent international multi-center study was conducted to specifically address weaknesses of previous trials implementing ECMO in early severe ARDS, the 2018 ECMO to Rescue Lung Injury in Severe ARDS (EOLIA) trial.⁷² Despite achieving a high quality of control for ventilation strategies in both groups and nearly universal implementation of ECMO in patients randomized to receive it, the results demonstrated that there was no significant difference in mortality between the ECMO group and the control group. Given the lack of strong evidence supporting the use of ECMO as a routine early treatment for ARDS, it is recommended that ECMO is reserved as rescue therapy in patients that remain hypoxemic despite conventional evidence-based approaches.

As a rescue therapy, inhaled nitric oxide (iNO) is used to target pulmonary vasodilation and improved oxygenation by reducing ventilation-perfusion mismatch.¹²² Although iNO improves short term oxygenation, randomized control trials were unsuccessful in demonstrating clinical benefits such as an increase in ventilator-free days or survival with iNO use in ARDS

patients.¹²³ Furthermore, in a 2016 systematic review, the use of iNO in ARDS was associated with a statistically increased risk of renal failure.¹²⁴

Other treatment concepts

A large number of pharmacologic approaches have been tested in large, randomized controlled trials in order to improve clinical outcomes in patients with ARDS. These trials have included approaches such as the use of β_2 -adrenergics, interferon β -1a, inhaled anticoagulants, selenium, ketoconazole, lisofylline, and statins (Figure 2).^{73-79, 125} However, clinical benefit for these interventions was not demonstrated in any of the trials.

1.5.1 Harnessing heterogeneity in ARDS to personalize therapy

Recent advancements in our understanding of ARDS pathophysiology demonstrate that there are likely important subtypes (or subendotypes) of ARDS that might be capable of better indicating prognosis, predicting response to particular interventions, and directing personalized therapies.¹²⁶ Subendotypes of ARDS can be partitioned using clinical data such as disease severity (i.e. degree of hypoxia),⁴ precipitating factors,¹²⁷ sepsis vs. non-sepsis causes of ARDS (the latter associated with better outcomes in mortality and ventilator free days),^{128, 129} and the presence of trauma-associated ARDS.¹³⁰ Genetic risk factors have also been discovered and partly explain underlying heterogeneity of ARDS, with over 30 identified genes shown to influence ARDS influence susceptibility.^{131, 132} Additionally, measured soluble biomarkers have been used to define subendotypes of ARDS that effectively predict severity and outcomes in patients.¹³³⁻¹³⁹ Though these clinical, genetic and soluble factors are capable of classifying ARDS patients' risk for outcome and severity of disease, an ideal utilization for subendotyping ARDS cases would be to direct treatment decisions. Indeed, such work has been performed by numerous investigators, mostly in a retrospective manner.

One method of subendotyping is by categorizing ARDS as being associated with direct lung injuries (e.g. pneumonia and caustic aspiration), versus indirect lung injuries (e.g. sepsis and non-pulmonary trauma). In particular, studies measuring systemic markers of injury have found that direct lung causes are associated with elevations in epithelial markers, such as surfactant proteins and soluble receptor for advanced glycation end products (sRAGE), while systemic injuries are associated with endothelial markers such as angiopoietin-2 and von Willebrand Factor.¹⁴⁰⁻¹⁴⁶ This distinction might suggest that the etiologic site of lung injury could influence targeted therapy towards epithelial and endothelial directed treatments.

Another method of anatomical subendotyping of ARDS injury is through radiographic approaches. In these classifications, ARDS was categorized as focal – defined as loss of airspace a particular region of the lung (e.g. a segment or lobe of lung) – and non-focal – defined as airspace attenuation evenly distributed amongst the entire lung fields.¹⁴⁷⁻¹⁵¹ In regards to treatment effects, it was found that lung recruitment maneuvers such as PEEP were more effective in non-focal ARDS and that such maneuvers resulted in significantly higher over-distention in the focal ARDS groups. Furthermore, systemic markers of sRAGE were elevated in patients with focal ARDS.¹⁵⁰ These findings are important in two regards: 1) the determination of focal versus non-focal ARDS is relatively easy and rapid as it can be achieved through computed tomography (CT) imaging and 2) the radiographic distinction could predict whether lung recruitment using PEEP is harmful or beneficial. Indeed, further prospective, large-cohort, randomized trials will be critical in demonstrating clinical efficacy in patient-centric outcomes such as mortality and ventilator free-days.

Among the most recent approaches to define subendotypes is by classifying ARDS cases as hyper- and hypo-inflammatory using specific inflammatory biomarkers.¹⁵² Using a statistical method called latent class analysis, which uses multivariate data to identify groups, investigators have been able to retrospectively detect hypo- and hyper-inflammatory subendotypes of ARDS.¹⁵³⁻¹⁵⁵ Inflammatory subendotypes have been classified with as few as three soluble markers (e.g. interleukin-8, bicarbonate, and tumor necrosis factor receptor-1)

and also by peripheral leukocyte transcriptional profiles.^{156, 157} Furthermore, when these subtypes were applied post-hoc to large scale clinical trials, it was found that there was a mortality benefit for simvastatin and a liberal-fluid strategy in hyper-inflammatory ARDS subendotypes.^{156, 158} The results of these analyses provide convincing inferences that there exist ARDS subtypes that are important for deciding personalized treatment approaches. As such, future clinical trials will likely need to implement subendotyping at the time of randomization to rigorously demonstrate efficacy of categorizing patients to choose the optimal treatment approaches. The undertaking of subendotyping ARDS patients will likely be met with many challenges: the acuity and haste of care needed in critical care patients might prevent the results of necessary studies prior to randomization and access to laboratories and technologies might not yet be universal for specific inflammatory biomarker measurements. Nonetheless, categorizing ARDS patients into groups that better allows for identification of disease severity, prognostication, and allocation to particular treatment regimens is an exciting and growing approach to ARDS research that will ideally lead to improved clinical outcomes.

1.6 Conclusion: The urgent need for novel ARDS treatment

The past 25 years of large, randomized clinical trial efforts have contributed a tremendous amount of insight that has advanced the clinical practice of lung-protective mechanical ventilation. Indeed, implementation of clinically proven management interventions, such as the use of low tidal volumes and prone positioning, have dramatically improved the outcomes for ARDS. However, mortality remains high and there is a lack of targeted treatment options. Nonetheless, emerging basic science research has resulted in novel therapeutic targets, such as hypoxia, adenosine, and microRNA signaling, that might pave the way for new pharmacologic ARDS treatments. Advancements in our appreciation for pathological and clinical subtypes of ARDS will likely also play a critical role in designing clinical trials to identify efficacy for treatments in specific cohorts of ARDS patients.¹²⁶ Furthermore, the recent COVID-

19 pandemic has stimulated the rapid initiation of clinical trials aimed at targeting ARDS. At the time of this writing, there are over 100 registered controlled trials for COVID-19 ARDS listed on ClinicalTrials.gov. Potential interventions that demonstrate clinical efficacy in COVID-19 ARDS could also provide usefulness in treating ARDS patients independent of SARS-CoV-2 infection. It is important to note, however, that insights gained from proven therapies for COVID-19 ARDS could translate to non-COVID-19 ARDS subtypes that share pathophysiological components with COVID-19 cases. For example, the efficacy reported with dexamethasone could indicate specific use for patients with viral-associated ARDS that are characterized by immune profiles similar to what is seen in COVID-19 and not for patients with other etiologic types of ARDS. Additional clinical studies will be required to carefully address such hypotheses. Lastly, to establish efficacy for novel ARDS interventions, collaborative efforts, such as the multicenter trials ongoing in the PETAL Network, will continue to be vital for the successful improvement of ARDS outcomes. In addition to these large scale studies, a network of smaller clinical trials investigating the efficacy of novel treatment concepts^{159, 160} may be required to identify new approaches for ARDS therapy. Channeling enthusiasm for new trials targeting COVID-19 ARDS may provide a catalyst and framework for these important collaborations going forward.

Chapter 2: Pre-clinical insights into ARDS

2.1 Modeling ARDS in the laboratory: acute lung injury

Key to understanding and developing targeted therapies for ARDS, as with any other organ injury, is the ability to model disease pathophysiology in a way that allows investigators to gain insight into disease progression, resolution and treatment responses. Lung biopsies from humans have been essential to the advancement of ARDS insights such as demonstrating the presence of inflammatory infiltration and diffuse alveolar damage, but these methods are both highly invasive or only account for patients that have died from their disease.¹⁶ Furthermore, human-derived tissue samples are typically limited to one or two time points of disease: after ARDS onset or post-mortem. Modeling ARDS in the laboratory setting allows for researchers to study disease pathophysiology serially among all time points. Additionally, a critical factor for ARDS research is the dissection of cellular and molecular contributions to pathophysiology, both of which are possible using modeling techniques. These techniques include cell culture, animal models, and protocols that utilize primary tissue isolated from both animal and human sources.

The following is a discussion of laboratory based techniques for modeling ARDS and previous work that has contributed the accumulated understanding of ARDS pathophysiology onset, progression, resolution, and potential novel treatment approaches. Lastly, an important distinction for the next discussion is that, in the pre-clinical research setting, ARDS research is referred to as acute lung injury (ALI). The reason for this is that 'ARDS' is typically reserved for the clinical definition for which it describes (i.e. it is dependent on a clinical set of criteria that are not relevant or readily measured in the pre-clinical setting).⁴ For this reason, ALI will be used henceforth to describe pre-clinical work in ARDS research, including the work presented in chapters 3 and 4.

2.1.1 Cell culture systems for studying ALI

Since the advent of obtaining single cell suspensions from tissues in early 20th century and the first established cell lines 1950s and 1960s, cell culture has been a vital tool for investigating biology and human diseases.^{161, 162} From understanding the mechanisms that drive cancerous transformation, to diagnosis of viral infection, to the generation of monoclonal antibodies, cell culture has been a critical player in the advancement of nearly all biomedical fields.¹⁶³⁻¹⁶⁶

Furthermore, comparative genetics have allowed for cells derived from distant species to reveal functional genes that are important for human physiology and disease, such as the discovery of toll-like receptors (TLRs) in *drosophila* that are found on mammalian cells which are responsible for recognizing foreign pathogens and initiating the innate immune response.^{167, 168}

In the context of ALI, cell culture can be used to investigate individual components of the microscopic lung environment (e.g. epithelial, endothelial, immune cells) or mediators of inflammation (e.g. cytokines, chemokines, and toxins). Alveolar epithelial cell (AECs) primary cells derived from mammals and immortalized cell lines (e.g. A549) have been used in cell-monolayer cultures to examine the role of lipopolysaccharide (LPS)-induced expression intercellular adhesion molecule-1 (ICAM-1), which promotes immune cell adherence to epithelial cells during lung inflammation.¹⁶⁹ Alveolar type II cells (ATII) isolated from human lungs have also been treated with LPS *in vitro* which demonstrated that alveolar epithelial cells also contribute to the expression of inflammatory cytokines.¹⁷⁰ Endothelial cell culture models have been used to demonstrate that endothelial cell apoptosis is a likely contributor to the onset of pulmonary microvascular leak during ALI during systemic inflammatory conditions such as sepsis.¹⁷¹⁻¹⁷³ Furthermore, cell culture systems that co-culture two or more cell types have been employed to study how cell-to-cell signaling plays a role in ALI. For example, co-culture of activated neutrophils and AECs was used to demonstrate that micro-particles containing miR-223 were transferred from neutrophils to AECs during ventilator induced lung injury, which played a protective role by dampening lung inflammation.¹⁷⁴

On the basis that inflammation plays a particularly important role in the pathogenesis of ALI, *in vitro* studies using immune cells are frequently performed to study their functions in orchestrating lung inflammation. Cells can be isolated from primary sources, usually from human peripheral blood, mouse blood, or mouse bone marrow. Using standardized centrifugation techniques, neutrophils, monocytes and T cells can be readily isolated from freshly isolated blood and then activated or differentiated into terminal cell types such as macrophages and subsets of T cells.¹⁷⁵⁻¹⁸⁰ Additionally, bone marrow can be isolated from mice and treated with granulocyte-macrophage colony-stimulating factor (GM-CSF) or macrophage colony-stimulating factor (M-CSF) to promote the differentiation of stem cells into dendritic and macrophage cells, respectively.^{181, 182} Isolation of immune cells from genetic knockout or transgenic mice also provides an advantage of genetic manipulation without the need for transfection or transduction methods that can potentially lead to unwanted activation or stimulation of cells.^{183, 184} Furthermore, immune cells can be isolated from the alveolar airspace using a bronchoalveolar lavage of either ARDS patients or healthy volunteers.¹⁸⁵⁻¹⁸⁷ In this way, the inflammatory signatures and functions of immune cells can be directly interrogated from the alveolar space during injury. A study by Morrell et al. demonstrated an important distinction between paired peripheral monocytes and alveolar macrophages transcriptional activation wherein they reported that enrichment in immune-inflammatory genes in alveolar macrophages or peripheral monocytes was associated with improved or worsened outcome, respectively.¹⁸⁸

Several more advanced *in vitro* systems also exist that closely model physiologic conditions of the lung. One such technique is the culturing of AECs on flexible membranes that can then be subjected to vacuum-mediated deformation to induce noxious strain in the cells.^{189, 190} Using a flexible membrane system to induce stretch-mediated injury in Calu-3 cells, Eckle et al. demonstrated that stretched cells become injured and upregulate inflammatory genes.¹⁸⁷ An even more complex *in vitro* system is the 'lung-on-a-chip' method.^{191, 192} The technology is a microphysiologic system allows for epithelial and endothelial cells to be plated on a flexible

membrane that also incorporates air and fluid flow approximated with the opposed cell layers. In this way organ-level pathophysiology can be modeled *in vitro*. For example, when human alveolar epithelial cells from asthma and chronic obstructive pulmonary disease patients were used in a lung-on-a-chip system, Benam et al. were able to closely model hyper-inflammatory responses that are dependent on the presence of endothelial cells as well as neutrophils.¹⁹³ Indeed, several components of ALI have been studied on microphysiologic systems that are able to demonstrate impaired gas exchange, edema, transmigration of neutrophils and fibrin deposition, exhibiting the utility of this *in vitro* system to model organ-level physiological processes.^{191, 192, 194}

2.1.2 Animal models of ALI

Though *in vitro* models have played, and continue to play, critical roles in the advancement of molecular and biochemical insights of ALI, they are limited by being pathophysiologically oversimplified. ALI is a complex syndrome that has multiple stages of disease that are defined by the participation of different cellular and molecular effectors.¹⁴ Furthermore, research focused on *in vitro* readouts such as inflammation and cell trafficking fall short in demonstrating meaningful organ- and organism-centered outcomes, including measures of respiration and mortality. As such, animal models of ALI are essential tools for realizing the implications for *in vitro* findings. Animal models can also serve as initial studies to begin understanding the mechanisms for lung injuries induced by a large number of etiologies and are used as platforms to test therapies for ALI.¹⁹⁵ Another useful characteristic of animal research is that human studies are rather slow and tissue is not typically readily available, both of which are not barriers in animal studies.

Among the most utilized animal models for studying ALI is rodents, particularly mice. There are numerous advantages to using mice to model ALI: they breed rapidly, have similar pulmonary anatomy to that of humans, and can develop a wide array of ALI types.¹⁹⁶ A unique

advantage to using mice to model ALI is the ability to readily develop genetically modified mice, which has become increasingly affordable and timely using modern technology based on clustered regularly interspaced short palindromic repeats (CRISPR).¹⁹⁷⁻²⁰⁰ Through deletion or insertion of genes of interest, genetically modified mice subjected to models of ALI can be utilized to precisely study the functions of proteins and non-coding RNAs.^{160, 190} Furthermore, genetic modifications in mice can be targeted to specific tissue compartments using Cre-Lox recombination whereby the deletion or alteration of a gene-of-interest is flanked by palindromic DNA sequences, called Loxp sites. DNA flanked by loxp sites is excised by the Cre-recombinase enzyme, which can be expressed in mice by introducing a second transgene that codes for Cre. If the transgene is placed under the upstream control of a promoter for a tissue specific gene (e.g. the albumin promoter is only active in hepatocytes), Cre is expressed in a targeted tissue compartment and subsequently deletes the loxp-flanked DNA sequence.^{200, 201} In this manner, not only can gene products be investigated genetically in mouse models of ALI, but they can also be interrogated specifically in tissues where they function. This consideration is of utmost importance when whole-body deletion of a targeted gene is embryonically lethal.

Mouse models of ALI can be performed using agents that typically correspond to ARDS risk factors in patients, such as sepsis, trauma, aspiration and ventilation induced lung injury (VILI).^{14, 127} Agents to induce lung injury can be injected systemically in the blood stream or intraperitoneal cavity, or directly into the alveolar airspace of mice through endotracheal catheterization.²⁰² Commonly administered agents used to induce acute lung injury in mice include, bacteria, viruses, lipopolysaccharide (LPS), hydrochloric acid (HCl), and high pressure ventilation.¹⁹⁵ The intratracheal injection of viruses or bacteria into mice causes pneumonia that can lead to acute lung injury and pathology in mice that is commonly seen in humans.²⁰³ For example, *Pseudomonas aeruginosa* instillation into the lungs of mice leads to acute pneumonia that is dependent on bacterial burden, with higher burdens resulting in worsened inflammation, respiratory failure, and increased mortality.²⁰⁴ Viruses are also commonly instilled into the lungs

of mice, though an important consideration is to establish the adaptability of viral strains that typically cause disease in humans to mice. A recent example of this is the inability for severe acute respiratory syndrome coronavirus coronavirus-2 (SARS-CoV-2) to infect mouse alveolar epithelial cells because the SARS-CoV-2 receptor, angiotensin-converting enzyme 2 (ACE2), does not efficiently bind to the virus.²⁰⁵ To circumvent this limitation, mice have to be genetically derived to express human-version of ACE2 or mouse-adapted strains for SARS-CoV-2 need to be generated, both of which have been utilized.²⁰⁶⁻²⁰⁸ Mouse adaptation of human viruses has been performed in several other viruses, including influenza.^{209, 210}

In addition to mice, many other animals are used to study ALI. Other species used to study ALI include hamsters, rats, rabbits, sheep, pigs, and non-human primates.²¹¹⁻²¹⁵ Using different species for ALI research requires several special considerations. Firstly, different animals developed evolutionary variations in their Toll-like receptor structures that recognize different structures on identical pathogen associated molecular patterns that result in different sensitivities and activities of receptors.^{216, 217} Secondly, species have differences in their mononuclear phagocyte systems. For example, species such as sheep, cattle, pigs, cats and goats have pulmonary intravascular macrophages (PIMs) that adhere to endothelial cells in lungs, while rats, mice, monkeys, and humans do not contain PIMs, which effects the development of ALI in experimental models.²¹⁸⁻²²⁰ Thirdly, animal size plays a large role in a number of ways: larger animals have easier vascular access allowing for monitoring of physiological parameters, but larger animals are also considerably more expensive.^{221, 222} Lastly, ALI studies can be limited in particular species due to a lack in species specific reagents, such as antibodies for Western blots and enzyme-linked immunosorbent assays (ELISA).^{223, 224}

As sepsis is among the leading causes of clinical ARDS, sepsis-related models of ALI are heavily utilized in animal models.^{6, 14, 45} Lipopolysaccharide (LPS) is commonly used to induce a form of ALI that models the systemic inflammation typically associated with bacterial

sepsis. LPS is an endotoxin present on the outer-membrane of gram-negative bacteria, which, when present in the blood stream, is recognized by Toll-like receptor-4 (TLR4) on the membrane of many cell types including macrophages, endothelial and epithelial cells, leading to the activation of inflammatory functions.²²⁵⁻²²⁸ When injected intravenously, the vascular endothelium is the first site of injury, resulting in decreased arterial tone and drop in blood pressure.²¹⁷ In the lungs, LPS-induced activation of capillary endothelial cells results in apoptosis, which precedes neutrophil entrapment.²²⁹⁻²³² Additionally, LPS stimulates resident alveolar macrophages in the lung to produce inflammatory mediators such as interleukin-1, tumor necrosis factor-alpha, and prostaglandin E₂ that all act to promote local inflammation leading to enhanced recruitment of neutrophils.^{233, 234} Excessive accumulation and activation of neutrophils in the lung is a key step to the onset of epithelial barrier damage resulting to pulmonary edema and hypoxemia associated with ALI.²³⁵⁻²³⁸ When LPS is administered intratracheally, as opposed to intravenously, recruitment of neutrophils is up to 10-fold higher.²³⁹ Indeed, LPS-induced ALI in mice is advantageous for its simplicity, its ability to model the pathophysiology resulting from bystander lung injury from the host's own inflammatory response (i.e. the scenario of ARDS in the setting of sepsis), and its reproducibility, however, it is limited for several reasons. Firstly, species' responses to LPS vary significantly. For example, mice require much higher doses of LPS to initiate pulmonary inflammation when compared with humans.²⁴⁰ Secondly, purified LPS does not cause severe epithelial and endothelial damage that is consistent with human ARDS, which is likely due to the fact that addition bacterial exotoxins and secreted proteins also contribute to the diffuse alveolar damage.^{239, 241, 242}

In order to more closely model microbial sepsis-induced ALI, animal models of peritonitis are used. The most common peritonitis model is the cecal ligation and puncture (CLP) model, which consists of ligating the cecum subsequently puncturing it three to five times to permit leakage of the colonic contents into the peritoneum.²⁴³ CLP results in sepsis, with

features of leukopenia, pulmonary hypertension, and lung injury within 18-72 hours²⁴⁴ CLP-associated ALI presents with features including hypoxemia, neutrophilic alveolitis, and edema²⁴⁵⁻²⁴⁷ Major limitations to the CLP model are that it requires a surgical procedure and has a mortality rate of 70-90% 30 hours after the procedure, which makes it difficult model to study recovery and treatment responses for ALI.^{244, 245}

Several models have also been utilized to directly injure the alveolar epithelium, which occurs in clinical scenarios of ARDS such as gastric contents aspiration and VILI.^{248, 249} As a method to mimic gastric content aspiration, hydrochloric acid (HCl) is instilled into the lungs of animals to reduce the alveolar pH to about 1.5. Instillation of HCl is followed by injury to the alveolar epithelium with loss of epithelial fluid transport function, which then undergoes a repair process including the renewal of epithelium by alveolar type II cells.²⁵⁰⁻²⁵³ The capillary endothelium is also injured during acid aspiration in a neutrophil-dependent manner.^{250, 251} Several considerations that limit the HCl aspiration model are that it requires pH levels that are much lower than typical human gastric contents to achieve alveolar injury (i.e. it requires a pH of about 1.5, whereas gastric contents are usually between pH 3.0 - 4.0) and that it does not account for the additional gastric contents aside from the acidity (e.g. food particles, bacterial products, and cytokines).²⁵⁴⁻²⁵⁶

Modeling ALI by primarily targeting the alveolar epithelium is also achieved by injurious mechanical ventilation.²⁵⁷⁻²⁵⁹ VILI studies in animals were the premise for the landmark ARDS Network trial that established lower tidal volumes were effective at reducing mortality in mechanically ventilated ARDS patients.⁶¹ Ventilation of animals with pressures resulting in injurious strain (i.e. over-distension) results in endothelial and epithelial disruptions and pulmonary edema.²⁶⁰ The presence of hyaline membrane formation and increased permeability of the alveolar blood-air barrier is dependent on the presence of neutrophils, indicating that inflammatory-mediated damage is required in addition to the injurious strain of mechanical ventilation.²⁶¹ One important consideration for the VILI model is that it involves the ventilation of

healthy lungs, as opposed to lungs that are already injured or at high risk for injury, such as in patients with pneumonia or sepsis.^{262, 263} Additionally, the VILI model is complex, requires practiced technical skills for accurate reproducibility, and varies significantly based on the ventilation modes used (e.g. pressure vs. volume modes, tidal volume and pressure levels, and whether the use of PEEP is incorporated).^{258, 259, 263}

2.2 The underlying role of dysregulated inflammation in ALI

Given that the large majority of risk factors for the development of ALI are conditions that cause systemic inflammation, such as sepsis and trauma, it is natural to consider that maladaptive inflammation is a likely culprit for the lung pathology of ALI.^{6, 14, 264} Indeed clinical and basic research have provided a breadth of insight demonstrating that triggering of the inflammatory response is critical to ALI pathogenesis.²⁶⁴ The initial event leading to the onset of ALI is the activation of the innate immune system. The resident cells in the lung that sense invasion of microbes or respond to systemic inflammatory signals are the alveolar macrophages.²⁶⁵ These cells work to sense pathogen associated molecular patterns (PAMPs) and damage associated molecular patterns (DAMPs) that may be present in the lung or in the blood from distant sites of infection or injury, leading to the secretion of cytokines and chemokines that recruit inflammatory monocytes and neutrophils to the lung. Together, these recruited inflammatory cells secrete proteases, reactive oxygen species (ROS), eicosanoids, phospholipids, and cytokines that further amplify inflammation and also have direct, tissue-damaging effects.²⁶⁵ In particular, injury to alveolar type II epithelial (ATII) cells leads to loss of surfactant production, alveolar cell thickening and leakage of protein rich fluid into the airspace (hyaline membranes), resulting in the pathological hallmark of ARDS, diffuse alveolar damage (DAD).^{266, 267} Furthermore, dysregulated inflammation in ALI is exemplified through clinical studies demonstrating that a prolonged inflammatory phenotype of invading monocytes, when

compared with resolution-type phenotypes, is associated with protracted cases of ARDS.²⁶⁸ Additional evidence for the critical role of inflammation in ALI pathogenesis is demonstrated by elevated levels of inflammatory cytokines interleukin-1-beta (IL1 β), tumor necrosis factor-alpha (TNF α), interleukin-6 (IL6), and interleukin-8 (IL-8) measured in the BAL and plasma of ARDS patients.²⁶⁹ Interestingly, there have also been measured humoral responses in ARDS patients: it was found that 57% of ARDS patients have at least one significantly elevated autoantibody either during or after the development of lung injury, though the implications of these findings are not yet understood.²⁷⁰

Among the several recruited cell types found in the lungs of ARDS patients, neutrophils are perhaps the most notorious cell for their role as effectors of inflammation and for causing destructive tissue injury in a large number of organ pathologies.²⁷¹⁻²⁷³ Indeed, neutrophilic inflammation is hallmark characteristic of DAD in ALI.²⁷⁴ Histologically, neutrophils accumulate early in the pulmonary microvasculature during ARDS.²⁷⁵ Furthermore, BAL samples also support the high concentration of neutrophils in the alveolar airspace.²³⁶ In addition to the presence of neutrophils in the BAL of ARDS patients, it was found that the BAL also has a profound chemoattractant activity to recruit neutrophils *ex vivo*, and that the extent of neutrophils in BAL is correlative with worse clinical outcomes, supporting the idea that neutrophil recruitment is a key event in disease pathophysiology.^{187, 276} Neutrophils collected from ARDS patients are also phenotypically more inflammatory when compared to healthy control patients. ARDS-associated neutrophils have increased expression of the inflammatory marker CD11b, increased oxidative burst capacity, and delayed constitutive apoptosis (i.e. they remain alive and performing tissue destructive activities for longer periods of time).^{277, 278} Indeed, targeted approaches aimed at inducing selective apoptosis of neutrophils using exogenous administration of interleukin-4 (IL4) have been demonstrated to be protective in a pre-clinical model of ALI.^{237, 279} Altogether, excessive neutrophil effector functions are strongly

associated with ALI severity and outcomes and their role in disease pathology builds upon the picture that dysregulated inflammation is the key process leading to ALI.

In addition to neutrophils, monocytes and macrophages have also been found to be key cell types that contribute to the inflammatory immunopathology of ALI. Peripheral monocytes develop in the bone marrow, where they are released into the circulating blood and recruited to sites of infection or tissue injury in response to cytokine and chemokine gradients.²⁸⁰ Once recruited into tissues, monocytes can differentiate into macrophages, amplify the immune response by secreting inflammatory cytokines and chemokines, partake in phagocytosis of pathogens and damaged tissues, and also play a role in tissue repair.²⁸⁰ Experimental models of ALI have revealed the importance of monocytes and macrophages for the initiation and maintenance of inflammatory responses and that their activities, when excessive, contribute to the lung pathology of ALI.²⁸¹ Though macrophages and monocytes are critical for controlling and neutralizing infectious pathogens that invade the lung and alveolar airspace, infectious models of viral- and fungal-related ALI have demonstrated that inflammatory monocytes and macrophages were also responsible for detrimental bystander injury to the lung.²⁸²⁻²⁸⁴ Similarly, in non-infectious (sterile) models of ALI, including allergic rhinitis, asthma, mechanical ventilation, intra-tracheal LPS, and intra-tracheal bleomycin models, recruited monocytes were found to promote injurious inflammation of the lung.²⁸⁵⁻²⁸⁸ The role of inflammatory monocytes in the initiation and progression of ALI is further demonstrated by evidence signifying that recruited monocyte apoptosis is a necessary step for the termination and resolution of inflammation and for the recovery of ALI.^{289, 290} Janssen et al. showed that in mice with monocytes that did not contain the cell death receptor, Fas, there was delayed resolution of ALI in both viral pneumonia models and intra-tracheal LPS-induced ALI.²⁹⁰ Furthermore, when Dhaliwal et al. performed monocyte depletion using clodronate nanoparticles, genetic inducible deletion, or antibody-mediated clearance in the intra-tracheal LPS-induced ALI mouse model, they reported significant decreases in emigration of neutrophils and measures of ALI.²⁸⁸ Taken

together, pre-clinical evidence strongly support the notion that both neutrophils and monocytes play an essential role in triggering immunopathology of the lungs that results in ALI.

Further convincing evidence for inflammation's role in the pathogenesis of ALI is the dependence on classical inflammatory cell-signaling pathways that are required for the development of ALI in systemic inflammatory models. Several pre-clinical investigations have revealed that Toll-like receptors (TLRs) are critical in the development of ALI. TLRs are an evolutionary conserved part of the innate immune system that act as receptors to recognize PAMPs (e.g. LPS, flagellin, and intracellular RNA/DNA) and DAMPs (e.g. hyaluronan, mitochondrial DNA, and histones) to initiate intracellular inflammatory signaling events such as the activation of mitogen-activated protein kinase pathways and activation of transcription factors, namely interferon regulatory factors (IRFs) and nuclear factor kappa-light-chain-enhancer of activated B cells (NF- κ B).^{291, 292} In a preclinical mouse-model of VILI, increased levels of degraded hyaluronan, an extracellular matrix glycosaminoglycan, were found in the lungs and plasma of mice and were responsible for the initiation of ALI through the recognition by TLR2 and TLR4.²⁹³ Furthermore, elevated levels of hyaluronan degradation products were also found in the plasma of ARDS patients.²⁹³ Similarly, mice with genetic deletion of TLR4 were protected from sepsis-induced models of ALI, which was demonstrated by reduced pulmonary microvascular leakage, neutrophil recruitment, and cytokine and chemokine production.²⁹⁴

Another critical mediator of inflammatory signaling in ALI is inflammasome signaling, especially the NOD-, LRR- and pyrin domain-containing protein 3 (NLRP3) inflammasome.²⁹⁵ The NLRP3 inflammasome is an intracellular sensor of both endogenous danger signals and pathogen associated molecules that when assembled, leads to the activation of caspase-1. Caspase-1 activity is necessary for the proteolytic cleavage and release of pro-IL-1 β and pro-IL-18, which are both pro-inflammatory cytokines that contribute to inflammatory pathologies, including ALI.²⁹⁶ In studies of models combining LPS- and mechanical ventilation- induced ALI,

it was shown that the NLRP3 inflammasome was required for the development of acute lung injury and hypoxemia.²⁹⁷ Lastly, in ARDS patients, NLRP3-regulated cytokines IL-1 β and IL-18 were found to be associated with severity of ARDS.²⁹⁸

2.2.1 Endogenous mechanisms for the regulation of inflammation and their potential as treatments for ALI

Given that inflammation is a critical driver for the pathogenesis of ARDS and ALI, there has been an enthusiastic effort to investigate the mechanisms that are involved. Many molecular pathways are currently under investigation that have the potential to modulate or limit the inflammatory processes in pulmonary inflammation, and several have shown the potential to be translated into clinical trials. In the next sections, some of these areas of active research are highlighted with a few examples for potential treatments that target excessive lung inflammation, which are unique in that current ARDS approaches are focused on ideal clinical management and the prevention of iatrogenic injury, such as with protective ventilation. The highlighted mechanisms include: hypoxia signaling, adenosine signaling, and the role of microRNAs with examples of recent discoveries that contribute to the current wealth of evidence for their protective effects. Studies have demonstrated that these mechanisms play several important functions in controlling of alveolar inflammation through a number of mechanisms such as the repression of pro-inflammatory pathways, the promotion of ALI resolution, and the optimization of carbohydrate metabolism.

2.2.1.1 The role of Hypoxia Inducible Factors

“The power to destroy a thing is the absolute control over it.”

— *Frank Herbert, Dune*

Hypoxia (defined as oxygen tensions below the necessary level to sustain cellular functions in organs or tissues) and inflammation are intimately linked conditions that are frequently encountered simultaneously in ARDS.²⁹⁹ Tissue hypoxia can occur during inflammation due to

increased consumption of oxygen by activated immune cells and invading pathogens, while hypoxia itself can induce inflammation, such as in hypoxic adipose tissue and in tumors.²⁹⁹ Cells are able to sense and respond to hypoxia through the activation of Hypoxia-inducible factors (HIFs), which are transcription factors that are stabilized and activated under hypoxic conditions (Figure 4). HIFs were first identified in 1991 as important transcription factors leading to the production of hypoxia-induced erythropoietin.³⁰⁰ Structurally, HIF works as a heterodimer with two distinct subunits (HIF- α and HIF- β), which dimerize during conditions such as hypoxia and inflammation.^{301, 302} HIF is regulated at the protein level, meaning that the α subunit of HIF is constitutively transcribed and translated into protein, but is constantly subjected to proteasome-dependent degradation under normoxic conditions. Oxygen sensing is not directly performed by HIFs themselves, instead enzymes called prolyl hydroxylase domain proteins (PHDs) act as oxygen sensors due to their requirement for molecular oxygen needed to hydroxylate HIF- α subunits. Hydroxylated HIF- α subunits are recognized by Von-Hippel Lindau (VHL) protein tumor suppressors, which then conjugate ubiquitin proteins to HIF- α , labeling it for targeted proteasomal degradation.^{303, 304} When cells become hypoxic, the lack of molecular oxygen renders PHDs inactive, preventing the hydroxylation and ultimate degradation of HIF- α (stabilization of HIF- α). Before translocating to the nucleus and initiating gene transcription, stabilized HIF- α dimerizes with a HIF- β subunit (Figure 4).³⁰⁵ HIF- α/β complexes activate hundreds of genes in the nucleus by recognition of the hypoxia response element (5'-RTGCG-3') in gene promoters.^{306, 307} Target genes of HIF are those that promote adaptations to the hypoxic environment, such as anaerobic ATP production, increased vasculogenesis, red blood cell production.^{302, 308, 309}

Although the lung is a highly oxygenated organ, it has been shown that HIFs are stabilized during ALI.¹⁹⁰ Stabilization of HIFs during ALI is likely due to several mechanisms, including local hypoxia resulting from pulmonary edema, the infiltration of immune cells with high levels of oxygen consumption, and through the accumulation of intermediate molecules

that act to inhibit PHDs, such as increased levels succinate.^{190, 299, 310} Additionally, HIF can be stabilized under normoxic conditions during acute lung injury.³¹¹ For example, mechanical stretch of alveolar epithelial cells results in the inhibition of succinate dehydrogenase (SDH) activity, leading to the accumulation of intracellular succinate. Accumulated succinate acts to directly inhibit PHD activity, leading to the stabilization of HIFs, even in the presence of molecular oxygen.^{311, 312}

Previous studies have shown that HIF is capable of regulating endogenous anti-inflammation pathways in multiple inflammatory organ injuries, including ARDS.^{311, 313, 314} For example, HIF-1 α stabilization in alveolar epithelial cells during models of VILI *in vitro* and *in vivo*, has been shown to be protective for cellular and organism survival.^{190, 315-318} These findings were confirmed when HIF-1 α deletion in alveolar-epithelial cells lead to increased mortality in murine models of VILI.¹⁹⁰ Mechanistically, HIF-1 α -mediated lung protection in VILI models was shown to be dependent on optimizing the glycolytic capacity and the reduction of oxygen consumption in alveolar epithelial cells, mediated through the induction of HIF target genes such as pyruvate dehydrogenase kinase 1 (PDK1) and glucose transporters GLUT1.^{308,}

319-321

As a result of the large amount of pre-clinical evidence demonstrating the protective role of HIFs in acute organ injuries, therapeutic targeting of HIFs has gathered much attention. Pharmacologic modulation of HIFs is achievable through both physiological and pharmacological interventions. Physiological interventions include permissive hypoxia, conservative oxygen administration for ventilated patients, and through the use of remote limb ischemia to precondition surgical patients.^{65, 66, 120, 322-324} Pharmacological approaches to stabilizing HIFs has been achieved with novel inhibitors of PHDs that enhance HIF signaling without modulation of oxygen therapy.^{325, 326} In mice, pharmacologic stabilization of HIF by PHD inhibition was found to be protective by reducing mortality and decreasing inflammation.¹⁹⁰ Several oral, small molecule PHD inhibitors have been developed: Roxadustat (FG-4592) by

FibroGen, Astellas, & AstraZeneca, Vadadustat (AKB-6548) by Akebia, and Daprodustat (GSK-1278863) by GlaxoSmithKline). Roxadustat has demonstrated significant efficacy in clinical trials for anemia associated with chronic kidney disease. Oral administration was shown to be safe and successfully enhanced HIF signaling, which was indicated by increased hemoglobin levels.^{327, 328} Furthermore, the oral HIF activator, Vadadustat, is currently under investigation as a therapy for the prevention and treatment of ARDS in hospitalized patients with COVID-19 (NCT04478071).

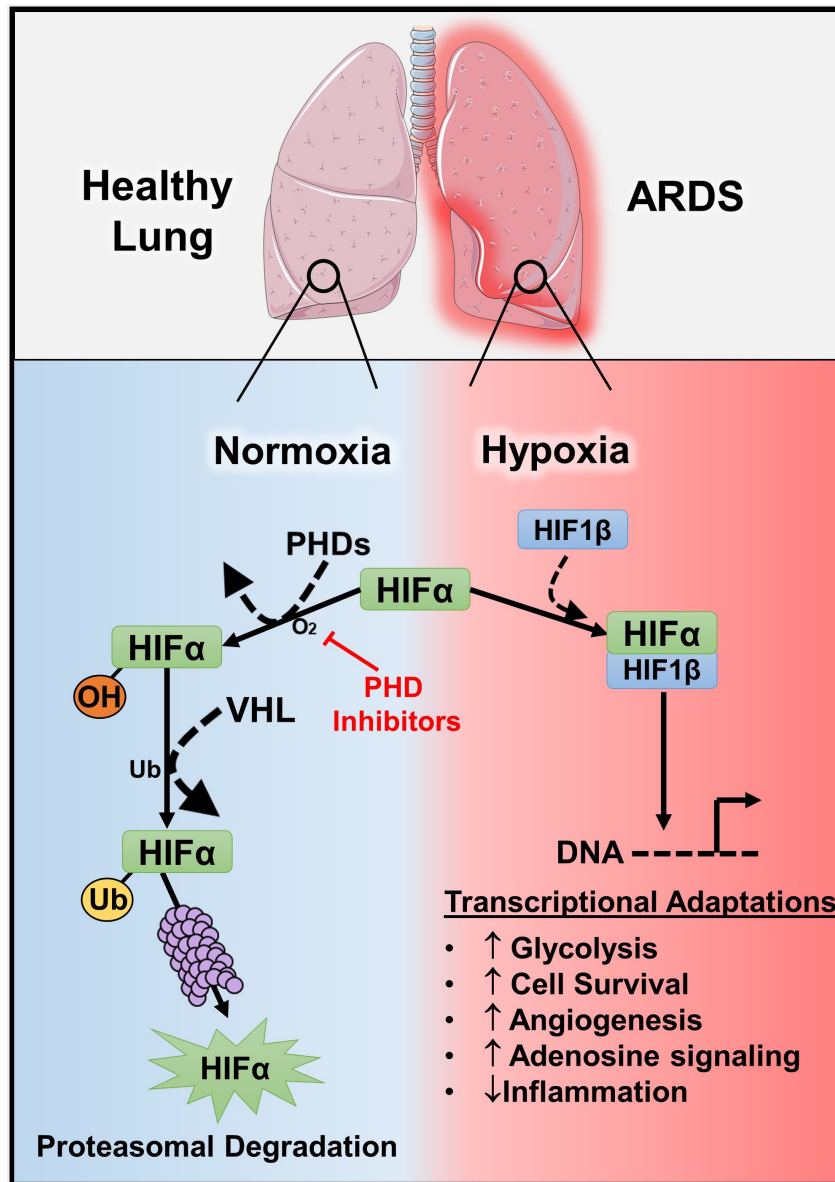


Figure 4: Hypoxia Inducible Factor (HIF)- α stabilization in the Acute Respiratory Distress Syndrome (ARDS) lung.

HIF α is a transcription factor that has two major isoforms (HIF1 α and HIF2 α) and that is constitutively transcribed and translated.³⁰⁰ Under normoxic conditions, proline hydroxylases (PHDs) use oxygen as a substrate to hydroxylate HIF α subunits, which targets them for ubiquitination by Von Hippel Lindau (VHL) for downstream proteolysis.^{303, 304} In conditions of cellular hypoxia, such as in the inflamed ARDS lung,^{190, 299} PHDs are inactive due to lack of oxygen substrate. HIF α isoforms dimerize with HIF1 β (a constitutively expressed binding

Figure 4 (Continued):

partner), which stabilizes them for translocation into the nucleus to induce gene transcription. Target genes of HIF include those that provide adaptation to hypoxic conditions, such as increasing glycolytic capacity and angiogenesis, and genes that contribute to the anti-inflammatory and tissue-protective functions.^{311, 313, 314} Indeed, pharmacologic HIF stabilization is targeted by an emerging class of PHD inhibiting drugs that provide exciting potential for the treatment of tissue inflammation during ARDS.^{325, 326}

2.2.1.2 The role of adenosine signaling

Adenosine is a purine nucleoside that is perhaps best known for its role as a building block for DNA nucleotides and as an energy carrier in the form of adenosine tri- and d-phosphate (ATP and ADP). In addition to these well-known roles, adenosine also acts as a signaling molecule in a wide array of biological processes.^{329, 330} Adenosine generation is first initiated by the enzymatic conversion of ATP and ADP to adenosine monophosphate (AMP) via the extracellular membrane bound protein, CD39, and then further processed into adenosine by another membrane bound enzyme, CD73 (Figure 5).³³¹ Adenosine initiates lung-protective signaling by interacting with one of its receptors that have been identified in multiple cell types such as immune cells, endothelial cells and alveolar epithelial cells.³³¹⁻³³⁹ For example, deletion of the A2B adenosine receptor (A2BAR) in alveolar epithelial cells results in worsened lung inflammation and pulmonary edema in a mouse model of ALI that combines intratracheal instillation of LPS and injurious mechanical ventilation.³¹⁶ A2BAR has also shown a protective role in models of hemorrhagic shock-induced lung injury.³⁴⁰ Exogenous administration of adenosine and a non-selective agonist of adenosine receptors, 5'-(N-Ethylcarboxamido) adenosine have been shown to promote endothelial barrier function *in vitro*, while pharmacologic antagonism or genetic deletion of A2AAR/A2BAR diminished this effect.³⁴¹ In contrast to the largely beneficial roles of adenosine during acute injury states, chronic and sustained elevation of adenosine can lead to tissue injury, fibrosis, and chronic pain via mechanisms that include IL-6 and soluble IL-6 receptors.³⁴²⁻³⁴⁴

Adenosine can be targeted therapeutically via multiple strategies. Several preclinical studies have indicated that direct administration of adenosine attenuates lung injury.^{345, 346} Furthermore, adenosine administration has been safely demonstrated in previous clinical studies.^{347, 348} For instance, a phase 3 trial published by Garcia-Dorado et al. recruited patients to investigate the impact of intracoronary adenosine treatment immediately before re-

vascularization and within six hours of ST-elevation myocardial infarction (STEMI).³⁴⁷ Although the study did not show a clinical benefit for adenosine treatment in terms of reducing infarct sizes, patients receiving adenosine showed a modest improvement in myocardial salvage and left ventricular failure evolution. A challenge to utilizing adenosine is that it has a relatively short half-life *in vivo*. Alternative methods to targeting adenosine is through the use of adenosine analogs or inhibitors of adenosine deaminase, which are responsible for the metabolism of adenosine. Furthermore, using selective adenosine receptor agonists could also serve as a feasible approach to harnessing adenosine signaling as a therapy. Previous studies in animal models demonstrated the protective role of BAY 60-6583, an A2BAR agonist, in ALI models.^{340,}³⁴⁹ Unfortunately, the efficacy and safety of these types of agonists have not yet been recorded in clinical studies. Finally, a third modality to target adenosine signaling is to use HIF activators, which are discussed in the previous section. As a direct transcriptional target of HIF-1 α , A2BAR levels can be enhanced through the stabilization and activation of HIF-1 α .³¹⁵ Additionally, extended use of therapeutic adenosine could potentially increase the risk for development of chronic lung disease such as fibrosis, given the fact that sustained adenosine has been shown to lead to have detrimental effects.³⁴²⁻³⁴⁴

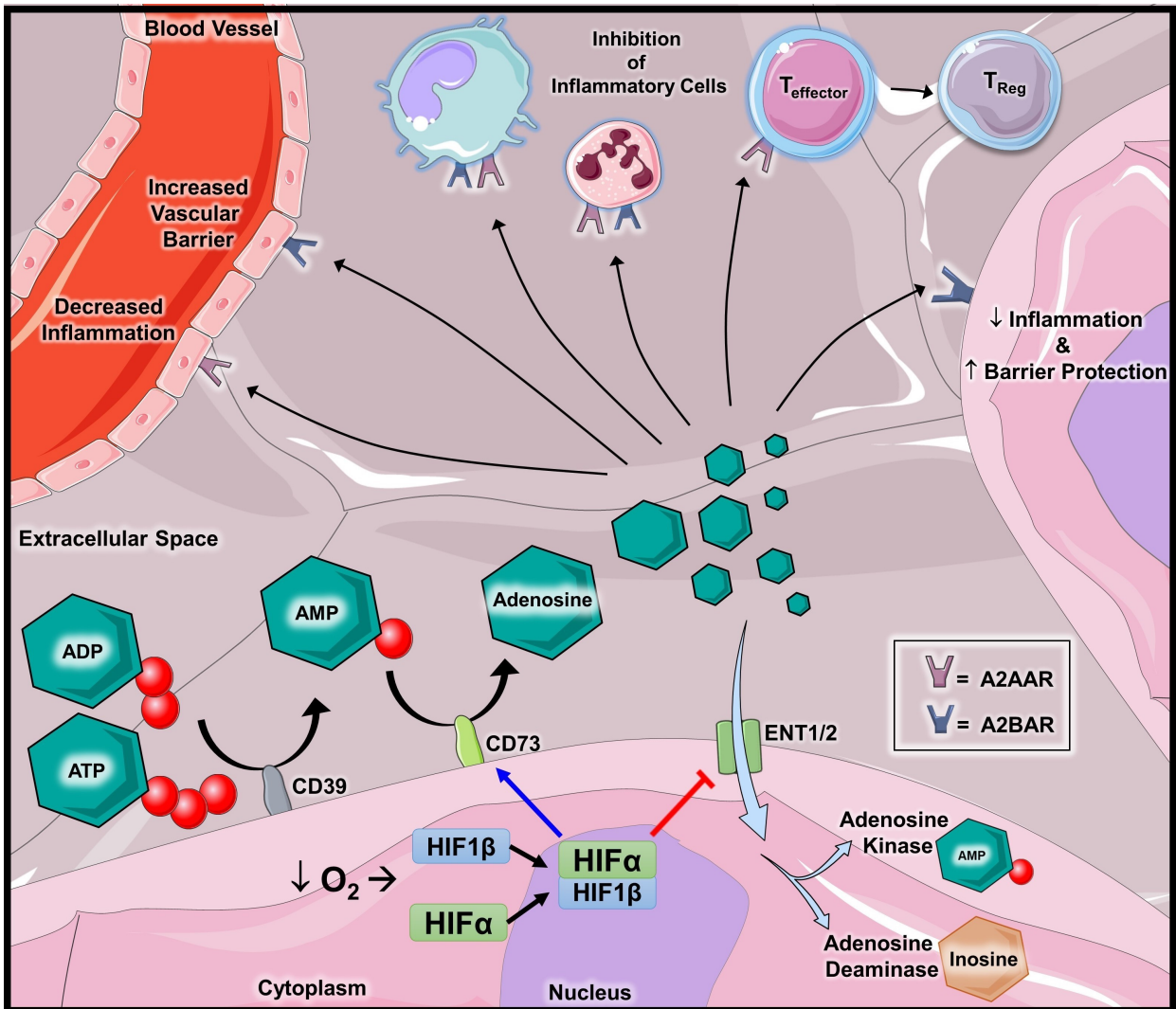


Figure 5: Adenosine signaling during inflammation.

The precursor to adenosine, Adenosine tri- and di-phosphate (ATP/ADP), is released into the extracellular space by activated or dying cells.³³¹ ATP is then converted to adenosine monophosphate (AMP) by membrane-bound ecto-nucleoside, CD39, and then subsequently into adenosine by the membrane-bound nucleotidase, CD73.³³¹ Once formed, extracellular adenosine plays several anti-inflammatory roles on numerous tissue compartments by interacting with surface A2A and A2B adenosine receptors (A2AAR/A2BAR).³³¹⁻³³⁹

Adenosine acts on epithelial and endothelial cells to promote barrier integrity and decrease inflammation.³⁴¹ Adenosine also acts on immune cells to dampen inflammatory activity.

Negative regulation of adenosine signaling occurs through re-uptake by equilibrative

Figure 5 (Continued):

nucleoside transporters 1 and 2 (ENT1/2), which results in the intracellular metabolism of adenosine by adenosine kinase or deaminase.³⁴¹ During hypoxic conditions, HIF-stabilization further promotes adenosine signaling by inducing expression of CD73 and repressing the expression of ENT1/2.^{317, 318}

2.2.1.3 The role of microRNAs

MicroRNAs (miRNAs) are members of the non-coding RNA family (i.e. they are nuclear coded genes whose transcripts aren't translated into proteins). miRNAs are initially transcribed as primary transcripts that can be several kilobases long (sometimes they are located inside of gene introns or exons) and are then enzymatically cleaved in a two-step process into approximately 22-25 nucleotides in length.³⁵⁰ miRNAs were initially discovered in the worm, *Caenorhabditis elegans*, but have since been found in the genomes of essentially all animal species, including mammals.³⁵¹⁻³⁵³ In the most recent miRBase database (an online library of known miRNAs, <http://www.mirbase.org/>), there were more than 2,500 miRNAs recorded in humans. miRNAs work to regulate gene expression by inhibiting the translation of mRNA targets via binding to specific sites in the 3'-untranslated region (UTR).³⁵⁰ Furthermore, miRNAs are capable of targeting multiple mRNAs at once and mRNAs can contain multiple sites in their 3'UTRs allowing them to be targeted by multiple miRNAs. In this way, individual miRNAs can regulate several biological pathways at multiple levels. It is hypothesized that more than half of the human genome is regulated by miRNAs.³⁵⁴ Indeed, leveraging miRNAs as a therapeutic approach for a number of diseases is under intense investigation.³⁵⁵ miRNAs have also been described to have important roles in regulating inflammation during ALI.³⁵⁶ One such miRNA is miR-155. Upon pulmonary infection or intratracheal instillation of LPS in mice, miR-155 is highly upregulated in the lungs.³⁵⁷⁻³⁵⁹ Mechanistically, miR-155 plays an important role in promoting inflammation by targeting suppressor of cytokine signaling-1 (SOCS-1), an important negative regulator in inflammatory signaling. Genetic deletion of *miR-155* in mice results in attenuated lung inflammation and injury during *Staphylococcal* enterotoxin B-induced and LPS-induced ALI models, suggesting that blocking miR-155 could be a potential therapeutic for ALI.^{358, 359} Another well-studied miRNA in the context of inflammation is miR-223.³⁶⁰ In a study by Neudecker et al. it was demonstrated that miR-223 is shuttled in microparticles that

originate from neutrophils into alveolar epithelial cells that served to attenuate lung inflammation in mouse models of VILI.¹⁷⁴ When miR-223 was deleted in mice, they experienced increased lung inflammation and edema when compared to wildtype mice after exposure to VILI. In addition to being more susceptible to VILI, *miR-223* knock-out mice also showed increased inflammation and mortality during *Staphylococcus aureus* pneumonia models.¹⁷⁴ Taken together, these studies are examples for how miRNAs can potentially be therapeutic targets for ALI.

Logistically, pharmacologic modulation of miRNA activity can be achieved through several strategies. These methods include administering synthetically created miRNA mimics to enhance function, anti-sense miRNA inhibitors to block miRNAs and small molecule drugs to up- or down-regulate specific miRNA expression. For example, in murine models of ALI, nanoparticle-packaged miR-223 mimics were effective at attenuating lung inflammation and injury when injected intravenously during murine VILI vili.¹⁷⁴ Furthermore, clinical trials have demonstrated that miRNA mimics can be safely and effectively utilized in human disease. The intradermal injection of Remlarsen (MRG-201), a miR-29 mimic, is being evaluated by two clinical trials in patients with keloid lesions (NCT02603224 and NCT03601052). Cobomarsen (MRG-106), a miR-155 inhibitor, is being evaluated by phase 2 clinical trials for patients with cutaneous T-cell lymphoma (NCT03713320 and NCT03837457). Small molecule drugs are another promising therapeutic strategy to modify miRNA functions in patients. ABX464, from Abivax S.A., works by promoting the splicing of non-coding RNAs to promote the expression of miR-124, which is an anti-inflammatory miRNA and is being investigated as a treatment for inflammatory conditions such as inflammatory bowel diseases and rheumatoid arthritis (NCT02735863, NCT03760003, and NCT03813199).³⁶¹ In an exciting next step, ABX464 is now being investigated as a therapeutic for COVID-19 in hopes of dampening lung inflammation and preventing the development of acute respiratory distress syndrome in hospitalized patients (NCT04393038).

2.3 Conclusion: The therapeutic potential for regulating inflammation of ARDS

Inflammation in the lung triggered by local (i.e. bacteria, aspirated contents, etc.) or systemic (i.e. sepsis, trauma, multiple transfusion, etc.) cues is well accepted as the key driver for both the initiation and progression of ALI. The immune-inflammatory pathology of ALI is multifaceted and involves many immune-cell types, a myriad of cytokines and chemokines, effector enzymes and molecules that directly induce tissue injury, and a complex web of cellular signaling pathways. As such, there is a great deal of knowledge still to be attained in understanding how exactly all these mediators function and contribute to lung pathology. Advancing our comprehension for the mechanisms that govern the pathophysiology of ALI is a critical step in identifying novel treatment approaches and for the improvement of prognostication and personalization of management approaches for ARDS patients.

Though there are many molecular and cellular components involved in ALI pathogenesis, the complex nature of the disease also implies that there is potentially a large number of novel treatment approaches to be discovered. As stated in the previous sections, there is already an expanding breadth of insights into how different cell types and molecular pathways contribute to ALI with several demonstrations of how they might be harnessed to promote the resolution of ALI. In this dissertation, I present work that resulted from our efforts to identify novel endogenous mechanisms that lead to the regulation of inflammation or the promotion of resolution during experimental models of ALI. While detailing new pathways that regulate inflammatory functions during ALI, I also present work that suggests these findings are targetable as treatment approaches and may lay the foundation for future translational research in clinical ARDS.

General methods and materials

The purpose of this section is to list the methods and materials that are common to both Chapter 3 and Chapter 4, in an effort to minimize the length of the dissertation and the need to duplicate the content in both chapters.

Isolation of human monocyte-derived macrophages (hMDMs). A protocol for the collection of blood from healthy donors was approved by the UTHealth Institutional Review Board and participants provided consent prior to collection. A 60 mL was pre-loaded with 10mL of citrate-dextrose buffer (Sigma-Aldrich), and then used to obtain 50 mL of blood by venipuncture. Next, the blood was centrifuged for 10 minutes at 400g. Centrifuge steps were all performed at 4 °C. The plasma supernatant was separated into two clean tubes and then centrifuged for 10 minutes at 400g. The cell pellets were then added back into previously centrifuged blood along with 20 ml of 3% dextran in normal saline and then allowed to incubate at room temperature for 40 minutes to promote sedimentation. After sedimentation, the upper layer was then moved into new conical tubes and filled to the top with HBSS (ThermoFisher, Waltham, MA) and subsequently centrifuged at for 10 minutes at 400g. Red-blood cell lysis was then performed using a Lysis Solution (Miltenyi Biotec, US) and then centrifuged at for 10 minutes at 400g. The cell pellet was then re-suspended in 2.5 mL of HBSS(-) +25mM HEPES + 1mM EDTA and delicately added on top of 10 mL of Ficoll-Paque PLUS (GE Healthcare, Sweden) and then centrifuged for 30 minutes at 700g with no brake. The interphase peripheral blood mononuclear cells (PBMCs) were pipetted into two tubes and washed twice with cold HBSS(-)+25mM HEPES+10% FCS. To differentiate PBMCs into hMDMs, we cultured PBMCs for 7 days in macrophage differentiation media (RPMI 1640 supplemented with 10% heat inactivated fetal bovine serum and 10 ng/mL recombinant human M-CSF (R&D, Minneapolis, MN)). Lipopolysaccharide (LPS, Sigma-Aldrich) stimulation was done using a concentration of 1 µg/mL in macrophage differentiation media.

RNA isolation, reverse transcription, and quantitative PCR. Isolation of RNA was achieved using a Trizol Reagent extraction method according to the protocol provided by the manufacturer (QIAzol Lysis Reagent, Qiagen). RNA concentrations were assessed with a BioTek Cytation 5 Take3 plate (Winooski, VT, USA). Reverse transcription was done using the Thermo Fisher Applied Biosystems High Capacity Reverse Transcription Kit on a Bio-Rad T100 thermal cycler (Hercules, CA, USA). Quantitative PCR was performed using TaqMan probes with the TaqMan Universal PCR Master Mix (ThermoFisher) on a Bio-Rad real-time PCR system

LPS-induced acute lung injury in mice. Acute lung injury (ALI) was modeled in mice aged 8-10 weeks old. Mice were anesthetized using an intraperitoneal injection of 70 mg/kg of pentobarbital. Intra-tracheal access was acquired utilizing the BioLite Intubation System (Braintree Scientific, Inc., Braintree, MA). Lipopolysaccharide (LPS, Sigma Aldrich, Escherichia coli O111:B4, Cat# L4391) was injected into lungs at a dose of 3.75ug/g. PBS was used for vehicle controls. Daily recording of mouse weights was performed. Humane euthanasia was performed when mice had two consecutive days of 25% or more weight loss, were unable to consume food or water, or had gross moribund appearance. Euthanasia was performed using pentobarbital overdose (250 mg/kg) (Socumb, animal NDC Code: 11695-4836-5, Henry Schein Animal Health, Melville, NY) and subsequent exsanguination. Bronchoalveolar lavage (BAL) was obtained with three 500 uL washes using ice-cold PBS. BAL cell densities were counted on a hemocytometer. 50 uL of BAL cells were spun onto glass slides with a Rotofix 32A centrifuge (Hettich, Tuttlingen, Germany). Slides were then stained using the Hema3 Stat Pack (Fisher Scientific, Waltham MA) and relative amounts of neutrophils were manually counted using light microscopy. The remaining BAL cells were centrifuged for 5 minutes at 300g. The resulting supernatant fluid (BAL Fluid) and cell pellets were separated into different tubes and flash frozen. 10 mL of pre-chilled PBS was injected into the right ventricle to perfuse the mouse

lungs and then the right lobes were excised and snap-frozen and the left upper lobe was inflated using 20 cmH₂O hydrostatic pressure of 10% formalin, then placed into 10% formalin.

Western blot. Specific information for the antibodies used in this work is listed in table 2.

Protein extraction was performed using RIPA Buffer (ThermoFisher, cat.# 89900) with freshly added phosphatase and protease inhibitors (New England Biolabs). For Hif-1 α and Hif-2 α Western blots, the NE-PER Nuclear and Cytoplasmic Extraction kit (ThermoScientific, Cat# 78835) was used with 60 mg of lung tissue to extract nuclear protein. Protein quantification was performed using a BCA method. Gel electrophoresis was followed by blocking of membranes for 1 hour at room temperature with 5% skim milk in PBS containing 0.1% tween. Primary antibodies were incubated with membranes overnight at 4°C. After subsequent incubation with HRP-conjugated secondary antibodies, chemiluminescence was captured on a Bio-Rad ChemiDoc Touch Imaging System. ImageJ software (National Institutes of Health) was used for protein quantification.

Hematoxylin and eosin staining of lung tissue and ALI scoring. Lungs were fixed in 10% formalin for 24-48 hours and then processed with a Leica TP1020 Semi-enclosed Benchtop Tissue Processor (Leica Camera, Wetzlar, Germany). Five-micrometer thick lung sections were stained with hematoxylin & eosin and then analyzed in a blinded fashion by a pathologist to assess for acute lung injury magnitude using a scoring system. Acute lung injury scoring was based on a previously described protocol with minor modification (0 = no injury; 1 = injury to 25% =; 2 = injury to 50%; 3 = injury to 75%; and 4 = diffuse injury).³⁶² Four categories of injury were assessed for separately on each lung section: (1) atelectasis; (2) cellularity; (3) alveolar wall thickening; (4) and alveolar over-distention. The total score was calculated as the sum of all the individual injury categories.

Measurements of BAL fluid cytokines, chemokines, and albumin. BAL fluid levels of Il-1 β (R&D Systems, Cat# DY401), Tnf- α (R&D Systems, Cat# DY410), Il-6 (BD Biosciences, Cat#

550950), and albumin (Bethyl Laboratories, Cat# E99-134) were measured using enzyme-linked immunosorbent assays (ELISA) according to the manufacturer's protocols.

days after the onset of LPS-induced ALI using 5 ug doses.

Transcriptomic profiling of BAL cells. BAL cells were collected from mice three days after the onset of ALI. After red blood cell lysis, neutrophil depletion was performed using a magnetic antibody-mediated positive selection method utilizing the MojoSort Mouse Ly-6g Selection Kit (BioLegend) and subsequent RNA was isolated (RNeasy Mini Kit, Qiagen, Cat#: 74104). RNA-sequencing was done at the UTHealth CPRIT Cancer Genomics Core. Libraries were generated with the KAPA mRNA Hyper Prep Kit (KK8581, Roche Holding AG, Switzerland). Pooled libraries underwent 75-cycle paired-end sequencing on the Illumina NextSeq 550 System (Illumina, Inc., USA) using the High Output Kit v2.5 (#20024907, Illumina, Inc., USA). Bases with quality scores less than 20 and adapter sequences were removed from raw data using Cutadapt (v1.15),³⁶³ followed by alignment to GRCm38 with STAR (v2.5.3a)³⁶⁴. Transcript abundance was quantified with HTseq-count uniquely-mapped reads number using default settings on GencodeM15. Transcripts with more than 5 reads in at least one sample were included in subsequent differential expression analysis using DESeq2.³⁶⁵ The *P*-values were adjusted using Benjamini and Hochberg's methods³⁶⁶ to account for false discovery rates (FDR). Transcripts with fold change > 2 and FDR < 0.05 were considered differentially expressed genes.

Chromatin immunoprecipitation-quantitative PCR. Human monocyte-derived macrophages (hMDMs) were treated with LPS for eight hours prior to cross-linking with a 1% methanol-free formaldehyde solution (ThermoFisher Scientific) for 8 minutes at room temperature. The formaldehyde was quenched with 140 mM glycine. Nuclei isolation was performed using lysis buffer I (50 mM HEPES-KOH pH 7.5, 10% glycerol, 1 mM EDTA, 140 mM NaCl, 0.5% NP-40, 1 mM PMSF, 0.25% Triton X-100, 1 µg/ml leupeptin, and 1X PIC) for 10 minutes with rotation at 4°C. Washing of nuclei was performed with lysis buffer II (10 mM

Tris-HCl pH 8.0, 200 mM NaCl, 1 mM EDTA, 0.5 mM EGTA, 1 mM PMSF, and 1X PIC for 10 minutes with rotation at 4°C. Shearing of nuclei was performed in lysis buffer III (10mM Tris-HCl pH 8.0, 100 mM NaCl, 1 mM EDTA, 0.5 mM EGTA, 0.5% sarkosyl, 1 mM PMSF, and 1X PIC) using 30 second cycles for eight minutes on a S220 focused-ultrasonicator (Covaris, Woburn, MA). Next, protein A/G UltraLink Resin (ThermoScientific) was to pre-clear samples at 4°C with rotation for one hour. 10% of the lysate was set aside to be used as the input sample, while primary antibodies, isotype control IgG (Cat#: ab171870, Abcam) and HIF-1 α (clone: D2U3T, Cell Signaling Technology), were added to separate 45% aliquots of the remaining lysate and allowed to incubate overnight with rotation at 4°C. The next day, antibody containing lysates were mixed with A/G UltraLink resin and then allowed to incubate while rotating at 4°C for 4 hours. The bead-conjugated antibody mixes were washed twice with high salt buffer (20 mM Tris-HCl pH7.5, 1% Triton X-100, 2 mM EDTA, 500 mM NaCl, 1 mM PMSF, and 1X PIC), then twice with a LiCl buffer (20 mM Tris-HCl pH 7.5, 250 mM LiCl, 2 mM EDTA, 0.5% NP-40, 1 mM PMSF, and 1X PIC), and then lastly washed once more with TE buffer (10 mM Tris-HCl pH7.5, 1 mM EDTA, and 1X PIC). Conjugates were then re-suspended in 100 ul of elution buffer (10 mM Tris-HCl pH 7.5, 5 mM EDTA, and 0.5% sodium dodecyl sulfate), and incubated for 15 hours at 65°C in order to reverse cross-link transcription factors from DNA. The transcription factor-enriched chromatin and 10% input samples were purified using the Qiagen PCR purification kit (Qiagen). The enrichment of ChIP was measured using qPCR. Primers flanking the promoter regions were designed (primers described in chapters 3 and 4). SYBR green supermix (Qiagen) was used to perform ChIP-qPCR. The following PCR cycling conditions were used: 1) 95°C for 15 minutes, 2) 35 cycles of 94°C for 15 seconds, 3) 60°C for 30 seconds, 4) and then 72°C for 30 seconds. Fold-enrichment was determined by calculating the ratio of HIF-1 α -enriched signals compared to input and then normalize them to isotype control IgG-enriched signals.

Statistical analysis. Data was analyzed using GraphPad Prism (version 7, San Diego, CA). Data are presented as mean and standard deviation (SD). We tested the normality of data using Shapiro-Wilk tests. F tests and Brown-Forsythe tests were used to assess for equal variances. We used unpaired t tests to compare means when the equal-variance assumption held and the data were found to be normal. Welch's t tests were used in normal data when variances were found to be significantly different. Mann-Whitney tests were used to compare medians when the data from two groups contained significantly different dispersions and locations. One-way ANOVA tests were performed for K-sample settings and the two-way ANOVA tests were used for experimental data containing two factors. P values were corrected by using the Dunnett method when comparisons were to a control group, the Bonferroni method in all other data sets, and the false discovery rate (FDR) method for genomic screens. For survival curve data, the Kaplan-Meier method was utilized to determine survival probabilities and a log-rank test was performed to assess survival outcomes. We considered P-values less than 0.05 to be statistically significant.

Chapter 3: The role of miR-147 in the regulation of inflammation during ALI

3.1 Introduction

Acute lung injuries (ALI), including the acute respiratory distress syndrome (ARDS), are devastating conditions defined by the rapid onset of pulmonary edema and hypoxemia and are a leading cause of death in critically-ill patients.³⁻⁶ Etiologies for ALI include pneumonia, sepsis and trauma, which are related in that they trigger potent systemic inflammatory responses.¹² Indeed, ALI is initiated by the activation of resident macrophages in the lung that amplify pulmonary inflammation via the recruitment of peripheral immune cells, such as pro-inflammatory neutrophils and monocytes.^{13, 14} In an appropriate response to infection or tissue injury, pulmonary inflammation achieves a necessary intensity and duration so that an infection is cleared or an injury is resolved, without causing harm to the lung parenchyma itself. However, during ALI, inflammation becomes dysregulated and results in injury to the alveoli, leading to a breakdown in the alveolar-capillary barrier with subsequent accumulation of pulmonary edema and hypoxemia.¹⁴ Targeting inflammation during ALI is a critical area for ongoing research for novel treatment approaches.

MicroRNAs (miRNAs) are a class of non-coding RNAs that are ~22 nucleotides in length and function as negative regulators of gene expression by blocking the translation of mRNA transcripts into protein.³⁵⁰⁻³⁵³ A growing body of evidence suggests that miRNAs partake in critical roles in controlling inflammatory processes in a large number of different organ injuries, including ALI.³⁵⁶ For instance, in a murine model of ventilation induced lung injury, miR-223 is transferred from infiltrating neutrophils into alveolar epithelial cells where it dampens inflammation by repressing poly(adenosine diphosphate-ribose) polymerase-1 (PARP-1).¹⁷⁴ Furthermore, miR-223 could be exogenously over-expressed in mice in order to therapeutically dampen pulmonary inflammation. However, most studies have focused on miRNAs during the onset of ALI, which does not address the challenge that ALI and ARDS are

not recognized until after a lung injury is established.³⁶⁷⁻³⁷⁴ To better our efforts in identifying novel miRNA-based treatment approaches that reverse inflammation and resolve lung function after ALI has already occurred, it is important to study the role of miRNAs during the period of time when lung injury is fully established.

In this work, we screened for miRNAs that were expressed after the onset of ALI in order to interrogate their ability their abilities to reverse lung injury. Our studies identified that miR-147 is significantly expressed in recruited pulmonary macrophages during the recovery-phase of ALI. Furthermore, we demonstrate that miR-147 functioned by modulating the accumulation of succinate within cells that, in turn, down-regulated inflammation by promoting the epigenetic silencing of pro-inflammatory genes.

3.2 Materials and Methods

Mouse Strains. Wild type (C57BL/6J), *Hif1 α* ^{loxp/loxp},³⁷⁵ *Hif2 α* ^{loxp/loxp},³⁷⁶ FVB.129S6-*Gt(ROSA)26Sor*^{tm2(HIF1A/luc)Kael/J} (ODD-Luc),³⁷⁷ and LysM Cre³⁷⁸ mice were purchased from Jackson Laboratory. *miR147*^{-/-} and *miR147*^{loxp/loxp} mice were generated as previously described.³⁷⁹ Mice were kept in a pathogen-free breeding facility at the Center for Laboratory Animal Medicine and Care at the University of Texas Health Science Center at Houston (UTHealth). Approved was granted by the UTHealth Institutional Animal Care and Use Committee for all mouse protocols utilized in this work. To account for sex as a biological variable, we performed experiments with equal numbers of male and female, age and weight-matched mice throughout all groups.

Generation of *miR147*^{loxp/loxp} LysM Cre, *Hif1 α* ^{loxp/loxp} LysM Cre, *Hif2 α* ^{loxp/loxp} LysM Cre, and B6-*Gt(ROSA)26Sor*^{tm2(HIF1A/luc)Kael/J} (B6.ODD-Luc) mice. Myeloid-cell specific genetic knockout mice were generated by crossing LysM Cre mice with *miR147*^{loxp/lox}, *Hif1 α* ^{loxp/loxp} and *Hif2 α* ^{loxp/loxp} mice. Efficiency of knockout in *miR147*^{loxp/loxp} LysM Cre mice was measured by performing RT-qPCR *miR-147* transcript expression in bronchoalveolar lavage (BAL) cells of intra-tracheal LPS-treated mice. *Hif1 α* ^{loxp/loxp} LysM Cre and *Hif2 α* ^{loxp/loxp} LysM Cre mice have been previously genotyped and characterized.^{380, 381} B6-*Gt(ROSA)26Sor*^{tm2(HIF1A/luc)Kael/J} (B6.ODD-Luc) mice were generated by crossing FVB.129S6-*Gt(ROSA)26Sor*^{tm2(HIF1A/luc)Kael/J} (ODD-Luc) with C57BL/6 mice for at least six generations.

Cells. All cells were kept at 37 °C and 5 % CO₂ in humidified incubators. Bone marrow-derived macrophages (BMDMs) from mice were harvested according to previously described protocols.³⁸² In short, bone marrow cells were incubated in RPMI containing 10 % heat inactivated fetal calf serum (FCS) and 1% antibiotic/antimycotic mix with 10 ng/mL of M-CSF (R&D Systems, cat# 416-ML) for 6 days, with fresh media added on day 3. HEK-293 cells were purchased from ATCC (CRL-1573) and cultured in DMEM containing 10 % heat inactivated

fetal calf serum (FCS) and 1% antibiotic/antimycotic mix. HEK-293 cells were sub-cultured 1:6 when they reached 90 % confluency.

CRISPR-mediated deletion of *NDUFA4* in THP-1 cells, as well as control THP-1 cells generated with non-gene-targeting guide RNA, was performed by Synthego (Redwood, CA). CRISPR editing efficiency was determined by the Inference of CRISPR Edits (ICE) tool, which demonstrated 95 % CRISPR editing efficiency.³⁸³ Knockout efficiency was verified with Western blot analysis for *NDUFA4* expression. THP-1 cells were cultured in RPMI containing 10 % heat inactivated fetal calf serum (FCS) and 1% antibiotic/antimycotic mix. To differentiate THP-1 cells into macrophage-like cells, cells were incubated in media containing phorbol 12-myristate 13-acetate (PMA) at a concentration of 100 nM for 24 hours. The next day, the media was replaced and cells were incubated for another 24 hours. Experiments were carried out the next day (48 total hours after starting differentiation).

Quantitative PCR. Specific probe information is listed in table 1.

Table 1: PCR probes used for Chapter 3.

Target Gene	Vendor / Source	Catalog Number
hsa-miR-16 (TaqMan Probe)	ThermoFisher	4427975-000391
hsa-miR-147b (TaqMan Probe)	ThermoFisher	4427975-002262
hsa-miR-155 (TaqMan Probe)	ThermoFisher	4427975-002623
hsa-miR-195 (TaqMan Probe)	ThermoFisher	4427975-000494
hsa-miR-27b (TaqMan Probe)	ThermoFisher	4427975-000409
hsa-miR-223* (TaqMan Probe)	ThermoFisher	4427975-002098
AA467197 (Mouse Nmes1) (Taqman Probe)	ThermoFisher	4351372-Mm01268692_m1
pre-miR-147 (Mouse) (Taqman Probe)	ThermoFisher	4427012-Mm03308429_pri
IL6 (Human)	ThermoFisher	4331182-Hs00174131_m1
Il6 (Mouse)	ThermoFisher	4331182-Mm00446190_m1
TNFA (Human)	ThermoFisher	4331182-Hs00174128_m1
Tnfa (Mouse)	ThermoFisher	4331182-Mm00443258_m1
IL1B (Human)	ThermoFisher	4331182-Hs01555410_m1
Il1b (Mouse)	ThermoFisher	4331182-Mm00434228_m1

MicroRNA microarray. Screening for up-regulated was performed using RNA isolated from mouse lungs three days after the onset of ALI. To analyze all current mature miRNA sequences provided in miRBase Release 20, we used the Affymetrix GeneChip miRNA 4.0. Data analysis was carried out using Transcriptome analysis Console (TAC) Software (Applied Biosystems). MicroRNAs with differential expression associated with an false discovery rate of less than 0.05 were considered to be significant.

***In vivo* locked nucleic acid miRNA antagomir (LNA) treatments.** LNAs targeting miR-147 and scrambled controls were purchased from Qiagen using the miRCURY LNA miRNA Inhibitor platform. Stock solutions of LNAs were re-suspended at a concentration of 50 mg/mL in sterile normal saline. One day prior to intra-tracheal LPS instillation, mice were given a 50 μ l of LNA solutions intra-tracheally. On the day of delivering intra-tracheal LPS, LNAs were added the LPS solutions at a concentration of 50 mg/mL. For each day after intra-tracheal LPS instillation, mice were given a 50 μ L intraperitoneal injection of stock LNA solutions.

Western blot. Specific information for the antibodies used in this work is listed in table 2.

Table 2: Antibodies used in Chapter 3.

Target antigen / Protein	Vendor / Source	Catalog Number	Working Concentration
Anti-mouse CD16/CD32	BioLegend	101301	Flow Cytometry 1:100
Anti-mouse AF488-B220	BioLegend	103228	Flow Cytometry 1:100
Anti-mouse FITC-CD3	BioLegend	100203	Flow Cytometry 1:100
Anti-mouse APC/Cyanine7-Ly6G	BioLegend	127623	Flow Cytometry 1:100
Anti-mouse PB-CD11b	BioLegend	101223	Flow Cytometry 1:100
Anti-mouse PE-CD11c	BioLegend	117307	Flow Cytometry 1:100
HIF-1 α (D2U3T)	Cell Signaling	14179	Western Blot 1:1000
HIF-2 α Polyclonal	Novus Biologicals	NB100-122	Western Blot 1:1000
TATA-binding protein (TBP)(D5G7Y)	Cell Signaling	12578	Western Blot 1:2000
NDUFA4 polyclonal	Invitrogen	PA5-50068	Western Blot 1:1000
β -Actin (C4)	Santa Cruz	sc-47778	Western Blot 1:2000
Phospho-NF- κ B p65 (Ser536) (93H1)	Cell Signaling	3033	Western Blot 1:1000
NF- κ B p65 (D14E12)	Cell Signaling	8242	Western Blot 1:1000
I κ B α (L35A5)	Cell Signaling	4814	Western Blot 1:1000
Phospho-I κ B α (Ser32) (14D4)	Cell Signaling	2859	Western Blot 1:1000
IRF-3 (D83B9)	Cell Signaling	4302	Western Blot 1:1000
Phospho-IRF-3 (Ser396) (4D4G)	Cell Signaling	4947	Western Blot 1:1000
Tri-Methyl-Histone H3 (Lys4) (C42D8)	Cell Signaling	9751	Western Blot 1:1000
Tri-Methyl-Histone H3 (Lys9) (D4W1U)	Cell Signaling	13969	Western Blot 1:1000
Tri-Methyl-Histone H3 (Lys27) (C36B11)	Cell Signaling	9733	Western Blot 1:1000
Histone H3 (D1H2)	Cell Signaling	4499	Western Blot 1:1000
Anti-rabbit IgG, HRP-linked	Cell Signaling	7074	Western Blot 1:2000
Anti-mouse IgG, HRP-linked	Cell Signaling	7076	Western Blot 1:2000

Lung imaging for luciferase bioluminescence. B6-*Gt(ROSA)26Sor^{tm2(HIF1A/luc)Kael/J}* (B6.ODD-Luc) mice were instilled with intra-tracheal LPS. On days 1, 3, 5, and 7 after the onset of ALI, B6.ODD-Luc mice were anesthetized with isoflurane (Henry Schein) and then administered 25 mg/kg D-luciferin diluted in sterile normal saline (Sigma, cat# L9504). Five minutes later, mice were euthanized with pentobarbital overdoses, lungs were excised and then imaged with an IVIS Lumina III Series (PerkinElmer). PBS treated mice were collected in parallel each day in order to have equal exposure-time controls. Fold change in luciferase activity was normalized to PBS control signals.

Lung digestion and CD45 enrichment. Three days after the onset of LPS-induced ALI, mice were euthanized and excised lungs were cut into small (0.2 to 0.4 cm) pieces and allowed to incubate with 2 mL of pre-warmed Dispase (Stemcell Technologies, cat# 07923) at 37 °C for one hour. Next lungs were ground through a 40 µM cell strainer into a 50 mL conical tube. Cells were then centrifuged at 300g for 5 minutes and treated with red blood cell lysis buffer (Miltenyi Biotec, US). After red blood cell lysis, CD45⁺ cell enrichment was performed using MojoSort magnetic beads (BioLegend, Cat# 480027). RNA was isolated from both CD45⁺ and CD45⁻ fractions for downstream qPCR.

Fluorescence activated cell sorting (FACS). BAL from three mice was pooled into a single sample. After collection red blood cell lysis was performed using Lysis Buffer (Miltenyi Biotec, US) and cells were pelleted and then re-suspended in FACS buffer (PBS + 1 % heat inactivated FCS). Blocking with anti-mouse CD16/32 Antibody (Clone 93, BioLegend, San Diego) was performed on ice for 10 minutes. Next, incubation with fluorophore conjugated antibodies (BioLegend) targeting B220-AF488 (Cat# 103228), CD3-FITC (Cat# 100203), Ly6G-APC/Cyanine7 (Cat# 127623), CD11b-Pacific Blue (Cat# 101223), and CD11c-PE (Cat# 117307) was carried out on ice for 30 minutes. After two washes with FACS buffer, cells were sorted using a BD FACS Aria II (BD BioSciences) directly into tubes containing Trizol LS

Reagent (ThermoFisher, Cat# 10296028). RNA isolation from sorted cells was performed using the RNeasy Mini Kit (Qiagen, Cat#: 74104).

***In vivo* microRNA mimic treatments.** miR-147 or scrambled mimic miRNAs (miRIDIAN microRNA mimics, Horizon Discovery Biosciences, Cambridge, UK) were incorporated into dioleoyl-phosphatidylcholine (DOPC) liposomes according to a previously described method.³⁸⁴ ³⁸⁵ DOPC and miRNA were combined in tertiary butanol in excess at a ratio of 1:10 (w/w) miRNA:DOPC. Then, Tween 20 was added at a ratio of 19:1 miRNA/DOPC mixture : Tween 20. After vortexing, the mixture was frozen in acetone chilled with dry ice and then lyophilized. Prior to intravenous injections, lyophilized preparations were hydrated in sterile normal saline at a concentration of 100 ug/mL. Intravenous injections of miRNA were performed two and four

Clodronate-mediated depletion of peripheral monocytes. Clodronate liposomes (5 mg/mL) and PBS control liposomes were purchased from Liposoma BV (Amsterdam, The Netherlands). 24 hours prior and 24 hours after intra-tracheal instillation of LPS, mice were given a 100 uL intravenous injection of clodronate or PBS liposomes.

Antibody-mediated depletion of PMNs. For PMN depletion, mice were treated with intraperitoneal injections of 1 mg anti-mouse Ly6G (clone 1A8, cat# BE0075-1) or IgG control (clone 2A3, Cat# BE0089) one day before and one day after intra-tracheal LPS instillation. Both antibodies were purchased from BioXCell (Lebanon, NH).

Chromatin immunoprecipitation-quantitative PCR. Primers flanking the promoter region of the *NMES1* gene were used for qPCR (Forward: ACAGAGGGGTGCAGACAGAA, Reverse: ACTCAGAGAGGCTCTGGTCA).

3' UTR luciferase reporter assays. miTarget™ 3' UTR miRNA Target Clones were purchased from GeneCopoeia (Rockville, MD). Two plasmid clones were generated: one containing the human NDUFA4 3' UTR inserted downstream of a secreted Gaussia luciferase (GeneCopoeia, product# HmiT102777) and another clone with the miR-147 binding-site in the NDUFA4 3' UTR

mutated from 5'-CCGCACA-3' to 5'-CCTACAA-3'. To account for transfection efficiency, both plasmids also encode for secreted alkaline phosphatase (SEAP) under the transcriptional control of the constitutively active CMV promoter. HEK-293 cells were transfected with 5 ug of reporter plasmids using Lipofectamine 2000 (ThermoFisher, cat# 11668019). The next day, the media was replaced and then subsequent transfection with 25 pmol of either miR-147 or scrambled mimic miRNAs (miRIDIAN microRNA mimics, Horizon Discovery Biosciences, Cambridge, UK) was performed using Lipofectamine RNAiMAX (ThermoFisher, Cat# 13778075). 48 hours after transfecting the miRNA mimics, 100 uL of media was removed from wells and luciferase and SEAP activity was assessed using the SecretE-Pair Dual Luminescence Assay Kit (GeneCopoeia, Cat# LF033) on a Cytation 5 Cell Imaging Multi-Mode Reader (BioTek, Winooski, VT). Luciferase activity was normalized by the SEAP activity for each individual sample.

Metabolic flux bioanalysis. To measure extracellular oxygen consumption rates (OCRs), 100,000 THP-1 cells were differentiated onto Seahorse XFp cell culture plates and analyzed on a Seahorse XFp Analyzer (Agilent, Santa Clara, CA). For mitochondrial function testing, we utilized the Seahorse XF Cell Mito Stress Test Kit according the manufacture protocol (Agilent, Cat# 103015-100) with the following concentration of reagents: 1 uM oligomycin, 1.5 uM Carbonyl cyanide-4-(trifluoromethoxy)phenylhydrazone (FCCP), and then 1 uM of rotenone and actinomycin A.

To measure redox capacity across individual mitochondrial electron transport chain (ETC) complexes, cells were permeabilized with Seahorse XF Plasma Permeabilizer (Agilent, Cat# 102504-100) at 1 nM in Mitochondrial Assay Buffer (220 mM mannitol, 70 mM sucrose, 10 mM KH₂PO₄, 5 mM MgCl₂, 2 mM HEPES, 1mM EGTA, 4mM adenosine diphosphate, and 0.2% w/v bovine serum albumin; all reagents acquired from Sigma). Next OCR was measured while cells were sequentially treated with 10 mM pyruvate and 1mM malonate (to provide electrons that enter the ETC at complex I), 2 uM rotenone, 10 mM succinate (to provide

electrons that enter the ETC at succinate dehydrogenase (SDH, complex II)), 2 mM actinomycin A, and then 10 mM ascorbate with 100 μ M tetramethyl-p-phenylene diamine (to provide electrons that enter the ETC at complex IV).³⁸⁶ All reagents were purchased from Sigma.

After Seahorse assays were complete, cells were stained with 2 mM Hoechst 33342 Solution (ThermoFisher, Cat# 62249) and then counted on a BioTex Lionheart LX (BioTek, Winooski, VT). Cell counts were then used to normalize OCR data.

Analysis of Polar metabolites by LC/IC-HRMS

To determine the incorporation of glucose and glutamine carbon the intracellular tricarboxylic acid (TCA) cycle, extracts were prepared and analyzed by high-resolution mass spectrometry (HRMS). Approximately 80% confluent cells were seeded in 60 mm dishes. Cells were washed with glutamine or glucose-free medium before incubated in fresh medium containing 11.1mM ¹³C₂-Glucose or 2mM ¹³C₅-Glutamine 6 hours. Cells were quickly washed with ice-cold deionized water to remove extra medium components. Metabolites were extracted using cold 80/20 (v/v) methanol/water with 0.1% ammonium hydroxide. Samples were centrifuged at 17,000 g for 5 minutes at 4 degree, and supernatants were transferred to clean tubes, followed by evaporation to dryness under nitrogen. Samples were reconstituted in deionized water, then 5 μ L was injected into a Thermo Scientific Dionex ICS-5000+ capillary ion chromatography (IC) system containing a Thermo IonPac AS11 250 \times 2 mm 4 μ m column for TCA cycle metabolites analysis. IC flow rate was 360 μ L/minute (at 30°C) and the gradient conditions are as follows: started with an initial 1mM KOH, increased to 35 mM at 25 minutes, then to 99 mM at 39 minutes, held 99 mM for 10 minutes. The total run time is 50 min. To assist the desolvation for better sensitivity, methanol was delivered by an external pump and combined with the eluent via a low dead volume mixing tee. Data were acquired using a Thermo Orbitrap Fusion Tribrid Mass Spectrometer under ESI negative mode.

For amino acid analysis, samples were diluted in 90/10 acetonitrile/water containing 1%

formic acid, then 15 μ L was injected into a Thermo Vanquish liquid chromatography (LC) system containing an Imtakt Intrada Amino Acid 2.1 x 150 mm column with 3 μ m particle size. Mobile phase A (MPA) was acetonitrile containing 0.1% formic acid. Mobile phase B (MPB) was 50 mM ammonium formate. The flow rate was 300 μ L/min (at 35°C), and the gradient conditions were: initial 15% MPB, increased to 30% MPB at 20 min, then increased to 95% MPB at 30 min, held at 95% MPB for 10 min, returned to initial conditions and equilibrated for 10 min. The total run time was 50 min. Data were acquired using a Thermo Orbitrap Fusion Tribrid mass spectrometer under ESI positive ionization mode at a resolution of 240,000. Then the raw files were imported to Thermo Trace Finder software for final analysis. The fractional abundance of each isotopologue is calculated by the peak area of the corresponding isotopology normalized by the sum of all isotopology areas.³⁸⁷ The relative abundance of each metabolite was normalized by total peak intensity.

Octyl- α -ketoglutarate and GSK126 cell culture treatments. Octyl- α -ketoglutarate was purchased from Sigma (Cat# SML2205), diluted in DMSO, and used *in vitro* at a concentration of 1.5 mM for 24 hours before cell collection or LPS stimulation. GSK126 was purchased from Cayman Chemical (Cat# 15415), diluted in DMSO, and used *in vitro* at a concentration of 2 μ M for 24 hours before cell collection or LPS stimulation.

3.3 Results

MicroRNA-147 is highly upregulated in lungs after the onset of ALI

We hypothesized that miRNAs could play an important role in the regulation of inflammation after the onset of ALI and promote recovery of injury. To this end, we utilized a survivable, sterile model of ALI using intra-tracheal LPS instillation that recapitulates many features of sepsis associated ALI such as the rapid onset of pulmonary leukocyte infiltration, disruption of the endothelial-epithelial barrier, and increased expression of inflammatory cytokines.³⁸⁸ In our hands, the weight-dosed intra-tracheal LPS model (2 mg/kg) resulted in a reproducible lung injury that peaks in severity around day three and resolves at around seven days, as demonstrated by measuring animal weight loss (Figure 6A). Because mice were at their peak phenotype around 3-days post LPS instillation, we considered this a critical time point when mice transitioned to recovery. We isolated RNA from the lungs of mice three days after the onset of ALI and submitted them for a miRNA microarray (Figure 6B). Compared to PBS-treated control mice, lungs from ALI mice were found to have significant differential expression of a large number for miRNAs (Figure 6C). After narrowing our list of differentially expressed miRNAs to those that are conserved within the human transcriptome, there was at least a twofold upregulation or downregulation in 12 and 5 miRNAs, respectively (Figure 6D). We next sought to investigate how the top upregulated miRNAs were expressed over the entire course of the ALI model. To do this, we measured the top six upregulated miRNAs in lung tissue over up to seven days after the onset of ALI using qPCR (Figure 6E). By performing an area-under-the-curve calculation for these six miRNAs, we found that miR-147 was the highest expressed miRNA over the course of ALI (Figure 6F). Interestingly, miR-147 expression was not substantially elevated until three days after the onset of ALI and peaked at 5 days post LPS instillation, indicating that it might potentially play a role during the timeframe in which mice recover from ALI (Figure 6E).

miR-147 is encoded in the genome within the 3' untranslated region (3' UTR) of the gene, normal mucosa of esophagus specific 1 (*Nmes1*).^{389, 390} *Nmes1* transcripts serve as the primary form for miR-147, which is processed into mature miR-147 via a pre-miR-147 intermediate. In order to determine if the increased pulmonary miR-147 expression during ALI was due to a transcriptional upregulation (as opposed to a purely stoichiometric upregulation contributed by infiltrating cells), we measured the expression of the *Nmes1* and pre-miR-147 in the lungs of ALI mice. We found that both *Nmes1* and pre-miR-147 transcripts were upregulated over the course of ALI, with a peak in expression three-days after the onset, which precedes the peak in miR-147 on day 5 (Figure 6G and H). In summary, we report that miR-147 is amongst the highest expressed miRNAs in lungs of mice during the course of ALI and that its increased expression is transcriptionally regulated.

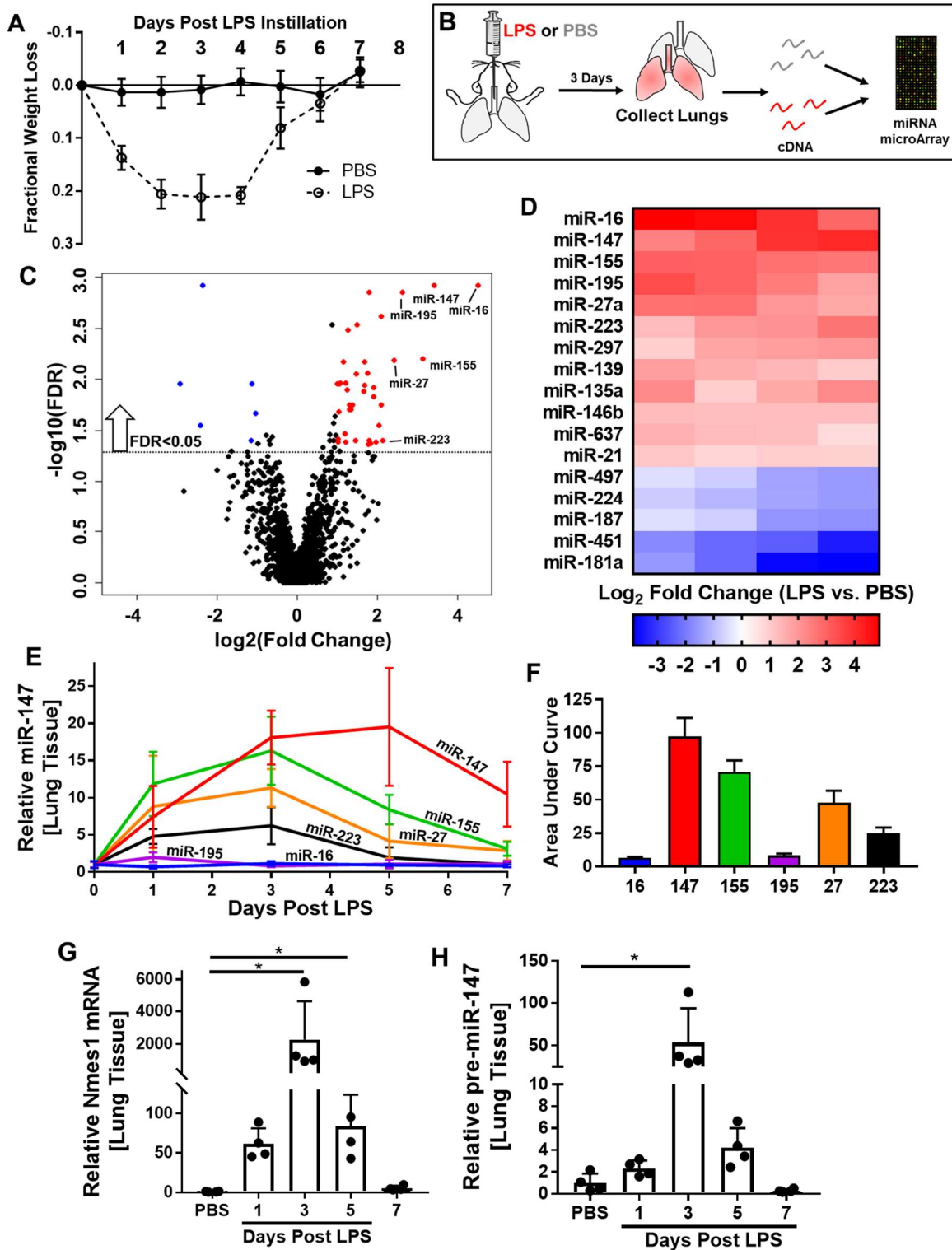


Figure 6: MicroRNA-147 is highly upregulated in lungs after the onset of ALI.

A) Calculated fractional weight loss curves for intra-tracheal LPS and PBS (controls) treated mice demonstrating peak weight loss at 3 days post ALI onset with subsequent recovery.

Figure 6 (Continued):

- B) Experimental schematic illustrating that RNA was isolated from ALI and control mice 3 days after the onset of ALI and submitted for microRNA microarray analysis.
- C) Volcano plot for up- and down-regulated miRNAs in the lungs of mice 3 days after the onset of ALI (n=4 mice in both groups, the designated threshold for significant changes was an FDR <0.05, miRNAs with fold change greater than 2 or less than 0.5 are portrayed as red or blue, respectively).
- D) Heat map listing the significantly differentially expressed miRNAs from the miRNA microarray results that are conserved with the human genome.
- E) Quantitative PCR measurements from mouse lung tissue for the top-six induced miRNAs identified from the miRNA microarray analysis (n>4 mice per group).
- F) Calculated area under the curve (AOC) for each of the top-six induced miRNAs over the entire seven days of the ALI model.
- G) Quantitative PCR results for *Nmes1* expression in the lungs of mice during ALI at the indicated time points. (n=4 per group, one-way ANOVA with Dunnett's correction for multiple comparisons).
- H) Quantitative PCR results for pre-miR-147 expression in the lungs of mice during ALI at the indicated time points. (n=4 per group, one-way ANOVA with Dunnett's correction for multiple comparisons).

All data are represented as mean \pm SD; * P-value <0.05.

Pharmacologic inhibition or genetic deletion of miR-147 exacerbates ALI

Next, we sought to determine if miR-147 is functionally important during the course of ALI. We first took a pharmacologic approach to inhibit miR-147 using locked nucleic acid (LNA) antisense oligonucleotides targeting the mature form of miR-147. LNAs are RNA derivatives that have chemically stabilized backbones that have previously been used *in vivo* systemically to effectively inhibit both mRNAs and miRNAs.³⁹¹⁻³⁹³ We treated mice with LNAs antisense to miR-147 directly into the lungs via intra-tracheal injections the day prior to and the day of LPS instillation. On the days after the onset of ALI, we gave mice daily LNA boosters via intraperitoneal injections (Figure 7A). This treatment regimen was effective at reducing the pulmonary expression of miR-147 as measured by qPCR (Figure 7B). Mice treated with miR-147-targeting LNAs had a significant increase in ALI mortality when compared with mice treated with scrambled control LNAs (Figure 7C). Furthermore, we found that mice treated with miR-147-targeting LNAs had increased residual pulmonary edema seven days after the onset, as measured by bronchoalveolar lavage fluid (BALF) albumin levels (Figure 7D).

As a next step, we utilized mice that have a genetic deletion for miR-147 (*miR147^{-/-}*). As previously described,³⁷⁹ *miR147^{-/-}* mice were generated by crossbreeding mice containing loxP sequences flanking the miR-147 loci (*miR147^{loxP/loxP}* mice) with mice encoding ubiquitously expressed Cre recombinase under the transcriptional regulation by the cytomegalovirus (CMV) promoter. We confirmed that there was efficient deletion of miR-147 by qPCR using RNA isolated from the lungs of *miR147^{-/-}* mice (Figure 7E). When given LPS-induced ALI, *miR147^{-/-}* mice experienced significantly increased mortality and a delayed recovery in their weight loss when compared with wild type (C57BL/6) mice (Figure 7F and G). Blinded histopathological analysis of hematoxylin and eosin stained lungs revealed that *miR147^{-/-}* mice had increased evidence for ALI (Figure 7H and I). Furthermore, *miR147^{-/-}* mice also developed worsened pulmonary edema as indicated by increased BALF albumin levels three and five days after the onset of ALI (Figure 7J). Lastly, *miR147^{-/-}* mice had increased neutrophilic inflammation during

ALI, indicated by increased levels of neutrophils counted in the BAL (Figure 7K). Altogether, these data support the notion that miR-147 plays a protective role in dampening inflammation and reducing tissue dysfunction during ALI.

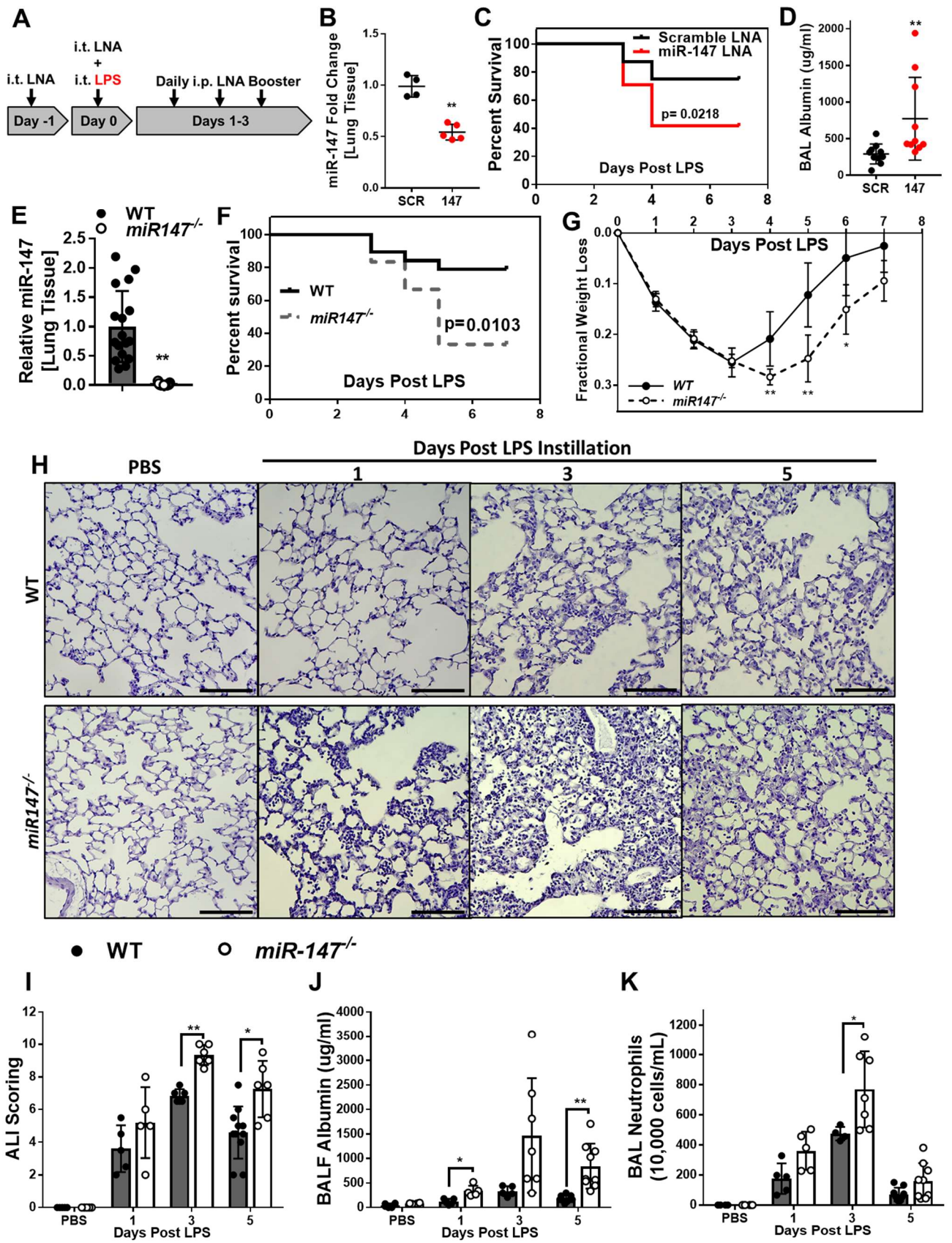


Figure 7: Pharmacologic inhibition or genetic deletion of miR-147 exacerbates ALI

Figure 8 (Continued):

- A) Experimental scheme for locked nucleic acid (LNA) antisense inhibition of miR-147 *in vivo*. Mice were injected with LNAs intra-tracheally (i.t.) 1 day prior to and on the day of i.t. LPS instillation. After the onset of ALI, mice were treated with intra-peritoneal (i.p.) doses daily.
- B) Quantitative PCR demonstrating reduced expression of miR-147 in lungs of mice treated with anti-miR-147 LNAs (147) compared with mice treated with scrambled control LNAs (SCR) (n=4 mice in the SCR group, n=5 mice in the 147 group, unpaired t-test).
- C) ALI-associated mortality in mice treated with either anti-miR-147 LNAs or scrambled controls (n=24 mice in each group, Kaplan-Meier curves, log-rank test).
- D) Pulmonary edema was determined by albumin concentration (ug/mL) in bronchoalveolar lavage fluid (BALF) using enzyme-linked immunosorbent assays (ELISA) in mice treated with anti-miR-147 and scrambled LNAs (n=10 mice in each group, Mann-Whitney test).
- E) Quantitative PCR for miR-147 expression in the lungs of wild type (WT) and *miR147^{-/-}* mice (n=17 mice in each group, Mann-Whitney test).
- F) ALI-associated mortality in WT and *miR147^{-/-}* mice (n=19 mice in the WT group, n=18 mice in the *miR147^{-/-}* group, Kaplan-Meier curves, log-rank test).
- G) ALI-associated fractional weight loss in WT and *miR147^{-/-}* mice (n=4-8 mice per group, Bonferroni-adjusted Welch's or unpaired t-tests).
- H and I) Representative hematoxylin and eosin stained sections and blinded ALI scoring of lungs collected from WT and *miR147^{-/-}* mice (40X magnification, n=5-11 mice per group, Bonferroni-adjusted unpaired t-tests).
- J) Pulmonary edema was determined by albumin concentration (ug/mL) in BALF using ELISA in WT and *miR147^{-/-}* mice (n=4-9 mice in each group, Bonferroni-adjusted unpaired t-tests).
- K) Quantification of neutrophils in the BAL of WT and *miR147^{-/-}* mice during ALI (n=4-9 mice in each group, Bonferroni-adjusted unpaired t-tests).

All data are represented as mean \pm SD; * P-value <0.05, ** P-value <0.01.

Liposomal miR-147-mimic treatment promotes resolution of ALI

Given that whole-body deletion of miR-147 resulted in increased tissue dysfunction and inflammation during ALI, we next investigated whether miR-147 over-expression could act in an opposite manner by reducing LPS-induced ALI. To do this, we delivered miR-147-mimic oligonucleotides that were packaged in liposomal 1,2-dioleoyl-sn-glycero-3-phosphatidylcholine (DOPC) intravenously two and four days after intra-tracheal LPS instillation (Figure 8A). DOPC liposomes have been shown to effectively deliver antisense oligonucleotides *in vivo* while also having minimal toxic properties.³⁹⁴⁻³⁹⁶ We confirmed that intravenous administration of liposomal miR-147 resulted in a significant over-expression of miR-147 in the lungs of mice using qPCR (Figure 8B). When treating mice with LPS-induced ALI, we observed a rebound in recovery of weight loss associated with ALI (Figure 8C). Histopathological analysis of hematoxylin and eosin stained lungs demonstrated decreased scores of ALI (Figure 8D and E). Lastly residual pulmonary edema at seven days after the onset of ALI was significantly reduced, as measured by BAL albumin levels (Figure 8D). Altogether, these findings demonstrate that miR-147 over-expression reduced ALI severity and promoted recovery in mice, which is in align with our previous results indicating miR-147 deficiency was associated with worsened ALI.

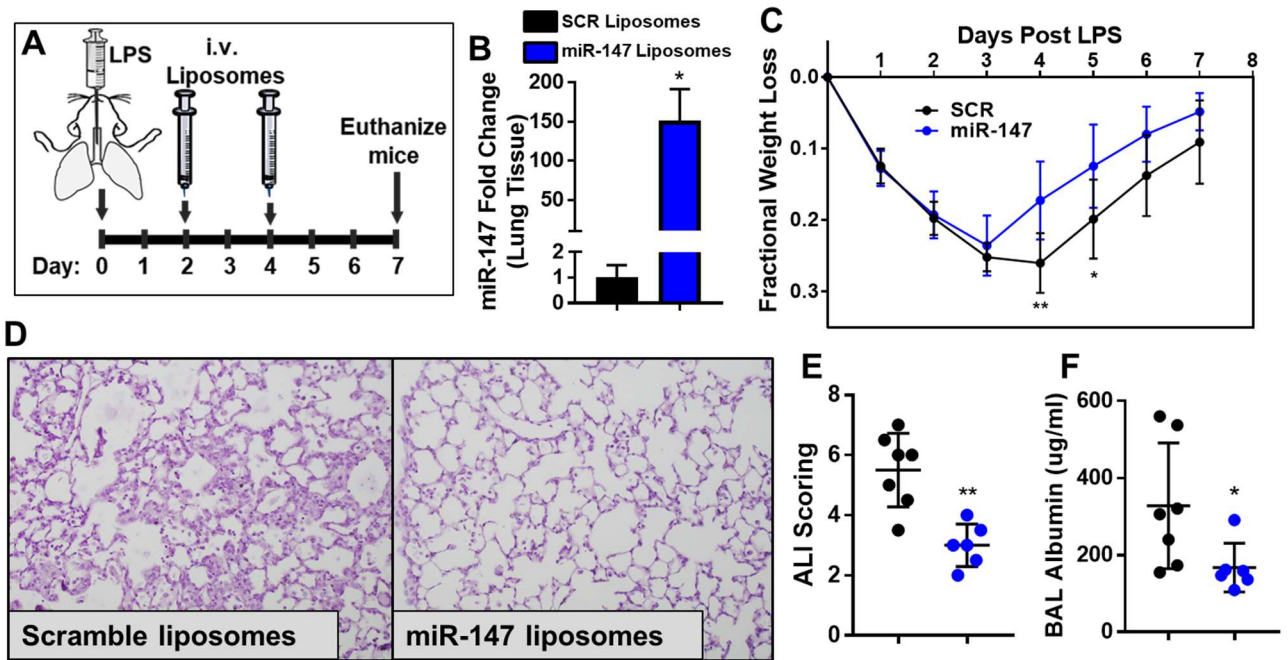


Figure 8: Liposomal miR-147-mimic treatment promotes resolution of ALI

A) Experimental scheme for liposomal miR-147 treatments. Mice were given intravenous (i.v.) injections of liposomal miR-147 mimics or scrambled controls 2 and 4 days after the onset of ALI.

B) Quantitative PCR measurements for miR-147 expression in lungs from mice treated with exogenous liposomal miR-147 (147) or scrambled controls (SCR) (n=4 mice in the SCR group, n=5 in the 147 group, Mann-Whitney test).

C) ALI-associated fractional weight loss in mice treated with liposomal miR-147 mimics or scrambled controls (n=6-8 mice per group, unpaired t-tests).

D and E) Representative hematoxylin and eosin stained sections and ALI scoring of lungs collected from mice treated with liposomal miR-147 mimics or scrambled controls (40X magnification, n=6-7 mice per group, unpaired t-test).

F) Pulmonary edema was determined by albumin concentration (ug/mL) in BALF using ELISA (n=6-7 mice per group, unpaired t-test).

All data are represented as mean \pm SD; * P-value <0.05, ** P-value <0.01.

Myeloid-specific deletion of miR-147 phenocopies whole-body deletion

To begin investigating the function for how miR-147 confers tissue protection during ALI, we first sought to identify in which cell(s) it is expressed. Given that ALI associated with intra-tracheal LPS instillation is characterized by the activation of resident alveolar macrophages followed by a substantial infiltration of inflammatory immune cells²³⁹ – both of which are cell types that highly express TLR4, the receptor for LPS – we first explored whether miR-147 expression was attributed to inflammatory immune cells. To do this, we digested lungs from mice three days after the onset of ALI into single cell suspensions and then used magnetically-conjugated antibodies to enrich for CD45 expressing cells, which is present on the surface of all hematopoietic lineage cells including, monocytes and macrophages.^{397, 398} There was a significantly increased expression of miR-147 in the CD45⁺ cells compared with CD45⁻ in digested lungs three days after the onset of ALI (Figure 9A). To further interrogate which of the CD45⁺ cells may be primarily expressing miR-147 during ALI, we used fluorescence activated cell sorting (FACS) of cells isolated from BAL of mice three days after the onset of ALI using a previously described strategy to gate for polymorphonuclear cells (PMNs, CD3⁻ B220⁻ Ly6G⁺), resident alveolar macrophages (CD3⁻ B220⁻ Ly6G⁻ CD11b^{low} CD11c^{high}), and peripherally recruited macrophages (CD3⁻ B220⁻ Ly6G⁻ CD11b^{high} CD11c^{low}).^{290, 399} After sorting for cells, qPCR-based measurements for miR-147 demonstrated that recruited macrophages contained significantly higher expression when compared with PMNs and alveolar macrophages (Figure 9B). Furthermore, by depleting circulating monocytes using liposomal clodronate, there was a decrease in the relative amount of miR-147 expression in the BAL cells three days after the onset of ALI (Figure 9C). Conversely, treating mice with intravenous PMN-depleting antibodies resulted in an increase in the relative expression of miR-147 in BAL cells isolated three days after intra-tracheal LPS instillation (Figure 9D). Altogether, these studies demonstrate that during ALI, miR-147 is highly expressed in recruitment macrophages.

To specifically address the function of miR-147 in the inflammatory immune compartment during ALI, we generated mice with myeloid-targeted deletion of miR-147 by crossbreeding *miR147^{loxp/loxp}* mice with mice encoding Cre recombinase under the transcriptional control by the lysozyme promoter (LysM Cre).³⁷⁸ We confirmed the knockout efficiency in BAL cells using qPCR which showed deletion for miR-147 expression (Figure 9E). When compared with LysM Cre control mice, *miR147^{loxp/loxp}* LysM Cre mice had a significantly increased mortality and delay in recovered weight loss associated with ALI (Figure 9F and G). Histopathologic analysis of hematoxylin and eosin stained lungs revealed significantly increased acute lung injury scores in *miR147^{loxp/loxp}* LysM Cre mice (Figure 9H and I). Furthermore, *miR147^{loxp/loxp}* LysM Cre mice also had significantly higher levels of pulmonary edema neutrophilic infiltration as measured by BALF albumin and BAL neutrophil counts, respectively (Figure 9J and K). In summary, these findings established that inflammatory immune cells, especially recruited macrophages, contributed to the expression of miR-147 during ALI and that specific deletion of miR-147 in the myeloid cell compartment was sufficient to phenocopy the exacerbated ALI we observed in the whole body deletion mouse.

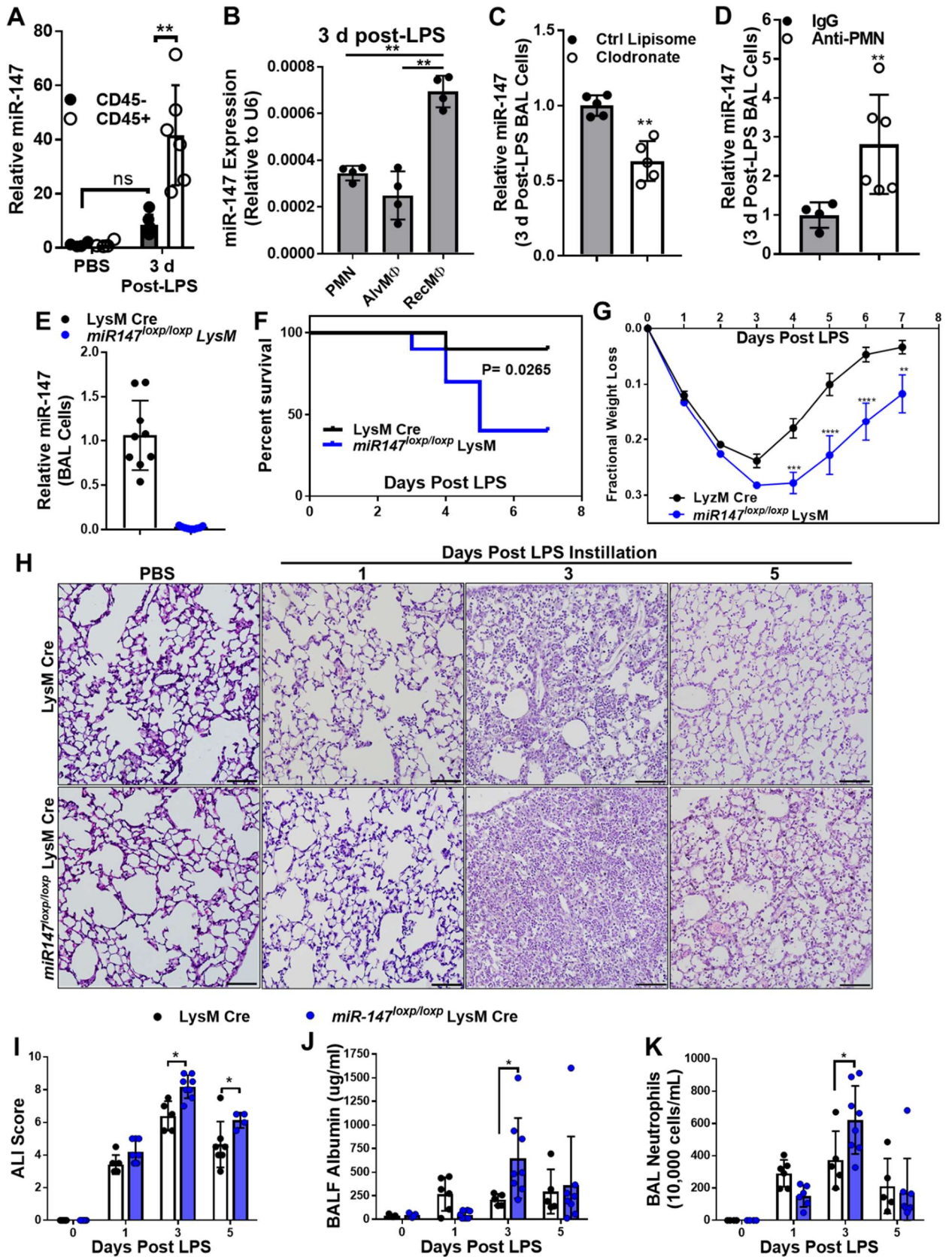


Figure 9: Myeloid-specific deletion of miR-147 phenocopies whole-body deletion

Figure 9 (Continued):

- A) Quantitative PCR measurements for miR-147 expression in CD45+ and CD45- cells after whole lung digestion of mouse lungs collected three days after the onset of ALI (n=4-6 mice in each group, Bonferroni-adjusted unpaired t-tests).
- B) Bronchoalveolar lavage (BAL) cells were collected three days after the onset of ALI and then separated into polymorphonuclear neutrophils (PMN), alveolar macrophages (AlvMΦ), and recruited macrophages (RecMΦ) populations using fluorescence assisted cell sorting (FACS). Quantitative PCR was used to determine the expression of miR-147 in each cell type (n=4 mice per group, Tukey-adjusted one-way ANOVA).
- C) BAL cells were collected three days after the onset of ALI from mice that were treated with either liposomal clodronate (to deplete peripheral monocytes) or liposomal PBS control (Ctrl). Quantitative PCR was used to determine the expression of miR-147 (n=5 mice per group, unpaired t-test).
- D) BAL cells were collected three days after the onset of ALI from mice that were treated with either PMN neutralizing (to deplete PMNs) or IgG control antibodies. Quantitative PCR was used to determine the expression of miR-147 (n=4-6 mice per group, Mann-Whitney test).
- E) BAL cells were collected from *miR147^{loxp/loxp}* LysM Cre and LysM Cre control mice. Quantitative PCR was used to determine the expression of miR-147 in order to confirm knockout efficiency (n=9 mice per group).
- F) ALI-associated survival in *miR147^{loxp/loxp}* LysM Cre and LysM Cre control mice. (n=10 mice per group, Kaplan-Meier curves, log-rank test).
- G) ALI-associated fractional weight loss in *miR147^{loxp/loxp}* LysM Cre and LysM Cre control mice. (n=7-10 mice per group, Bonferroni-adjusted Welch's or unpaired t-tests).
- H and I) Representative hematoxylin and eosin stained sections and ALI scoring of lungs collected from *miR147^{loxp/loxp}* LysM Cre and LysM Cre mice (40X magnification, n=4-8 mice per group, unpaired t-test).

Figure 9 (Continued):

J) Pulmonary edema was determined by albumin concentration (ug/mL) in BALF using ELISA in *miR147^{loxp/loxp}* LysM Cre and LysM Cre mice (n=5-8 mice in each group, Bonferroni-adjusted unpaired t-tests).

K) Quantification of neutrophils in the BAL of *miR147^{loxp/loxp}* LysM Cre and LysM Cre mice (n=4-8 mice in each group, Bonferroni-adjusted unpaired t-tests).

All data are represented as mean \pm SD; * P-value <0.05, ** P-value <0.01.

***miR147^{loxp/loxp}* LysM Cre mice have higher levels of inflammation during ALI**

We next sought to determine whether exacerbated ALI in *miR147^{loxp/loxp}* LysM Cre mice was associated with increased levels of inflammatory cytokine expression. We measured mRNA levels of the inflammatory genes *Il1b*, *Tnfa*, and *Il6* in the BAL cells of mice with LPS-induced ALI and found that *miR147^{loxp/loxp}* LysM Cre mice had significantly increased levels of inflammatory transcripts when compared with LysM Cre controls (Figure 10A, B, and C). These findings were also consistent with the protein levels of inflammatory cytokines measured in the BALF isolated from *miR147^{loxp/loxp}* LysM Cre mice (Figure 10D, E and F). These findings, in combination with the presence of increased infiltration of PMNs (Figure 9K), indicate that increased levels of inflammation are responsible for exacerbated ALI in *miR147^{loxp/loxp}* LysM Cre mice and that miR-147 is a critical regulator of inflammation.

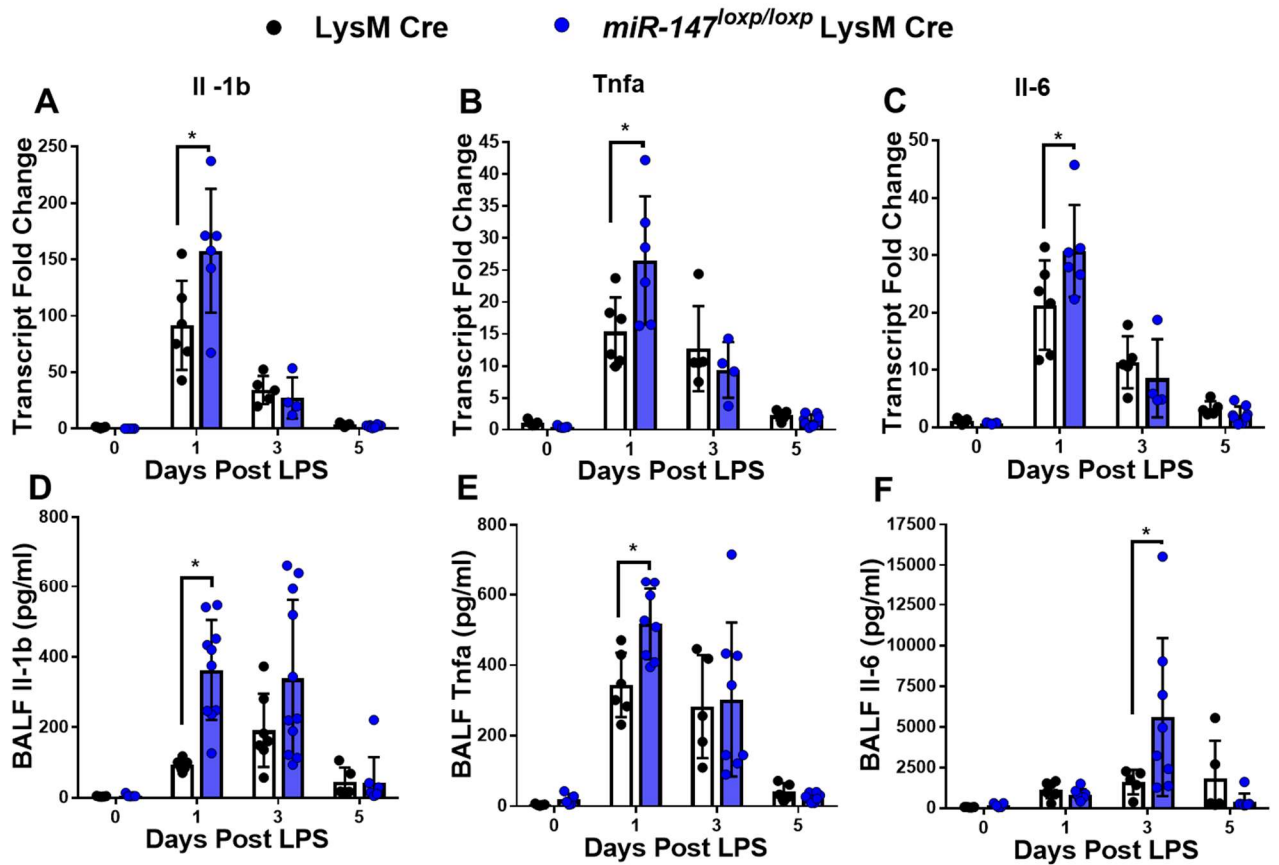


Figure 10: *miR147^{loxp/loxp}* LysM Cre mice have higher levels of inflammation during ALI

A, B and C) Il-1b, Tnf- α , and Il-6 protein concentration were measured using enzyme-linked immunosorbent assays in bronchoalveolar lavage fluid (BALF) collected from *miR147^{loxp/loxp}* LysM Cre and LysM Cre mice with ALI at the indicated time points (n=4-8 mice per group, Bonferroni-adjusted unpaired t-tests).

D, E and F) *Il1b*, *Tnfa* and *Il6* transcript levels were quantified using PCR in BAL cells collected from *miR147^{loxp/loxp}* LysM Cre and LysM Cre mice with ALI at the indicated time points (n=5-11 mice per group, Bonferroni-adjusted unpaired t-tests).

All data are represented as mean \pm SD; * P-value <0.05, ** P-value <0.01.

miR-147 is induced during ALI in a Hif1 α -dependent manner

We next investigated how miR-147 expression is regulated. First, we confirmed that miR-147 was transcriptionally up-regulated in LPS treated macrophage cells *in vitro* using mouse bone marrow-derived macrophages (BMDMs) and human peripheral monocyte-derived macrophages (hMDMs). Both cell lines showed upregulated expression of miR-147 in response to LPS stimulation (Figure 11A and B). By analyzing the promoter region of the NMES1 gene (which codes for the primary transcript that contains miR-147), we identified several regulatory elements that are associated with inflammatory signaling, including NF- κ B binding motifs and hypoxia response elements (HREs) (Figure 11C). Inflammation and hypoxia commonly co-exist during organ injuries, including in the lung, where hypoxia inducible factors (HIFs) and NF- κ B partake in complex bi-directional crosstalk.^{299, 400-404} We therefore hypothesized that HIFs could function as transcriptional regulators for miR-147 during LPS stimulation of macrophages. First, we isolated BMDMs from mice lacking functional genes for either the Hif1 α or Hif2 α isoforms in the myeloid compartment by isolating bone marrow from *Hif1a*^{loxp/loxp} LysM Cre or *Hif2a*^{loxp/loxp} LysM Cre mice, respectively. After treating the BMDMs with LPS for 24 hours, we measured a significant decrease in miR-147 expression by about 50 % specifically in the Hif1 α -deficient macrophages and not in the Hif2 α -deficient macrophages (Figure 11D). Next, to confirm that Hif1 α associates with the promoter of NMES1 in response to LPS stimulation, we performed a chromatin immunoprecipitation (ChIP)-qPCR which showed that there was a significant increase in enrichment in Hif1 α binding to the NMES1 promoter (Figure 11E).

In order to demonstrate the transcriptional role of Hif1 α for miR-147 expression *in vivo* we first assessed, indirectly, whether HIFs are stabilized in the lungs of mice with ALI mice using a HIF-reporter mouse (ODD-Luc mice).³⁷⁷ ODD-Luc mice have a constitutively expressed luciferase tagged with the oxygen dependent domain (ODD) of HIFs, which is the targeted domain for hydroxylation that labels HIFs for subsequent proteasome-dependent degradation. In this way, ODD-Luc mice express luciferase that is regulated at the protein level in the exact

manner as HIFs and can be measured for bioluminescent activity *in vivo* or *ex vivo*. After giving ODD-Luc mice intra-tracheal instillation of LPS, we measured significantly elevated bioluminescent activity in excised lungs up to five days after the onset of ALI (Figure 11F and G). To confirm HIF stabilization, specifically, in the lungs from mice with ALI, we performed Western blot analysis and found elevated Hif1 α protein levels the nuclear extracts isolated from lung tissues of mice with ALI, which peaked three days after the onset (Figure 11H and I). Interestingly, Hif2 α protein levels in the lungs did not change significantly (Figure 11H and J). Lastly, to test whether the presence of Hif1 α was also critical for the expression of miR-147 *in vivo*, we induced ALI in *Hif1a*^{loxp/loxp} LysM Cre and *Hif2a*^{loxp/loxp} LysM Cre mice and measured for miR-147 in the BAL cells three days after the onset of ALI. Hif1 α deletion resulted in abrogated miR-147 upregulation in the BAL cells after LPS instillation, while Hif2 α deletion did not have any effect (Figure 11K). Altogether, these experiments demonstrated that Hif1 α , but not Hif2 α , played an important role in expressing miR-147 in infiltrating alveolar compartment inflammatory cells during LPS-induced ALI.

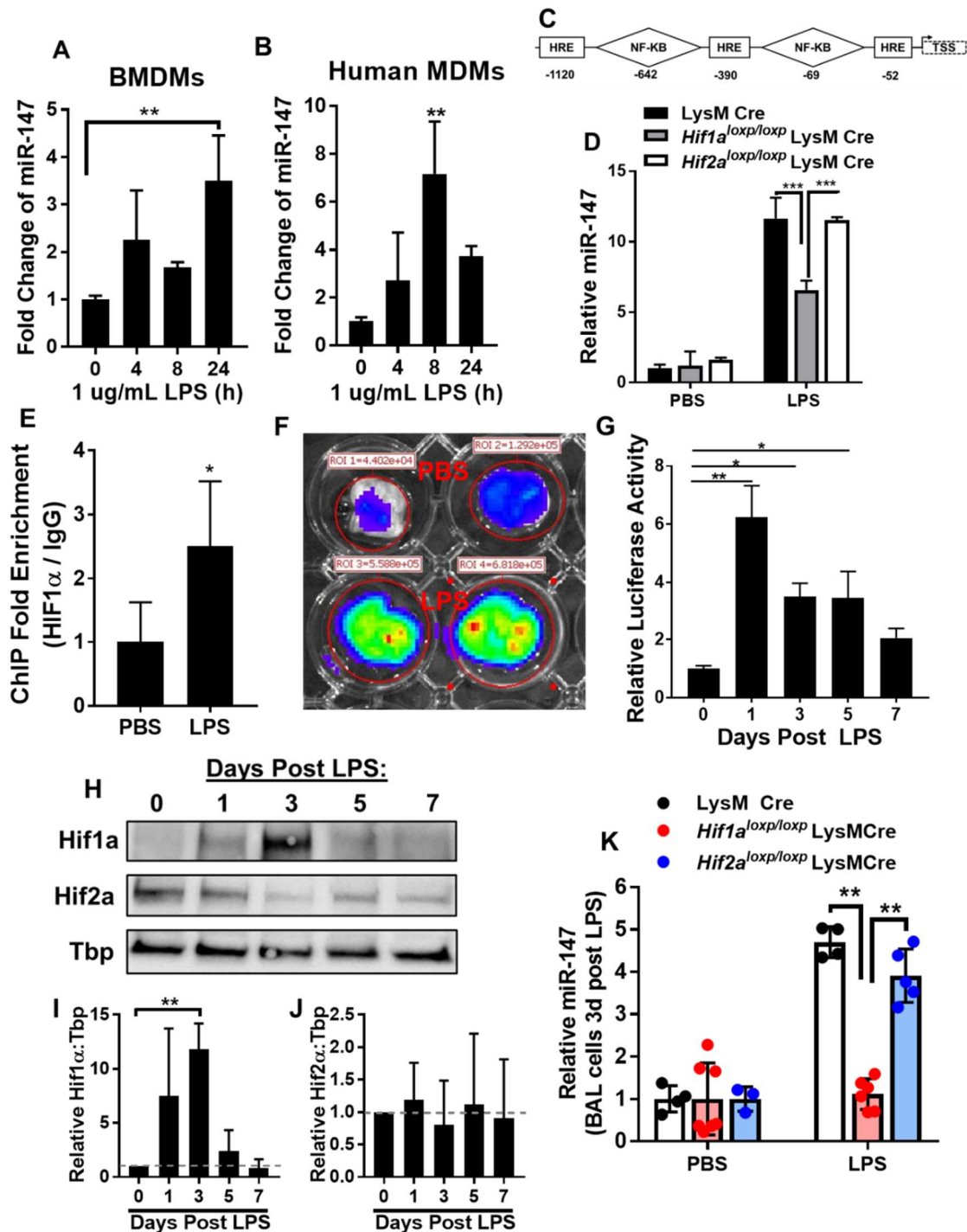


Figure 11: miR-147 is induced during ALI in a Hif1 α -dependent manner.

A) Mouse bone marrow-derived macrophages were stimulated with 1 ug/mL lipopolysaccharide for the indicated time points and then assayed for miR-147 expression using quantitative PCR (n=3 biological replicates, one-way ANOVA with Dunnett's test).

Figure 11 (Continued):

- B) Human peripheral monocyte-derived macrophages (hMDMs) were stimulated with 1 ug/mL lipopolysaccharide for the indicated time points and then assayed for miR-147 expression using quantitative PCR (n=3 biological replicates, one-way ANOVA with Dunnett's test).
- C) Diagram of transcription factor response element motifs in the promoter region of NEMS1. Hypoxia response elements (HRE) and NF-KB response elements are listed as being upstream by the indicated number of base pairs from the transcription start site (TSS).
- D) BMDMs isolated from LysM Cre, *Hif1a*^{loxp/loxp} LysM Cre and *Hif2a*^{loxp/loxp} LysM Cre mice were treated with 1ug/mL LPS for 24 hours and then assayed for miR-147 expression using quantitative PCR (n=3 biological replicates, Tukey-adjusted two-way ANOVA).
- E) Human MDMs were treated with LPS (1 µg/mL) for 8 hours. Chromatin Immunoprecipitation (ChIP)-PCR targeting a sequence in the NEMS1 promoter was performed to assess fold enrichment for HIF-1α association with the promoter of *NMES1* compared with IgG isotype control. Data are relative to PBS groups (n=3 biological replicates, one-tailed paired t-test).
- F and G) Representative images and quantification of bioluminescent activity from ODD-LUC mouse lungs after the onset of ALI. Luciferase activity is relative to PBS treated mice collected and imaged at the same time as ALI lungs (n=3-8 mice per group, one-way ANOVA with Dunnett's test).
- H, I and J) Representative Western blots and densitometry for Hif-1α and Hif-2α protein expression in nuclear extracts isolated from mice with ALI at the indicated time points. Tata-box binding protein (TbP) was used as the loading control. Densitometry data are relative to day 0 signals (n=mice per group, one-way ANOVA with Dunnett's test).
- K) Quantitative PCR was used to measure the expression of miR-147 in the BAL cells isolated from LysM Cre, *Hif1a*^{loxp/loxp} LysM Cre and *Hif2a*^{loxp/loxp} LysM Cre mice three days after the onset of ALI (n=3-6 mice per group, Tukey-adjusted two-way ANOVA).

All data are represented as mean ± SD; * P-value <0.05, ** P-value <0.01.

miR-147 targets the mitochondrial complex IV subunit, NDUFA4

Given that miRNAs function by inhibiting the expression of mRNA targets, we sought to determine the functional role of miR-147 in macrophages by identifying putative target mRNAs. To do this, we performed mRNA sequencing using cells from the BAL of *miR147^{loxp/loxp}* LysM Cre mice three days after the onset of ALI that were depleted of neutrophils, which enriched the samples for infiltrating macrophages that highly express miR-147 in control mice (Figure 12A). We found a large number of significantly up- and down-regulated genes in the *miR147^{loxp/loxp}* LysM Cre mice BAL macrophages when compared with LysM Cre controls (Figure 12B). Because miRNAs work by repressing their mRNA targets, we focused on the up-regulated differentially expressed genes in the *miR147^{loxp/loxp}* LysM Cre BAL macrophages, presuming at least one of them were up-regulated due to the absence of miR-147. There were 21 significantly up-regulated mRNAs in *miR147^{loxp/loxp}* LysM Cre BAL macrophages, of which we then cross-referenced with a list of predicted target genes based on the *in silico* prediction software, TargetScan.⁴⁰⁵ The comparison of up-regulated genes with the predicted target list yielded a single common gene, NADH dehydrogenase (ubiquinone) 1 alpha subcomplex 4 (NDUFA4), which codes for mitochondrial complex IV subunit, (Figure 12C).⁴⁰⁶⁻⁴⁰⁸ Using qPCR, we confirmed that *Ndufa4* expression was significantly up-regulated in *miR147^{loxp/loxp}* LysM Cre BAL cells (Figure 12D). We next sought to confirm the specific target of miR-147 to the predicted 3'UTR binding site using a reporter system that consisted of a plasmid coding for luciferase, but with the 3'UTR of NDUFA4. We also constructed another plasmid that is identical except for a four base mutation in the NDUFA4 3'UTR where the binding site for miR-147 is predicted to be located (Figure 12E). In this way, when the plasmids are transfected, the transcribed luciferase mRNAs will artificially be regulated by miR-147. We then co-transfected the plasmids into HEK293 cells with either miR-147 mimics or scramble controls. We measured significantly reduced luciferase activity in cells co-transfected with the wild type 3'UTR plasmid and miR-147 mimics, which was reversed in the cells transfected with the construct containing

the mutated miR-147 binding site (Figure 12F). The loss of repressed luciferase by miR-147 in the mutated construct demonstrated that the binding of miR-147 to the 3'UTR of NDUFA4 is site specific and indicated that NDUFA4 is a bona fide target gene for miR-147. To determine that miR-147 regulation of NDUFA4 mRNA levels also resulted in differential protein expression, we performed western blots in BMDMs derived from *miR147^{loxp/loxp}* LysM Cre mice and found a significant upregulation of Ndufa4 protein when compared to LysM Cre control cells (Figure G). Conversely, when we transfected the monocytic cell line, THP-1 cells, with miR-147 mimics, we measured a significant reduction in NDUFA4 protein levels, further supporting that miR-147 regulates both mRNA and protein expression of NDUFA4 (Figure 12H). Altogether, these findings reveal that during ALI, miR-147 targets NDUFA4, which is a bona fide target gene, and results in regulation of its protein levels.

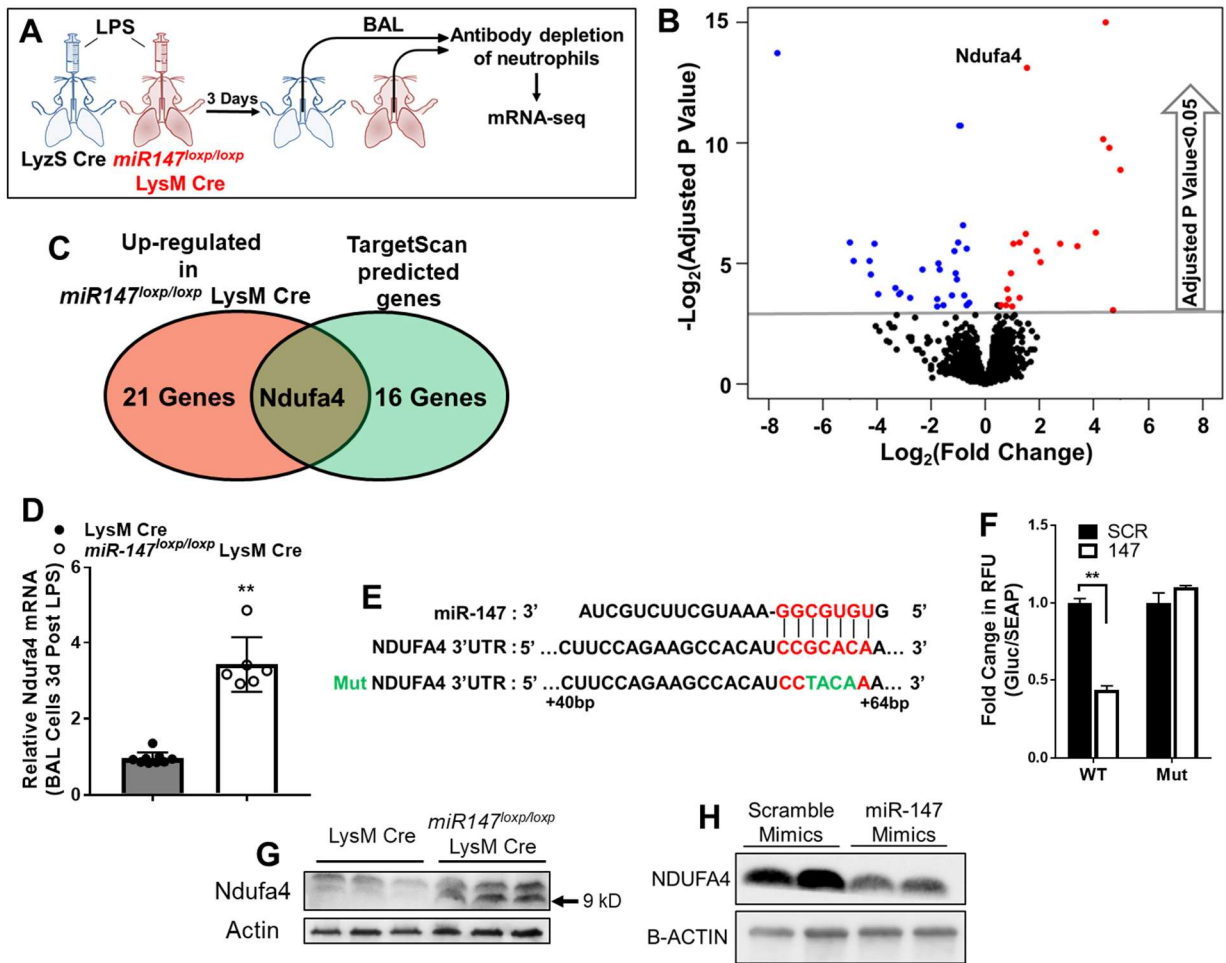


Figure 12: miR-147 targets the mitochondrial complex IV subunit, NDUFA4

- A) Experimental scheme demonstrating how bronchoalveolar lavage (BAL) cells were collected from LysM Cre and *miR147^{loxp/loxp}* LysM Cre mice three days after onset of ALI and then depleted for neutrophils using prior to RNA isolation. RNA was subsequently submitted for mRNA-seq.
- B) Differentially expressed genes in BAL cells isolated from *miR147^{loxp/loxp}* LysM Cre mice vs. LysM Cre controls. An adjusted P-value (False discovery rate) of less than 0.05 was considered significant. Genes with fold change greater than 2 are colored red and genes with fold change less than 0.5 are colored blue.

Figure 12 (Continued):

- C) Venn diagram illustrating the common gene (NDUFA4) in both the up-regulated differentially expressed genes and the predicted target genes for miR-147 determined by the *in silico* software, TargetScan.
- D) Quantitative PCR measurement of Ndufa4 mRNA expression in the BAL cells collected from LysM Cre and *miR147^{loxp/loxp}* LysM Cre three days after the onset of ALI (n=9 mice in the LysM Cre group, n=6 mice in the *miR147^{loxp/loxp}* LysM Cre group, Mann-Whitney test).
- E) Sequence details for 3' untranslated region (UTR) reporter plasmids. Luciferase coding regions were engineered with the wild type 3'UTR of NDUFA4 that contain the putative binding site for miR-147. In a separate plasmid, the 3'UTR contains a 4 base pair mutation in the miR-147 binding site, indicated in green.
- F) Fold changes in relative fluorescent units (RFU) in the supernatants of luciferase-3' UTR reporter expressing HEK-293 cells. Cells were transfected with either the wild type (WT) 3'UTR plasmid or the mutated 3'UTR plasmid (Mut). The cells were subsequently transfected with miR-147 mimics (147) or scrambled controls (SCR) (n=3 replicates, Bonferroni-adjusted multiple t-tests).
- G) Western blots for Ndufa4 protein expression in mouse bone marrow-derived macrophages isolated from LysM Cre and *miR147^{loxp/loxp}* LysM Cre mice (n=3 replicates).
- H) Western blots for Ndufa4 protein expression in THP-1 cells transfected with miR-147 or scramble control mimics (n=3 replicates).

All data are represented as mean \pm SD; * P-value <0.05, ** P-value <0.01.

NDUFA4 deletion dampens inflammatory gene expression independent of LPS-TLR4 signaling

Having identified NDUFA4 as a target gene regulated by miR-147, we next addressed whether NDUFA4 could play a role in regulation of inflammation in a manner consistent with the dysregulated inflammatory phenotype we observed during ALI in *miR147^{loxp/loxp}* LysM Cre mice. Using the acute monocytic leukemia cell line, THP-1 cells, we used CRISPR-mediated gene editing to develop NDUFA4-knockout cells (*NDUFA4^{-/-}*) in addition to control cells that were transfected with guide-RNA targeting a non-coding region of the genome. Western blotting for NDUFA4 levels demonstrated high efficiency for protein knockout in *NDUFA4^{-/-}* cells (Figure 13A). When *NDUFA4^{-/-}* cells were treated with LPS, we measured a significant reduction in the inflammatory cytokine genes *IL1B*, *IL6* and *TNFA*, when compared with the control cells (Figure 13B, C, and D). These results suggest that the deletion of NDUFA4 results in reduced inflammatory cytokine expression, which is consistent with our data in *miR147^{loxp/loxp}* LysM Cre mice, in which NDUFA4 and inflammatory cytokine expressions were elevated.

We next investigated whether the reduction in cytokine expression in *NDUFA4^{-/-}* LPS-stimulated THP-1 cells was associated with a decrease in the activation of intracellular pathways downstream of the LPS-TLR4 signaling. Upon binding to TLR4, LPS stimulation results in a cascade of intracellular events that result in the expression of inflammatory genes orchestrated by several transcription factors, including NF- κ B, IRF3 and AP-1, which are activated when in a phosphorylated state.^{409, 410} We performed Western blot analysis to measure the phosphorylated levels of p65 (a subunit of NF- κ B), I κ B α (an inhibitor of NF- κ B that is inactivated by phosphorylation), c-Jun (a member of the AP-1 transcription factor), and IRF3. We did not observe any significant changes in the phosphorylation state of any of these proteins in the *NDUFA4^{-/-}* THP-1 cells after LPS stimulation (Figure 13E and F). These data indicate that the down-regulated transcription of inflammatory cytokines in the *NDUFA4^{-/-}* THP-1 cells was not a result of inhibited signaling by the LPS-TLR4 axis.

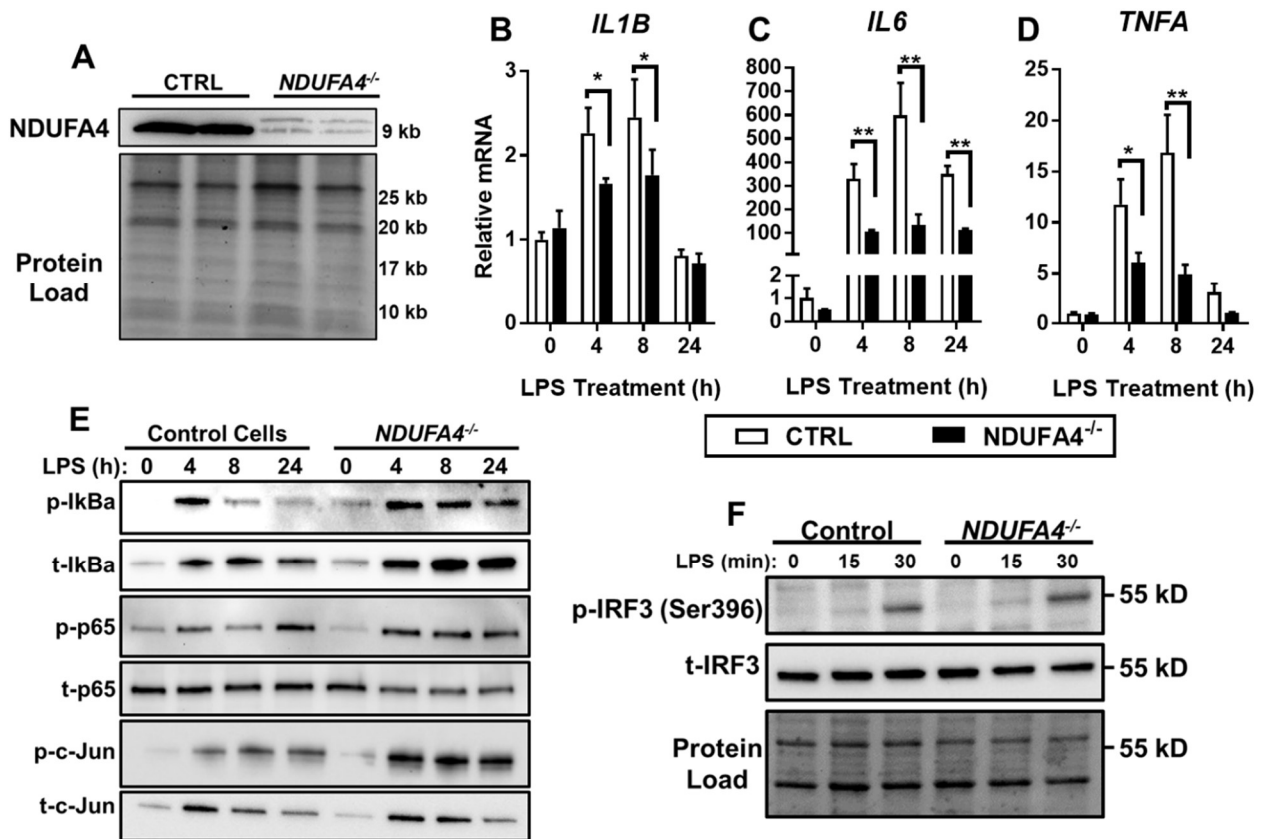


Figure 13: NDUFA4 deletion dampens inflammatory gene expression independent of LPS-TLR4 signaling

- A) Western blot of NDUFA4 protein expression in control (CTRL) and *NDUFA4*^{-/-} THP-1 cells (n=4 biological replicates).
- B, C and D) *IL1B*, *IL6* and *TNFA* mRNA expression measured by quantitative PCR in CTRL and *NDUFA4*^{-/-} THP-1 cells stimulated with 1 ug/mL lipopolysaccharide (LPS) for the indicated time points (n=3 biological replicates, Bonferroni-adjusted multiple t-tests).
- E) Western blot of NF-κB pathway total protein (t) and phospho-protein (p) expression in CTRL and *NDUFA4*^{-/-} THP-1 cells stimulated with 1 ug/mL lipopolysaccharide (LPS) for the indicated time points (n=3 biological replicates).
- F) Western blot of total IRF3 and phosphor-IRF3 protein expression in CTRL and *NDUFA4*^{-/-} THP-1 cells stimulated with 1 ug/mL lipopolysaccharide (LPS) for the indicated time points (n=3 biological replicates).

All data are represented as mean ± SD; * P-value <0.05, ** P-value <0.01.

NDUFA4 deletion leads to succinate accumulation via dampening the electron transport chain

Given that *NDUFA4*^{-/-} THP-1 cells expressed less inflammatory cytokines independent of LPS-TLR4 signaling, we hypothesized that – because NDUFA4 is a subunit of the mitochondrial complex IV⁴⁰⁶⁻⁴⁰⁸ – a metabolic mechanism might play a role in *NDUFA4*^{-/-} THP-1 cell inflammatory signaling. Indeed, metabolic programming of macrophages has been demonstrated to be a critical factor in governing their inflammatory phenotypes, especially in the context of mitochondria-derived factors such as reactive oxidative species and biologically active metabolites.⁴¹¹⁻⁴¹⁵ We first interrogated the mitochondrial function of the *NDUFA4*^{-/-} THP-1 cells by measuring their oxygen consumption rates (OCR, an indicator of oxidative phosphorylation activity) while sequentially treating cells with oligomycin (an adenosine triphosphate synthase inhibitor), cyanide p-trifluoromethoxyphenyl-hydrazone (FCCP, an uncoupler of oxidative phosphorylation), and rotenone combined with actinomycin A (Rot/AA, inhibitors of mitochondrial complex I and III, respectively). *NDUFA4*^{-/-} THP-1 cells had a significant reduction in measured OCR, including reduced calculated basal-, max- and ATP linked-OCR when compared with control cells (Figure 14A and B). To determine whether the reduction in mitochondrial function in *NDUFA4*^{-/-} cells was associated with a reduction in redox capacity across the mitochondrial electron transport chain (ETC) complexes, we measured OCRs in permeabilized cells that were sequentially treated with pyruvate and malonate (to provide electrons that enter the ETC at complex I), rotenone, succinate (to provide electrons that enter the ETC at succinate dehydrogenase (SDH, complex II)), actinomycin A, and then ascorbate with tetramethyl-p-phenylene diamine (to provide electrons that enter the ETC at complex IV).³⁸⁶ In this fashion, we were able to measure the oxidative phosphorylation-coupled redox activities of complex I, SDH, and complex IV in live cells with intact mitochondria. Consistent with previous reports that NDUFA4 knockdown results in decreased complex IV activity,^{407, 408} we observed decreased OCR associated with complex IV redox activity in

NDUFA4^{-/-} cells (Figure 14C and D). Interestingly, we also measured decreased OCR associated with complex I and SDH redox activities, suggesting that *NDUFA4* deletion had an effect on upstream ETC complex activities in addition to complex IV (Figure 14C and D).

We next sought to determine whether the reduction in mitochondrial oxidative phosphorylation capacity and redox activities of ETC complexes in *NDUFA4*^{-/-} cells resulted in alterations of mitochondrial matrix-associated metabolites by using high-resolution mass spectrometry to measure levels of tricarboxylic acid (TCA) cycle metabolites. There was a significant increase in the intracellular levels of succinate in *NDUFA4*^{-/-} cells when compared with controls (Figure 14E). Because succinate accumulation can occur by several means, such as through the increased generation or the decreased oxidation of succinate, we performed carbon tracing experiments to first interrogate the carbon source for the elevated succinate levels. Given that glucose (through glycolysis) and glutamine (through glutaminolysis) are both critical carbon sources for macrophages,^{416, 417} we performed heavy-isotope (¹³C) carbon tracing experiments by incubating cells with either ¹³C₆-glucose or ¹³C₅-glutamine (Figure 14F). Carbons from glucose sources enter the TCA cycle as the two-carbon metabolite, acetyl-CoA, resulting in succinate with two ¹³C isotopes (m+2), while carbons from glutamine sources are incorporated into the TCA cycle as five-carbon glutamate, resulting in succinate with four ¹³C isotopes (m+4) (Figure 14F). When tracing with ¹³C₆-glucose, we measured a reduction in m+2 succinate ions in the *NDUFA4*^{-/-} cells, whereas when incubation of cells with ¹³C₅-glutamine, we measured a significant increase in m+4 succinate ions in *NDUFA4*^{-/-} cells, indicating that the accumulation of succinate in *NDUFA4*^{-/-} cells is derived from a glutamine source (Figure 14G and H). Next, we investigated whether succinate accumulation was a result of increased glutamine incorporation or decreased succinate oxidation by SDH. By measuring the ratios of all ¹³C-labeled α -ketoglutarate ions (the metabolite through which glutamine enters the TCA cycle) and un-labeled α -ketoglutarate ions, we found no significant differences in the amount of glutamine entering the TCA cycle, demonstrating that succinate accumulation in *NDUFA4*^{-/-}

cells is not due to an increase in its generation (Figure 14I). To assess for the oxidation of succinate, we calculated the fraction of m+4 succinate to m+4 fumarate (the product of succinate oxidation by SDH). We calculated a significantly increased relative fraction of m+4 succinate to m+4 fumarate, indicating that succinate accumulation in *NDUFA4*^{-/-} cells is due to a decrease in succinate oxidation, presumably due to the reduction in redox activity of SDH as a result of decreased activity of the NDUFA4-deficient complex IV (Figure 14J). Altogether, these findings demonstrate that when the miR-147 target gene, NDUFA4, is deleted, there is a resulting dampening of ETC function with a subsequent accumulation of succinate due to a decrease in the redox activity of SDH.

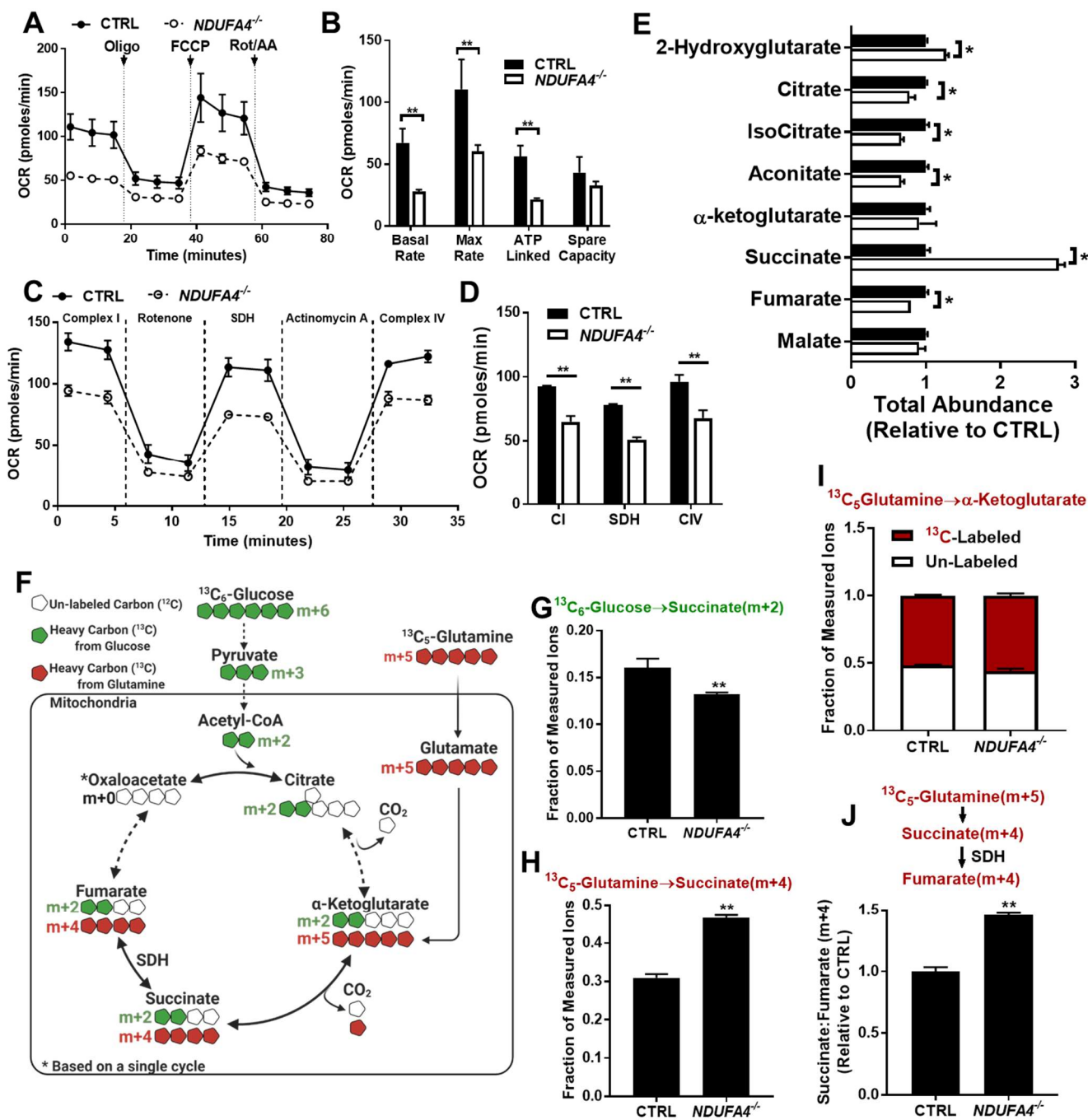


Figure 14: NDUFA4 deletion leads to succinate accumulation via dampening the electron transport chain

A) Extracellular oxygen consumption rates (OCR) of control (CTRL) and *NDUFA4*^{-/-} THP-1 cells treated sequentially with oligomycin (oligo), Carbonyl cyanide-4-phenylhydrazone (FCCP), and then a combination of rotenone with actinomycin A (rot/AA). Data are normalized by cell counts for each sample (n=3 biological replicates).

Figure 14 (Continued):

- B) Calculated basal, max, ATP-linked, and spare capacity rates of extracellular oxygen consumption of CTRL and *NDUFA4*^{-/-} THP-1 cells (n=3 biological replicates, Bonferonni-adjusted unpaired t-tests).
- C) OCR associated with coupled redox activities of mitochondrial complex I, succinate dehydrogenase (SDH), and mitochondrial complex IV in CTRL and *NDUFA4*^{-/-} THP-1 cells (n=3 biological replicates).
- D) Calculated rates of extracellular oxygen consumption coupled with the redox capacities of mitochondrial complex I, succinate dehydrogenase (SDH), and mitochondrial complex IV in CTRL and *NDUFA4*^{-/-} THP-1 cells (n=3 biological replicates, unpaired t-tests).
- E) Tricarboxylic acid cycle metabolites were measured in CTRL and *NDUFA4*^{-/-} THP-1 cells using high-resolution mass spectrometry. Data for abundances are normalized to the CTRL group for each metabolite (n=6 replicates in each group, Bonferonni-adjusted multiple t-tests).
- F) Diagram of heavy carbon (¹³C) tracing experimental design. ¹³C₆-glucose (green) or ¹³C₅-glutamine (red) were supplemented into cell growth media for six hours before collection. Isotopes of metabolites are referred to by their number of ¹³C atoms (i.e. m+2 citrate contains two ¹³C atoms, and so on). White symbols denote un-labeled carbons (¹²C).
- G) Fraction of measured m+2 succinate ions that were derived from ¹³C₆-glucose tracing in CTRL and *NDUFA4*^{-/-} THP-1 cells (n=3 replicates per group, unpaired t-test).
- H) Fraction of measured m+4 succinate ions that were derived from ¹³C₅-glutamine tracing in CTRL and *NDUFA4*^{-/-} THP-1 cells (n=3 replicates per group, unpaired t-test).
- I) Fraction of total labeled (m+1, m+2, m+3, and m+4) and un-labeled α-ketoglutarate ions that were derived from ¹³C₅-glutamine tracing in CTRL and *NDUFA4*^{-/-} THP-1 cells (n=3 replicates per group).

Figure 14 (Continued):

- J) Ratio of m+4 succinate:m+4 fumarate derived from $^{13}\text{C}_5$ -glutamine tracing in CTRL and *NDUFA4*^{-/-} THP-1 cells (n=3 replicates per group, unpaired t-test).

All data are represented as mean \pm SD; * P-value <0.05, ** P-value <0.01.

Succinate accumulation in *NDUFA4* knockout cells epigenetically regulates inflammation

Previous work has demonstrated that succinate is an important metabolite for the control of transcriptional activity and in the functional status of macrophages. In macrophages, succinate oxidation was shown to promote pro-inflammatory functions through the generation of mitochondrial reactive oxygen species.⁴¹⁴ Succinate has also been shown to play a potent role in competitively inhibiting α -ketoglutarate (α -KG)-dependent dioxygenases, including lysine histone demethylases (KDMs).⁴¹⁸⁻⁴²⁰ Furthermore, epigenetic regulation of inflammatory genes by KDMs has been shown to control phenotypes of macrophages.⁴²¹⁻⁴²³ We consequently sought to investigate whether *NDUFA4*^{-/-} cell accumulation of succinate was associated with epigenetic regulation of inflammatory cytokines. We first performed Western blot analysis to assess for genome-wide tri-methylation marks on histone-3 lysine-27 (H3K27me3), histone-3 lysine-9 (H3K9me3), and histone-3 lysine-4 (H3K4me3) and found a significant upregulation in H3K27me3 and H3K9me3 marks, both of which are gene-activating marks, in *NDUFA4*^{-/-} THP-1 cells (Figure 15A and B). Interestingly, we did not observe any significant increase in the gene-silencing mark, H3K4me3 (Figure 14A and B). To test whether the up-regulation in tri-methylation of H3K27 could be attributed to succinate accumulation, we treated cells with a competitive activator of KDMs, octyl- α -ketoglutarate (octyl- α -KG). After treatment of with octyl- α -KG, we observed a reversal of H3K27me3 in *NDUFA4*^{-/-} cells back to the levels seen in control cells (Figure 15E and F). In order to investigate whether reversal of H3K27me3 in *NDUFA4*^{-/-} cells could also reverse the decrease in inflammatory cytokine gene expression, we treated cells with GSK126, a specific inhibitor of enhancer of zeste homolog 2 (EZH2), which is a lysine methyl transferase that catalyzes the addition of methyl groups onto H3K27me3. After treating cells with GSK126, we observed a reversal of H3K27me3 in *NDUFA4*^{-/-} and a restoration in the expression of *IL6* during stimulation with LPS (Figure 15G and H). In summary, these results suggest that succinate accumulation in *NDUFA4*^{-/-} cells resulted in

increased epigenetic gene silencing marks via the inhibition of KDMs. Furthermore, reversal of elevated levels of H3K27me3 in *NDUFA4*^{-/-} cells was associated with restored expression of inflammatory cytokine transcription, thus providing a mechanistic link for how miR-147 targeting of NDUFA4 could result in the regulation of macrophage inflammatory processes through epigenetic modification.

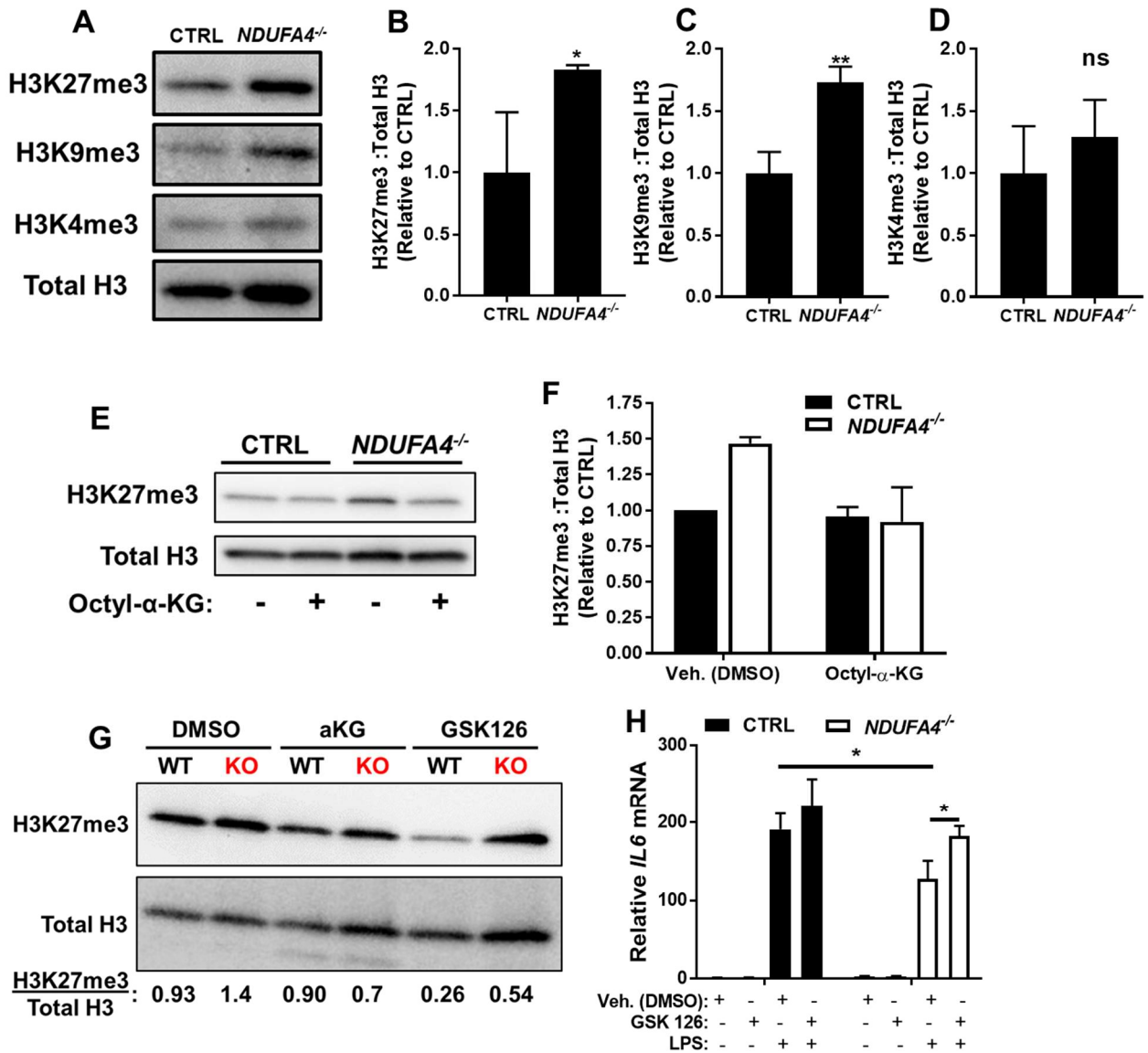


Figure 15: Succinate accumulation in NDUFA4 knockout cells epigenetically regulates inflammation

- A) Western blot of modified Tri-methyl marks on Histone H3 – Tri-Methyl-Histone H3 at lysine 27 (H3K27me3), Tri-Methyl-Histone H3 at lysine 9 (H3K9me3), and Tri-Methyl-Histone H3 at lysine 4 (H3K4me3) – in control (CTRL) and *NDUFA4*^{-/-} THP-1 cells (n=3 biological replicates).
- B, C and D) Western blot densitometry for H3K27me3, H3K9me3, and H3K4me3 relative to total Histone H3 in CTRL and *NDUFA4*^{-/-} THP-1 cells (n=3 biological replicates, unpaired t-tests).

Figure 15 (Continued):

- E) Western blot for H3K27me3 modification in CTRL and *NDUFA4*^{-/-} THP-1 cells that are treated with octyl- α -ketoglutarate or DMSO vehicle for 24 hours (n=2 biological replicates).
- F) Western blot densitometry for H3K27me3 modification relative to total Histone H3 in CTRL and *NDUFA4*^{-/-} THP-1 cells that are treated with octyl- α -ketoglutarate or DMSO vehicle for 24 hours (n=2 biological replicates).
- G) Western blot for H3K27me3 modification in CTRL and *NDUFA4*^{-/-} THP-1 cells that are treated with octyl- α -ketoglutarate, GSK126, or DMSO vehicle for 24 hours. Ratio of H3K27me3:total H3 are calculated at the bottom (n=1 biological replicate).
- H) Quantitative PCR measurement of *IL6* mRNA in CTRL and *NDUFA4*^{-/-} THP-1 cells that are treated with DMSO or GSK126 for 24 hours, then with 1ug/mL of LPS or PBS (negative control) for 4 hours (n=1 biological replicate, Bonferonni-adjusted multiple t-tests).

All data are represented as mean \pm SD; * P-value <0.05, ** P-value <0.01.

3.4 Conclusions and Significance

Through their function as inhibitors of gene expression, miRNAs provide a unique opportunity to intimately understand endogenous regulatory nodes that control biological processes, including inflammation.³⁵⁶ Here we hypothesized that unique miRNAs expressed after the onset of ALI may promote recovery and serve as novel therapeutic targets. Through a miRNA targeted microarray, we screened for the expression of all currently annotated miRNAs in the lungs of mice with sepsis-associated ALI three days after the onset of ALI and discovered that miR-147 expression was significantly enriched, particularly during the middle and later time points of the injury. Using both pharmacologic and genetic approaches, we showed that loss of miR-147 function resulted in worsened outcomes of ALI in mice. Furthermore, exogenously overexpressing miR-147 in mice through the utilization of liposome-packaged miR-147 mimics during peak inflammatory time points accelerated the recovery of ALI in mice, supporting the protective role of miR-147. By enriching for hematopoietic-lineage positive cells in digested lungs and sorting BAL cells in ALI mice, we demonstrated that miR-147 is predominantly expressed in the myeloid cell compartment, particularly in recruited macrophages. Indeed, specific deletion of miR-147 in the myeloid compartment recapitulated the worsened ALI phenotype observed in the whole-body deleted mice and also demonstrated increased expression of inflammatory mediators in the alveolar space. After surveying the promoter region of primary transcript for miR-147 (*NMES1*), we established that miR-147 expression in macrophages is dependent on Hif-1 α both *in vitro* and *in vivo*. Utilizing a transcriptomic approach, we identified the mitochondrial complex IV subunit, *NDUFA4*, as a putative target gene for miR-147. Through a CRISPR-mediated deletion of *NDUFA4* in the monocytic cell line, THP-1, we measured decreased expression of inflammatory cytokines upon LPS stimulation, which is consistent with our findings that miR-147 deletion – causing upregulation of *NDUFA4* – resulted in increased inflammation. Using extracellular oxygen consumption rate assays and

metabolomics, we reveal that NDUFA4 deletion promotes the accumulation of succinate via dampening the coupled activity of electron transport chain complex II (succinate dehydrogenase) redox activity. Succinate, in turn, promoted the epigenetic silencing of inflammatory genes by inhibiting the demethylation of Histone H3. Together, these findings reveal an intracellular network in myeloid cells beginning with the expression of miR-147 that works to modulate the signaling metabolite, succinate, which modifies the epigenetic landscape to limit the expression of inflammatory cytokines during lung inflammation.

The anti-inflammatory role of miR-147 during lung inflammation adds to a growing body of evidence that implies the importance of miRNA-mediated negative-feedback regulation of inflammation in macrophages.^{424, 425} MiR-146 is upregulated in macrophages upon LPS stimulation and was found to target IL-1 associated kinase-1 (IRAK1), IRAK2, and TNF associated factor 6 (TRAF6), all of which are transduction molecules that mediate TLR4 signaling to activate NF- κ B and inflammatory gene expression, in order to promote negative feedback. Furthermore, miR-146 was shown to be induced by the pro-resolving mediator, Resolvin D1, and to mediate the development of endotoxin-induced tolerance in macrophages upon subsequent stimulations by LPS.⁴²⁶⁻⁴³³ Other miRNAs have also been found to be up-regulated by LPS-TLR4 activation and subsequently dampen NF- κ B activation in a negative feedback manner. These include miR-149 that targets Myd88, which is an adapter protein that relays the TLR4 signaling into the cell, and miR-21, which acts to negatively regulate NF- κ B activation by targeting the tumor suppressor PDCD4.^{433, 434} Indeed, a prior study also identified miR-147 as a suppressor of inflammatory gene expression in macrophages, but did not implicate a target gene or mechanism for this function.³⁹⁰ Additionally, another study by Vlacil et al. found miR-147 to be down-regulated by the activation of nucleotide-binding oligomerization domain-containing proteins (NOD) 1 and 2, which resulted in increased levels of *Il-6* and *Tnf- α* transcript levels in endothelial cells.⁴³⁵ Our work showed that, unlike the previously mentioned miRNAs, miR-147 did not regulate the expression of inflammatory genes by acting on

intracellular signaling events or the activation of NF- κ B, but by altering the epigenomic landscape of macrophages. Though we demonstrate that miR-147's ability to alter the epigenome was attributed to the accumulation of the known lysine demethylase (KDM) inhibitor succinate as a result of the inhibition of NDUFA4, it is possible that there are additional targets for miR-147 that regulate inflammatory signaling at the level of signal transduction initiated by TLR4 activation by LPS. Our discovery of NDUFA4 as a miR-147 target was based on a transcriptomic approach, but it may not have identified target genes that are regulated on a protein level (i.e. miR-147 inhibits the translation of a gene without degrading its mRNA). Proteomic or tagged-argonaute2 pull-down assays could be used to more inclusively screen for additional target genes for miR-147.⁴³⁶

Epigenetic regulation of macrophage inflammatory functions is a rapidly expanding field with several studies showing that pro-inflammatory gene expression is both promoted and suppressed via post-translational modifications of histones.^{437, 438} Among the most reported epigenetic modifiers in macrophages is the lysine-specific demethylase, jumonji domain containing-3 (JMJD3). JMJD3 is normally induced in LPS stimulated macrophages, where it acts as an eraser of methyl groups on H3K27me2/3 – a gene silencing mark – and was shown to promote transcriptional activity.^{422,434} The induction of pro-inflammatory cytokines in macrophages in response to serum amyloid A stimulation has also been shown to be dependent on the activity of JMJD3^{439, 440} Furthermore, JMJD3 is α -ketoglutarate-dependent and studies have shown that α -ketoglutarate accumulation in macrophages can promote epigenetic activation of gene transcription.⁴⁴¹ In contrast, treating macrophages with a specific inhibitor of JMJD3 reduces LPS induced pro-inflammatory cytokine gene expression.⁴²¹ Similarly, succinate accumulation secondary to succinate dehydrogenase inhibition has been shown to inactivate JMJD3, leading to hyper-methylation of histones.^{418, 419, 442} Though our findings demonstrate an endogenous network for epigenomic regulation of pro-inflammatory cytokines via the accumulation of succinate, it remains to be established whether H3K27me3

marks are associated with pro-inflammatory genes and whether the regulation by succinate occurs in a JMJD3-dependent manner. Further studies using pharmacologic and genetic inhibition of JMJD3 and chromatin immunoprecipitation (ChIP)-seq studies are currently being pursued to answer these questions. Furthermore, LPS stimulation has also been shown to induce histone activating marks, such as histone H3 and H4 acetylation at the IL-12 p40 loci, to activate gene transcription.^{443, 444} Whether other histone modifications, such as acetylation, are altered downstream of the miR-147:NDUFA4 axis were not explored and remains an additional possibility.

Succinate and the activity of succinate dehydrogenase (SDH) has demonstrated a growing role in inflammatory functions of macrophages.^{430,438} Early reports suggested that exogenous succinate promoted IL-1 β expression via increased reactive oxygen species (ROS) and HIF-1 α -stabilization, though later studies specified that the oxidation of succinate by SDH is the critical event leading to HIF-1 stabilization and IL-1 β expression.^{445 414} Targeting SDH with an inhibitor or through genetic knockdown resulted in the accumulation of succinate in macrophages and dampened inflammatory gene expression.⁴¹⁴ This phenomenon mirrors our findings that inhibition of SDH as a result of NDUFA4 targeting by miR-147 promoted the accumulation of succinate and dampened inflammatory cytokine expression. Other mechanisms of inhibiting SDH in macrophages have also been described, such as the accumulation of itaconate, which is produced by the upregulation of the mitochondrial enzyme, immune-Responsive Gene 1 (Irg1), in response to LPS stimulation. Itaconate is a potent inhibitor of SDH and results in succinate accumulation, leading to anti-inflammatory phenotypes in macrophages both *in vitro* and *in vivo*.⁴⁴⁶ In our studies, it does not appear that itaconate contributed to the inhibition of SDH due to its lack of accumulation in *NDUFA4*^{-/-} THP-1 cells (data not shown). Succinate has also been shown to act via its cellular surface G-protein coupled receptor, SUNCR1. Depending on the pathophysiological context, the activation of SUNCR1 by succinate can induce either pro- or anti-inflammatory effects in macrophages.⁴⁴⁷⁻

⁴⁴⁹ Our data did indicate that there was also an accumulation of extracellular succinate in *NDUFA4*^{-/-} THP-1 cells (data not shown), but whether there is a contributory role for SUNCR1 was not investigated and is still a possibility.

Early studies have established that macrophages are critical players in both the initiation and resolution of ALI, with functions depending on the type of insult, chronicity, and severity.²⁸¹ Though macrophages are considered initiators of lung inflammation during ALI, macrophage phenotypic switching towards decreasing pro-inflammatory functions and increasing resolving functions is an important event that limits the duration and severity of lung injury.⁴⁵⁰ Furthermore, the clearance of pro-inflammatory macrophages is also a protective mechanism during acute lung injury. As an example, macrophage depletion using liposomal clodronate or genetic approaches reduced the severity of inflammation and tissue injury in murine models of ALI.^{451, 452} Additionally, Fas-mediated apoptosis of pro-inflammatory recruited macrophages is a requirement for resolution of LPS-induced ALI.²⁹⁰ Our results are in agreement that recruited macrophages require restraint in their inflammatory phenotypes in order to prevent tissue injury. Through the induction of miR-147, we demonstrate that dampening the electron transport chain is another mechanism by which macrophage inflammation is regulated to limit tissue injury in ALI.

Our findings that miR-147 expression is dependent on HIF-1 α also adds to an established line of work that HIF-1 α is a critical player in macrophage inflammatory processes. HIF-1 α has been shown to have both anti- and pro-inflammatory roles in macrophages. In an early genetic study, Cramer et al. demonstrated in *Hif1a*^{loxp/loxp} LysM Cre mice that HIF-1 α is essential for pro-inflammatory macrophage activity in an LPS-induced sepsis model.⁴⁵³ Furthermore, HIF-1 α has also been shown to act as a transcription factor for IL-1 β , IL-6 and inducible nitric oxide synthase.^{445, 454} On the other hand, myeloid-cell stabilization of HIF-1 α has also been demonstrated as a key regulator in the promotion of resolution in murine colitis models and also in murine *Helicobacter pylori*-induced gastritis models^{454, 455} Furthermore, HIF-

1 α is a critical regulator of inflammation in alveolar epithelial cells during ALI, and promotes the expression of the anti-inflammatory neuronal guidance protein, Netrin1.^{190, 456}

There are recognizably several limitations to our work. Firstly, the use of the LysM Cre mouse to target myeloid cells is not perfect. The LysM Cre promoter targets all granulocytes, including neutrophils, and has also been reported to have activity in alveolar type II cells.^{457, 458} Further *in vivo* studies will benefit this work by using macrophage specific recombinase for miR-147 deletion, such as the hCD68-rtTA/Teto-Cre, which is specifically expressed in peripheral recruited monocytes.⁴⁵⁹ Additionally, our data lack translational significance with human subjects. Currently we are gathering BAL samples from ARDS patients with the intent on answering whether miR-147 expression, succinate levels, and ARDS outcomes are correlated.

Altogether, our findings highlight a novel role in which myeloid cell-derived miR-147 is upregulated in response to stimulation by bacterial endotoxin during ALI to repress excessive inflammation. The impact of miR-147 is mediated through its regulation of NDUFA4, with subsequent dampening of the electron transport chain and accumulation of the metabolite, succinate, which acts as an epigenetic repressor of inflammatory gene expression. Further investigating the specific enzyme(s) that succinate interacts with to regulate the epigenome will be important moving forward because it may contribute towards identifying a drug target that may translate into novel ALI treatment. Additionally, our work suggests that miR-147 might be targeted directly as a therapeutic using nano-particle packaged mimics. Future work should be focused on utilizing miR-147 therapeutically in additional models of ALI, including more clinically-relevant infectious models, to further establish its pre-clinical efficacy and safety as a treatment modality.

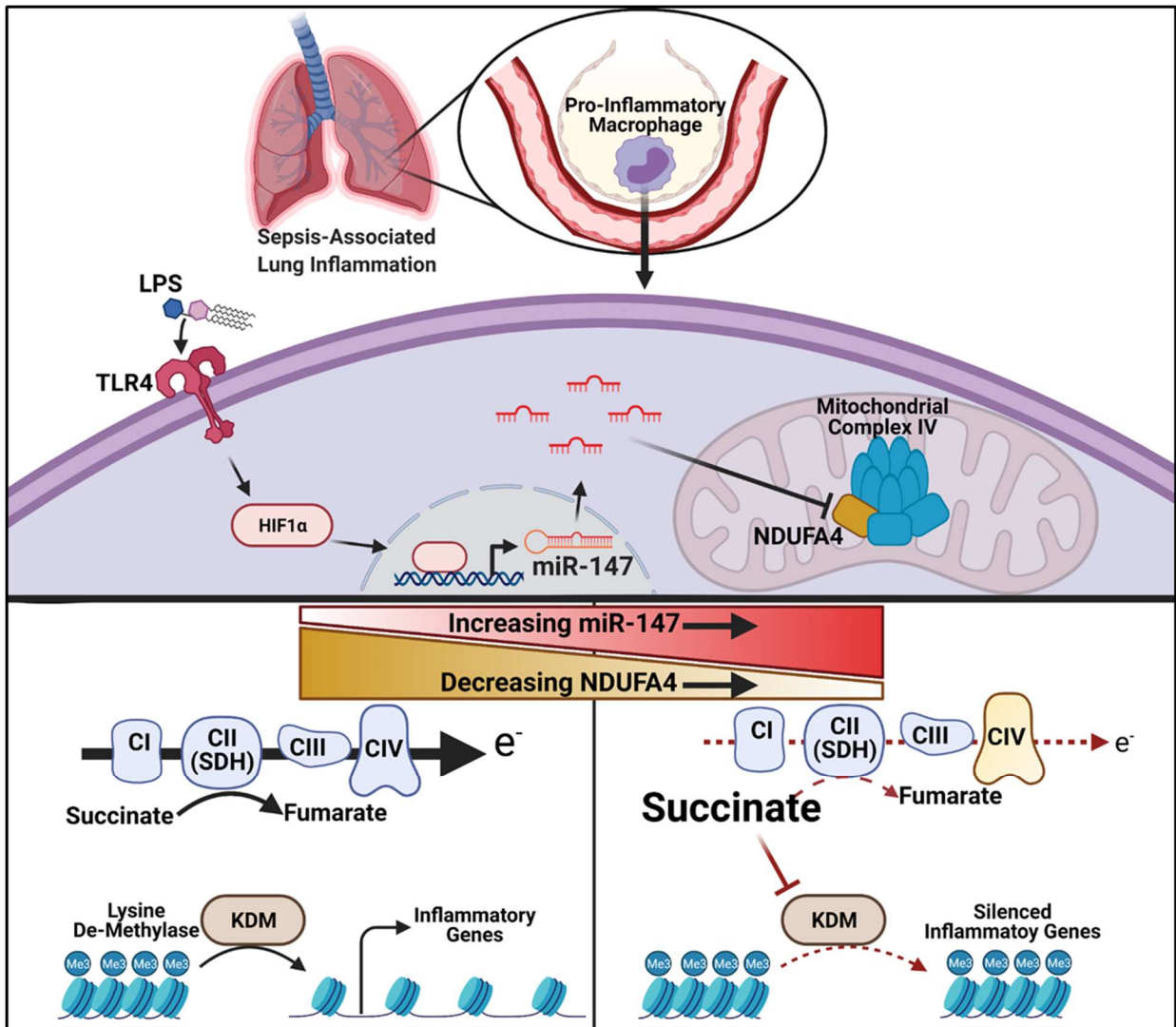


Figure 16: Proposed mechanism for miR-147-mediated regulation of inflammation during ALI

During ALI, pro-inflammatory recruited macrophages are activated through TLR4 by LPS which results in HIF-1 α stabilization and translocation to the nucleus where it activates the transcription of miR-147. MiR-147 then acts by blocking the translation of NDUFA4 subunits, which are a subunit of the mitochondrial complex IV. Decreasing NDUFA4 levels results in dampened electron transport chain activity, resulting in diminished redox activity of succinate dehydrogenase (SDH). The reduced activity of SDH leads to an accumulation of succinate, which then acts to inhibit lysine-specific demethylases (KDMs) and promote the epigenetic silencing of inflammatory cytokine genes. Created with BioRender.com.

Chapter 4: The role of netrin-1 in the regulation of inflammation during ALI

Work presented this chapter was previously published in:

Nathaniel K Berg*; Jiwen Li*; Boyun Kim; Tingting Mills; Guangsheng Pei, Zhongming Zhao, Xiangyun Li; Xu Zhang; Wei Ruan; Holger K Eltzschig; Xiaoyi Yuan. Hypoxia-inducible factor-dependent induction of myeloid-derived netrin-1 attenuates natural killer cell infiltration during endotoxin-induced lung injury. *The FASEB Journal*. 2020. Doi: 10.1096/fj.202002407R

*Denotes co-first authorship

Re-use of these materials for this dissertation were allowed with permission from the publisher and the terms of the Creative Commons Attribution-NonCommercial-NoDerivs License.

4.1 Introduction

Persistent and uncontrolled inflammation is the hallmark of sepsis, and sepsis-associated lung inflammation, which significantly contributes to morbidity and mortality of critical illness.^{460, 461} Inflammation by itself is an essential adaptive response to noxious stimuli such as infection and tissue injury.^{331, 462-465} However, in situations where an infectious burden is excessive or inflammation becomes dysregulated (i.e. fails to terminate or resolve), inflammation can result in profound collateral tissue damage and systemic impact.^{14, 466-472} Indeed, endogenous mechanisms and immune-modulators are programmed to limit inflammation and restore tissue homeostasis.^{360, 473-479} Such mechanisms include negative feedback pathways that serve to dampen inflammation and active stimulation by pro-resolution mediators that coordinate the termination of inflammation.^{477, 480-486} Myeloid cells, such as macrophages and neutrophils, are a crucial part of innate immunity and key drivers of the initiation and resolution of inflammation. For example, during lung inflammation, monocytes are recruited to the inflamed air space to differentiate into macrophages secreting cytokines that act locally to stimulate chemotaxis and

activate neutrophils.⁴⁸⁷ Therefore, understanding how myeloid cells contribute to the proper inflammatory responses are areas of intense investigation.⁴⁸⁸⁻⁴⁹⁴

Neuronal guidance proteins (NGPs) were first characterized for their role in neurogenesis through their ability to act as chemoattractant and chemorepellent cues to guide axons to their target synapses.⁴⁹⁵⁻⁴⁹⁸ However, increasing evidence has recognized NGPs as a class of immune-modulators⁴⁹⁹, which can regulate inflammatory processes by limiting or promoting the migration of leukocytes during acute and chronic inflammatory conditions.⁵⁰⁰⁻⁵¹⁰ For example, netrin 1, as one of the most investigated NGPs in immune modulation, is expressed by endothelial cells and plays a crucial role in inhibiting the migration of neutrophils to different chemoattractants.⁵¹¹ In addition, several lines of evidence from mice with partial deletion of netrin 1 (*Ntn1*^{+/-}) indicated that netrin-1 plays an important role in limiting the transmigration of leukocytes during models of acute lung injury, peritonitis, and colitis.^{502, 503, 505, 512} Additionally, exposure of hypoxia results in netrin 1 induction in mucosal epithelial cells in a hypoxia-inducible factor HIF-1 α dependent manner, and *Ntn1*^{+/-} mice exhibit increased myeloperoxidase activity in the colon tissue upon hypoxia exposure.⁵⁰³ Furthermore, recombinant netrin 1 treatment inhibits chemokine (C-C motif) ligand 2 (CCL2) and chemokine (C-C motif) ligand 19 driven macrophage migration *in vitro*.⁵¹³ Besides its role in leukocyte migration, netrin-1 was shown to suppress inflammatory macrophage functions^{514, 515} and to promote resolution of inflammation by stimulating the production of specialized pro-resolving mediators and tissue regeneration.^{516, 517} However, the functional role of myeloid cells-derived netrin 1 during lung inflammation has not been elucidated. Our studies demonstrated that, for the first time, myeloid cell-specific expression of netrin 1 confers lung protection through the modulation of CCL2 dependent natural killer (NK) cell migration.

4.2 Materials and Methods

Mice. Wild type (C57BL/6J), *Ntn1*^{loxp/loxp} 518, *Hif1 α* ^{loxp/loxp} 375, and LysM Cre³⁷⁸ mice were purchased from Jackson Laboratory. Detailed information on the mice strains is listed in table 3. Mice were housed and bred in a pathogen-free suite at the Center for Laboratory Animal Medicine and Care at the University of Texas Health Science Center at Houston (UTHealth). All experimental animal protocols were approved by the UTHealth Institutional Animal Care and Use Committee. Accounting for sex as a variable, for experiments using C57BL/6J or *Ntn1*^{loxp/loxp} LysM Cre mice, experiments were performed with age and weight-matched equal numbers of male and female mice throughout all groups. In our experiments using *Hif1 α* ^{loxp/loxp} LysM Cre mice, sex-dependent differences in mice were not observed and we used age and weight-matched mice (Figure 17).

Table 3: Mouse strain details for chapter 4.

Species	Vendor or Source	Background Strain	Sex	Persistent ID / URL
mice	Jackson Laboratory	C57BL/6J	Male	https://www.jax.org/strain/000664
mice	Jackson Laboratory	C57BL/6J	female	https://www.jax.org/strain/000664

	Species	Vendor or Source	Background Strain	Other Information	Persistent ID / URL
Parent - Male	Mice, <i>Netrin-1^{loxP/loxP}</i>	Jackson Laboratory	(129X1/SvJ x 129S1/Sv)F1-Kitl+	B6.129(SJL)-Ntn1tm1.1Tek/J	https://www.jax.org/strain/028038
Parent - Female	Mice, <i>Netrin-1^{loxP/loxP}</i>	Jackson Laboratory	(129X1/SvJ x 129S1/Sv)F1-Kitl+	B6.129(SJL)-Ntn1tm1.1Tek/J	https://www.jax.org/strain/028038
Parent - Male	Mice, Lyz2 Cre ⁺	Jackson Laboratory	129P2/OlaHsd	B6.129P2-Lyz2tm1(cre)Ifo/J	https://www.jax.org/strain/004781
Parent - Female	Mice, Lyz2 Cre ⁺	Jackson Laboratory	129P2/OlaHsd	B6.129P2-Lyz2tm1(cre)Ifo/J	https://www.jax.org/strain/004781
Parent - Male	Mice, <i>Hif1a^{loxP/loxP}</i>	Jackson Laboratory	(129X1/SvJ x 129S1/Sv)F1-Kitl+	B6.129-Hif1atm3Rsjo/J	https://www.jax.org/strain/007561
Parent - Female	Mice, <i>Hif1a^{loxP/loxP}</i>	Jackson Laboratory	(129X1/SvJ x 129S1/Sv)F1-Kitl+	B6.129-Hif1atm3Rsjo/J	https://www.jax.org/strain/007561

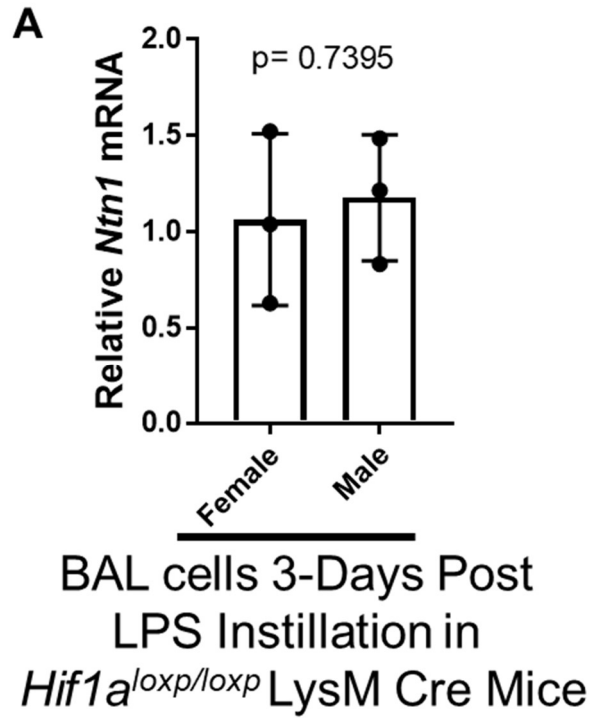


Figure 17: Lack of significant sex differences in *Hif1a*^{loxp/loxp} LysM Cre Mice.

A) Relative expression of *Ntn1* transcript in bronchoalveolar lavage (BAL) cells isolated from LysM cre and *Hif1a*^{loxp/loxp} LysM Cre mice 3 days after lipopolysaccharide (LPS)-induced lung inflammation (n=3 mice per group, unpaired t-test). Data are represented as mean +/- SD.

Generation of *Ntn1*^{loxp/loxp} LysM Cre⁺ and *Hif1α*^{loxp/loxp} LysM Cre⁺ mice. To conditionally achieve myeloid-cell specific deletion, *Ntn1*^{loxp/loxp} and *Hif1α*^{loxp/loxp} mice were crossbred with LysM Cre⁺ to generate *Ntn1*^{loxp/loxp} LysM Cre and *Hif1α*^{loxp/loxp} LysM Cre mice, respectively. Knock out in *Ntn1*^{loxp/loxp} LysM Cre mice was confirmed by performing RT-qPCR measuring knockout efficiency of the *Ntn1* mRNA transcript levels in bone marrow and in bronchoalveolar lavage (BAL) cells of intratracheal LPS-treated mice (Figure 18). *Hif1α*^{loxp/loxp} LysM Cre mice have been previously genotyped and characterized.³⁸⁰

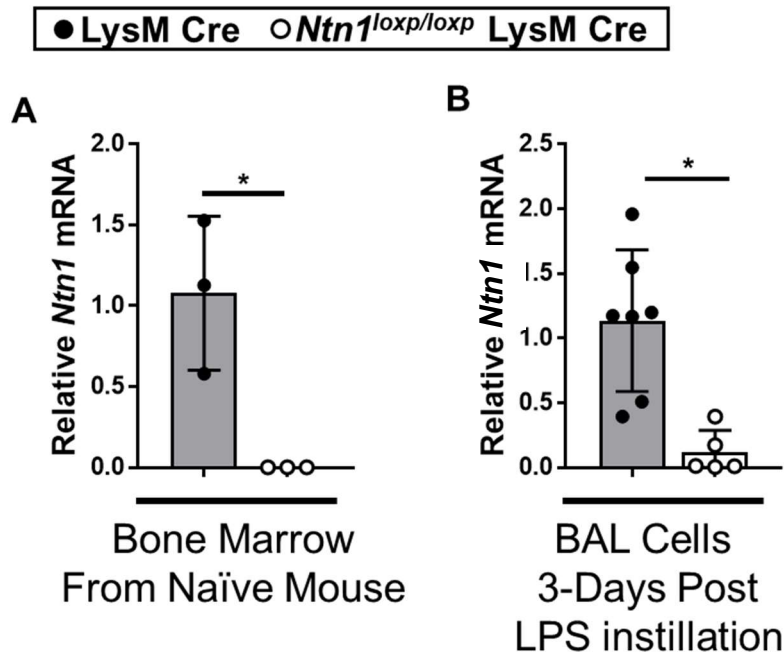


Figure 18: Confirmation of *Ntn1* knockout in *Ntn1^{loxp/loxp}* LysM Cre mice.

A) Relative expression of *Ntn1* transcript in bone marrow cells isolated from naïve LysM cre and *Ntn1^{loxp/loxp}* LysM Cre mice (n=3 mice per group, * p-value = 0.05, Mann-Whitney test). B) Relative expression of *Ntn1* transcript in bronchoalveolar lavage (BAL) cells isolated from LysM cre and *Ntn1^{loxp/loxp}* LysM Cre mice 3 days after LPS-induced lung inflammation (n=5-8 mice per group, * p-value < 0.01, Mann-Whitney test). All data are represented as mean +/- SD.

Isolation of human polymorphonuclear cells (PMNs) After isolation of human monocyte derived macrophages (described in the general materials and methods), the remaining cell pellet, which consists of PMNs were also washed twice with cold HBSS+25mM HEPES+10% FCS. PMNs were then cultured for experiments in DMEM+25mM HEPES+20%FCS, 2mM Gln, 1% Antibiotic/Antimycotic solution. To obtain hMDMs, PBMCs were cultured for 7 days in macrophage differentiation media: RPMI 1640 (supplemented with 10% heat inactivated fetal bovine serum and 10 ng/mL recombinant human M-CSF). Treatment with lipopolysaccharide (LPS, Sigma-Aldrich) was performed using a concentration of 1 µg/mL.

Table 4: Reagents for chapter 4

Description	Source / Repository	Catalog number #
Ficoll-Paque PLUS	GE Healthcare	17-1440-02
Red Blood Cell Lysis Solution	Miltenyi Biotec	130-094-183
citrate-dextrose buffer	Sigma-Aldrich	C3821
recombinant human M-CSF	R&D Systems	216-MC
lipopolysaccharide (LPS, <i>Escherichia coli</i> 0111:B4)	Sigma-Aldrich	L4391
QIAzol Lysis Reagent	Qiagen	79306
Applied Biosystems High Capacity Reverse Transcription Kit	Thermo Fisher	4368814
TaqMan Universal PCR Master Mix	ThermoFisher	4305719
TB Green Premix Ex Taq II (Tli RNase H Plus)	Takara Bio Inc	RR820A
protease inhibitor cocktails	New England Biolabs	5871S
phosphatase inhibitor cocktails	New England Biolabs	5870S
BCA protein assay	ThermoFisher	23225
SuperSignal West Femto Maximum Sensitivity Substrate	Thermo Scientific	34094
pentobarbital (Nembutal)	Akorn Inc	76478050150
Albumin ELISA	Bethyl Laboratories	E90-134
IL-6 ELISA	BD Biosciences	555240
IL-1 β ELISA	R&D Systems	DY401
CCL2 ELISA	R&D Systems	DY479
the citric acid-based antigen unmasking solution	Vector Laboratories	H-3300
normal goat serum	Vector Laboratories	S-1000
VECTASTAIN Elite ABC-HRP Kit	Vector Laboratories	PK-6101
DAB (3,3'-diaminobenzidine) Substrate Kit	Vector Laboratories	SK-4100
Red Blood Cell Lysis Solution	Promega	Z3141
RNeasy Mini Kit	Qiagen	74104
MojoSort Mouse Ly-6g Selection Kit	BioLegend	480123
Proteome Profiler Mouse Cytokine Panel A	R&D Systems	ARY006

RT-qPCR. Quantitative PCR was performed using TaqMan probes targeting netrin-1 (ThermoFisher, Human: Cat# 4331182 and Mouse: Cat# 4331182) and 18S for control (ThermoFisher, cat# 4331182).

Neuronal Guidance Peptide mRNA array. hMDMs were stimulated with LPS for 8 hours and then collected for RNA isolation. Screening for Neuronal Guidance Peptide mRNA expression was performed using the Axon Guidance PrimerArray (cat.# PH006) and TB Green Premix Ex Taq II from Takara Bio Inc. (Shiga, Japan) according to the manufacture's protocols.

Western Blotting. Detailed information on the antibodies is listed in table 5.

Immunohistochemistry. The lung slices were cut in 5 μ m in thickness and mounted on glass slides. Antigen retrieval was performed with the citric acid-based solution (Vector Laboratories) using a pressure cooker following deparaffinization and rehydration. The BAL cell slides were prepared with cytospin (Hettich ROTOFIX 32A centrifuge, Germany) and cells were fixed with freshly made 4% Paraformaldehyde (PFA) for 20 minutes (room temperature) followed by permeabilization (0.3% Triton X-100, 20 minutes). Endogenous peroxidase activity was quenched (3% hydrogen peroxide solution, 5 minutes). After blocking with 2.5% normal goat serum, slices were incubated with primary antibodies (4°C, overnight). The following steps were performed with ABC-HRP Kit (Vector Laboratories) and DAB (3,3'-diaminobenzidine) according to the manual instruction followed by hematoxylin counterstaining. Negative control slides were incubated with the recombinant rabbit IgG (Abcam, Cat#ab172730) instead of primary antibody at the same concentration. A Leica DM2500 light microscope was used to evaluate the staining and pictures were taken with a Leica DMC5400 digital camera. Detailed information on the antibodies is listed in table 5.

Table 5: Antibodies used in chapter 4.

Target antigen	Vendor or Source	Catalog number	Working concentration
Anti-mouse CD16/CD32 recombinant rabbit IgG	BioLegend	101301	Flow cytometry 1:100
FITC-anti-NK1.1 (Clone PL136)	ThermoFisher	11-5941-82	Flow cytometry 1:100
APC-anti-CD3 (Clone 17A2)	ThermoFisher	17-0032-82	Flow cytometry 1:100
Alexa Fluor 546 goat anti-rabbit IgG(H+L)	Invitrogen	A11010	Immunofluorescence 1:200
anti-F4/80 antibody (FITC)	Abcam	ab60343	Immunofluorescence 1:200
Netrin-1 Antibody	LifeSpan BioSciences	LS-C743016	immunohistochemistry paraffin 1:200
Netrin-1 Antibody	Abcam	ab126729	western blot 1:1000 Immunofluorescence 1:200
β -Actin Antibody	Santa Cruz	sc-47778	western blot 1:2000
Anti-rabbit IgG, HRP-linked Antibody	Cellsignaling	7074	western blot 1:5000
Anti-mouse IgG, HRP-linked Antibody	Cellsignaling	7076	western blot 1:5000

Flow cytometry of BAL cells. After collection and red blood cell lysis, BAL cells were blocked with anti-mouse CD16/32 Antibody (Clone 93, BioLegend) for 10 minutes on ice and then stained with FITC-anti-NK1.1 (Clone PL136, ThermoFisher) and APC-anti-CD3 (Clone 17A2, ThermoFisher) for 30 minutes on ice. After two washes with flow cytometry buffer, cells were analyzed on a CytoFLEX LX (Beckman Coulter, Indianapolis IN). Detailed information on the antibodies is listed in table 5.

Immunofluorescence. The BAL cell slides were prepared with cytospin (Hettich ROTOFIX 32A centrifuge, Germany) and cells were fixed with freshly made 4% Paraformaldehyde solution for 20 minutes at room temperature. Following blocking with 2.5% normal goat serum at room temperature for 1 hour, the slides were incubated with primary antibody at 4°C overnight. Negative control slides were incubated with the recombinant rabbit IgG. Conjugated secondary antibodies were used to apply the fluorescence dye. Slides were mounted after counterstaining with DAPI. A confocal microscope (Leica, Germany) was used to observe and document the staining. Detailed information on the antibodies is listed in table 5.

mRNA-sequencing of bronchoalveolar lavage (BAL) cells. After mRNA sequencing described in the general materials and methods standard Gene Ontology (GO) and KEGG pathway enrichment analyses were performed using the online tool WebGestalt (v0.4.3)⁵¹⁹. Up-regulated differentially expressed genes were matched to cell-type ontology using the CellKb database (v2.0) software.

Antibody-mediated neutralization of CCL2. For CCL2 neutralization, mice were treated with intraperitoneal injections of 10ug/g of body weight of anti-mouse CCL2 (clone 2H5, Cat# BE0185) or control IgG (Cat# BE0091). Both antibodies were purchased from BioXCell (Lebanon, NH).

Profiling for cytokine and chemokine expression in mouse BAL fluid. To screen for expression of cytokine and chemokines in the BAL fluid of mice, we performed the Proteome

Profiler Mouse Cytokine Panel A (R&D Systems, Minneapolis, MN) using 100 uL of mouse BAL fluid. Dot blot membranes were imaged and densitometry was performed using ImageJ software (National Institutes of Health).

Chromatin immunoprecipitation-quantitative PCR. Primers for the Netrin1 promoter were as follows: Forward: TCCTCCTCCTCTTCCTCACG, Reverse: CTCTAACCCAGCCTGATGGC.

4.3 Results

Netrin-1 is upregulated in endotoxin stimulated myeloid cells

Previous studies have demonstrated that NGPs play significant roles in regulating the inflammatory processes of macrophages.^{506, 512, 514, 515, 520, 521} Along these lines of evidence, we hypothesized that NGPs may be upregulated by macrophages in response to inflammatory stimuli as a potential endogenous anti-inflammatory mechanism. To investigate the induction of NGP expression in macrophages, we treated human monocyte-derived macrophages (MΦs) with LPS for 8 hours and then performed an RT-qPCR array for NGP gene expression (Figure 19A). *NTN1* (the gene encoding for netrin-1) was the highest expressed NPG in the array reaching statistical significance, and the result was further confirmed using an alternate TaqMan based qPCR assay (Figures 19B, C). Besides the upregulation of *NTN1*, cell lysates also demonstrated increased levels of netrin-1 protein following LPS exposure (Figures 19D, E). In addition, we investigated the expression of netrin-1 in LPS treated human polymorphonuclear cells (PMNs) and found increased levels of netrin-1 transcript and protein levels (Figure 19F, G, H). Together these results demonstrate that netrin-1 expression is significantly induced in myeloid cells during treatment with LPS.

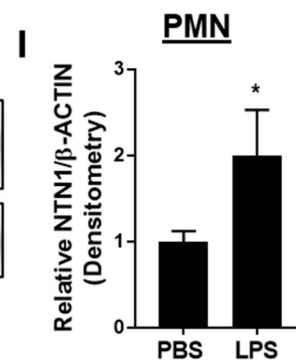
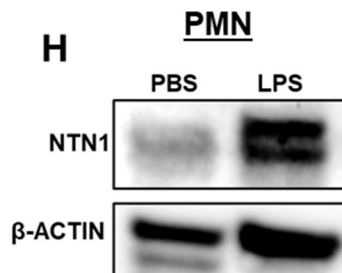
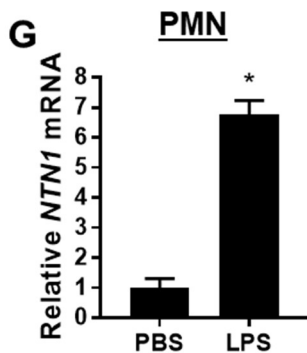
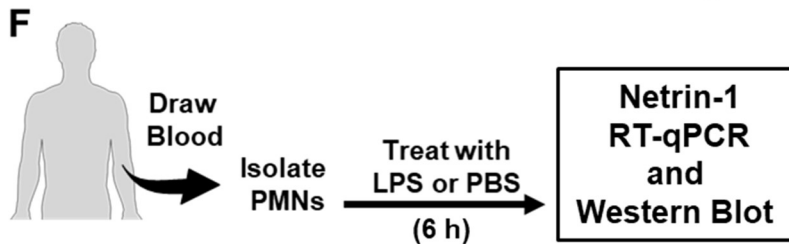
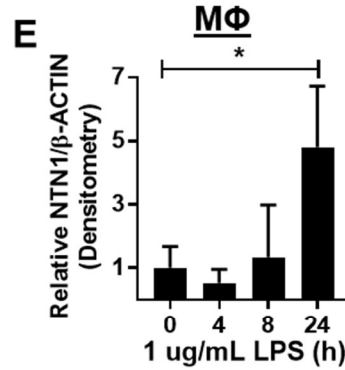
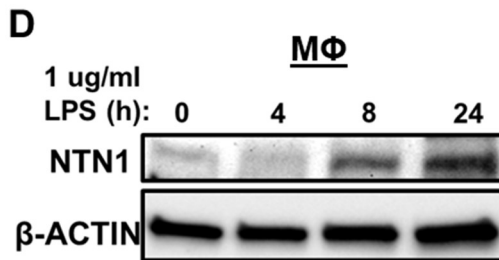
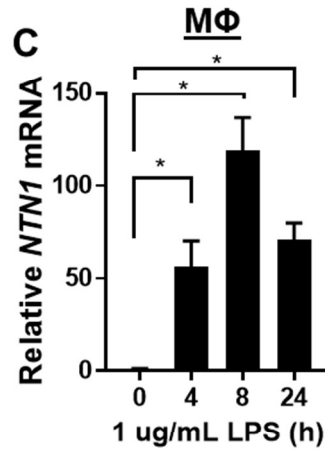
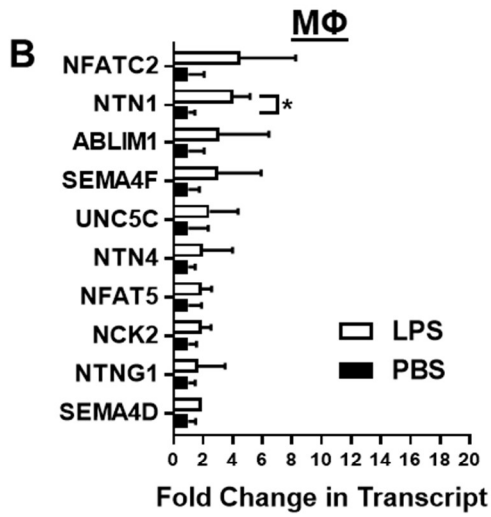
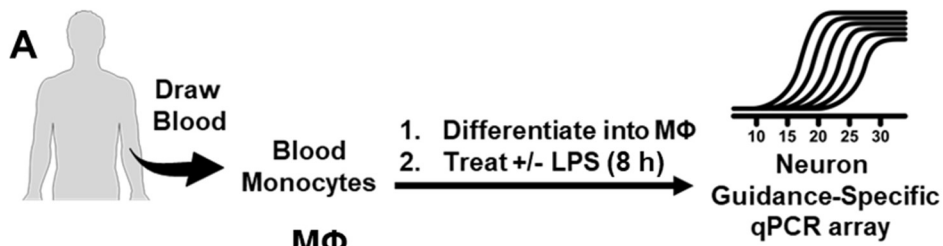


Figure 19: Netrin-1 is significantly upregulated in endotoxin treated myeloid cells.

(Figure on previous page)

A) Monocytes were isolated from blood of healthy donors and differentiated into macrophages (MΦs) then treated with LPS (1 ug/mL for 8 hours). RNA was isolated and used to perform a neuron guidance-specific RT-qPCR array.

B) The top upregulated genes from the array demonstrated the netrin-1 gene (*NTN1*) as the top-statistically significant induced gene (n=4, Bonferroni adjusted unpaired or Welch's t test).

C) PCR confirmation of *NTN1* upregulation in LPS stimulated human blood-derived MΦs (n=3 per group, one-way ANOVA with Dunnett's post-hoc tests).

D and E) Representative image and quantification for Western blot for netrin-1 protein expression in LPS treated MΦs (n=3 per group, one-way ANOVA with Dunnett's post-hoc tests).

F) Peripheral polymorphonuclear neutrophils (PMNs) were isolated from healthy donors and treated with 1 ug/mL of LPS for 8 hours.

G) *NTN1* RT-qPCR using RNA isolation from LPS treated PMNs (n=3 per group, unpaired t-test).

H and I) Representative image and quantification for Western blot for netrin-1 protein expression in LPS treated PMNs (n=3, unpaired t-test).

All data are represented as mean \pm SD; * p-value <0.05.

Myeloid cells express high levels of netrin-1 during LPS-induced lung injury

In order to investigate whether netrin-1 is expressed in myeloid cells during sepsis-associated lung inflammation, we utilized a murine model of LPS-induced lung injury, which results in significant recruitment and activation of leukocytes.^{349, 522-525} After intratracheal (i.t.) instillation of a weight-based dose of LPS (Figure 20A), Mice had the highest measured peak weight loss and bronchoalveolar lavage (BAL) cell counts 3 days after LPS challenge (Figure 20B, C). Because peak leukocyte infiltration was observed 3 days post LPS instillation, we performed western blot analysis for netrin-1 protein expression in lung tissue lysates collected at this time point. Netrin-1 protein was significantly upregulated in lung tissue lysates (Figure 20D, E). Next, we further characterized the localization of netrin-1 in the lungs of mice with LPS-induced lung injury by immunohistochemistry staining for netrin-1. Netrin-1 staining was observed primarily in alveolar airspace infiltrating leukocytes (Figure 20F). Furthermore, we quantified the netrin-1 expression on the surface of naïve alveolar macrophages (Ly6G⁻ F4/80⁺, collected from i.t. PBS-treated controls), BAL macrophages (Ly6G⁻ F4/80⁺), and PMNs (Ly6G⁺ F4/80⁻) isolated from mice 3 days after i.t. instillation of LPS by flow cytometry. Netrin-1 levels were significantly elevated in BAL macrophages after i.t. LPS instillation when compared to naïve alveolar macrophages (Figure 20G, H). Interestingly, netrin-1 expression was significantly reduced in infiltrating PMNs when compared with both naïve alveolar macrophages and macrophages collected from i.t. LPS-treated mice (Figure 20G, H). Finally, immunofluorescence staining of BAL cells demonstrated macrophage dominant netrin-1 expression 3 days after i.t. LPS treatment (Figure 20I). Taken together, these data indicate that netrin-1 is highly expressed in BAL macrophages during i.t. LPS-induced lung injury.

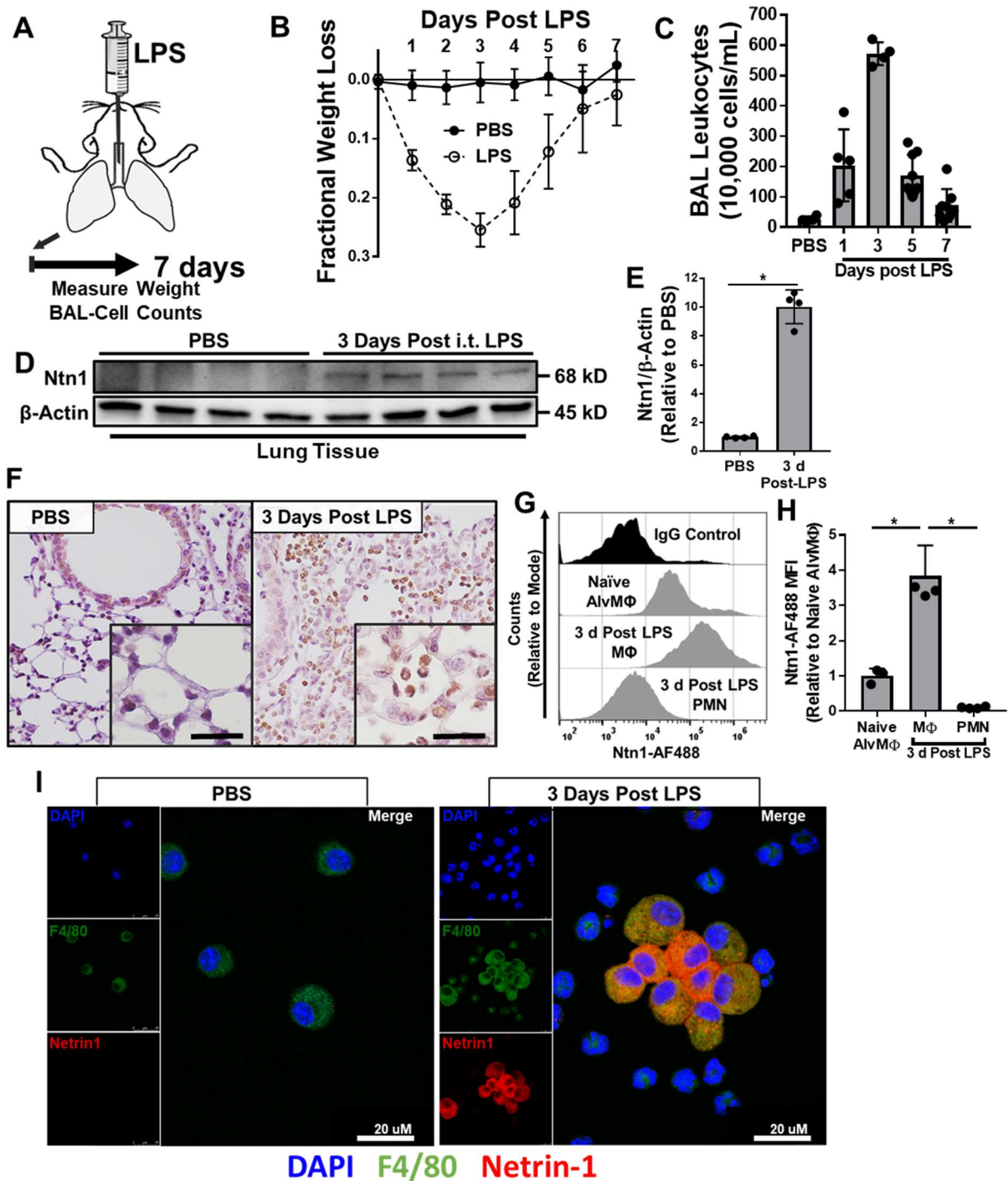


Figure 20: Myeloid cells recruited during endotoxin-induced lung injury have high levels of netrin-1.

A) Schematic for LPS-induced lung injury in mice. Mice were administered intra-tracheal instillation of LPS (3.75 $\mu\text{g/g}$ of body weight) or PBS for control and then monitored for weight

Figure 20 (Continued):

loss or collected 1, 3, 5, or 7 days later for quantification of bronchoalveolar lavage (BAL) leukocytes.

B) Fractional weight loss measured in mice during LPS-induced lung injury (n=10 in the PBS group, n=29 in the LPS group).

C) BAL leukocytes counts in mice collected 1, 3, 5, or 7 days after LPS-induced lung injury (n=4-9 per group, one-way ANOVA with Bonferroni post-hoc tests).

D and E) Image and densitometry quantification for Western blot for netrin-1 protein expression in lung tissue isolated from mice 3 days after LPS or PBS instillation (n=4 mice per group, Mann-Whitney test).

F) Representative immunohistochemistry staining for netrin-1 in formalin-fixed paraffin-embedded lung from mice 3 days after LPS or PBS instillation (n=3 replicates per group, images are magnified 40X with 120X inserts).

G) Representative flow cytometry histogram counts for netrin-1 expression in PBS control BAL alveolar macrophages (Naïve Alveolar Macrophage, Ly6G⁻ F4/80⁺) or in BAL macrophages (Macrophage, Ly6G⁻ F4/80⁺) and neutrophils (PMN, Ly6G⁺ F4/80⁻) from mice 3 days after LPS instillation (n=3-4 mice per group, counts relative to mode).

H) Netrin-1 flow cytometry mean fluorescent intensity quantification (n=3-4 per group, one-way ANOVA with Bonferroni post-hoc tests).

I) Representative immunofluorescence staining of BAL leukocytes isolated 3 days after LPS or PBS instillation demonstrating co-staining for F4/80 with netrin-1 (n=3 mice per group).

All data are represented as mean \pm SD; * p-value <0.05.

Netrin1 expression in myeloid cells is dependent on HIF-1 α

Previous work has demonstrated that HIF-1 α directly targets the promoter of the netrin-1 to induce its transcription.⁵⁰³ Consistently, we identified an essential DNA binding element for HIF-1 α , named hypoxia response element (HRE; 5'-GCGTG-3')³⁰⁹, located 303 nucleotide base pairs upstream from the transcriptional start site of netrin-1 (Figure 21A). To investigate the role of HIF-1 α in the expression of netrin-1 in LPS-stimulated human monocyte derived M Φ s, we performed chromatin immunoprecipitation (ChIP) quantitative PCR to assess HIF-1 α binding to the HRE located in the netrin-1 promoter. After stimulation with LPS for 8 hours, we observed a significant increase in HIF-1 α association to the netrin-1 promoter compared with PBS treated controls (Figure 21B). Next, we sought to determine if the expression of netrin-1 in BAL leukocytes is dependent on HIF-1 α during LPS-induced lung injury *in vivo*. To address this question, we utilized *Hif1a*^{loxp/loxp} LysM Cre mice that contain a conditional deletion for *Hif1a* in myeloid cells.⁵²⁶ On day 3 after LPS instillation, BAL leukocytes isolated from *Hif1a*^{loxp/loxp} LysM Cre mice had a significant reduction in netrin-1 transcript levels when compared to LysM Cre control mice (Figure 21C). Similarly, immunohistochemistry staining revealed abrogated netrin-1 protein in BAL cells collected from *Hif1a*^{loxp/loxp} LysM Cre mice on day 3 after LPS-induced lung injury (Figure 21D). In order to assess for potential non-myeloid contributions of netrin-1 during lung inflammation, we measured the protein level of netrin-1 in total lung tissue of *Hif1a*^{loxp/loxp} LysM Cre mice 3 days after LPS instillation. As we previously observed in C57BL/6 mice, netrin-1 expression is increased in lung tissue of LysM Cre control mice 3 days after LPS instillation, which was completely abolished in *Hif1a*^{loxp/loxp} LysM Cre mice (Figure 21E, F). These results indicate that netrin-1 expression in infiltrating myeloid cells during LPS-induced lung injury is dependent on HIF-1 α and support the importance of myeloid cells in netrin-1 induction during lung inflammation.

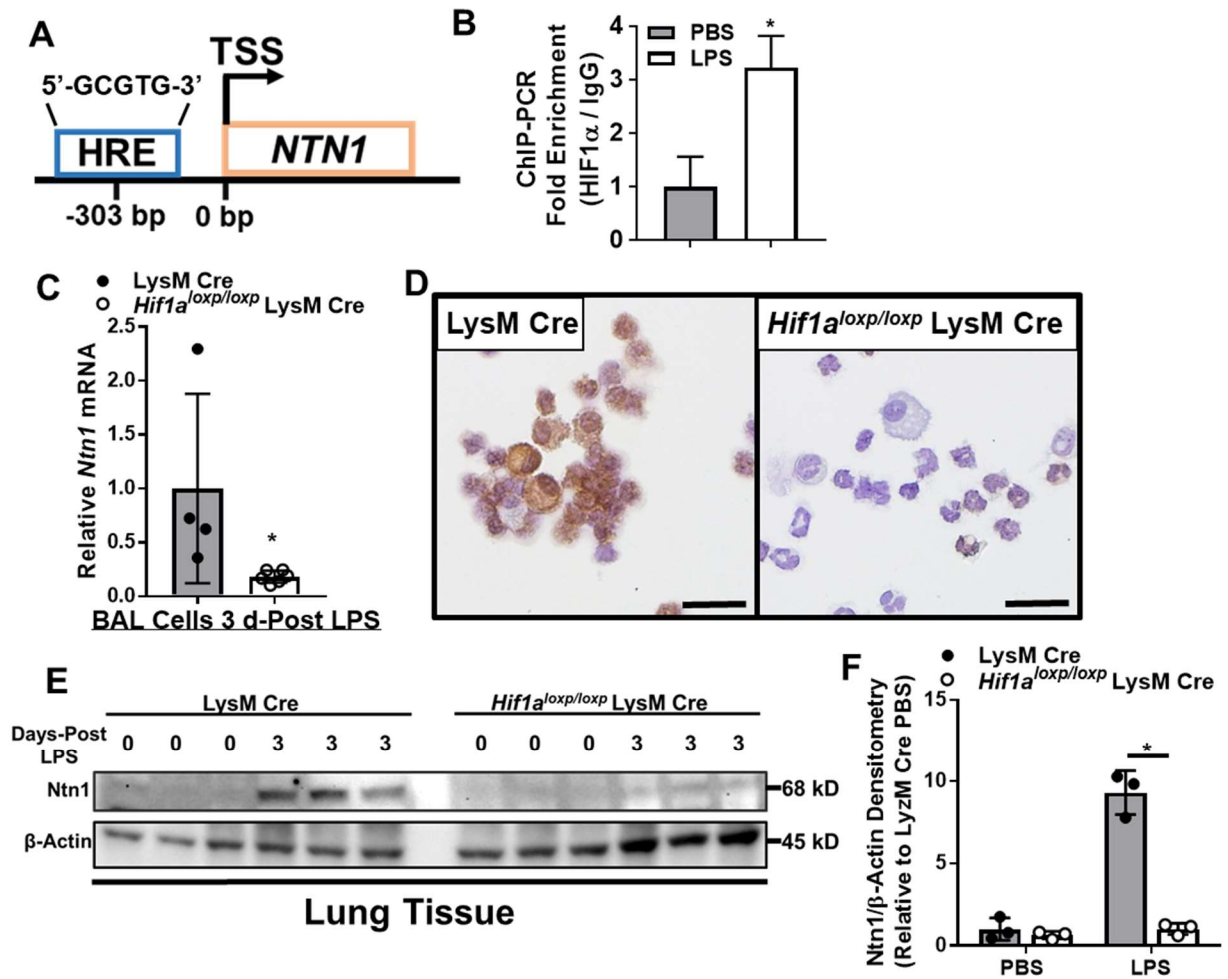


Figure 21: LPS-induced netrin-1 expression in myeloid cells is regulated by HIF-1 α .

A) Schematic illustrating the location of a hypoxia response element (HRE) 303 base pairs upstream of the transcriptional start site (TSS) of *NTN1*.

B) Human monocyte-derived M Φ s were treated with LPS (1 μ g/mL) for 8 h and then fixed to induce DNA-protein cross-linking. Chromatin Immunoprecipitation (ChIP)-PCR targeting a sequence proximal to the HRE was performed to demonstrate fold enrichment for HIF-1 α association with the promoter of *NTN1* compared with IgG isotype control. Data are normalized relative to PBS treated M Φ s (n=3, unpaired t-test).

Figure 21 (Continued):

C) Relative expression of *Ntn1* in BAL cells collected from mice with conditional genetic deletion of *Hif1 α* in myeloid cells (*Hif1 α ^{loxp/loxp}* LysM Cre) 3 days after onset of LPS-induced lung injury compared with LysM Cre mice for control (n=4-6 mice per group, Mann-Whitney test).

D) Representative immunohistochemistry staining for netrin-1 protein in BAL cells isolated from *Hif1 α ^{loxp/loxp}* LysM Cre mice 3 days after onset of LPS-induced lung injury compared with LysM Cre mice (n=3).

E and F) Densitometry and western blot image and quantification for netrin-1 protein expression in lung tissue of LysM Cre and *Hif1 α ^{loxp/loxp}* LysM Cre 3 days after the onset of LPS-induced lung injury (n=3 mice per group, two-way ANOVA with Bonferroni post-hoc tests).

All data are represented as mean \pm SD; * p-value <0.05.

Netrin-1 deletion in myeloid cells results in exacerbated LPS-induced lung injury

In order to investigate the functional role for myeloid-cell derived netrin-1 during LPS-induced lung injury, we cross-bred *Ntn1^{loxp/loxp}* mice with LysM Cre mice to generate offspring that are deficient for netrin-1 in myeloid cells (*Ntn1^{loxp/loxp}* LysM Cre). Following LPS instillation, *Ntn1^{loxp/loxp}* LysM Cre mice had statistically increased mortality and delayed recovery of weight loss in surviving mice compared to LysM Cre mice (Figure 22A, B). Additionally, increased albumin concentration was observed in bronchoalveolar lavage fluid (BALF) from *Ntn1^{loxp/loxp}* LysM Cre mice at 3 days post LPS instillation, suggesting elevated pulmonary edema (Figure 22C). Additionally, we observed elevated BAL neutrophil counts and BALF IL-1 β and IL-6 protein levels in *Ntn1^{loxp/loxp}* LysM Cre mice 3 days after LPS instillation compared with LysM Cre controls, suggesting increased levels of pulmonary inflammation in these animals (Figure 22D, E, F). Finally, blinded pathological scoring of lung tissue harvested from mice 3 days after LPS instillation suggested increased lung pathology in *Ntn1^{loxp/loxp}* LysM Cre mice (Figure 22G, H). Altogether, netrin-1 deletion in myeloid cells results in a worsened outcome, increased inflammatory markers and lung pathology during LPS-induced lung injury.

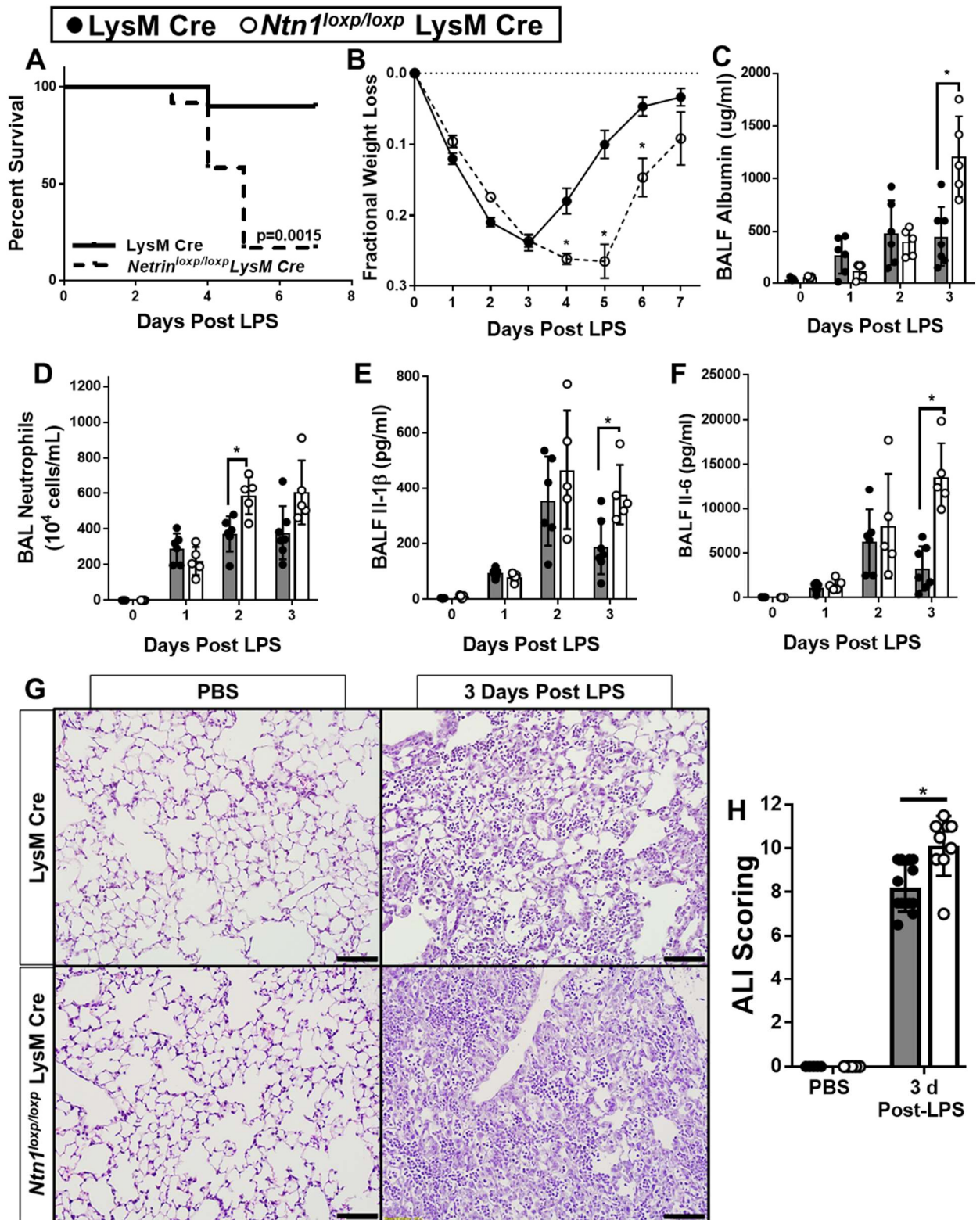


Figure 22: Netrin-1 deletion in myeloid cells exacerbates LPS-induced lung injury.

A) Mortality of mice with conditional deletion of *Ntn1* in myeloid cells (*Ntn1^{loxp/loxp} LysM Cre*) compared with *LysM Cre* control mice in LPS-induced lung injury (n=10 mice in *LysM Cre*

Figure 22 (Continued):

group, n=12 mice in *Ntn1^{loxp/loxp}* LysM Cre group, Kaplan-Meier curves, log-rank test).

B) Fractional weight loss in *Ntn1^{loxp/loxp}* LysM Cre mice compared with LysM Cre controls (n=10-12 mice per group, Bonferroni-adjusted Welch's or unpaired t test).

C) Pulmonary edema was assessed by enzyme-linked immunosorbent assay (ELISA) quantification of bronchoalveolar lavage fluid (BALF) albumin in *Ntn1^{loxp/loxp}* LysM Cre and LysM Cre mice with LPS-induced lung injury at indicated time points (n=5-7 mice per group, Bonferroni-adjusted unpaired t-test).

D) Quantification of BAL neutrophils in *Ntn1^{loxp/loxp}* LysM Cre and LysM Cre mice with LPS-induced lung injury at indicated time points (n=5-7 mice per group, Bonferroni-adjusted unpaired t-tests).

E and F) ELISA quantification of inflammatory cytokines, IL-1 β and IL-6, in BALF collected from *Ntn1^{loxp/loxp}* LysM Cre and LysM Cre mice with LPS-induced lung injury at indicated time points (n=5-7 mice per group, Bonferroni-adjusted unpaired t-test).

G and H) Representative sections and lung injury scoring of hematoxylin and eosin stained lung tissue collected from *Ntn1^{loxp/loxp}* LysM Cre and LysM Cre mice 3 days after onset of LPS-induced lung injury (40X magnification, n=5-13 mice per group, unpaired t-test).

All data are represented as mean \pm SD. * p-value <0.05.

Increased NK cell infiltration in *Ntn1^{loxp/loxp}* LysM Cre mice during LPS-induced lung injury

Based on the profound increase in lung inflammation in *Ntn1^{loxp/loxp}* LysM Cre mice following i.t. LPS instillation, we next set out to gain mechanistic insight on the regulatory role of myeloid-derived netrin-1 by transcriptomic approach. Because we initially demonstrated an insignificant contribution of neutrophils in netrin-1 expression, we performed mRNA sequencing using RNA isolated from BAL cells collected on day 3 after LPS instillation that was depleted of neutrophils (Figure 23A). Differential gene regulation analysis revealed 105 down-regulated (fold change <0.5) and 145 up-regulated (fold change >2) statistically significant (False Discovery Rate < 0.05) genes (Figure 23B). Gene Ontology and KEGG pathway enrichment analysis of down-regulated genes did not identify any enriched pathways, but up-regulated genes revealed an increase in multiple pathways, with the highest enrichment being in NK cell-mediated cytotoxicity (Figure 23C). To determine if the enrichment in the NK-cell mediated cytotoxicity KEGG pathway was attributed to an increased number of NK cells in the total BAL cells, we first analyzed the up-regulated genes using CellKB, which uses a rank-biased overlap method to match the up-regulated genes to cell-type marker sets that are published in the literature (CellKB, <https://cellkb.combinatics.com/>). We found that 87 of the 145 up-regulated genes were matched to NK cell gene sets, with an expression-weighted match score of 66.31, both of which were the strongest signals amongst other cell types that were matched (Figure 23D). Interestingly, the macrophage cell type represented the weakest match result from the CellKB algorithm (Figure 23D), suggesting differential gene regulation was not a result of transcriptomic changes between *Ntn1^{loxp/loxp}* LysM Cre and LysM Cre control macrophages. In order to investigate whether there is an increase in NK cell numbers in the alveolar airspace during LPS-induced lung injury in *Ntn1^{loxp/loxp}* LysM Cre mice, we performed flow cytometry using BAL cells collected 3 days after LPS instillation and gated for NK cells (CD3⁻ NK1.1⁺). Consistent with our transcriptomic results, we observed an increased percentage and the total number of NK cells in the BAL of *Ntn1^{loxp/loxp}* LysM Cre mice when compared with LysM Cre

controls (Figure 23F, G). Altogether, these results demonstrate that myeloid-cell derived netrin-1 plays a critical role in NK cell recruitment during LPS-induced lung injury.

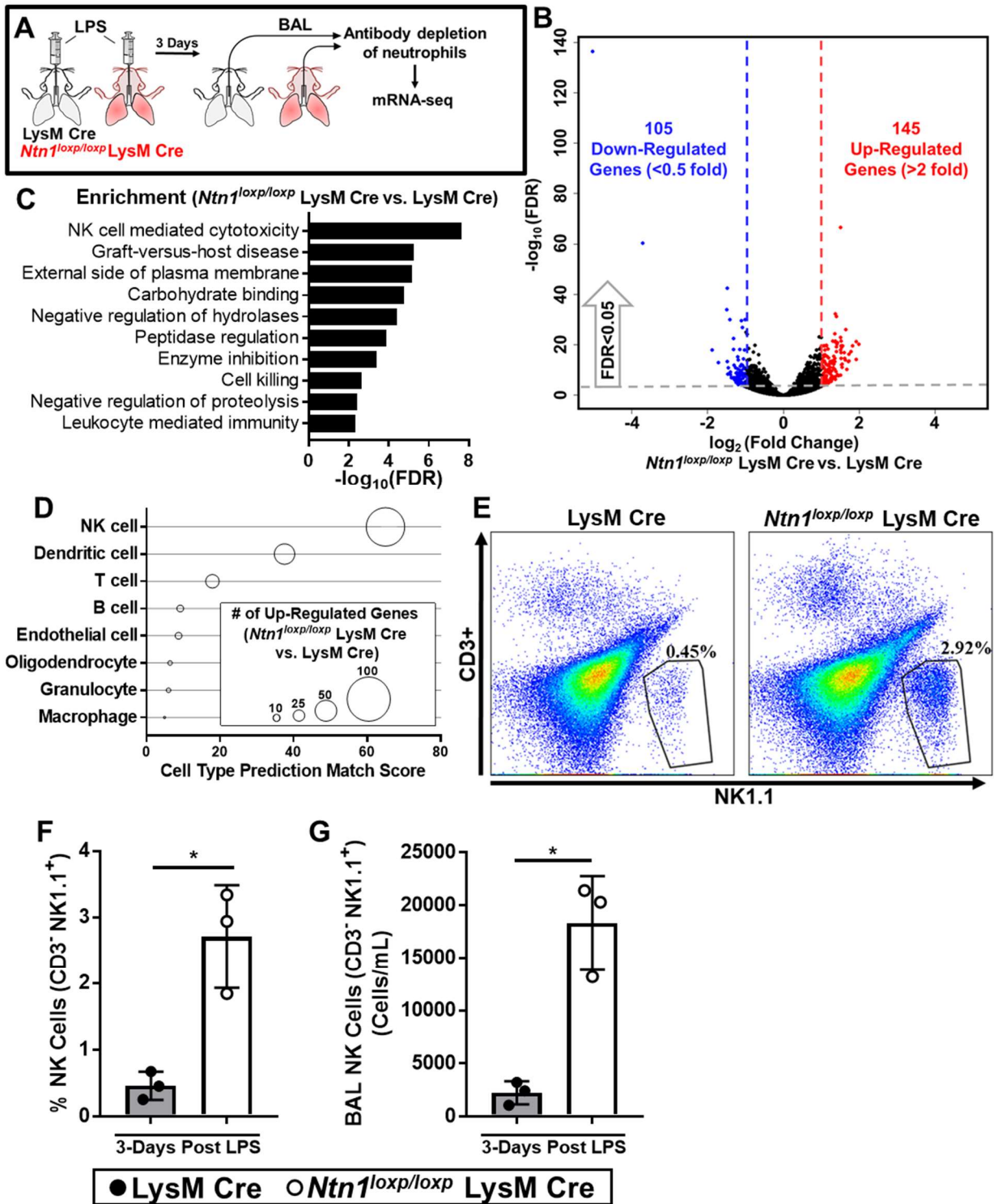


Figure 23: *Ntn1^{loxp/loxp}* LysM Cre mice display increased natural killer (NK) cell infiltration in the airway during LPS-induced lung injury.

A) Experimental scheme: bronchia alveolar lavage (BAL) cells were collected from LysM Cre and *Ntn1^{loxp/loxp}* LysM Cre mice 3 days after onset of LPS-induced lung injury and then depleted

Figure 23 (Continued):

for neutrophils before RNA isolation. RNA was then submitted for analysis via mRNA-seq.

B) Volcano plot of up- and down-regulated genes in BAL cells collected from *Ntn1^{loxp/loxp}* LysM Cre mice when compared with LysM Cre controls (n=3 mice the *Ntn1^{loxp/loxp}* LysM Cre group, n=4 in LysM Cre group, the threshold for FDR was < 0.05, thresholds for fold change were <0.5 or >2).

C) Pathway enrichment analysis for up-regulated genes in BAL cells collected from *Ntn1^{loxp/loxp}* LysM Cre mice when compared with LysM Cre controls.

D) CellKB analysis was used to match up-regulated genes with cell-type marker sets that are published in the literature. Diameters of circles indicate the number of genes matching to each cell-type marker set and the prediction match score is weighted by the fold enrichment of the corresponding matching genes.

E, F, and G) Representative gating and quantification (percentage and total) for NK cells (CD3⁻ NK1.1⁺) in the BAL of LysM Cre and *Ntn1^{loxp/loxp}* LysM Cre mice 3 days after onset of LPS-induced lung injury (n=3 mice per group, unpaired t-test).

All data are represented as mean ± SD; * p-value <0.05.

CCL2 elevation in *Ntn1*^{loxp/loxp} LysM Cre mice is associated with increased NK cell levels and inflammation

After having shown an increased NK cell infiltration in *Ntn1*^{loxp/loxp} LysM Cre mice during LPS-induced inflammation, we subsequently pursued studies to address a potential mechanistic cause. Previous studies of lung inflammation have demonstrated a role for chemokine-mediated recruitment of NK cells.⁵²⁷⁻⁵²⁹ We, therefore, hypothesized that chemoattractant signal is responsible for the increased accumulation of NK cells in *Ntn1*^{loxp/loxp} LysM Cre mice during LPS-induced lung injury. To identify potential chemokine or cytokine mediators, we performed a membrane-based antibody array to measure relative levels of cytokines and chemokines in the BALF of *Ntn1*^{loxp/loxp} LysM Cre mice and LysM Cre mice 3 days after intratracheal LPS instillation. We found protein expression of CCL2, a chemoattractant for NK cells^{527, 530, 531}, to be the most elevated cytokine or chemokine in BALF of *Ntn1*^{loxp/loxp} LysM Cre mice (Figure 24A, B). Using ELISA, we confirmed the elevation of CCL2 in the BALF of *Ntn1*^{loxp/loxp} LysM Cre mice compared with LysM Cre mice 3 days after intratracheal LPS instillation (Figure 24C). Consequently, we pursued the notion that CCL2 inhibition might reverse the elevated NK cell recruitment and lung inflammation in *Ntn1*^{loxp/loxp} LysM Cre mice. Thus, we treated *Ntn1*^{loxp/loxp} LysM Cre mice with intraperitoneal neutralizing antibodies against CCL2 on days 1 and 2 after intratracheal instillation of LPS, and then assessed NK cell recruitment and lung inflammation on day 3 (Figure 24D). Compared with IgG treated controls, *Ntn1*^{loxp/loxp} LysM Cre mice treated with CCL2 neutralizing antibodies had a statistically significant reduction in total BAL NK cells via flow cytometry (Figure 24E). *Ntn1*^{loxp/loxp} LysM Cre mice treated with CCL2 neutralizing antibodies also had a significant reduction in infiltrating BAL neutrophils and in alveolar barrier permeability, as indicated by reduced BALF albumin concentration (Figure 24F, G). Upon histological evaluation of hematoxylin and eosin-stained lung tissue, there was a statistically significant reduction in lung pathology as determined by blinded pathological scoring (Figure 24H, I). Taken together, these studies support the role of myeloid-derived netrin-1 in limiting CCL2-mediated NK cell recruitment during lung inflammation.

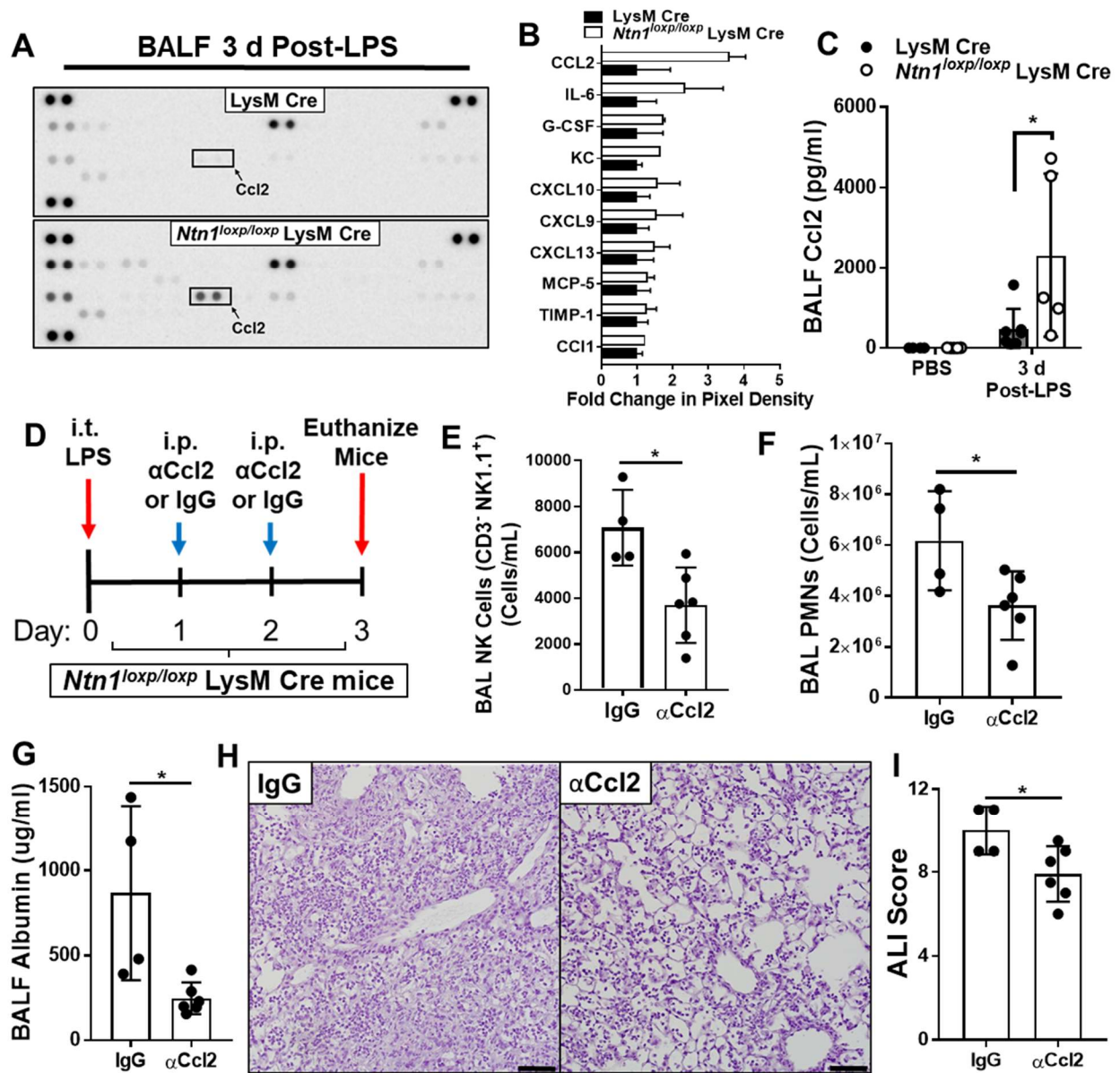


Figure 24: C-C motif chemokine ligand 2 (CCL2) neutralization in *Ntn1^{loxp/loxp}* LysM Cre mice reduces natural killer (NK) cell infiltration in the airway and improves LPS-induced lung injury.

A) Using Bronchoalveolar lavage fluid (BALF) collected from LysM Cre and *Ntn1^{loxp/loxp}* LysM Cre mice 3 days after onset of LPS-induced lung injury, we performed a membrane-based sandwich immunoassay to profile for changes in inflammatory cytokines and chemokines. Representative dot-blots of the membrane-based immunoassay.

Figure 24 (Continued):

B) Quantified pixel density of the top ten up-regulated cytokines/chemokines in *Ntn1*^{loxp/loxp} LysM Cre mice relative to LysM Cre controls (n=2 per group).

C) CCL2 up-regulation was confirmed in BALF of *Ntn1*^{loxp/loxp} LysM Cre mice relative to LysM Cre mice 3 days after onset of LPS-induced lung injury using enzyme-linked immunosorbent assay (ELISA) (n=4-7 mice per group, Bonferroni-adjusted unpaired t-test).

D) Experimental scheme: *Ntn1*^{loxp/loxp} LysM Cre were given LPS-induced lung injury and then subsequently given intraperitoneal (i.p.) injections of neutralizing CCL2 antibodies (α CCL2) or IgG isotype control (10 μ g/g of body weight) on days 1 and 2 after the onset of lung inflammation. Mice were subsequently euthanized for analysis on day 3 after the onset of lung inflammation.

E) Quantification of total NK cells (CD3⁻ NK1.1⁺) in the BAL collected from α CCL2-treated *Ntn1*^{loxp/loxp} LysM Cre mice 3 days after onset of LPS-induced inflammation was measured by flow cytometry (n=4-6 mice per group, unpaired t-test).

F) Quantification of total polymorphonuclear neutrophils (PMNs) in the BAL collected from α CCL2-treated *Ntn1*^{loxp/loxp} LysM Cre mice 3 days after onset of LPS-induced lung injury (n=4-6 mice per group, unpaired t-test).

G) Pulmonary edema was assessed by enzyme-linked immunosorbent assay (ELISA) quantification of bronchoalveolar lavage fluid (BALF) albumin in α CCL2-treated *Ntn1*^{loxp/loxp} LysM Cre mice (n=4-6 mice per group, Mann-Whitney test).

H and I) Representative hematoxylin and eosin staining and lung pathology scoring of lung sections from α CCL2-treated *Ntn1*^{loxp/loxp} LysM Cre mice (n=4-6 mice per group, unpaired t-test).

All data are represented as mean \pm SD; * p-value <0.05.

4.4 Conclusions and Significance

An increasingly recognized class of immune-modulators is the NGPs.⁴⁹⁹ The present studies aim at investigating the role of myeloid cell-derived NGPs during sepsis-associated lung inflammation. Through a qPCR-based screen, we identified netrin-1 to be highly upregulated in LPS stimulated human monocyte-derived macrophages, as well as in peripheral circulating neutrophils. During LPS-induced lung injury in mice, pulmonary netrin-1 was significantly elevated 3 days after the onset of inflammation, which coincided with the peak infiltration of immune cells into the alveolar airspace. Using immunohistochemistry and flow cytometry, we localized netrin-1 expression to infiltrating immune cells, particularly in macrophages. Subsequent transcriptional studies identified Hif-1 α as a key transcriptional factor for netrin-1 regulation, and transgenic mice lacking HIF-1 α in the myeloid compartment failed to induce netrin 1 during LPS-induced lung injury. Furthermore, the deletion of netrin-1 in the myeloid cell compartment (*Ntn1*^{loxp/loxp} LysM Cre) resulted in worsened outcomes during LPS-induced lung injury in mice, indicating a protective role for myeloid cell-derived netrin-1. Surprisingly, increased NK cell and CCL2 accumulation are observed in *Ntn1*^{loxp/loxp} LysM Cre mice. Lastly, when *Ntn1*^{loxp/loxp} LysM Cre mice were treated with CCL2 neutralizing antibodies, we observed a reduction in NK cell recruitment and improvement in lung inflammation. Together, these data reveal myeloid-derived netrin-1 as a critical negative feedback mechanism during lung inflammation.

Our findings that myeloid-derived netrin-1 protects mice against lung inflammation are in alignment with other studies. Netrin-1 has been reported to dampen inflammation in several models of inflammatory conditions including peritonitis,⁵¹² acute lung injury^{502, 532} kidney ischemia-reperfusion injury,^{514, 533} arthritis,⁵³⁴ and colitis.⁵³⁵ Mechanistically, netrin-1 serves to limit inflammation by regulation of leukocyte migration and accumulation^{534, 536-538} and is also shown to facilitate the active resolution of inflammation by promoting pro-resolving mediator expression during peritonitis⁵¹⁷ and liver ischemia-reperfusion injury.⁵³⁹ *Ex vivo* netrin-1

treatment of macrophages and endogenous overexpression of netrin-1 *in vivo* was found to promote the transition to an anti-inflammatory M2-like phenotype macrophage, which acts to limit inflammation and encourage wound healing.^{514, 533, 538} Previous studies have also demonstrated that netrin-1 is expressed by myeloid cells and plays a functional role in disease conditions. For example, macrophage-derived netrin-1 has been shown to promote retention of adipose tissue macrophages leading to insulin resistance,⁵⁴⁰ promote the development of atherosclerosis,⁵⁰⁴ and to support the progression of aortic aneurysms.⁵⁴¹ Thus, myeloid cell-derived netrin-1 plays diverse regulatory roles under different inflammatory conditions, such as in the case of adenosine signaling.^{331, 344}

Several previous studies have demonstrated hypoxia and HIF-1 α -dependent expression of netrin-1 during inflammatory conditions. HIF-1 α -dependence netrin-1 induction in mucosal epithelial cells has been illustrated in models of hypoxia-induced mucosal inflammation.⁵⁰³ In addition, macrophages found in hypoxic regions of atherosclerotic show increased netrin-1 level in both human and mouse studies, and HIF activation induces netrin-1 expression in macrophages in a HIF-1 α dependent manner.⁵⁴² Besides HIF-1 α dependent induction, netrin-1 expression is also controlled by NF- κ B, and NF- κ B can act as both a transcriptional activator⁵⁴³ and repressor.⁵⁰² Furthermore, vagal nerve innervation has also been shown to regulate pulmonary expression of netrin-1 as unilateral vagotomy decreases netrin-1 expression in the lung.⁵¹⁷ However, the neuronal stimulation of netrin-1 expression in myeloid cells is unknown.

Netrin-1 imparts cellular functions through interacting with its receptors. The best described netrin-1 receptors during inflammatory regulation are uncoordinated receptor 5 (UNC5b), the neogenin receptor, and the adenosine 2B (A2B) receptor.^{502, 503, 505, 512} Netrin-1 interacting with UNC5b on leukocytes has been implicated in regulating migratory functions as well as dampening inflammatory cytokine expression.^{504, 540, 541, 544} The A2B receptor is involved in regulating inflammation in response to elevated extracellular adenosine levels that are commonly present during settings of tissue injury and has also been demonstrated to be a

critical mediator for netrin-1 regulation of inflammation.^{340, 525, 537, 545, 546} Previous studies have shown that the A2B receptor mediates netrin-1 induced expression of resolution mediators to promote regeneration during liver inflammation,⁵³⁹ dampening of inflammation during peritonitis,⁵¹² attenuate experimental colitis,⁵³⁵ and limit pulmonary inflammation.⁵⁰² In contrast with UNC5b and the A2B receptor, the netrin-1 receptor, neogenin, has been shown to promote acute inflammation and inhibit monocyte polarization toward anti-inflammatory and pro-resolution phenotypes.^{547, 548}

The present studies have established an exciting new link between myeloid-derived netrin 1 and NK cell migration during endotoxin-induced lung injury. Indeed, others have reported NK cells as drivers of immune-pathology in several models of organ injuries.⁵⁴⁹⁻⁵⁵² For example, tissue-resident NK cells promote ischemic kidney injury by mediating local responses.⁵⁵⁰ During LPS-induced lung injury, it was shown that NK cell depletion in mice resulted in reduced chemokine-mediated neutrophil recruitment and improved outcomes.⁵⁵¹ Additionally, NK cells were reported to be primary drivers of immune-pathology during a model of interstitial pneumonia.⁵⁵² In models of viral infection, NK cells were implicated as the critical players in causing excessive inflammation leading to bystander lung tissue injury which was reversed by antibody-mediated depletion.^{553, 554} Interestingly, pre-infecting mice with *Klebsiella pneumoniae* provided protection in subsequent lethal challenges of influenza virus, which was attributed to *K. pneumoniae*-conditioned reduction of NK cell recruitment and inflammation.⁵⁵⁵ Consistent with our findings of CCL2-driven NK cell accumulation in *Ntn1^{loxp/loxp}* LysM Cre mice, previous work has implicated CCL2 in the recruitment of NK cells during a model of invasive pulmonary aspergillosis infection.⁵²⁷

Our studies have several limitations. *Ntn1^{loxp/loxp}* LysM Cre mice have a deletion of netrin 1 in macrophage and neutrophil populations, as well as in other granulocytes^{457, 458}. Thus, the profound phenotype in these mice could be mediated by several cell types together. To further dissect the specific role of netrin 1 in macrophages and neutrophils during endotoxin-induced

lung injury, *Ntn1*^{loxP/loxP} mice could be cross-bred with hCD68-rtTA/ Teto-Cre mice, and MRP8-Cre mice, respectively. Furthermore, the contribution of myeloid netrin 1 in NK cell recruitment was only indicated in *in vivo* studies. Further *in vitro* experiments will facilitate the determination of direct or indirect interaction between these two cell populations. Finally, although we have identified the upregulation of netrin 1 in human neutrophils and macrophages during inflammatory stimulation, the functional role of netrin 1 in NK cell recruitment during human endotoxin-induced lung injury was not explored in our study. Additional studies employing lung tissues and cells isolated from respiratory washout from patients suffering from lung gram-negative bacteria infection or sepsis would be crucial to illustrate this particular interaction.

Altogether, these findings highlight a novel role of myeloid cell-derived netrin-1 during pulmonary inflammation in limiting excessive inflammation. The impact of myeloid-derived netrin 1 is achieved by orchestrating CCL2 mediated NK cell infiltration during lung inflammation. Our studies indicate a novel mechanism for the immune-modulatory effect of netrin-1 in myeloid cells, particularly during lung injury. Our studies have also implied a functional role of myeloid-derived netrin 1 in NK cell recruitment, which contributes to the complexity of netrin 1 biology for the field. Moreover, our studies suggest that myeloid-derived netrin 1 might play an important role in other diseases where NK cells play major functional roles, e.g. cancer⁵⁵⁶, autoimmune diseases⁵⁵⁷, and viral infection⁵⁵⁸. Thus, investigating how myeloid-derived netrin 1 contributes to the pathophysiology of these conditions could be of great interest to the field. Finally, future work should focus on dissecting the target cells of myeloid-derived netrin-1 as the sources of CCL2, as well as the receptor that mediates its immune-modulatory effects.

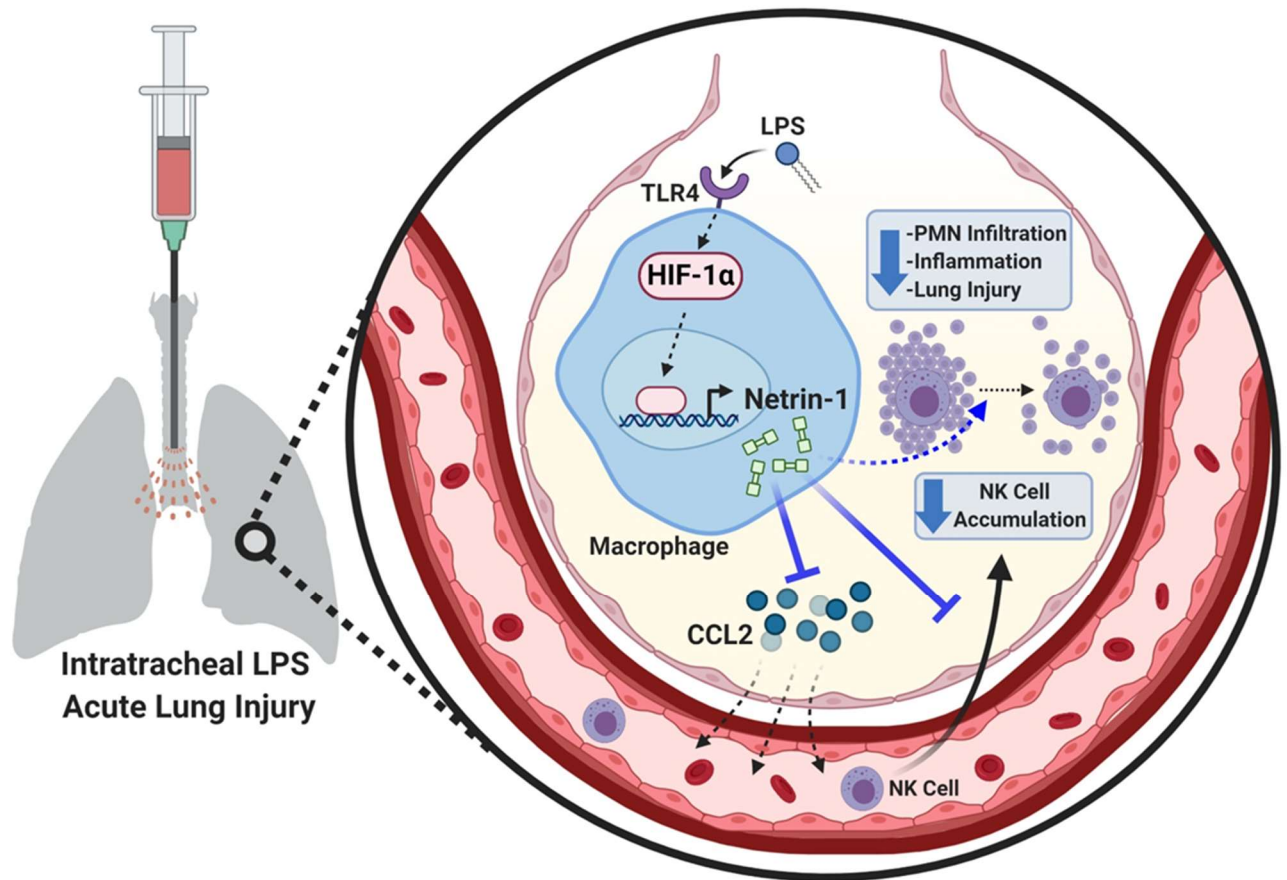


Figure 25: Proposed mechanism for myeloid cell-derived Netrin-1 during LPS-induced acute lung injury.

During acute lung injury initiated by intratracheal injection of LPS, macrophages are activated through toll-like receptor 4. Netrin-1 is expressed by activated macrophages via stabilization of the transcription factor, hypoxia inducible factor-1 alpha (Hif-1 α), which binds to and activates the promoter of Netrin-1. Myeloid-derived Netrin-1 plays a critical role in regulating chemokine (C-C motif) ligand 2 (CCL2) and subsequently limits the recruitment of proinflammatory natural killer (NK) cells. The ultimate effect of regulating NK cell accumulation by myeloid-derived Netrin-1 is to dampen inflammation, polymorphonuclear neutrophil (PMN) accumulation and lung injury. Created with BioRender.com.

Chapter 5: Conclusion of dissertation

The findings reported in this dissertation highlight several endogenous mechanisms in myeloid cells that work to regulate inflammation during ALI. In the first study (Chapter 3), we demonstrate the novel role for miR-147 in regulating macrophage-mediated inflammation by dampening their inflammatory functions via the epigenetic silencing of cytokine gene expression. In the second study (Chapter 4), the neuronal guidance peptide, Netrin-1, expressed in macrophages during ALI played an important role in the regulation of excessive inflammation associated with NK cell infiltration. Both findings are consistent with previous works establishing that the regulation of pro-inflammatory macrophages is critical for the proper resolution of ALI.^{281, 450, 452} Genetic deletion of either miR-147 or Netrin-1 resulted in exacerbated inflammation and tissue injury during LPS-induced ALI. As a consequence, we posit that these two regulatory genes might be leveraged as therapeutic targets.

In Chapter 3, we demonstrated that exogenous administration of liposome-packaged miR-147 mimics provided a therapeutic benefit for mice with LPS-induced ALI. This pre-clinical finding is exciting and invokes the potential for clinical translation. MicroRNA-based therapeutics have previously been proposed and are currently under investigation.^{559, 560} The first microRNA-based therapy was miR-34a. As a transcriptional target of p53 and potent tumor suppressor, miR-34a has shown potent pre-clinical evidence for controlling tumors and became the first miRNA-mediated treatment to enter clinical trials.⁵⁶¹⁻⁵⁶³ To date, there are over 15 miRNA-targeting therapies in development (clinical and pre-clinical trials).⁵⁶⁴ Though our results suggested that NDUFA4 is the primary target for miR-147 that is responsible for limiting inflammation in macrophages, it is possible there are other targets we did not identify in our RNA-based screen that work in concert with NDUFA4. An added benefit to a therapeutic miRNA approach is that exogenous administration of miR-147 would also account for these additional targets.

An important consideration of utilizing miR-147, as with most anti-inflammatory treatments (e.g. anti-TNF agents, steroids, etc.) is the concern that it may dampen the host's ability to clear or contain infection. Subsequent studies in our lab are already underway investigating the effects and timing of miR-147 treatment in infectious ALI models in mice in order to address these possibilities.

Therapeutic leveraging of Netrin-1 is another translational approach under investigation and has been studied as a biomarker for several disease types, but has not yet been utilized in clinical trials.⁵⁶⁵⁻⁵⁷⁰ In pre-clinical work, Netrin-1 imparts anti-inflammatory effects to protect a number of organ injuries, including acute lung injury,^{502, 532} peritonitis,⁵¹² arthritis,⁵³⁴ kidney ischemia-reperfusion injury,^{514, 533} myocardial ischemia,⁵⁷⁰ and colitis.⁵³⁵ With such strong pre-clinical evidence for Netrin-1 treatment as an anti-inflammatory agent, clinical trials in patients will be crucial in translating these findings.

In both Chapters of this dissertation, there is a commonality for the dependence on Hif-1 α . Both miR-147 and Netrin-1 were established as Hif-1 α transcriptional targets in macrophages, signifying that targeting hypoxia and Hif-1 α might also provide for a therapeutic approach for ALI and ARDS. HIF-stabilizing drugs have been developed and have demonstrated safe and effective use for anemia associated with chronic kidney disease.^{325, 326} With great excitement, a clinical trial utilizing the oral HIF activator, Vadadustat, is currently ongoing as a treatment for the prevention and treatment of ARDS in patients with COVID-19 (NCT04478071). The results of this trial could be the first to demonstrate whether there is efficacious use of HIF-stabilizing drugs in an inflammatory organ injury in human patients.

Regulating inflammatory processes of macrophages is a highly desirable approach to limiting inflammatory tissue damage leading to ALI and ARDS. Altogether, the work in this dissertation outlines two endogenous pathways that could provide targeted treatments towards dampening inflammation and promoting recovery from lung injury.

Bibliography:

1. Bernard, G. (2017) Acute Lung Failure - Our Evolving Understanding of ARDS. *N Engl J Med* **377**, 507-509
2. Ashbaugh, D., Boyd Bigelow, D., Petty, T., and Levine, B. (1967) ACUTE RESPIRATORY DISTRESS IN ADULTS. *The Lancet* **290**, 319-323
3. Bernard, G. R., Artigas, A., Brigham, K. L., Carlet, J., Falke, K., Hudson, L., Lamy, M., LeGall, J. R., Morris, A., and Spragg, R. (1994) Report of the American-European consensus conference on ARDS: definitions, mechanisms, relevant outcomes and clinical trial coordination. The Consensus Committee. *Intensive Care Med* **20**, 225-232
4. Ranieri, V. M., Rubenfeld, G. D., Thompson, B. T., Ferguson, N. D., Caldwell, E., Fan, E., Camporota, L., Slutsky, A. S., and Force, A. D. T. (2012) Acute respiratory distress syndrome: the Berlin Definition. *JAMA* **307**, 2526-2533
5. Thompson, B. T., Chambers, R. C., and Liu, K. D. (2017) Acute Respiratory Distress Syndrome. *New England Journal of Medicine* **377**, 562-572
6. Williams, G. W., Berg, N. K., Reskallah, A., Yuan, X., and Eltzschig, H. K. (2021) Acute Respiratory Distress Syndrome: Contemporary Management and Novel Approaches during COVID-19. *Anesthesiology* **134**, 270-282
7. Chen, L., Zhao, H., Alam, A., Mi, E., Eguchi, S., Yao, S., and Ma, D. (2019) Postoperative remote lung injury and its impact on surgical outcome. *BMC Anesthesiology* **19**, 30
8. Rubenfeld, G. D., Caldwell, E., Peabody, E., Weaver, J., Martin, D. P., Neff, M., Stern, E. J., and Hudson, L. D. (2005) Incidence and Outcomes of Acute Lung Injury. *New England Journal of Medicine* **353**, 1685-1693
9. Eworuke, E., Major, J. M., and Gilbert McClain, L. I. (2018) National incidence rates for Acute Respiratory Distress Syndrome (ARDS) and ARDS cause-specific factors in the United States (2006-2014). *J Crit Care* **47**, 192-197

10. Bellani, G., Laffey, J. G., Pham, T., Fan, E., Brochard, L., Esteban, A., Gattinoni, L., van Haren, F., Larsson, A., McAuley, D. F., Ranieri, M., Rubenfeld, G., Thompson, B. T., Wrigge, H., Slutsky, A. S., Pesenti, A., Investigators, L. S., and Group, E. T. (2016) Epidemiology, Patterns of Care, and Mortality for Patients With Acute Respiratory Distress Syndrome in Intensive Care Units in 50 Countries. *JAMA* **315**, 788-800
11. Association, A. H. (2015) *AHA Hospital Statistics 2015 Edition*, Health Forum Publishing Company. Accessed: January 30, 2021. ISBN: 13: 978-0872589551
12. Thompson, B. T., Chambers, R. C., and Liu, K. D. (2017) Acute Respiratory Distress Syndrome. *N Engl J Med* **377**, 562-572
13. Opitz, B., Laak, V. v., Eitel, J., and Suttorp, N. (2010) Innate Immune Recognition in Infectious and Noninfectious Diseases of the Lung. *American Journal of Respiratory and Critical Care Medicine* **181**, 1294-1309
14. Matthay, M. A., Zemans, R. L., Zimmerman, G. A., Arabi, Y. M., Beitler, J. R., Mercat, A., Herridge, M., Randolph, A. G., and Calfee, C. S. (2019) Acute respiratory distress syndrome. *Nature Reviews Disease Primers* **5**, 18
15. Matthay, M. A., Ware, L. B., and Zimmerman, G. A. (2012) The acute respiratory distress syndrome. *J Clin Invest* **122**, 2731-2740
16. Cardinal-Fernandez, P., Lorente, J. A., Ballen-Barragan, A., and Matute-Bello, G. (2017) Acute Respiratory Distress Syndrome and Diffuse Alveolar Damage. New Insights on a Complex Relationship. *Annals of the American Thoracic Society* **14**, 844-850
17. Lorente, J. A., Cardinal-Fernández, P., Muñoz, D., Frutos-Vivar, F., Thille, A. W., Jaramillo, C., Ballén-Barragán, A., Rodríguez, J. M., Peñuelas, O., Ortiz, G., Blanco, J., Pinheiro, B. V., Nin, N., del Carmen Marin, M., Esteban, A., and Thompson, T. B. (2015) Acute respiratory distress syndrome in patients with and without diffuse alveolar damage: an autopsy study. *Intensive Care Med* **41**, 1921-1930

18. Cardinal-Fernandez, P., Ortiz, G., Chang, C. H., Kao, K. C., Bertreau, E., Philipponnet, C., Casero-Alonso, V. M., Souweine, B., Charbonney, E., and Guérin, C. (2019) Predicting the Impact of Diffuse Alveolar Damage through Open Lung Biopsy in Acute Respiratory Distress Syndrome-The PREDATOR Study. *J Clin Med* **8**
19. Moss, M., Bucher, B., Moore, F. A., Moore, E. E., and Parsons, P. E. (1996) The role of chronic alcohol abuse in the development of acute respiratory distress syndrome in adults. *Jama* **275**, 50-54
20. Calfee, C. S., Matthay, M. A., Eisner, M. D., Benowitz, N., Call, M., Pittet, J.-F., and Cohen, M. J. (2011) Active and passive cigarette smoking and acute lung injury after severe blunt trauma. *American journal of respiratory and critical care medicine* **183**, 1660-1665
21. Hsieh, S. J., Zhuo, H., Benowitz, N. L., Thompson, B. T., Liu, K. D., Matthay, M. A., Calfee, C. S., National Heart, L., Blood Institute Acute Respiratory Distress Syndrome, N., National Heart, L., and Blood Institute Acute Respiratory Distress Syndrome, N. (2014) Prevalence and impact of active and passive cigarette smoking in acute respiratory distress syndrome. *Crit Care Med* **42**, 2058-2068
22. Ware, L. B., Zhao, Z., Koyama, T., May, A. K., Matthay, M. A., Lurmann, F. W., Balmes, J. R., and Calfee, C. S. (2016) Long-Term Ozone Exposure Increases the Risk of Developing the Acute Respiratory Distress Syndrome. *Am J Respir Crit Care Med* **193**, 1143-1150
23. Reilly, J. P., Zhao, Z., Shashaty, M. G. S., Koyama, T., Christie, J. D., Lancken, P. N., Wang, C., Balmes, J. R., Matthay, M. A., Calfee, C. S., and Ware, L. B. (2019) Low to Moderate Air Pollutant Exposure and Acute Respiratory Distress Syndrome after Severe Trauma. *Am J Respir Crit Care Med* **199**, 62-70
24. Mangialardi, R. J., Martin, G. S., Bernard, G. R., Wheeler, A. P., Christman, B. W., Dupont, W. D., Higgins, S. B., and Swindell, B. B. (2000) Hypoproteinemia predicts

- acute respiratory distress syndrome development, weight gain, and death in patients with sepsis. Ibuprofen in Sepsis Study Group. *Crit Care Med* **28**, 3137-3145
25. Ni, Y.-N., Luo, J., Yu, H., Wang, Y.-W., Hu, Y.-H., Liu, D., Liang, B.-M., and Liang, Z.-A. (2017) Can body mass index predict clinical outcomes for patients with acute lung injury/acute respiratory distress syndrome? A meta-analysis. *Critical Care* **21**, 36
26. Zhi, G., Xin, W., Ying, W., Guohong, X., and Shuying, L. (2016) "Obesity Paradox" in Acute Respiratory Distress Syndrome: Asystematic Review and Meta-Analysis. *PLoS One* **11**, e0163677-e0163677
27. Stapleton, R. D., Dixon, A. E., Parsons, P. E., Ware, L. B., and Suratt, B. T. (2010) The association between BMI and plasma cytokine levels in patients with acute lung injury. *Chest* **138**, 568-577
28. Schenkeveld, L., Magro, M., Oemrawsingh, R. M., Lenzen, M., de Jaegere, P., van Geuns, R.-J., Serruys, P. W., and van Domburg, R. T. (2012) The influence of optimal medical treatment on the 'obesity paradox', body mass index and long-term mortality in patients treated with percutaneous coronary intervention: a prospective cohort study. *BMJ Open* **2**, e000535-e000535
29. Zhou, P., Yang, X.-L., Wang, X.-G., Hu, B., Zhang, L., Zhang, W., Si, H.-R., Zhu, Y., Li, B., Huang, C.-L., Chen, H.-D., Chen, J., Luo, Y., Guo, H., Jiang, R.-D., Liu, M.-Q., Chen, Y., Shen, X.-R., Wang, X., Zheng, X.-S., Zhao, K., Chen, Q.-J., Deng, F., Liu, L.-L., Yan, B., Zhan, F.-X., Wang, Y.-Y., Xiao, G.-F., and Shi, Z.-L. (2020) A pneumonia outbreak associated with a new coronavirus of probable bat origin. *Nature* **579**, 270-273
30. Wu, F., Zhao, S., Yu, B., Chen, Y.-M., Wang, W., Song, Z.-G., Hu, Y., Tao, Z.-W., Tian, J.-H., Pei, Y.-Y., Yuan, M.-L., Zhang, Y.-L., Dai, F.-H., Liu, Y., Wang, Q.-M., Zheng, J.-J., Xu, L., Holmes, E. C., and Zhang, Y.-Z. (2020) A new coronavirus associated with human respiratory disease in China. *Nature* **579**, 265-269
31. Dong, E., Du, H., and Gardner, L. An interactive web-based dashboard to track COVID-19 in real time. *The Lancet Infectious Diseases*

32. Hoffmann, M., Kleine-Weber, H., Schroeder, S., Krüger, N., Herrler, T., Erichsen, S., Schiergens, T. S., Herrler, G., Wu, N.-H., Nitsche, A., Müller, M. A., Drosten, C., and Pöhlmann, S. (2020) SARS-CoV-2 Cell Entry Depends on ACE2 and TMPRSS2 and Is Blocked by a Clinically Proven Protease Inhibitor. *Cell* **181**, 271-280.e278
33. Du, L., He, Y., Zhou, Y., Liu, S., Zheng, B., and Jiang, S. (2009) The spike protein of SARS-CoV - A target for vaccine and therapeutic development. *Nature reviews. Microbiology* **7**, 226-236
34. Tay, M. Z., Poh, C. M., Rénia, L., MacAry, P. A., and Ng, L. F. P. (2020) The trinity of COVID-19: immunity, inflammation and intervention. *Nature Reviews Immunology*
35. Huang, C., Wang, Y., Li, X., Ren, L., Zhao, J., Hu, Y., Zhang, L., Fan, G., Xu, J., and Gu, X. (2020) Clinical features of patients infected with 2019 novel coronavirus in Wuhan, China. *The Lancet* **395**, 497-506
36. Zhou, F., Yu, T., Du, R., Fan, G., Liu, Y., Liu, Z., Xiang, J., Wang, Y., Song, B., and Gu, X. (2020) Clinical course and risk factors for mortality of adult inpatients with COVID-19 in Wuhan, China: a retrospective cohort study. *The Lancet*
37. Blanco-Melo, D., Nilsson-Payant, B. E., Liu, W.-C., Uhl, S., Hoagland, D., Møller, R., Jordan, T. X., Oishi, K., Panis, M., Sachs, D., Wang, T. T., Schwartz, R. E., Lim, J. K., Albrecht, R. A., and tenOever, B. R. Imbalanced Host Response to SARS-CoV-2 Drives Development of COVID-19. *Cell*
38. Tian, S., Hu, W., Niu, L., Liu, H., Xu, H., and Xiao, S.-Y. (2020) Pulmonary pathology of early phase 2019 novel coronavirus (COVID-19) pneumonia in two patients with lung cancer. *Journal of Thoracic Oncology*
39. Xu, Z., Shi, L., Wang, Y., Zhang, J., Huang, L., Zhang, C., Liu, S., Zhao, P., Liu, H., and Zhu, L. (2020) Pathological findings of COVID-19 associated with acute respiratory distress syndrome. *The Lancet respiratory medicine* **8**, 420-422
40. Tay, M. Z., Poh, C. M., Renia, L., MacAry, P. A., and Ng, L. F. P. (2020) The trinity of COVID-19: immunity, inflammation and intervention. *Nat Rev Immunol* **20**, 363-374

41. Cao, W., and Li, T. (2020) COVID-19: towards understanding of pathogenesis. *Cell Res* **30**, 367-369
42. McGonagle, D., O'Donnell, J. S., Sharif, K., Emery, P., and Bridgewood, C. (2020) Immune mechanisms of pulmonary intravascular coagulopathy in COVID-19 pneumonia. *The Lancet Rheumatology* **2**, e437-e445
43. Teuwen, L. A., Geldhof, V., Pasut, A., and Carmeliet, P. (2020) COVID-19: the vasculature unleashed. *Nat Rev Immunol* **20**, 389-391
44. Tang, N., Li, D., Wang, X., and Sun, Z. (2020) Abnormal coagulation parameters are associated with poor prognosis in patients with novel coronavirus pneumonia. *J Thromb Haemost* **18**, 844-847
45. Wu, C., Chen, X., Cai, Y., Xia, J. a., Zhou, X., Xu, S., Huang, H., Zhang, L., Zhou, X., Du, C., Zhang, Y., Song, J., Wang, S., Chao, Y., Yang, Z., Xu, J., Zhou, X., Chen, D., Xiong, W., Xu, L., Zhou, F., Jiang, J., Bai, C., Zheng, J., and Song, Y. (2020) Risk Factors Associated With Acute Respiratory Distress Syndrome and Death in Patients With Coronavirus Disease 2019 Pneumonia in Wuhan, China. *JAMA Internal Medicine*
46. McGonagle, D., O'Donnell, J. S., Sharif, K., Emery, P., and Bridgewood, C. Immune mechanisms of pulmonary intravascular coagulopathy in COVID-19 pneumonia. *The Lancet Rheumatology*
47. Teuwen, L.-A., Geldhof, V., Pasut, A., and Carmeliet, P. (2020) COVID-19: the vasculature unleashed. *Nature Reviews Immunology*
48. Tang, N., Li, D., Wang, X., and Sun, Z. (2020) Abnormal coagulation parameters are associated with poor prognosis in patients with novel coronavirus pneumonia. *Journal of Thrombosis and Haemostasis*
49. Cao, W., and Li, T. (2020) COVID-19: towards understanding of pathogenesis. *Cell Research*

50. Arentz, M., Yim, E., Klaff, L., Lokhandwala, S., Riedo, F. X., Chong, M., and Lee, M. (2020) Characteristics and outcomes of 21 critically ill patients with COVID-19 in Washington State. *Jama*
51. Grasselli, G., Zangrillo, A., Zanella, A., Antonelli, M., Cabrini, L., Castelli, A., Cereda, D., Coluccello, A., Foti, G., and Fumagalli, R. (2020) Baseline characteristics and outcomes of 1591 patients infected with SARS-CoV-2 admitted to ICUs of the Lombardy Region, Italy. *Jama*
52. Cummings, M. J., Baldwin, M. R., Abrams, D., Jacobson, S. D., Meyer, B. J., Balough, E. M., Aaron, J. G., Claassen, J., Rabbani, L. E., Hastie, J., Hochman, B. R., Salazar-Schicchi, J., Yip, N. H., Brodie, D., and O'Donnell, M. R. Epidemiology, clinical course, and outcomes of critically ill adults with COVID-19 in New York City: a prospective cohort study. *The Lancet*
53. Wadman, M., Couzin-Frankel, J., Kaiser, J., and Maticic, C. (2020) A rampage through the body. *Science* **368**, 356-360
54. Couzin-Frankel, J. (2020) The mystery of the pandemic's 'happy hypoxia'. *Science* **368**, 455-456
55. Brochard, L., Slutsky, A., and Pesenti, A. (2017) Mechanical ventilation to minimize progression of lung injury in acute respiratory failure. *American journal of respiratory and critical care medicine* **195**, 438-442
56. Marini, J. J., and Gattinoni, L. (2020) Management of COVID-19 Respiratory Distress. *JAMA*
57. Arulkumaran, N., Brealey, D., Howell, D., and Singer, M. (2020) Use of non-invasive ventilation for patients with COVID-19: a cause for concern? *The Lancet Respiratory Medicine* **8**, e45
58. Sartini, C., Tresoldi, M., Scarpellini, P., Tettamanti, A., Carcò, F., Landoni, G., and Zangrillo, A. (2020) Respiratory Parameters in Patients With COVID-19 After Using

- Noninvasive Ventilation in the Prone Position Outside the Intensive Care Unit. *JAMA* **323**, 2338-2340
59. Thompson, B. T., and Bernard, G. R. (2011) ARDS Network (NHLBI) studies: successes and challenges in ARDS clinical research. *Crit Care Clin* **27**, 459-468
 60. Schoenfeld, D. A., and Bernard, G. R. (2002) Statistical evaluation of ventilator-free days as an efficacy measure in clinical trials of treatments for acute respiratory distress syndrome. *Crit Care Med* **30**, 1772-1777
 61. Brower, R. G., Matthay, M. A., Morris, A., Schoenfeld, D., Thompson, B. T., Wheeler, A., and Network, A. R. D. S. (2000) Ventilation with lower tidal volumes as compared with traditional tidal volumes for acute lung injury and the acute respiratory distress syndrome. *N Engl J Med* **342**, 1301-1308
 62. Guérin, C., Reignier, J., Richard, J. C., Beuret, P., Gacouin, A., Boulain, T., Mercier, E., Badet, M., Mercat, A., Baudin, O., Clavel, M., Chatellier, D., Jaber, S., Rosselli, S., Mancebo, J., Sirodot, M., Hilbert, G., Bengler, C., Richecoeur, J., Gainnier, M., Bayle, F., Bourdin, G., Leray, V., Girard, R., Baboi, L., Ayzac, L., and Group, P. S. (2013) Prone positioning in severe acute respiratory distress syndrome. *N Engl J Med* **368**, 2159-2168
 63. Wiedemann, H. (2006) National Heart, Lung, and Blood Institute acute respiratory distress syndrome (ARDS) clinical trials network, comparison of two fluid-management strategies in acute lung injury. *N Engl J Med* **354**, 2564-2575
 64. Girardis, M., Busani, S., Damiani, E., Donati, A., Rinaldi, L., Marudi, A., Morelli, A., Antonelli, M., and Singer, M. (2016) Effect of conservative vs conventional oxygen therapy on mortality among patients in an intensive care unit: the oxygen-ICU randomized clinical trial. *Jama* **316**, 1583-1589
 65. Mackle, D., Bellomo, R., Bailey, M., Beasley, R., Deane, A., Eastwood, G., Finfer, S., Freebairn, R., King, V., and Linke, N. (2019) Conservative Oxygen Therapy during Mechanical Ventilation in the ICU. *The New England journal of medicine*

66. Barrot, L., Asfar, P., Mauny, F., Winiszewski, H., Montini, F., Badie, J., Quenot, J.-P., Pili-Floury, S., Bouhemad, B., and Louis, G. (2020) Liberal or conservative oxygen therapy for acute respiratory distress syndrome. *New England Journal of Medicine* **382**, 999-1008
67. Papazian, L., Forel, J. M., Gacouin, A., Penot-Ragon, C., Perrin, G., Loundou, A., Jaber, S., Arnal, J. M., Perez, D., Seghboyan, J. M., Constantin, J. M., Courant, P., Lefrant, J. Y., Guérin, C., Prat, G., Morange, S., Roch, A., and Investigators, A. S. (2010) Neuromuscular blockers in early acute respiratory distress syndrome. *N Engl J Med* **363**, 1107-1116
68. Moss, M., Huang, D. T., Brower, R. G., Ferguson, N. D., Ginde, A. A., Gong, M. N., Grissom, C. K., Gundel, S., Hayden, D., Hite, R. D., Hou, P. C., Hough, C. L., Iwashyna, T. J., Khan, A., Liu, K. D., Talmor, D., Thompson, B. T., Ulysse, C. A., Yealy, D. M., Angus, D. C., and National Heart, Lung, and Blood Institute PETAL Clinical Trials Network. (2019) Early Neuromuscular Blockade in the Acute Respiratory Distress Syndrome. *N Engl J Med* **380**, 1997-2008
69. (2004) Higher versus Lower Positive End-Expiratory Pressures in Patients with the Acute Respiratory Distress Syndrome. *New England Journal of Medicine* **351**, 327-336
70. Rice, T. W., Wheeler, A. P., Thompson, B. T., Steingrub, J., Hite, R. D., Moss, M., Morris, A., Dong, N., and Rock, P. (2012) Initial trophic vs full enteral feeding in patients with acute lung injury: the EDEN randomized trial. *Jama* **307**, 795-803
71. Peek, G. J., Mugford, M., Tiruvoipati, R., Wilson, A., Allen, E., Thalanany, M. M., Hibbert, C. L., Truesdale, A., Clemens, F., Cooper, N., Firmin, R. K., and Elbourne, D. (2009) Efficacy and economic assessment of conventional ventilatory support versus extracorporeal membrane oxygenation for severe adult respiratory failure (CESAR): a multicentre randomised controlled trial. *Lancet (London, England)* **374**, 1351-1363
72. Combes, A., Hajage, D., Capellier, G., Demoule, A., Lavoué, S., Guervilly, C., Da Silva, D., Zafrani, L., Tirot, P., Veber, B., Maury, E., Levy, B., Cohen, Y., Richard, C., Kalfon,

- P., Bouadma, L., Mehdaoui, H., Beduneau, G., Lebreton, G., Brochard, L., Ferguson, N. D., Fan, E., Slutsky, A. S., Brodie, D., Mercat, A., and EOLIA Trial Group, R. E. V. A., and ECMONet. (2018) Extracorporeal Membrane Oxygenation for Severe Acute Respiratory Distress Syndrome. *N Engl J Med* **378**, 1965-1975
73. Matthay, M. A., Brower, R. G., Carson, S., Douglas, I. S., Eisner, M., Hite, D., Holets, S., Kallet, R. H., Liu, K. D., MacIntyre, N., Moss, M., Schoenfeld, D., Steingrub, J., and Thompson, B. T. (2011) Randomized, placebo-controlled clinical trial of an aerosolized beta(2)-agonist for treatment of acute lung injury. *Am J Respir Crit Care Med* **184**, 561-568
74. Ranieri, V. M., Pettilä, V., Karvonen, M. K., Jalkanen, J., Nightingale, P., Brealey, D., Mancebo, J., Ferrer, R., Mercat, A., Patroniti, N., Quintel, M., Vincent, J. L., Okkonen, M., Meziani, F., Bellani, G., MacCallum, N., Creteur, J., Kluge, S., Artigas-Raventos, A., Maksimow, M., Piippo, I., Elima, K., Jalkanen, S., Jalkanen, M., Bellingan, G., and Group, I. S. (2020) Effect of Intravenous Interferon β -1a on Death and Days Free From Mechanical Ventilation Among Patients With Moderate to Severe Acute Respiratory Distress Syndrome: A Randomized Clinical Trial. *JAMA*
75. Miller, A. C., Elamin, E. M., and Suffredini, A. F. (2014) Inhaled anticoagulation regimens for the treatment of smoke inhalation-associated acute lung injury: a systematic review. *Crit Care Med* **42**, 413-419
76. Mahmoodpoor, A., Hamishehkar, H., Shadvar, K., Ostadi, Z., Sanaie, S., Saghaleini, S. H., and Nader, N. D. (2019) The Effect of Intravenous Selenium on Oxidative Stress in Critically Ill Patients with Acute Respiratory Distress Syndrome. *Immunol Invest* **48**, 147-159
77. (2002) Randomized, placebo-controlled trial of lisofylline for early treatment of acute lung injury and acute respiratory distress syndrome. *Crit Care Med* **30**, 1-6

78. (2000) Ketoconazole for early treatment of acute lung injury and acute respiratory distress syndrome: a randomized controlled trial. The ARDS Network. *Jama* **283**, 1995-2002
79. McAuley, D. F., Laffey, J. G., O'Kane, C. M., Perkins, G. D., Mullan, B., Trinder, T. J., Johnston, P., Hopkins, P. A., Johnston, A. J., McDowell, C., and McNally, C. (2014) Simvastatin in the Acute Respiratory Distress Syndrome. *New England Journal of Medicine* **371**, 1695-1703
80. Villar, J., Ferrando, C., Martinez, D., Ambros, A., Munoz, T., Soler, J. A., Aguilar, G., Alba, F., Gonzalez-Higueras, E., Conesa, L. A., Martin-Rodriguez, C., Diaz-Dominguez, F. J., Serna-Grande, P., Rivas, R., Ferreres, J., Belda, J., Capilla, L., Tallet, A., Anon, J. M., Fernandez, R. L., and Gonzalez-Martin, J. M. (2020) Dexamethasone treatment for the acute respiratory distress syndrome: a multicentre, randomised controlled trial. *The Lancet. Respiratory medicine* **8**, 267-276
81. (2006) Efficacy and Safety of Corticosteroids for Persistent Acute Respiratory Distress Syndrome. *New England Journal of Medicine* **354**, 1671-1684
82. Rice, T. W., Wheeler, A. P., Thompson, B. T., deBoisblanc, B. P., Steingrub, J., Rock, P., and Investigators, N. N. A. R. D. S. N. o. (2011) Enteral omega-3 fatty acid, gamma-linolenic acid, and antioxidant supplementation in acute lung injury. *JAMA* **306**, 1574-1581
83. Serpa Neto, A., Cardoso, S. O., Manetta, J. A., Pereira, V. G. M., Espósito, D. C., Pasqualucci, M. d. O. P., Damasceno, M. C. T., and Schultz, M. J. (2012) Association Between Use of Lung-Protective Ventilation With Lower Tidal Volumes and Clinical Outcomes Among Patients Without Acute Respiratory Distress Syndrome: A Meta-analysis. *JAMA* **308**, 1651-1659
84. Investigators, W. G. f. t. P. (2018) Effect of a Low vs Intermediate Tidal Volume Strategy on Ventilator-Free Days in Intensive Care Unit Patients Without ARDS: A Randomized Clinical Trial. *JAMA* **320**, 1872-1880

85. Güldner, A., Kiss, T., Serpa Neto, A., Hemmes, S. N. T., Canet, J., Spieth, P. M., Rocco, P. R. M., Schultz, M. J., Pelosi, P., and Gama de Abreu, M. (2015) Intraoperative Protective Mechanical Ventilation for Prevention of Postoperative Pulmonary Complications: A Comprehensive Review of the Role of Tidal Volume, Positive End-expiratory Pressure, and Lung Recruitment Maneuvers. *Anesthesiology: The Journal of the American Society of Anesthesiologists* **123**, 692-713
86. Severgnini, P., Selmo, G., Lanza, C., Chiesa, A., Frigerio, A., Bacuzzi, A., Dionigi, G., Novario, R., Gregoretti, C., de Abreu, M. G., Schultz, M. J., Jaber, S., Futier, E., Chiaranda, M., and Pelosi, P. (2013) Protective Mechanical Ventilation during General Anesthesia for Open Abdominal Surgery Improves Postoperative Pulmonary Function. *Anesthesiology: The Journal of the American Society of Anesthesiologists* **118**, 1307-1321
87. Mathis, M. R., Duggal, N. M., Likosky, D. S., Haft, J. W., Douville, N. J., Vaughn, M. T., Maile, M. D., Blank, R. S., Colquhoun, D. A., Strobel, R. J., Janda, A. M., Zhang, M., Kheterpal, S., and Engoren, M. C. (2019) Intraoperative Mechanical Ventilation and Postoperative Pulmonary Complications after Cardiac Surgery. *Anesthesiology: The Journal of the American Society of Anesthesiologists* **131**, 1046-1062
88. Tremblay, L. N., and Slutsky, A. S. (2006) Ventilator-induced lung injury: from the bench to the bedside. *Intensive Care Med* **32**, 24-33
89. Amato, M. B., Barbas, C. S., Medeiros, D. M., Magaldi, R. B., Schettino, G. P., Lorenzi-Filho, G., Kairalla, R. A., Deheinzelin, D., Munoz, C., Oliveira, R., Takagaki, T. Y., and Carvalho, C. R. (1998) Effect of a protective-ventilation strategy on mortality in the acute respiratory distress syndrome. *N Engl J Med* **338**, 347-354
90. Villar, J., Kacmarek, R. M., Pérez-Méndez, L., and Aguirre-Jaime, A. (2006) A high positive end-expiratory pressure, low tidal volume ventilatory strategy improves outcome in persistent acute respiratory distress syndrome: a randomized, controlled trial. *Crit Care Med* **34**, 1311-1318

91. Meade, M. O., Cook, D. J., Guyatt, G. H., Slutsky, A. S., Arabi, Y. M., Cooper, D. J., Davies, A. R., Hand, L. E., Zhou, Q., Thabane, L., Austin, P., Lapinsky, S., Baxter, A., Russell, J., Skrobik, Y., Ronco, J. J., Stewart, T. E., and Lung Open Ventilation Study Investigators, f. t. (2008) Ventilation Strategy Using Low Tidal Volumes, Recruitment Maneuvers, and High Positive End-Expiratory Pressure for Acute Lung Injury and Acute Respiratory Distress Syndrome: A Randomized Controlled Trial. *JAMA* **299**, 637-645
92. Walkey, A. J., Del Sorbo, L., Hodgson, C. L., Adhikari, N. K. J., Wunsch, H., Meade, M. O., Uleryk, E., Hess, D., Talmor, D. S., Thompson, B. T., Brower, R. G., and Fan, E. (2017) Higher PEEP versus Lower PEEP Strategies for Patients with Acute Respiratory Distress Syndrome. A Systematic Review and Meta-Analysis. *Annals of the American Thoracic Society* **14**, S297-s303
93. Guo, L., Xie, J., Huang, Y., Pan, C., Yang, Y., Qiu, H., and Liu, L. (2018) Higher PEEP improves outcomes in ARDS patients with clinically objective positive oxygenation response to PEEP: a systematic review and meta-analysis. *BMC Anesthesiology* **18**, 172
94. Weber, J., Gutjahr, J., Schmidt, J., Lozano-Zahonero, S., Borgmann, S., Schumann, S., and Wirth, S. (2020) Effect of individualized PEEP titration guided by intratidal compliance profile analysis on regional ventilation assessed by electrical impedance tomography - a randomized controlled trial. *BMC Anesthesiol* **20**, 42
95. Pintado, M. C., de Pablo, R., Trascasa, M., Milicua, J. M., Rogero, S., Daguerre, M., Cambronero, J. A., Arribas, I., and Sánchez-García, M. (2013) Individualized PEEP setting in subjects with ARDS: a randomized controlled pilot study. *Respiratory care* **58**, 1416-1423
96. Hess, D. R. (2015) Recruitment Maneuvers and PEEP Titration. *Respiratory care* **60**, 1688-1704
97. Goligher, E. C., Hodgson, C. L., Adhikari, N. K. J., Meade, M. O., Wunsch, H., Uleryk, E., Gajic, O., Amato, M. P. B., Ferguson, N. D., Rubenfeld, G. D., and Fan, E. (2017)

- Lung Recruitment Maneuvers for Adult Patients with Acute Respiratory Distress Syndrome. A Systematic Review and Meta-Analysis. *Annals of the American Thoracic Society* **14**, S304-S311
98. Investigators, W. G. f. t. A. R. f. A. R. D. S. T. (2017) Effect of Lung Recruitment and Titrated Positive End-Expiratory Pressure (PEEP) vs Low PEEP on Mortality in Patients With Acute Respiratory Distress Syndrome: A Randomized Clinical Trial. *JAMA* **318**, 1335-1345
99. Lamm, W. J., Graham, M. M., and Albert, R. K. (1994) Mechanism by which the prone position improves oxygenation in acute lung injury. *Am J Respir Crit Care Med* **150**, 184-193
100. Broccard, A., Shapiro, R. S., Schmitz, L. L., Adams, A. B., Nahum, A., and Marini, J. J. (2000) Prone positioning attenuates and redistributes ventilator-induced lung injury in dogs. *Crit Care Med* **28**, 295-303
101. Munshi, L., Del Sorbo, L., Adhikari, N. K. J., Hodgson, C. L., Wunsch, H., Meade, M. O., Uleryk, E., Mancebo, J., Pesenti, A., Ranieri, V. M., and Fan, E. (2017) Prone Position for Acute Respiratory Distress Syndrome. A Systematic Review and Meta-Analysis. *Annals of the American Thoracic Society* **14**, S280-S288
102. Fan, E., Del Sorbo, L., Goligher, E. C., Hodgson, C. L., Munshi, L., Walkey, A. J., Adhikari, N. K. J., Amato, M. B. P., Branson, R., Brower, R. G., Ferguson, N. D., Gajic, O., Gattinoni, L., Hess, D., Mancebo, J., Meade, M. O., McAuley, D. F., Pesenti, A., Ranieri, V. M., Rubenfeld, G. D., Rubin, E., Seckel, M., Slutsky, A. S., Talmor, D., Thompson, B. T., Wunsch, H., Uleryk, E., Brozek, J., and Brochard, L. J. (2017) An Official American Thoracic Society/European Society of Intensive Care Medicine/Society of Critical Care Medicine Clinical Practice Guideline: Mechanical Ventilation in Adult Patients with Acute Respiratory Distress Syndrome. *Am J Respir Crit Care Med* **195**, 1253-1263

103. Albert, R. K. (2020) Prone Ventilation for Patients with Mild or Moderate Acute Respiratory Distress Syndrome. *Annals of the American Thoracic Society* **17**, 24-29
104. Slutsky, A. S. (2010) Neuromuscular blocking agents in ARDS. Mass Medical Soc
105. Pohlman, M. C., McCallister, K. E., Schweickert, W. D., Pohlman, A. S., Nigos, C. P., Krishnan, J. A., Charbeneau, J. T., Gehlbach, B. K., Kress, J. P., and Hall, J. B. (2008) Excessive tidal volume from breath stacking during lung-protective ventilation for acute lung injury. *Crit Care Med* **36**, 3019-3023
106. Weigelt, J. A., Norcross, J. F., Borman, K. R., and Snyder, W. H. (1985) Early steroid therapy for respiratory failure. *Archives of surgery* **120**, 536-540
107. Bernard, G. R., Luce, J. M., Sprung, C. L., Rinaldo, J. E., Tate, R. M., Sibbald, W. J., Kariman, K., Higgins, S., Bradley, R., and Metz, C. A. (1987) High-dose corticosteroids in patients with the adult respiratory distress syndrome. *New England Journal of Medicine* **317**, 1565-1570
108. Meduri, G. U., Headley, A. S., Golden, E., Carson, S. J., Umberger, R. A., Kelso, T., and Tolley, E. A. (1998) Effect of prolonged methylprednisolone therapy in unresolving acute respiratory distress syndrome: a randomized controlled trial. *Jama* **280**, 159-165
109. Group, R. C., Horby, P., Lim, W. S., Emberson, J. R., Mafham, M., Bell, J. L., Linsell, L., Staplin, N., Brightling, C., Ustianowski, A., Elmahi, E., Prudon, B., Green, C., Felton, T., Chadwick, D., Rege, K., Fegan, C., Chappell, L. C., Faust, S. N., Jaki, T., Jeffery, K., Montgomery, A., Rowan, K., Juszczak, E., Baillie, J. K., Haynes, R., and Landray, M. J. (2020) Dexamethasone in Hospitalized Patients with Covid-19 - Preliminary Report. *N Engl J Med*
110. COVID-19 Treatment Guidelines Panel. Coronavirus Disease 2019 (COVID-19) Treatment Guidelines. National Institutes of Health. Available at <https://www.covid19treatmentguidelines.nih.gov/>. Accessed July 12, 2020.

111. Gumbert, S. D., Kork, F., Jackson, M. L., Vanga, N., Ghebremichael, S. J., Wang, C. Y., and Eltzschig, H. K. (2020) Perioperative Acute Kidney Injury. *Anesthesiology: The Journal of the American Society of Anesthesiologists* **132**, 180-204
112. Jolley, S. E., Hough, C. L., Clermont, G., Hayden, D., Hou, S., Schoenfeld, D., Smith, N. L., Thompson, B. T., Bernard, G. R., and Angus, D. C. (2017) Relationship between Race and the Effect of Fluids on Long-term Mortality after Acute Respiratory Distress Syndrome. Secondary Analysis of the National Heart, Lung, and Blood Institute Fluid and Catheter Treatment Trial. *Annals of the American Thoracic Society* **14**, 1443-1449
113. Silversides, J. A., Fitzgerald, E., Manickavasagam, U. S., Lapinsky, S. E., Nisenbaum, R., Hemmings, N., Nutt, C., Trinder, T. J., Pogson, D. G., Fan, E., Ferguson, A. J., McAuley, D. F., and Marshall, J. C. (2018) Deresuscitation of Patients With Iatrogenic Fluid Overload Is Associated With Reduced Mortality in Critical Illness. *Crit Care Med* **46**, 1600-1607
114. Fowler, A. A., Truwit, J. D., Hite, R. D., Morris, P. E., DeWilde, C., Priday, A., Fisher, B., Thacker, L. R., Natarajan, R., Brophy, D. F., Sculthorpe, R., Nanchal, R., Syed, A., Sturgill, J., Martin, G. S., Sevransky, J., Kashiouris, M., Hamman, S., Egan, K. F., Hastings, A., Spencer, W., Tench, S., Mehkri, O., Bindas, J., Duggal, A., Graf, J., Zellner, S., Yanny, L., McPolin, C., Hollrith, T., Kramer, D., Ojielo, C., Damm, T., Cassity, E., Wieliczko, A., and Halquist, M. (2019) Effect of Vitamin C Infusion on Organ Failure and Biomarkers of Inflammation and Vascular Injury in Patients With Sepsis and Severe Acute Respiratory Failure: The CITRIS-ALI Randomized Clinical Trial. *JAMA* **322**, 1261-1270
115. (2019) Early High-Dose Vitamin D3 for Critically Ill, Vitamin D–Deficient Patients. *New England Journal of Medicine* **381**, 2529-2540
116. McClave, S. A., Taylor, B. E., Martindale, R. G., Warren, M. M., Johnson, D. R., Braunschweig, C., McCarthy, M. S., Davanos, E., Rice, T. W., Cresci, G. A., Gervasio, J. M., Sacks, G. S., Roberts, P. R., and Compher, C. (2016) Guidelines for the

- Provision and Assessment of Nutrition Support Therapy in the Adult Critically Ill Patient: Society of Critical Care Medicine (SCCM) and American Society for Parenteral and Enteral Nutrition (A.S.P.E.N.). *JPEN. Journal of parenteral and enteral nutrition* **40**, 159-211
117. Helmerhorst, H. J., Roos-Blom, M.-J., van Westerloo, D. J., and de Jonge, E. (2015) Association between arterial hyperoxia and outcome in subsets of critical illness: a systematic review, meta-analysis, and meta-regression of cohort studies. *Crit Care Med* **43**, 1508-1519
118. Asfar, P., Schortgen, F., Boisramé-Helms, J., Charpentier, J., Guérot, E., Megarbane, B., Grimaldi, D., Grelon, F., Anguel, N., Lasocki, S., Henry-Lagarrigue, M., Gonzalez, F., Legay, F., Guitton, C., Schenck, M., Doise, J. M., Devaquet, J., Van Der Linden, T., Chatellier, D., Rigaud, J. P., Dellamonica, J., Tamion, F., Meziani, F., Mercat, A., Dreyfuss, D., Seegers, V., and Radermacher, P. (2017) Hyperoxia and hypertonic saline in patients with septic shock (HYPER2S): a two-by-two factorial, multicentre, randomised, clinical trial. *The Lancet Respiratory Medicine* **5**, 180-190
119. Siemieniuk, R. A., Chu, D. K., Kim, L. H.-Y., Güell-Rous, M.-R., Alhazzani, W., Soccia, P. M., Karanickolas, P. J., Farhoumand, P. D., Siemieniuk, J. L., and Satia, I. (2018) Oxygen therapy for acutely ill medical patients: a clinical practice guideline. *Bmj* **363**
120. Perner, A., De Jong, A., and Shankar-Hari, M. (2020) Trials on oxygen supplementation in sepsis: better late than never. *Intensive Care Medicine* **46**, 116-118
121. April, I. (2009) Extracorporeal membrane oxygenation for 2009 influenza A (H1N1) acute respiratory distress syndrome. *Jama* **302**, 1888-1895
122. Griffiths, M. J., and Evans, T. W. (2005) Inhaled nitric oxide therapy in adults. *New England Journal of Medicine* **353**, 2683-2695
123. Taylor, R. W., Zimmerman, J. L., Dellinger, R. P., Straube, R. C., Criner, G. J., Davis Jr, K., Kelly, K. M., Smith, T. C., Small, R. J., and Group, I. N. O. i. A. S. (2004) Low-dose

- inhaled nitric oxide in patients with acute lung injury: a randomized controlled trial. *Jama* **291**, 1603-1609
124. Gebistorf, F., Karam, O., Wetterslev, J., and Afshari, A. (2016) Inhaled nitric oxide for acute respiratory distress syndrome (ARDS) in children and adults. *The Cochrane database of systematic reviews*, Cd002787
125. (2014) Rosuvastatin for Sepsis-Associated Acute Respiratory Distress Syndrome. *New England Journal of Medicine* **370**, 2191-2200
126. Wilson, J. G., and Calfee, C. S. (2020) ARDS Subphenotypes: Understanding a Heterogeneous Syndrome. *Critical Care* **24**, 102
127. Hudson, L. D., Milberg, J. A., Anardi, D., and Maunder, R. J. (1995) Clinical risks for development of the acute respiratory distress syndrome. *American journal of respiratory and critical care medicine* **151**, 293-301
128. Sheu, C. C., Gong, M. N., Zhai, R., Chen, F., Bajwa, E. K., Clardy, P. F., Gallagher, D. C., Thompson, B. T., and Christiani, D. C. (2010) Clinical characteristics and outcomes of sepsis-related vs non-sepsis-related ARDS. *Chest* **138**, 559-567
129. Sevransky, J. E., Martin, G. S., Shanholtz, C., Mendez-Tellez, P. A., Pronovost, P., Brower, R., and Needham, D. M. (2009) Mortality in sepsis versus non-sepsis induced acute lung injury. *Critical care* **13**, 1-6
130. Calfee, C. S., Eisner, M. D., Ware, L. B., Thompson, B. T., Parsons, P. E., Wheeler, A. P., Korpak, A., Matthay, M. A., Acute Respiratory Distress Syndrome Network, N. H. L., and Blood, I. (2007) Trauma-associated lung injury differs clinically and biologically from acute lung injury due to other clinical disorders. *Crit Care Med* **35**, 2243-2250
131. Meyer, N. J., and Christie, J. D. (2013) Genetic Heterogeneity and Risk of Acute Respiratory Distress Syndrome. *Semin Respir Crit Care Med* **34**, 459-474
132. Meyer, N. J., Li, M., Feng, R., Bradfield, J., Gallop, R., Bellamy, S., Fuchs, B. D., Lanken, P. N., Albelda, S. M., and Rushefski, M. (2011) ANGPT2 genetic variant is

- associated with trauma-associated acute lung injury and altered plasma angiopoietin-2 isoform ratio. *American journal of respiratory and critical care medicine* **183**, 1344-1353
133. Meyer, N. J., Reilly, J. P., Anderson, B. J., Palakshappa, J. A., Jones, T. K., Dunn, T. G., Shashaty, M. G. S., Feng, R., Christie, J. D., and Opal, S. M. (2018) Mortality Benefit of Recombinant Human Interleukin-1 Receptor Antagonist for Sepsis Varies by Initial Interleukin-1 Receptor Antagonist Plasma Concentration. *Crit Care Med* **46**, 21-28
134. Sapru, A., Calfee, C. S., Liu, K. D., Kangelaris, K., Hansen, H., Pawlikowska, L., Ware, L. B., Alkhouli, M. F., Abbot, J., Matthay, M. A., and The, N. A. N. (2015) Plasma soluble thrombomodulin levels are associated with mortality in the acute respiratory distress syndrome. *Intensive Care Medicine* **41**, 470-478
135. Ware, L. B., Koyama, T., Zhao, Z., Janz, D. R., Wickersham, N., Bernard, G. R., May, A. K., Calfee, C. S., and Matthay, M. A. (2013) Biomarkers of lung epithelial injury and inflammation distinguish severe sepsis patients with acute respiratory distress syndrome. *Critical care* **17**, 1-7
136. Eisner, M., Parsons, P., Matthay, M., Ware, L., and Greene, K. (2003) Plasma surfactant protein levels and clinical outcomes in patients with acute lung injury. *Thorax* **58**, 983-988
137. Jabaudon, M., Blondonnet, R., Pereira, B., Cartin-Ceba, R., Lichtenstern, C., Mauri, T., Determann, R. M., Drabek, T., Hubmayr, R. D., and Gajic, O. (2018) Plasma sRAGE is independently associated with increased mortality in ARDS: a meta-analysis of individual patient data. *Intensive care medicine* **44**, 1388-1399
138. Calfee, C. S., Eisner, M. D., Parsons, P. E., Thompson, B. T., Conner, E. R., Matthay, M. A., Ware, L. B., and the, N. A. R. D. S. C. T. N. (2009) Soluble intercellular adhesion molecule-1 and clinical outcomes in patients with acute lung injury. *Intensive Care Medicine* **35**, 248-257
139. Agrawal, A., Matthay, M. A., Kangelaris, K. N., Stein, J., Chu, J. C., Imp, B. M., Cortez, A., Abbott, J., Liu, K. D., and Calfee, C. S. (2013) Plasma angiopoietin-2 predicts the

- onset of acute lung injury in critically ill patients. *American journal of respiratory and critical care medicine* **187**, 736-742
140. Shaver, C. M., and Bastarache, J. A. (2014) Clinical and biological heterogeneity in acute respiratory distress syndrome: direct versus indirect lung injury. *Clin Chest Med* **35**, 639-653
141. Pelosi, P., D'onofrio, D., Chiumello, D., Paolo, S., Chiara, G., Capelozzi, V., Barbas, C., Chiaranda, M., and Gattinoni, L. (2003) Pulmonary and extrapulmonary acute respiratory distress syndrome are different. *European Respiratory Journal* **22**, 48s-56s
142. Calfee, C. S., Janz, D. R., Bernard, G. R., May, A. K., Kangelaris, K. N., Matthay, M. A., and Ware, L. B. (2015) Distinct molecular phenotypes of direct vs indirect ARDS in single-center and multicenter studies. *Chest* **147**, 1539-1548
143. Rubin, D. B., Wiener-Kronish, J. P., Murray, J. F., Green, D. R., Turner, J., Luce, J. M., Montgomery, A. B., Marks, J. D., and Matthay, M. A. (1990) Elevated von Willebrand factor antigen is an early plasma predictor of acute lung injury in nonpulmonary sepsis syndrome. *The Journal of Clinical Investigation* **86**, 474-480
144. Calfee, C. S., Gallagher, D., Abbott, J., Thompson, B. T., Matthay, M. A., and Network, N. A. (2012) Plasma angiopoietin-2 in clinical acute lung injury: prognostic and pathogenetic significance. *Crit Care Med* **40**, 1731-1737
145. van der Heijden, M., Pickkers, P., van Nieuw Amerongen, G. P., van Hinsbergh, V. W., Bouw, M. P., van der Hoeven, J. G., and Groeneveld, A. J. (2009) Circulating angiopoietin-2 levels in the course of septic shock: relation with fluid balance, pulmonary dysfunction and mortality. *Intensive care medicine* **35**, 1567-1574
146. Uchida, T., Shirasawa, M., Ware, L. B., Kojima, K., Hata, Y., Makita, K., Mednick, G., Matthay, Z. A., and Matthay, M. A. (2006) Receptor for advanced glycation end-products is a marker of type I cell injury in acute lung injury. *American journal of respiratory and critical care medicine* **173**, 1008-1015

147. Puybasset, L., Cluzel, P., Gusman, P., Grenier, P., Preteux, F., and Rouby, J.-J. (2000) Regional distribution of gas and tissue in acute respiratory distress syndrome. I. Consequences for lung morphology. *Intensive care medicine* **26**, 857-869
148. Puybasset, L., Gusman, P., Muller, J. C., Cluzel, P., Coriat, P., and Rouby, J. J. (2000) Regional distribution of gas and tissue in acute respiratory distress syndrome. III. Consequences for the effects of positive end-expiratory pressure. CT Scan ARDS Study Group. Adult Respiratory Distress Syndrome. *Intensive Care Med* **26**, 1215-1227
149. Constantin, J.-M., Grasso, S., Chanques, G., Aufort, S., Futier, E., Sebbane, M., Jung, B., Gallix, B., Bazin, J. E., and Rouby, J.-J. (2010) Lung morphology predicts response to recruitment maneuver in patients with acute respiratory distress syndrome. *Crit Care Med* **38**, 1108-1117
150. Mrozek, S., Jabaudon, M., Jaber, S., Paugam-Burtz, C., Lefrant, J.-Y., Rouby, J.-J., Asehnoune, K., Allaouchiche, B., Baldesi, O., and Leone, M. (2016) Elevated plasma levels of sRAGE are associated with nonfocal CT-based lung imaging in patients with ARDS: a prospective multicenter study. *Chest* **150**, 998-1007
151. Rouby, J.-J., Puybasset, L., Cluzel, P., Richecoeur, J., Lu, Q., and Grenier, P. (2000) Regional distribution of gas and tissue in acute respiratory distress syndrome. II. Physiological correlations and definition of an ARDS Severity Score. *Intensive care medicine* **26**, 1046-1056
152. Bos, L. D., Schouten, L. R., van Vught, L. A., Wiewel, M. A., Ong, D. S. Y., Cremer, O., Artigas, A., Martin-Loeches, I., Hoogendijk, A. J., van der Poll, T., Horn, J., Juffermans, N., Calfee, C. S., and Schultz, M. J. (2017) Identification and validation of distinct biological phenotypes in patients with acute respiratory distress syndrome by cluster analysis. *Thorax* **72**, 876-883
153. Sinha, P., Delucchi, K. L., Thompson, B. T., McAuley, D. F., Matthay, M. A., and Calfee, C. S. (2018) Latent class analysis of ARDS subphenotypes: a secondary analysis of the

- statins for acutely injured lungs from sepsis (SAILS) study. *Intensive care medicine* **44**, 1859-1869
154. Delucchi, K., Famous, K. R., Ware, L. B., Parsons, P. E., Thompson, B. T., and Calfee, C. S. (2018) Stability of ARDS subphenotypes over time in two randomised controlled trials. *Thorax* **73**, 439-445
155. Calfee, C. S., Delucchi, K., Parsons, P. E., Thompson, B. T., Ware, L. B., Matthay, M. A., and Network, N. A. (2014) Subphenotypes in acute respiratory distress syndrome: latent class analysis of data from two randomised controlled trials. *The Lancet Respiratory Medicine* **2**, 611-620
156. Famous, K. R., Delucchi, K., Ware, L. B., Kangelaris, K. N., Liu, K. D., Thompson, B. T., and Calfee, C. S. (2017) Acute Respiratory Distress Syndrome Subphenotypes Respond Differently to Randomized Fluid Management Strategy. *American Journal of Respiratory and Critical Care Medicine* **195**, 331-338
157. Bos, L. D. J., Scicluna, B. P., Ong, D. S. Y., Cremer, O., Poll, T. v. d., and Schultz, M. J. (2019) Understanding Heterogeneity in Biologic Phenotypes of Acute Respiratory Distress Syndrome by Leukocyte Expression Profiles. *American Journal of Respiratory and Critical Care Medicine* **200**, 42-50
158. Calfee, C. S., Delucchi, K. L., Sinha, P., Matthay, M. A., Hackett, J., Shankar-Hari, M., McDowell, C., Laffey, J. G., O'Kane, C. M., and McAuley, D. F. (2018) Acute respiratory distress syndrome subphenotypes and differential response to simvastatin: secondary analysis of a randomised controlled trial. *The Lancet Respiratory medicine* **6**, 691-698
159. Lee, T. J., Yuan, X., Kerr, K., Yoo, J. Y., Kim, D. H., Kaur, B., and Eltzschig, H. K. (2020) Strategies to Modulate MicroRNA Functions for the Treatment of Cancer or Organ Injury. *Pharmacological Reviews* **72**, 639-667
160. Neudecker, V., Haneklaus, M., Jensen, O., Khailova, L., Masterson, J. C., Tye, H., Biette, K., Jedlicka, P., Brodsky, K. S., Gerich, M. E., Mack, M., Robertson, A. A. B., Cooper, M. A., Furuta, G. T., Dinarello, C. A., O'Neill, L. A., Eltzschig, H. K., Masters, S.

- L., and McNamee, E. N. (2017) Myeloid-derived miR-223 regulates intestinal inflammation via repression of the NLRP3 inflammasome. *J Exp Med* **214**, 1737-1752
161. Merten, O.-W. (2006) Introduction to animal cell culture technology—past, present and future. *Cytotechnology* **50**, 1
162. Rous, P., and Jones, F. S. (1916) A method for obtaining suspensions of living cells from the fixed tissues, and for the plating out of individual cells. *The Journal of experimental medicine* **23**, 549-555
163. Milstein, C. (1999) The hybridoma revolution: an offshoot of basic research. *BioEssays* **21**, 966-973
164. Leland, D. S., and Ginocchio, C. C. (2007) Role of cell culture for virus detection in the age of technology. *Clin Microbiol Rev* **20**, 49-78
165. Leighton, J. (1957) Contributions of tissue culture studies to an understanding of the biology of cancer: a review. *Cancer research* **17**, 929-941
166. Sanford, K. K. (1965) Malignant transformation of cells in vitro. *Int. Rev. Cytol* **18**, 1
167. Beutler, B., Jiang, Z., Georgel, P., Crozat, K., Croker, B., Rutschmann, S., Du, X., and Hoebe, K. (2006) Genetic analysis of host resistance: Toll-like receptor signaling and immunity at large. *Annual review of immunology* **24**, 353-389
168. Vijay, K. (2018) Toll-like receptors in immunity and inflammatory diseases: Past, present, and future. *International Immunopharmacology* **59**, 391-412
169. Beck-Schimmer, B., Madjdpour, C., Kneller, S., Ziegler, U., Pasch, T., Wüthrich, R. P., Ward, P. A., and Schimmer, R. C. (2002) Role of alveolar epithelial ICAM-1 in lipopolysaccharide-induced lung inflammation. *European Respiratory Journal* **19**, 1142-1150
170. Thorley, A. J., Ford, P. A., Giembycz, M. A., Goldstraw, P., Young, A., and Tetley, T. D. (2007) Differential regulation of cytokine release and leukocyte migration by lipopolysaccharide-stimulated primary human lung alveolar type II epithelial cells and macrophages. *Journal of immunology (Baltimore, Md. : 1950)* **178**, 463-473

171. Hu, H., Li, X., Li, Y., Wang, L., Mehta, S., Feng, Q., Chen, R., and Peng, T. (2009) Calpain-1 induces apoptosis in pulmonary microvascular endothelial cells under septic conditions. *Microvascular research* **78**, 33-39
172. Hotchkiss, R. S., Tinsley, K. W., Swanson, P. E., and Karl, I. E. (2002) Endothelial cell apoptosis in sepsis. *Crit Care Med* **30**, S225-S228
173. Basuroy, S., Bhattacharya, S., Leffler, C. W., and Parfenova, H. (2009) Nox4 NADPH oxidase mediates oxidative stress and apoptosis caused by TNF- α in cerebral vascular endothelial cells. *American Journal of Physiology-Cell Physiology* **296**, C422-C432
174. Neudecker, V., Brodsky, K. S., Clambey, E. T., Schmidt, E. P., Packard, T. A., Davenport, B., Standiford, T. J., Weng, T., Fletcher, A. A., Barthel, L., Masterson, J. C., Furuta, G. T., Cai, C., Blackburn, M. R., Ginde, A. A., Graner, M. W., Janssen, W. J., Zemans, R. L., Evans, C. M., Burnham, E. L., Homann, D., Moss, M., Kreth, S., Zacharowski, K., Henson, P. M., and Eltzschig, H. K. (2017) Neutrophil transfer of miR-223 to lung epithelial cells dampens acute lung injury in mice. *Sci Transl Med* **9**
175. Oh, H., Siano, B., and Diamond, S. (2008) Neutrophil isolation protocol. *J Vis Exp*, 745
176. Lozano-Ojalvo, D., López-Fandiño, R., and López-Expósito, I. (2015) PBMC-Derived T Cells. In *The Impact of Food Bioactives on Health: in vitro and ex vivo models* (Verhoeckx, K., Cotter, P., López-Expósito, I., Kleiveland, C., Lea, T., Mackie, A., Requena, T., Swiatecka, D., and Wichers, H., eds) pp. 169-180, Springer International Publishing, Cham
177. Zhu, J., and Paul, W. E. (2010) Peripheral CD4⁺ T-cell differentiation regulated by networks of cytokines and transcription factors. *Immunological reviews* **238**, 247-262
178. Safi, W., Kuehnl, A., Nüssler, A., Eckstein, H.-H., and Pelisek, J. (2016) Differentiation of human CD14⁺ monocytes: an experimental investigation of the optimal culture medium and evidence of a lack of differentiation along the endothelial line. *Experimental & Molecular Medicine* **48**, e227-e227

179. Italiani, P., and Boraschi, D. (2014) From Monocytes to M1/M2 Macrophages: Phenotypical vs. Functional Differentiation. *Frontiers in Immunology* **5**
180. Panda, S. K., and Ravindran, B. (2013) Isolation of Human PBMCs. *Bio-protocol* **3**, e323
181. Geissmann, F., Manz, M. G., Jung, S., Sieweke, M. H., Merad, M., and Ley, K. (2010) Development of monocytes, macrophages, and dendritic cells. *Science (New York, N.Y.)* **327**, 656-661
182. Na, Y. R., Jung, D., Gu, G. J., and Seok, S. H. (2016) GM-CSF Grown Bone Marrow Derived Cells Are Composed of Phenotypically Different Dendritic Cells and Macrophages. *Mol Cells* **39**, 734-741
183. Zhang, X., Edwards, J. P., and Mosser, D. M. (2009) The expression of exogenous genes in macrophages: obstacles and opportunities. *Methods in molecular biology (Clifton, N.J.)* **531**, 123-143
184. Moradian, H., Roch, T., Lendlein, A., and Gossen, M. (2020) mRNA Transfection-Induced Activation of Primary Human Monocytes and Macrophages: Dependence on Carrier System and Nucleotide Modification. *Scientific Reports* **10**, 4181
185. Pinilla-Vera, M., Xiong, Z., Zhao, Y., Zhao, J., Donahoe, M. P., Barge, S., Horne, W. T., Kolls, J. K., McVerry, B. J., Birukova, A., Tighe, R. M., Foster, W. M., Hollingsworth, J., Ray, A., Mallampalli, R., Ray, P., and Lee, J. S. (2016) Full Spectrum of LPS Activation in Alveolar Macrophages of Healthy Volunteers by Whole Transcriptomic Profiling. *PLoS One* **11**, e0159329
186. Tighe, R. M., Redente, E. F., Yu, Y.-R., Herold, S., Sperling, A. I., Curtis, J. L., Duggan, R., Swaminathan, S., Nakano, H., Zacharias, W. J., Janssen, W. J., Freeman, C. M., Brinkman, R. R., Singer, B. D., Jakubzick, C. V., and Misharin, A. V. (2019) Improving the Quality and Reproducibility of Flow Cytometry in the Lung. An Official American Thoracic Society Workshop Report. *American Journal of Respiratory Cell and Molecular Biology* **61**, 150-161

187. Steinberg, K. P., Milberg, J. A., Martin, T. R., Maunder, R. J., Cockrill, B. A., and Hudson, L. D. (1994) Evolution of bronchoalveolar cell populations in the adult respiratory distress syndrome. *Am J Respir Crit Care Med* **150**, 113-122
188. Morrell, E. D., II, F. R., Manicone, A. M., Mikacenic, C., Stapleton, R. D., Gharib, S. A., and Wurfel, M. M. (2018) Peripheral and Alveolar Cell Transcriptional Programs Are Distinct in Acute Respiratory Distress Syndrome. *American Journal of Respiratory and Critical Care Medicine* **197**, 528-532
189. Vlahakis, N. E., Schroeder, M. A., Limper, A. H., and Hubmayr, R. D. (1999) Stretch induces cytokine release by alveolar epithelial cells in vitro. *American Journal of Physiology-Lung Cellular and Molecular Physiology* **277**, L167-L173
190. Eckle, T., Brodsky, K., Bonney, M., Packard, T., Han, J., Borchers, C. H., Mariani, T. J., Kominsky, D. J., Mittelbronn, M., and Eltzschig, H. K. (2013) HIF1A reduces acute lung injury by optimizing carbohydrate metabolism in the alveolar epithelium. *PLoS Biol* **11**, e1001665
191. Huh, D., Leslie, D. C., Matthews, B. D., Fraser, J. P., Jurek, S., Hamilton, G. A., Thorneloe, K. S., McAlexander, M. A., and Ingber, D. E. (2012) A human disease model of drug toxicity–induced pulmonary edema in a lung-on-a-chip microdevice. *Science translational medicine* **4**, 159ra147-159ra147
192. Huh, D., Matthews, B. D., Mammoto, A., Montoya-Zavala, M., Hsin, H. Y., and Ingber, D. E. (2010) Reconstituting organ-level lung functions on a chip. *Science* **328**, 1662-1668
193. Benam, K. H., Villenave, R., Lucchesi, C., Varone, A., Hubeau, C., Lee, H.-H., Alves, S. E., Salmon, M., Ferrante, T. C., Weaver, J. C., Bahinski, A., Hamilton, G. A., and Ingber, D. E. (2016) Small airway-on-a-chip enables analysis of human lung inflammation and drug responses in vitro. *Nature Methods* **13**, 151-157
194. Viola, H., Chang, J., Grunwell, J. R., Hecker, L., Tirouvanziam, R., Grotberg, J. B., and Takayama, S. (2019) Microphysiological systems modeling acute respiratory distress

- syndrome that capture mechanical force-induced injury-inflammation-repair. *APL Bioeng* **3**, 041503-041503
195. Matute-Bello, G., Frevert, C. W., and Martin, T. R. (2008) Animal models of acute lung injury. *American Journal of Physiology-Lung Cellular and Molecular Physiology* **295**, L379-L399
 196. Matute-Bello, G., Downey, G., Moore, B. B., Groshong, S. D., Matthay, M. A., Slutsky, A. S., and Kuebler, W. M. (2011) An official American Thoracic Society workshop report: features and measurements of experimental acute lung injury in animals. *American journal of respiratory cell and molecular biology* **44**, 725-738
 197. Bouabe, H., and Okkenhaug, K. (2013) Gene targeting in mice: a review. *Methods in molecular biology (Clifton, N.J.)* **1064**, 315-336
 198. Bockamp, E., Maringer, M., Spangenberg, C., Fees, S., Fraser, S., Eshkind, L., Oesch, F., and Zabel, B. (2002) Of mice and models: improved animal models for biomedical research. *Physiological genomics* **11**, 115-132
 199. Jinek, M., Chylinski, K., Fonfara, I., Hauer, M., Doudna, J. A., and Charpentier, E. (2012) A Programmable Dual-RNA–Guided DNA Endonuclease in Adaptive Bacterial Immunity. *Science* **337**, 816-821
 200. Modzelewski, A. J., Chen, S., Willis, B. J., Lloyd, K. C. K., Wood, J. A., and He, L. (2018) Efficient mouse genome engineering by CRISPR-EZ technology. *Nature Protocols* **13**, 1253-1274
 201. Gurumurthy, C. B., O'Brien, A. R., Quadros, R. M., Adams, J., Alcaide, P., Ayabe, S., Ballard, J., Batra, S. K., Beauchamp, M.-C., Becker, K. A., Bernas, G., Brough, D., Carrillo-Salinas, F., Chan, W., Chen, H., Dawson, R., DeMambro, V., D'Hont, J., Dibb, K. M., Eudy, J. D., Gan, L., Gao, J., Gonzales, A., Guntur, A. R., Guo, H., Harms, D. W., Harrington, A., Hentges, K. E., Humphreys, N., Imai, S., Ishii, H., Iwama, M., Jonasch, E., Karolak, M., Keavney, B., Khin, N.-C., Konno, M., Kotani, Y., Kunihiro, Y., Lakshmanan, I., Larochelle, C., Lawrence, C. B., Li, L., Lindner, V., Liu, X.-D., Lopez-

- Castejon, G., Loudon, A., Lowe, J., Jerome-Majewska, L. A., Matsusaka, T., Miura, H., Miyasaka, Y., Morpurgo, B., Motyl, K., Nabeshima, Y.-i., Nakade, K., Nakashiba, T., Nakashima, K., Obata, Y., Ogiwara, S., Ouellet, M., Oxburgh, L., Piltz, S., Pinz, I., Ponnusamy, M. P., Ray, D., Redder, R. J., Rosen, C. J., Ross, N., Ruhe, M. T., Ryzhova, L., Salvador, A. M., Alam, S. S., Sedlacek, R., Sharma, K., Smith, C., Staes, K., Starrs, L., Sugiyama, F., Takahashi, S., Tanaka, T., Trafford, A. W., Uno, Y., Vanhoutte, L., Vanrockeghem, F., Willis, B. J., Wright, C. S., Yamauchi, Y., Yi, X., Yoshimi, K., Zhang, X., Zhang, Y., Ohtsuka, M., Das, S., Garry, D. J., Hochepped, T., Thomas, P., Parker-Thornburg, J., Adamson, A. D., Yoshiki, A., Schmouth, J.-F., Golovko, A., Thompson, W. R., Lloyd, K. C. K., Wood, J. A., Cowan, M., Mashimo, T., Mizuno, S., Zhu, H., Kasperek, P., Liaw, L., Miano, J. M., and Burgio, G. (2019) Reproducibility of CRISPR-Cas9 methods for generation of conditional mouse alleles: a multi-center evaluation. *Genome Biol* **20**, 171
202. Das, S., MacDonald, K., Chang, H.-Y. S., and Mitzner, W. (2013) A simple method of mouse lung intubation. *J Vis Exp*, e50318-e50318
203. Mizgerd, J. P., and Skerrett, S. J. (2008) Animal models of human pneumonia. *American Journal of Physiology-Lung Cellular and Molecular Physiology* **294**, L387-L398
204. Kukavica-Ibrulj, I., Facchini, M., Cigana, C., Levesque, R. C., and Bragonzi, A. (2014) Assessing *Pseudomonas aeruginosa* virulence and the host response using murine models of acute and chronic lung infection. *Methods Mol Biol* **1149**, 757-771
205. Wan, Y., Shang, J., Graham, R., Baric, R. S., and Li, F. (2020) Receptor recognition by the novel coronavirus from Wuhan: an analysis based on decade-long structural studies of SARS coronavirus. *Journal of virology* **94**
206. Johansen, M. D., Irving, A., Montagutelli, X., Tate, M. D., Rudloff, I., Nold, M. F., Hansbro, N. G., Kim, R. Y., Donovan, C., Liu, G., Faiz, A., Short, K. R., Lyons, J. G., McCaughan, G. W., Gorrell, M. D., Cole, A., Moreno, C., Couteur, D., Hesselton, D.,

- Triccas, J., Neely, G. G., Gamble, J. R., Simpson, S. J., Saunders, B. M., Oliver, B. G., Britton, W. J., Wark, P. A., Nold-Petry, C. A., and Hansbro, P. M. (2020) Animal and translational models of SARS-CoV-2 infection and COVID-19. *Mucosal Immunology* **13**, 877-891
207. Israelow, B., Song, E., Mao, T., Lu, P., Meir, A., Liu, F., Alfajaro, M. M., Wei, J., Dong, H., and Homer, R. J. (2020) Mouse model of SARS-CoV-2 reveals inflammatory role of type I interferon signaling. *Journal of Experimental Medicine* **217**
208. Leist, S. R., Dinnon III, K. H., Schäfer, A., Longping, V. T., Okuda, K., Hou, Y. J., West, A., Edwards, C. E., Sanders, W., and Fritch, E. J. (2020) A mouse-adapted SARS-CoV-2 induces acute lung injury and mortality in standard laboratory mice. *Cell* **183**, 1070-1085. e1012
209. Raut, S., Hurd, J., Cureton, R., Blandford, G., and Heath, R. (1975) The pathogenesis of infections of the mouse caused by virulent and avirulent variants of an influenza virus. *Journal of medical microbiology* **8**, 127-136
210. Hirst, G. K. (1947) Studies on the mechanism of adaptation of influenza virus to mice. *The Journal of experimental medicine* **86**, 357-366
211. Schneemann, M., Schoedon, G., Hofer, S., Blau, N., Guerrero, L., and Schaffner, A. (1993) Nitric oxide synthase is not a constituent of the antimicrobial armature of human mononuclear phagocytes. *Journal of Infectious Diseases* **167**, 1358-1363
212. Jungi, T., Adler, H., Adler, B., Thöny, M., Krampe, M., and Peterhans, E. (1996) Inducible nitric oxide synthase of macrophages. Present knowledge and evidence for species-specific regulation. *Veterinary immunology and immunopathology* **54**, 323-330
213. Jesch, N. K., Dörger, M., Enders, G., Rieder, G., Vogelmeier, C., Messmer, K., and Krombach, F. (1997) Expression of inducible nitric oxide synthase and formation of nitric oxide by alveolar macrophages: an interspecies comparison. *Environmental health perspectives* **105**, 1297-1300

214. Dörger, M., Jesch, N. K., Rieder, G., Hirvonen, M.-R., Savolainen, K., Krombach, F., and Messmer, K. (1997) Species differences in NO formation by rat and hamster alveolar macrophages in vitro. *American journal of respiratory cell and molecular biology* **16**, 413-420
215. Raj, J. U., Hazinski, T. A., and Bland, R. D. (1985) Oxygen-induced lung microvascular injury in neutropenic rabbits and lambs. *Journal of Applied Physiology* **58**, 921-927
216. Hajjar, A. M., Ernst, R. K., Tsai, J. H., Wilson, C. B., and Miller, S. I. (2002) Human Toll-like receptor 4 recognizes host-specific LPS modifications. *Nature immunology* **3**, 354-359
217. Kuida, H., Hinshaw, L. B., Gilbert, R. P., and Visscher, M. B. (1958) Effect of gram-negative endotoxin on pulmonary circulation. *American Journal of Physiology-Legacy Content* **192**, 335-344
218. Sone, Y., Serikov, V. B., and Staub Sr, N. C. (1999) Intravascular macrophage depletion attenuates endotoxin lung injury in anesthetized sheep. *Journal of Applied Physiology* **87**, 1354-1359
219. Warner, A. E. (1996) Pulmonary intravascular macrophages: role in acute lung injury. *Clin Chest Med* **17**, 125-135
220. Brain, J. D., Molina, R. M., DeCamp, M. M., and Warner, A. E. (1999) Pulmonary intravascular macrophages: their contribution to the mononuclear phagocyte system in 13 species. *American Journal of Physiology-Lung Cellular and Molecular Physiology* **276**, L146-L154
221. MATUTE-BELLO, G., Frevert, C. W., Kajikawa, O., SKERRETT, S. J., GOODMAN, R. B., PARK, D. R., and MARTIN, T. R. (2001) Septic shock and acute lung injury in rabbits with peritonitis: failure of the neutrophil response to localized infection. *American journal of respiratory and critical care medicine* **163**, 234-243

222. Butz, G. M., and Davisson, R. L. (2001) Long-term telemetric measurement of cardiovascular parameters in awake mice: a physiological genomics tool. *Physiological genomics* **5**, 89-97
223. Kajikawa, O., Johnson II, M. C., Goodman, R. B., Frevert, C. W., and Martin, T. R. (1997) A sensitive immunoassay to detect the α -chemokine GRO in rabbit blood and lung fluids. *Journal of immunological methods* **205**, 135-143
224. Kajikawa, O., Goodman, R., Johnson, M., and Martin, T. (1996) Sensitive and specific immunoassays for rabbit IL-8 and MCP-1: two important cytokines that regulate leukocyte migration in the lungs. *J Immunol Methods* **197**, 19-29
225. Tapping, R. I., Akashi, S., Miyake, K., Godowski, P. J., and Tobias, P. S. (2000) Toll-like receptor 4, but not toll-like receptor 2, is a signaling receptor for Escherichia and Salmonella lipopolysaccharides. *The Journal of Immunology* **165**, 5780-5787
226. Wright, S. D., Ramos, R. A., Tobias, P. S., Ulevitch, R. J., and Mathison, J. C. (1990) CD14, a receptor for complexes of lipopolysaccharide (LPS) and LPS binding protein. *Science* **249**, 1431-1433
227. Martin, T. R., Mathison, J. C., Tobias, P. S., Leturcq, D., Moriarty, A., Maunder, R., and Ulevitch, R. (1992) Lipopolysaccharide binding protein enhances the responsiveness of alveolar macrophages to bacterial lipopolysaccharide. Implications for cytokine production in normal and injured lungs. *The Journal of clinical investigation* **90**, 2209-2219
228. Tobias, P. S., Soldau, K., and Ulevitch, R. J. (1986) Isolation of a lipopolysaccharide-binding acute phase reactant from rabbit serum. *The Journal of experimental medicine* **164**, 777-793
229. Kawasaki, M., Kuwano, K., Hagimoto, N., Matsuba, T., Kunitake, R., Tanaka, T., Maeyama, T., and Hara, N. (2000) Protection from lethal apoptosis in lipopolysaccharide-induced acute lung injury in mice by a caspase inhibitor. *The American journal of pathology* **157**, 597-603

230. Wang, H. L., Akinci, I. O., Baker, C. M., Urich, D., Bellmeyer, A., Jain, M., Chandel, N. S., Mutlu, G. M., and Budinger, G. S. (2007) The intrinsic apoptotic pathway is required for lipopolysaccharide-induced lung endothelial cell death. *The Journal of Immunology* **179**, 1834-1841
231. Fujita, M., Kuwano, K., Kunitake, R., Hagimoto, N., Miyazaki, H., Kaneko, Y., Kawasaki, M., Maeyama, T., and Hara, N. (1998) Endothelial cell apoptosis in lipopolysaccharide-induced lung injury in mice. *International archives of allergy and immunology* **117**, 202-208
232. Reutershan, J., Cagnina, R. E., Chang, D., Linden, J., and Ley, K. (2007) Therapeutic anti-inflammatory effects of myeloid cell adenosine receptor A2a stimulation in lipopolysaccharide-induced lung injury. *The Journal of Immunology* **179**, 1254-1263
233. O'GRADY, N. P., PREAS, H. L., Pugin, J., Fiuza, C., Tropea, M., Reda, D., Banks, S. M., and Suffredini, A. F. (2001) Local inflammatory responses following bronchial endotoxin instillation in humans. *American journal of respiratory and critical care medicine* **163**, 1591-1598
234. Smith, P. D., Suffredini, A. F., Allen, J. B., Wahl, L. M., Parrillo, J. E., and Wahl, S. M. (1994) Endotoxin administration to humans primes alveolar macrophages for increased production of inflammatory mediators. *Journal of clinical immunology* **14**, 141-148
235. Abraham, E. (2003) Neutrophils and acute lung injury. *Crit Care Med* **31**, S195-199
236. Lee, W. L., and Downey, G. P. (2001) Neutrophil activation and acute lung injury. *Current opinion in critical care* **7**, 1-7
237. Harris, A. J., Mirchandani, A. S., Lynch, R. W., Murphy, F., Delaney, L., Small, D., Coelho, P., Watts, E. R., Sadiku, P., Griffith, D., Dickinson, R. S., Clark, E., Willson, J. A., Morrison, T., Mazzone, M., Carmeliet, P., Ghesquiere, B., O'Kane, C., McAuley, D., Jenkins, S. J., Whyte, M. K. B., and Walmsley, S. R. (2019) IL4R α Signaling Abrogates Hypoxic Neutrophil Survival and Limits Acute Lung Injury Responses In Vivo. *American journal of respiratory and critical care medicine* **200**, 235-246

238. Sadiku, P., Willson, J. A., Dickinson, R. S., Murphy, F., Harris, A. J., Lewis, A., Sammut, D., Mirchandani, A. S., Ryan, E., Watts, E. R., Thompson, A. A. R., Marriott, H. M., Dockrell, D. H., Taylor, C. T., Schneider, M., Maxwell, P. H., Chilvers, E. R., Mazzone, M., Moral, V., Pugh, C. W., Ratcliffe, P. J., Schofield, C. J., Ghesquiere, B., Carmeliet, P., Whyte, M. K., and Walmsley, S. R. (2017) Prolyl hydroxylase 2 inactivation enhances glycogen storage and promotes excessive neutrophilic responses. *The Journal of clinical investigation* **127**, 3407-3420
239. Wiener-Kronish, J., Albertine, K., and Matthay, M. (1991) Differential responses of the endothelial and epithelial barriers of the lung in sheep to Escherichia coli endotoxin. *The Journal of clinical investigation* **88**, 864-875
240. Winkler, G. C. (1989) Review of the significance of pulmonary intravascular macrophages with respect to animal species and age. *Pathobiology* **57**, 281-286
241. Roy-Burman, A., Savel, R. H., Racine, S., Swanson, B. L., Revadigar, N. S., Fujimoto, J., Sawa, T., Frank, D. W., and Wiener-Kronish, J. P. (2001) Type III protein secretion is associated with death in lower respiratory and systemic Pseudomonas aeruginosa infections. *The Journal of infectious diseases* **183**, 1767-1774
242. Kudoh, I., Wiener-Kronish, J. P., Hashimoto, S., Pittet, J.-F., and Frank, D. (1994) Exoproduct secretions of Pseudomonas aeruginosa strains influence severity of alveolar epithelial injury. *American Journal of Physiology-Lung Cellular and Molecular Physiology* **267**, L551-L556
243. Walley, K. R., Lukacs, N. W., Standiford, T. J., Strieter, R. M., and Kunkel, S. L. (1996) Balance of inflammatory cytokines related to severity and mortality of murine sepsis. *Infection and immunity* **64**, 4733-4738
244. Goya, T., Abe, M., Shimura, H., and Torisu, M. (1992) Characteristics of alveolar macrophages in experimental septic lung. *Journal of leukocyte biology* **52**, 236-243

245. Villar, J., Ribeiro, S. P., Mullen, J., Kuliszewski, M., Post, M., and Slutsky, A. S. (1994) Induction of the heat shock response reduces mortality rate and organ damage in a sepsis-induced acute lung injury model. *Crit Care Med* **22**, 914-921
246. Lomas-Neira, J. L., Chung, C. S., Wesche, D. E., Perl, M., and Ayala, A. (2005) In vivo gene silencing (with siRNA) of pulmonary expression of MIP-2 versus KC results in divergent effects on hemorrhage-induced, neutrophil-mediated septic acute lung injury. *Journal of leukocyte biology* **77**, 846-853
247. Gnidec, A. G., Sibbald, W. J., Cheung, H., and Metz, C. A. (1988) Ibuprofen reduces the progression of permeability edema in an animal model of hyperdynamic sepsis. *Journal of Applied Physiology* **65**, 1024-1032
248. Mendelson, C. L. (1946) The aspiration of stomach contents into the lungs during obstetric anesthesia. *Obstetrical & Gynecological Survey* **1**, 837-839
249. Slutsky, A. S., and Ranieri, V. M. (2013) Ventilator-Induced Lung Injury. *New England Journal of Medicine* **369**, 2126-2136
250. Knight, P. R., Druskovich, G., Tait, A. R., and Johnson, K. J. (1992) The role of neutrophils, oxidants, and proteases in the pathogenesis of acid pulmonary injury. In *The Journal of the American Society of Anesthesiologists* Vol. 77 pp. 772-778, The American Society of Anesthesiologists
251. Folkesson, H., Matthay, M., Hebert, C., and Broaddus, V. (1995) Acid aspiration-induced lung injury in rabbits is mediated by interleukin-8-dependent mechanisms. *The Journal of clinical investigation* **96**, 107-116
252. Modelska, K., Pittet, J.-F., Folkesson, H. G., Courtney Broaddus, V., and Matthay, M. A. (1999) Acid-induced lung injury: protective effect of anti-interleukin-8 pretreatment on alveolar epithelial barrier function in rabbits. *American journal of respiratory and critical care medicine* **160**, 1450-1456
253. McAuley, D. F., Frank, J. A., Fang, X., and Matthay, M. A. (2004) Clinically relevant concentrations of β 2-adrenergic agonists stimulate maximal cyclic adenosine

- monophosphate-dependent airspace fluid clearance and decrease pulmonary edema in experimental acid-induced lung injury. *Crit Care Med* **32**, 1470-1476
254. Raghavendran, K., Davidson, B. A., Mullan, B. A., Hutson, A. D., Russo, T. A., Manderscheid, P. A., Woytash, J. A., Holm, B. A., Notter, R. H., and Knight, P. R. (2005) Acid and particulate-induced aspiration lung injury in mice: importance of MCP-1. *American Journal of Physiology-Lung Cellular and Molecular Physiology* **289**, L134-L143
255. Knight, P. R., Rutter, T., Tait, A. R., Coleman, E., and Johnson, K. (1993) Pathogenesis of gastric particulate lung injury: a comparison and interaction with acidic pneumonitis. *Anesthesia and analgesia* **77**, 754-760
256. Bonten, M., Gaillard, C. A., Van der Geest, S., Van Tiel, F., Beysens, A. J., Smeets, H., and Stobberingh, E. E. (1995) The role of intragastric acidity and stress ulcer prophylaxis on colonization and infection in mechanically ventilated ICU patients. A stratified, randomized, double-blind study of sucralfate versus antacids. *American journal of respiratory and critical care medicine* **152**, 1825-1834
257. Koeppen, M., Eckle, T., and Eltzschig, H. K. (2011) Pressure Controlled Ventilation to Induce Acute Lung Injury in Mice. *JoVE*, e2525
258. Dreyfuss, D., and Saumon, G. (1998) Ventilator-induced lung injury: lessons from experimental studies. *American journal of respiratory and critical care medicine* **157**, 294-323
259. Dos Santos, C., and Slutsky, A. (2000) Invited review: mechanisms of ventilator-induced lung injury: a perspective. *Journal of applied physiology* **89**, 1645-1655
260. Fu, Z., Costello, M. L., Tsukimoto, K., Prediletto, R., Elliott, A., Mathieu-Costello, O., and West, J. B. (1992) High lung volume increases stress failure in pulmonary capillaries. *Journal of Applied Physiology* **73**, 123-133

261. Kawano, T., Mori, S., Cybulsky, M., Burger, R., Ballin, A., Cutz, E., and Bryan, A. (1987) Effect of granulocyte depletion in a ventilated surfactant-depleted lung. *Journal of applied physiology* **62**, 27-33
262. O'Mahony, D., Liles, W., Altemeier, W. A., Dhanireddy, S., Frevert, C. W., Liggitt, D., Martin, T. R., and Matute-Bello, G. (2006) Mechanical ventilation interacts with endotoxemia to induce extrapulmonary organ dysfunction. *Critical Care* **10**, 1-9
263. Dhanireddy, S., Altemeier, W. A., Matute-Bello, G., O'Mahony, D. S., Glenny, R. W., Martin, T. R., and Liles, W. C. (2006) Mechanical ventilation induces inflammation, lung injury, and extra-pulmonary organ dysfunction in experimental pneumonia. *Laboratory Investigation* **86**, 790-799
264. Han, S., and Mallampalli, R. K. (2015) The acute respiratory distress syndrome: from mechanism to translation. *Journal of immunology (Baltimore, Md. : 1950)* **194**, 855-860
265. Aggarwal, N. R., King, L. S., and D'Alessio, F. R. (2014) Diverse macrophage populations mediate acute lung inflammation and resolution. *Am J Physiol Lung Cell Mol Physiol* **306**, L709-725
266. Castro, C. Y. (2006) ARDS and diffuse alveolar damage: a pathologist's perspective. *Seminars in thoracic and cardiovascular surgery* **18**, 13-19
267. Geiser, T., Atabai, K., Jarreau, P. H., Ware, L. B., Pugin, J., and Matthay, M. A. (2001) Pulmonary edema fluid from patients with acute lung injury augments in vitro alveolar epithelial repair by an IL-1beta-dependent mechanism. *Am J Respir Crit Care Med* **163**, 1384-1388
268. Rosseau, S., Hammerl, P., Maus, U., Walmrath, H. D., Schütte, H., Grimminger, F., Seeger, W., and Lohmeyer, J. (2000) Phenotypic characterization of alveolar monocyte recruitment in acute respiratory distress syndrome. *Am J Physiol Lung Cell Mol Physiol* **279**, L25-35

269. Meduri, G. U., Annane, D., Chrousos, G. P., Marik, P. E., and Sinclair, S. E. (2009) Activation and regulation of systemic inflammation in ARDS: rationale for prolonged glucocorticoid therapy. *Chest* **136**, 1631-1643
270. Burbelo, P. D., Seam, N., Groot, S., Ching, K. H., Han, B. L., Meduri, G. U., Iadarola, M. J., and Suffredini, A. F. (2010) Rapid induction of autoantibodies during ARDS and septic shock. *Journal of translational medicine* **8**, 97
271. Rosales, C. (2018) Neutrophil: A Cell with Many Roles in Inflammation or Several Cell Types? *Frontiers in Physiology* **9**
272. Jasper, A. E., McIver, W. J., Sapey, E., and Walton, G. M. (2019) Understanding the role of neutrophils in chronic inflammatory airway disease. *F1000Res* **8**, F1000 Faculty Rev-1557
273. Fournier, B. M., and Parkos, C. A. (2012) The role of neutrophils during intestinal inflammation. *Mucosal Immunology* **5**, 354-366
274. Cowburn, A. S., Condliffe, A. M., Farahi, N., Summers, C., and Chilvers, E. R. (2008) Advances in neutrophil biology: clinical implications. *Chest* **134**, 606-612
275. Bachofen, M., and Weibel, E. R. (1977) Alterations of the gas exchange apparatus in adult respiratory insufficiency associated with septicemia. *The American review of respiratory disease* **116**, 589-615
276. Parsons, P. E., Fowler, A. A., Hyers, T. M., and Henson, P. M. (1985) Chemotactic activity in bronchoalveolar lavage fluid from patients with adult respiratory distress syndrome. *The American review of respiratory disease* **132**, 490-493
277. Dorward, D. A., Felton, J. M., Robb, C. T., Craven, T., Kipari, T., Walsh, T. S., Haslett, C., Kefala, K., Rossi, A. G., and Lucas, C. D. (2017) The cyclin-dependent kinase inhibitor AT7519 accelerates neutrophil apoptosis in sepsis-related acute respiratory distress syndrome. *Thorax* **72**, 182-185
278. Juss, J. K., House, D., Amour, A., Begg, M., Herre, J., Storisteanu, D. M., Hoenderdos, K., Bradley, G., Lennon, M., Summers, C., Hessel, E. M., Condliffe, A., and Chilvers, E.

- R. (2016) Acute Respiratory Distress Syndrome Neutrophils Have a Distinct Phenotype and Are Resistant to Phosphoinositide 3-Kinase Inhibition. *Am J Respir Crit Care Med* **194**, 961-973
279. Sadiku, P., Willson, J. A., Dickinson, R. S., Murphy, F., Harris, A. J., Lewis, A., Sammut, D., Mirchandani, A. S., Ryan, E., Watts, E. R., Thompson, A. A. R., Marriott, H. M., Dockrell, D. H., Taylor, C. T., Schneider, M., Maxwell, P. H., Chilvers, E. R., Mazzone, M., Moral, V., Pugh, C. W., Ratcliffe, P. J., Schofield, C. J., Ghesquiere, B., Carmeliet, P., Whyte, M. K., and Walmsley, S. R. (2017) Prolyl hydroxylase 2 inactivation enhances glycogen storage and promotes excessive neutrophilic responses. *J Clin Invest* **127**, 3407-3420
280. Shi, C., and Pamer, E. G. (2011) Monocyte recruitment during infection and inflammation. *Nature reviews immunology* **11**, 762-774
281. Aggarwal, N. R., King, L. S., and D'Alessio, F. R. (2014) Diverse macrophage populations mediate acute lung inflammation and resolution. *American journal of physiology. Lung cellular and molecular physiology* **306**, L709-L725
282. Heung, L. J., and Hohl, T. M. (2019) Inflammatory monocytes are detrimental to the host immune response during acute infection with *Cryptococcus neoformans*. *PLoS pathogens* **15**, e1007627
283. Coates, B. M., Staricha, K. L., Koch, C. M., Cheng, Y., Shumaker, D. K., Budinger, G. R. S., Perlman, H., Misharin, A. V., and Ridge, K. M. (2018) Inflammatory Monocytes Drive Influenza A Virus–Mediated Lung Injury in Juvenile Mice. *The Journal of Immunology* **200**, 2391-2404
284. Lee, A. J., Chen, B., Chew, M. V., Barra, N. G., Shenouda, M. M., Nham, T., van Rooijen, N., Jordana, M., Mossman, K. L., and Schreiber, R. D. (2017) Inflammatory monocytes require type I interferon receptor signaling to activate NK cells via IL-18 during a mucosal viral infection. *Journal of Experimental Medicine* **214**, 1153-1167

285. Tang, H., Li, T., Han, X., and Sun, J. (2019) TLR4 antagonist ameliorates combined allergic rhinitis and asthma syndrome (CARAS) by reducing inflammatory monocytes infiltration in mice model. *International immunopharmacology* **73**, 254-260
286. Wilson, M. R., O'Dea, K. P., Zhang, D., Shearman, A. D., Rooijen, N. v., and Takata, M. (2009) Role of Lung-marginated Monocytes in an In Vivo Mouse Model of Ventilator-induced Lung Injury. *American Journal of Respiratory and Critical Care Medicine* **179**, 914-922
287. Zaslona, Z., Przybranowski, S., Wilke, C., van Rooijen, N., Teitz-Tennenbaum, S., Osterholzer, J. J., Wilkinson, J. E., Moore, B. B., and Peters-Golden, M. (2014) Resident alveolar macrophages suppress, whereas recruited monocytes promote, allergic lung inflammation in murine models of asthma. *The Journal of Immunology* **193**, 4245-4253
288. Dhaliwal, K., Scholefield, E., Ferenbach, D., Gibbons, M., Duffin, R., Dorward, D. A., Morris, A. C., Humphries, D., MacKinnon, A., Wilkinson, T. S., Wallace, W. A. H., van Rooijen, N., Mack, M., Rossi, A. G., Davidson, D. J., Hirani, N., Hughes, J., Haslett, C., and Simpson, A. J. (2012) Monocytes control second-phase neutrophil emigration in established lipopolysaccharide-induced murine lung injury. *American journal of respiratory and critical care medicine* **186**, 514-524
289. McCubbrey, A. L., Barthel, L., Mohning, M. P., Redente, E. F., Mould, K. J., Thomas, S. M., Leach, S. M., Danhorn, T., Gibbings, S. L., Jakubzick, C. V., Henson, P. M., and Janssen, W. J. (2018) Deletion of c-FLIP from CD11bhi Macrophages Prevents Development of Bleomycin-induced Lung Fibrosis. *American Journal of Respiratory Cell and Molecular Biology* **58**, 66-78
290. Janssen, W. J., Barthel, L., Muldrow, A., Oberley-Deegan, R. E., Kearns, M. T., Jakubzick, C., and Henson, P. M. (2011) Fas determines differential fates of resident and recruited macrophages during resolution of acute lung injury. *American journal of respiratory and critical care medicine* **184**, 547-560

291. Kawai, T., and Akira, S. (2010) The role of pattern-recognition receptors in innate immunity: update on Toll-like receptors. *Nat Immunol* **11**, 373-384
292. Rock, F. L., Hardiman, G., Timans, J. C., Kastelein, R. A., and Bazan, J. F. (1998) A family of human receptors structurally related to Drosophila Toll. *Proc Natl Acad Sci U S A* **95**, 588-593
293. Jiang, D., Liang, J., Fan, J., Yu, S., Chen, S., Luo, Y., Prestwich, G. D., Mascarenhas, M. M., Garg, H. G., Quinn, D. A., Homer, R. J., Goldstein, D. R., Bucala, R., Lee, P. J., Medzhitov, R., and Noble, P. W. (2005) Regulation of lung injury and repair by Toll-like receptors and hyaluronan. *Nat Med* **11**, 1173-1179
294. Jeyaseelan, S., Chu, H. W., Young, S. K., Freeman, M. W., and Worthen, G. S. (2005) Distinct roles of pattern recognition receptors CD14 and Toll-like receptor 4 in acute lung injury. *Infection and immunity* **73**, 1754-1763
295. Franchi, L., Muñoz-Planillo, R., and Núñez, G. (2012) Sensing and reacting to microbes through the inflammasomes. *Nat Immunol* **13**, 325-332
296. Swanson, K. V., Deng, M., and Ting, J. P. Y. (2019) The NLRP3 inflammasome: molecular activation and regulation to therapeutics. *Nature Reviews Immunology* **19**, 477-489
297. Jones, H. D., Crother, T. R., Gonzalez-Villalobos, R. A., Jupelli, M., Chen, S., Dagvadorj, J., Arditi, M., and Shimada, K. (2014) The NLRP3 inflammasome is required for the development of hypoxemia in LPS/mechanical ventilation acute lung injury. *Am J Respir Cell Mol Biol* **50**, 270-280
298. Dolinay, T., Kim, Y. S., Howrylak, J., Hunninghake, G. M., An, C. H., Fredenburgh, L., Massaro, A. F., Rogers, A., Gazourian, L., Nakahira, K., Haspel, J. A., Landazury, R., Eppanapally, S., Christie, J. D., Meyer, N. J., Ware, L. B., Christiani, D. C., Ryter, S. W., Baron, R. M., and Choi, A. M. (2012) Inflammasome-regulated cytokines are critical mediators of acute lung injury. *Am J Respir Crit Care Med* **185**, 1225-1234

299. Eltzschig, H. K., and Carmeliet, P. (2011) Hypoxia and inflammation. *N Engl J Med* **364**, 656-665
300. Semenza, G. L., Neifelt, M. K., Chi, S. M., and Antonarakis, S. E. (1991) Hypoxia-inducible nuclear factors bind to an enhancer element located 3' to the human erythropoietin gene. *Proc Natl Acad Sci U S A* **88**, 5680-5684
301. Wang, G. L., and Semenza, G. L. (1995) Purification and characterization of hypoxia-inducible factor 1. *J Biol Chem* **270**, 1230-1237
302. Wang, G. L., Jiang, B. H., Rue, E. A., and Semenza, G. L. (1995) Hypoxia-inducible factor 1 is a basic-helix-loop-helix-PAS heterodimer regulated by cellular O₂ tension. *Proc Natl Acad Sci U S A* **92**, 5510-5514
303. Ohh, M., Park, C. W., Ivan, M., Hoffman, M. A., Kim, T. Y., Huang, L. E., Pavletich, N., Chau, V., and Kaelin, W. G. (2000) Ubiquitination of hypoxia-inducible factor requires direct binding to the beta-domain of the von Hippel-Lindau protein. *Nat Cell Biol* **2**, 423-427
304. Ivan, M., Kondo, K., Yang, H., Kim, W., Valiando, J., Ohh, M., Salic, A., Asara, J. M., Lane, W. S., and Kaelin, W. G., Jr. (2001) HIF α targeted for VHL-mediated destruction by proline hydroxylation: implications for O₂ sensing. *Science* **292**, 464-468
305. Jaakkola, P., Mole, D. R., Tian, Y. M., Wilson, M. I., Gielbert, J., Gaskell, S. J., von Kriegsheim, A., Hebestreit, H. F., Mukherji, M., Schofield, C. J., Maxwell, P. H., Pugh, C. W., and Ratcliffe, P. J. (2001) Targeting of HIF- α to the von Hippel-Lindau ubiquitylation complex by O₂-regulated prolyl hydroxylation. *Science* **292**, 468-472
306. Kimura, H., Weisz, A., Kurashima, Y., Hashimoto, K., Ogura, T., D'Acquisto, F., Addeo, R., Makuuchi, M., and Esumi, H. (2000) Hypoxia response element of the human vascular endothelial growth factor gene mediates transcriptional regulation by nitric oxide: control of hypoxia-inducible factor-1 activity by nitric oxide. *Blood* **95**, 189-197

307. O'Rourke, J. F., Dachs, G. U., Gleadle, J. M., Maxwell, P. H., Pugh, C. W., Stratford, I. J., Wood, S. M., and Ratcliffe, P. J. (1997) Hypoxia response elements. *Oncology research* **9**, 327-332
308. Kim, J. W., Tchernyshyov, I., Semenza, G. L., and Dang, C. V. (2006) HIF-1-mediated expression of pyruvate dehydrogenase kinase: a metabolic switch required for cellular adaptation to hypoxia. *Cell Metab* **3**, 177-185
309. Dengler, V. L., Galbraith, M. D., and Espinosa, J. M. (2014) Transcriptional regulation by hypoxia inducible factors. *Critical reviews in biochemistry and molecular biology* **49**, 1-15
310. Yuan, X., Lee, J. W., Bowser, J. L., Neudecker, V., Sridhar, S., and Eltzschig, H. K. (2018) Targeting Hypoxia Signaling for Perioperative Organ Injury. *Anesth Analg* **126**, 308-321
311. Haeberle, H. A., Dürrstein, C., Rosenberger, P., Hosakote, Y. M., Kuhlicke, J., Kempf, V. A., Garofalo, R. P., and Eltzschig, H. K. (2008) Oxygen-independent stabilization of hypoxia inducible factor (HIF)-1 during RSV infection. *PLoS One* **3**
312. Vohwinkel, C. U., Coit, E. J., Burns, N., Elajaili, H., Hernandez-Saavedra, D., Yuan, X., Eckle, T., Nozik, E., Tuder, R. M., and Eltzschig, H. K. (2021) Targeting alveolar-specific succinate dehydrogenase A attenuates pulmonary inflammation during acute lung injury. *The FASEB Journal* **35**, e21468
313. Ju, C., Colgan, S. P., and Eltzschig, H. K. (2016) Hypoxia-inducible factors as molecular targets for liver diseases. *Journal of Molecular Medicine* **94**, 613-627
314. Poth, J. M., Brodsky, K., Ehrentraut, H., Grenz, A., and Eltzschig, H. K. (2013) Transcriptional control of adenosine signaling by hypoxia-inducible transcription factors during ischemic or inflammatory disease. *Journal of molecular medicine* **91**, 183-193
315. Eckle, T., Kewley, E. M., Brodsky, K. S., Tak, E., Bonney, S., Gobel, M., Anderson, D., Glover, L. E., Riegel, A. K., Colgan, S. P., and Eltzschig, H. K. (2014) Identification of hypoxia-inducible factor HIF-1A as transcriptional regulator of the A2B adenosine

- receptor during acute lung injury. *Journal of immunology (Baltimore, Md. : 1950)* **192**, 1249-1256
316. Hoegl, S., Brodsky, K. S., Blackburn, M. R., Karmouty-Quintana, H., Zwissler, B., and Eltzschig, H. K. (2015) Alveolar Epithelial A2B Adenosine Receptors in Pulmonary Protection during Acute Lung Injury. *Journal of immunology (Baltimore, Md. : 1950)* **195**, 1815-1824
317. Eckle, T., Fullbier, L., Wehrmann, M., Khoury, J., Mittelbronn, M., Ibla, J., Rosenberger, P., and Eltzschig, H. K. (2007) Identification of ectonucleotidases CD39 and CD73 in innate protection during acute lung injury. *Journal of immunology (Baltimore, Md. : 1950)* **178**, 8127-8137
318. Reutershan, J., Vollmer, I., Stark, S., Wagner, R., Ngamsri, K. C., and Eltzschig, H. K. (2009) Adenosine and inflammation: CD39 and CD73 are critical mediators in LPS-induced PMN trafficking into the lungs. *FASEB J* **23**, 473-482
319. Ebert, B. L., Firth, J. D., and Ratcliffe, P. J. (1995) Hypoxia and mitochondrial inhibitors regulate expression of glucose transporter-1 via distinct Cis-acting sequences. *J Biol Chem* **270**, 29083-29089
320. Semenza, G. L., Roth, P. H., Fang, H. M., and Wang, G. L. (1994) Transcriptional regulation of genes encoding glycolytic enzymes by hypoxia-inducible factor 1. *J Biol Chem* **269**, 23757-23763
321. Papandreou, I., Cairns, R. A., Fontana, L., Lim, A. L., and Denko, N. C. (2006) HIF-1 mediates adaptation to hypoxia by actively downregulating mitochondrial oxygen consumption. *Cell Metab* **3**, 187-197
322. Wever, K. E., Warlé, M. C., Wagener, F. A., van der Hoorn, J. W., Masereeuw, R., van der Vliet, J. A., and Rongen, G. A. (2011) Remote ischaemic preconditioning by brief hind limb ischaemia protects against renal ischaemia-reperfusion injury: the role of adenosine. *Nephrology Dialysis Transplantation* **26**, 3108-3117

323. Przyklenk, K., and Whittaker, P. (2011) Remote ischemic preconditioning: current knowledge, unresolved questions, and future priorities. *Journal of cardiovascular pharmacology and therapeutics* **16**, 255-259
324. Wang, F., Yin, J., Lu, Z., Zhang, G., Li, J., Xing, T., Zhuang, S., and Wang, N. (2016) Limb ischemic preconditioning protects against contrast-induced nephropathy via renalase. *EBioMedicine* **9**, 356-365
325. Hill, P., Shukla, D., Tran, M. G., Aragonés, J., Cook, H. T., Carmeliet, P., and Maxwell, P. H. (2008) Inhibition of hypoxia inducible factor hydroxylases protects against renal ischemia-reperfusion injury. *J Am Soc Nephrol* **19**, 39-46
326. Ahn, J. M., You, S. J., Lee, Y. M., Oh, S. W., Ahn, S. Y., Kim, S., Chin, H. J., Chae, D. W., and Na, K. Y. (2012) Hypoxia-inducible factor activation protects the kidney from gentamicin-induced acute injury. *PLoS One* **7**, e48952
327. Chen, N., Hao, C., Liu, B. C., Lin, H., Wang, C., Xing, C., Liang, X., Jiang, G., Liu, Z., Li, X., Zuo, L., Luo, L., Wang, J., Zhao, M. H., Liu, Z., Cai, G. Y., Hao, L., Leong, R., Wang, C., Liu, C., Neff, T., Szczech, L., and Yu, K. P. (2019) Roxadustat Treatment for Anemia in Patients Undergoing Long-Term Dialysis. *N Engl J Med* **381**, 1011-1022
328. Chen, N., Hao, C., Peng, X., Lin, H., Yin, A., Hao, L., Tao, Y., Liang, X., Liu, Z., Xing, C., Chen, J., Luo, L., Zuo, L., Liao, Y., Liu, B. C., Leong, R., Wang, C., Liu, C., Neff, T., Szczech, L., and Yu, K. P. (2019) Roxadustat for Anemia in Patients with Kidney Disease Not Receiving Dialysis. *N Engl J Med* **381**, 1001-1010
329. Liu, H., and Xia, Y. (2015) Beneficial and detrimental role of adenosine signaling in diseases and therapy. *Journal of Applied Physiology* **119**, 1173-1182
330. Eltzschig, H. K. (2013) Extracellular adenosine signaling in molecular medicine. *Journal of molecular medicine (Berlin, Germany)* **91**, 141-146
331. Le, T. T., Berg, N. K., Harting, M. T., Li, X., Eltzschig, H. K., and Yuan, X. (2019) Purinergic Signaling in Pulmonary Inflammation. *Front Immunol* **10**, 1633

332. Ehrentraut, H., Clambey, E. T., McNamee, E. N., Brodsky, K. S., Ehrentraut, S. F., Poth, J. M., Riegel, A. K., Westrich, J. A., Colgan, S. P., and Eltzschig, H. K. (2013) CD73+ regulatory T cells contribute to adenosine-mediated resolution of acute lung injury. *The FASEB Journal* **27**, 2207-2219
333. Grenz, A., Homann, D., and Eltzschig, H. K. (2011) Extracellular adenosine: a safety signal that dampens hypoxia-induced inflammation during ischemia. *Antioxidants & redox signaling* **15**, 2221-2234
334. Eltzschig, H. K., Bonney, S. K., and Eckle, T. (2013) Attenuating myocardial ischemia by targeting A2B adenosine receptors. *Trends in molecular medicine* **19**, 345-354
335. Eltzschig, H. K., Weissmüller, T., Mager, A., and Eckle, T. (2006) Nucleotide metabolism and cell-cell interactions. In *Cell-Cell Interactions* pp. 73-87, Springer
336. Eckle, T., Hughes, K., Ehrentraut, H., Brodsky, K. S., Rosenberger, P., Choi, D.-S., Ravid, K., Weng, T., Xia, Y., and Blackburn, M. R. (2013) Crosstalk between the equilibrative nucleoside transporter ENT2 and alveolar Adora2b adenosine receptors dampens acute lung injury. *The FASEB Journal* **27**, 3078-3089
337. Ehrentraut, H., Westrich, J. A., Eltzschig, H. K., and Clambey, E. T. (2012) Adora2b adenosine receptor engagement enhances regulatory T cell abundance during endotoxin-induced pulmonary inflammation. *PLoS One* **7**
338. Koeppen, M., Eckle, T., and Eltzschig, H. K. (2009) Selective deletion of the A1 adenosine receptor abolishes heart-rate slowing effects of intravascular adenosine in vivo. *PLoS One* **4**, e6784
339. Busca, A., Saxena, M., Kryworuchko, M., and Kumar, A. (2009) Anti-apoptotic genes in the survival of monocytic cells during infection. *Current genomics* **10**, 306-317
340. Koscsó, B., Trepakov, A., Csóka, B., Németh, Z. H., Pacher, P., Eltzschig, H. K., and Haskó, G. (2013) Stimulation of A2B adenosine receptors protects against trauma-hemorrhagic shock-induced lung injury. *Purinergic signalling* **9**, 427-432

341. Lu, Q., Harrington, E. O., Newton, J., Casserly, B., Radin, G., Warburton, R., Zhou, Y., Blackburn, M. R., and Rounds, S. (2010) Adenosine protected against pulmonary edema through transporter- and receptor A2-mediated endothelial barrier enhancement. *Am J Physiol Lung Cell Mol Physiol* **298**, L755-767
342. Hu, X., Adebisi, M. G., Luo, J., Sun, K., Le, T.-T. T., Zhang, Y., Wu, H., Zhao, S., Karmouty-Quintana, H., Liu, H., Huang, A., Wen, Y. E., Zaika, O. L., Mamenko, M., Pochynyuk, O. M., Kellems, R. E., Eltzschig, H. K., Blackburn, M. R., Walters, E. T., Huang, D., Hu, H., and Xia, Y. (2016) Sustained Elevated Adenosine via ADORA2B Promotes Chronic Pain through Neuro-immune Interaction. *Cell reports* **16**, 106-119
343. Pedroza, M., Schneider, D. J., Karmouty-Quintana, H., Coote, J., Shaw, S., Corrigan, R., Molina, J. G., Alcorn, J. L., Galas, D., Gelinas, R., and Blackburn, M. R. (2011) Interleukin-6 contributes to inflammation and remodeling in a model of adenosine mediated lung injury. *PLoS One* **6**, e22667-e22667
344. Karmouty-Quintana, H., Xia, Y., and Blackburn, M. R. (2013) Adenosine signaling during acute and chronic disease states. *J Mol Med (Berl)* **91**, 173-181
345. Lu, Q., Harrington, E. O., Newton, J., Casserly, B., Radin, G., Warburton, R., Zhou, Y., Blackburn, M. R., and Rounds, S. (2010) Adenosine protected against pulmonary edema through transporter- and receptor A2-mediated endothelial barrier enhancement. *Am J Physiol Lung Cell Mol Physiol* **298**, 12
346. Gonzales, J. N., Gorshkov, B., Varn, M. N., Zemskova, M. A., Zemskov, E. A., Sridhar, S., Lucas, R., and Verin, A. D. (2014) Protective effect of adenosine receptors against lipopolysaccharide-induced acute lung injury. *Am J Physiol Lung Cell Mol Physiol* **306**, 10
347. Garcia-Dorado, D., Garcia-del-Blanco, B., Otaegui, I., Rodriguez-Palomares, J., Pineda, V., Gimeno, F., Ruiz-Salmeron, R., Elizaga, J., Evangelista, A., Fernandez-Aviles, F., San-Roman, A., and Ferreira-Gonzalez, I. (2014) Intracoronary injection of adenosine

- before reperfusion in patients with ST-segment elevation myocardial infarction: a randomized controlled clinical trial. *Int J Cardiol* **177**, 935-941
348. Jin, Z., Duan, W., Chen, M., Yu, S., Zhang, H., Feng, G., Xiong, L., and Yi, D. (2011) The myocardial protective effects of adenosine pretreatment in children undergoing cardiac surgery: a randomized controlled clinical trial. *Eur J Cardiothorac Surg* **39**, e90-96
349. Schingnitz, U., Hartmann, K., Macmanus, C. F., Eckle, T., Zug, S., Colgan, S. P., and Eltzschig, H. K. (2010) Signaling through the A2B adenosine receptor dampens endotoxin-induced acute lung injury. *J Immunol* **184**, 5271-5279
350. O'Brien, J., Hayder, H., Zayed, Y., and Peng, C. (2018) Overview of MicroRNA Biogenesis, Mechanisms of Actions, and Circulation. *Frontiers in Endocrinology* **9**
351. Lee, R. C., Feinbaum, R. L., and Ambros, V. (1993) The *C. elegans* heterochronic gene *lin-4* encodes small RNAs with antisense complementarity to *lin-14*. *Cell* **75**, 843-854
352. Wightman, B., Ha, I., and Ruvkun, G. (1993) Posttranscriptional regulation of the heterochronic gene *lin-14* by *lin-4* mediates temporal pattern formation in *C. elegans*. *Cell* **75**, 855-862
353. Bartel, D. P. (2009) MicroRNAs: target recognition and regulatory functions. *Cell* **136**, 215-233
354. Friedman, R. C., Farh, K. K., Burge, C. B., and Bartel, D. P. (2009) Most mammalian mRNAs are conserved targets of microRNAs. *Genome research* **19**, 92-105
355. Lee, T. J., Yuan, X., K., K., Yoo, J. Y., Kim, D. H., Kaur, B., and Eltzschig, H. K. (2020) Strategies to Modulate MicroRNA Functions for the Treatment of Cancer or Organ Injury. *Pharmacol Rev.*, epub ahead of print.
356. Lee, L. K., Medzikovic, L., Eghbali, M., Eltzschig, H. K., and Yuan, X. (2020) The Role of MicroRNAs in Acute Respiratory Distress Syndrome and Sepsis, From Targets to Therapies: A Narrative Review. *Anesthesia & Analgesia* **131**, 1471-1484

357. McAdams, R. M., Bierle, C. J., Boldenow, E., Weed, S., Tsai, J., Beyer, R. P., MacDonald, J. W., Bammler, T. K., Liggitt, H. D., Farin, F. M., Vanderhoeven, J., Rajagopal, L., and Adams Waldorf, K. M. (2015) Choriodecidual Group B Streptococcal Infection Induces miR-155-5p in the Fetal Lung in *Macaca nemestrina*. *Infect Immun* **83**, 3909-3917
358. Wang, W., Liu, Z., Su, J., Chen, W. S., Wang, X. W., Bai, S. X., Zhang, J. Z., and Yu, S. Q. (2016) Macrophage micro-RNA-155 promotes lipopolysaccharide-induced acute lung injury in mice and rats. *Am J Physiol Lung Cell Mol Physiol* **311**, L494-506
359. Rao, R., Rieder, S. A., Nagarkatti, P., and Nagarkatti, M. (2014) Staphylococcal enterotoxin B-induced microRNA-155 targets SOCS1 to promote acute inflammatory lung injury. *Infect Immun* **82**, 2971-2979
360. Yuan, X., Berg, N., Lee, J. W., Le, T. T., Neudecker, V., Jing, N., and Eltzschig, H. (2018) MicroRNA miR-223 as regulator of innate immunity. *J Leukoc Biol* **104**, 515-524
361. Vautrin, A., Manchon, L., Garcel, A., Campos, N., Lapasset, L., Laaref, A. M., Bruno, R., Gislard, M., Dubois, E., Scherrer, D., Ehrlich, J. H., and Tazi, J. (2019) Both anti-inflammatory and antiviral properties of novel drug candidate ABX464 are mediated by modulation of RNA splicing. *Scientific Reports* **9**, 792
362. Yang, Y.-L., Tang, G.-J., Wu, Y.-L., Yien, H.-W., Lee, T.-S., and Kou, Y. R. (2008) Exacerbation of wood smoke-induced acute lung injury by mechanical ventilation using moderately high tidal volume in mice. *Respir Physiol Neurobiol* **160**, 99-108
363. Martin, M. (2011) Cutadapt removes adapter sequences from high-throughput sequencing reads. *EMBnet.journal* **17**, 10-12
364. Dobin, A., Davis, C. A., Schlesinger, F., Drenkow, J., Zaleski, C., Jha, S., Batut, P., Chaisson, M., and Gingeras, T. R. (2013) STAR: ultrafast universal RNA-seq aligner. *Bioinformatics* **29**, 15-21
365. Anders, S., and Huber, W. (2010) Differential expression analysis for sequence count data. *Genome Biol* **11**, R106

366. Benjamini, Y., and Hochberg, Y. (1995) Controlling the False Discovery Rate: A Practical and Powerful Approach to Multiple Testing. *J R Statist Soc B* **57**, 289-300
367. Xie, T., Liang, J., Liu, N., Wang, Q., Li, Y., Noble, P. W., and Jiang, D. (2012) MicroRNA-127 Inhibits Lung Inflammation by Targeting IgG Fcγ Receptor I. *The Journal of Immunology* **188**, 2437-2444
368. Lee, L. K., Medzikovic, L., Eghbali, M., Eltzschig, H. K., and Yuan, X. (2020) The Role of MicroRNAs in Acute Respiratory Distress Syndrome and Sepsis, From Targets to Therapies: A Narrative Review. *Anesthesia & Analgesia* **131**
369. Ling, Y., Li, Z.-Z., Zhang, J.-F., Zheng, X.-W., Lei, Z.-Q., Chen, R.-Y., and Feng, J.-H. (2018) MicroRNA-494 inhibition alleviates acute lung injury through Nrf2 signaling pathway via NQO1 in sepsis-associated acute respiratory distress syndrome. *Life Sciences* **210**, 1-8
370. Zhao, J., Xie, F., Chen, R., Zhang, Z., Dai, R., Zhao, N., Wang, R., Sun, Y., and Chen, Y. (2020) Transcription factor NF-κB promotes acute lung injury via microRNA-99b-mediated PRDM1 down-regulation. *Journal of Biological Chemistry* **295**, 18638-18648
371. Good, R. J., Hernandez-Lagunas, L., Allawzi, A., Maltzahn, J. K., Vohwinkel, C. U., Upadhyay, A. K., Kompella, U. B., Birukov, K. G., Carpenter, T. C., Sucharov, C. C., and Nozik-Grayck, E. (2018) MicroRNA dysregulation in lung injury: the role of the miR-26a/EphA2 axis in regulation of endothelial permeability. *American Journal of Physiology-Lung Cellular and Molecular Physiology* **315**, L584-L594
372. Bobba, C. M., Fei, Q., Shukla, V., Lee, H., Patel, P., Putman, R. K., Spitzer, C., Tsai, M., Wewers, M. D., Lee, R. J., Christman, J. W., Ballinger, M. N., Ghadiali, S. N., and Englert, J. A. (2021) Nanoparticle delivery of microRNA-146a regulates mechanotransduction in lung macrophages and mitigates injury during mechanical ventilation. *Nature communications* **12**, 289

373. Liu, Y., Wang, X., Li, P., Zhao, Y., Yang, L., Yu, W., and Xie, H. (2021) Targeting MALAT1 and miRNA-181a-5p for the intervention of acute lung injury/acute respiratory distress syndrome. *Respiratory Research* **22**, 1
374. Rajput, C., Tauseef, M., Farazuddin, M., Yazbeck, P., Amin, M.-R., BR, V. A., Sharma, T., and Mehta, D. (2016) MicroRNA-150 Suppression of Angiopoetin-2 Generation and Signaling Is Crucial for Resolving Vascular Injury. *Arteriosclerosis, Thrombosis, and Vascular Biology* **36**, 380-388
375. Ryan, H. E., Poloni, M., McNulty, W., Elson, D., Gassmann, M., Arbeit, J. M., and Johnson, R. S. (2000) Hypoxia-inducible factor-1 α is a positive factor in solid tumor growth. *Cancer research* **60**, 4010-4015
376. Gruber, M., Hu, C. J., Johnson, R. S., Brown, E. J., Keith, B., and Simon, M. C. (2007) Acute postnatal ablation of Hif-2 α results in anemia. *Proc Natl Acad Sci U S A* **104**, 2301-2306
377. Safran, M., Kim, W. Y., O'Connell, F., Flippin, L., Günzler, V., Horner, J. W., Depinho, R. A., and Kaelin, W. G., Jr. (2006) Mouse model for noninvasive imaging of HIF prolyl hydroxylase activity: assessment of an oral agent that stimulates erythropoietin production. *Proc Natl Acad Sci U S A* **103**, 105-110
378. Clausen, B. E., Burkhardt, C., Reith, W., Renkawitz, R., and Förster, I. (1999) Conditional gene targeting in macrophages and granulocytes using LysMcre mice. *Transgenic research* **8**, 265-277
379. Kim, B., Guaregua, V., Chen, X., Zhao, C., Yeow, W., Berg, N. K., Eltzschig, H. K., and Yuan, X. (2021) Characterization of a Murine Model System to Study MicroRNA-147 During Inflammatory Organ Injury. *Inflammation*, 1-15
380. Cramer, T., Yamanishi, Y., Clausen, B. E., Förster, I., Pawlinski, R., Mackman, N., Haase, V. H., Jaenisch, R., Corr, M., and Nizet, V. (2003) HIF-1 α is essential for myeloid cell-mediated inflammation. *Cell* **112**, 645-657

381. Imtiyaz, H. Z., Williams, E. P., Hickey, M. M., Patel, S. A., Durham, A. C., Yuan, L.-J., Hammond, R., Gimotty, P. A., Keith, B., and Simon, M. C. (2010) Hypoxia-inducible factor 2alpha regulates macrophage function in mouse models of acute and tumor inflammation. *The Journal of clinical investigation* **120**, 2699-2714
382. Trouplin, V., Boucherit, N., Gorvel, L., Conti, F., Mottola, G., and Ghigo, E. (2013) Bone marrow-derived macrophage production. *J Vis Exp*, e50966-e50966
383. Hsiau, T., Maures, T., Waite, K., Yang, J., Kelso, R., Holden, K., and Stoner, R. (2018) Inference of CRISPR edits from Sanger trace data. *BioRxiv*, 251082
384. Pecot, C. V., Rupaimoole, R., Yang, D., Akbani, R., Ivan, C., Lu, C., Wu, S., Han, H. D., Shah, M. Y., Rodriguez-Aguayo, C., Bottsford-Miller, J., Liu, Y., Kim, S. B., Unruh, A., Gonzalez-Villasana, V., Huang, L., Zand, B., Moreno-Smith, M., Mangala, L. S., Taylor, M., Dalton, H. J., Sehgal, V., Wen, Y., Kang, Y., Baggerly, K. A., Lee, J. S., Ram, P. T., Ravoori, M. K., Kundra, V., Zhang, X., Ali-Fehmi, R., Gonzalez-Angulo, A. M., Massion, P. P., Calin, G. A., Lopez-Berestein, G., Zhang, W., and Sood, A. K. (2013) Tumour angiogenesis regulation by the miR-200 family. *Nature communications* **4**, 2427
385. Landen, C. N., Jr., Chavez-Reyes, A., Bucana, C., Schmandt, R., Deavers, M. T., Lopez-Berestein, G., and Sood, A. K. (2005) Therapeutic EphA2 gene targeting in vivo using neutral liposomal small interfering RNA delivery. *Cancer research* **65**, 6910-6918
386. Salabei, J. K., Gibb, A. A., and Hill, B. G. (2014) Comprehensive measurement of respiratory activity in permeabilized cells using extracellular flux analysis. *Nature protocols* **9**, 421-438
387. Du, D., Tan, L., Wang, Y., Peng, B., Weinstein, J. N., Wondisford, F. E., Su, X., and Lorenzi, P. L. (2019) ElemCor: accurate data analysis and enrichment calculation for high-resolution LC-MS stable isotope labeling experiments. *BMC Bioinformatics* **20**, 89
388. Ehrentraut, H., Weisheit, C. K., Frede, S., and Hilbert, T. (2019) Inducing Acute Lung Injury in Mice by Direct Intratracheal Lipopolysaccharide Instillation. *J Vis Exp*

389. Zhou, J., Wang, H., Lu, A., Hu, G., Luo, A., Ding, F., Zhang, J., Wang, X., Wu, M., and Liu, Z. (2002) A novel gene, NMES1, downregulated in human esophageal squamous cell carcinoma. *International journal of cancer* **101**, 311-316
390. Liu, G., Friggeri, A., Yang, Y., Park, Y.-J., Tsuruta, Y., and Abraham, E. (2009) miR-147, a microRNA that is induced upon Toll-like receptor stimulation, regulates murine macrophage inflammatory responses. *Proceedings of the National Academy of Sciences* **106**, 15819-15824
391. Di Martino, M. T., Gullà, A., Gallo Cantafio, M. E., Altomare, E., Amodio, N., Leone, E., Morelli, E., Lio, S. G., Caracciolo, D., Rossi, M., Frandsen, N. M., Tagliaferri, P., and Tassone, P. (2014) In Vitro and In Vivo Activity of a Novel Locked Nucleic Acid (LNA)-Inhibitor-miR-221 against Multiple Myeloma Cells. *PLoS One* **9**, e89659
392. Fluiter, K., ten Asbroek, A. L., de Wissel, M. B., Jakobs, M. E., Wissenbach, M., Olsson, H., Olsen, O., Oerum, H., and Baas, F. (2003) In vivo tumor growth inhibition and biodistribution studies of locked nucleic acid (LNA) antisense oligonucleotides. *Nucleic Acids Res* **31**, 953-962
393. Braasch, D. A., and Corey, D. R. (2001) Locked nucleic acid (LNA): fine-tuning the recognition of DNA and RNA. *Chemistry & Biology* **8**, 1-7
394. Gutiérrez-Puente, Y., Tari, A. M., Stephens, C., Rosenblum, M., Guerra, R. T., and Lopez-Berestein, G. (1999) Safety, Pharmacokinetics, and Tissue Distribution of Liposomal P-Ethoxy Antisense Oligonucleotides Targeted to Bcl-2. *Journal of Pharmacology and Experimental Therapeutics* **291**, 865-869
395. Landen, C. N., Chavez-Reyes, A., Bucana, C., Schmandt, R., Deavers, M. T., Lopez-Berestein, G., and Sood, A. K. (2005) Therapeutic EphA2 Gene Targeting *In vivo* Using Neutral Liposomal Small Interfering RNA Delivery. *Cancer research* **65**, 6910-6918
396. Wagner, M. J., Mitra, R., McArthur, M. J., Baze, W., Barnhart, K., Wu, S. Y., Rodriguez-Aguayo, C., Zhang, X., Coleman, R. L., Lopez-Berestein, G., and Sood, A. K. (2017)

- Preclinical Mammalian Safety Studies of EPHARNA (DOPC Nanoliposomal EphA2-Targeted siRNA). *Molecular Cancer Therapeutics* **16**, 1114-1123
397. Hermiston, M. L., Xu, Z., and Weiss, A. (2003) CD45: a critical regulator of signaling thresholds in immune cells. *Annu Rev Immunol* **21**, 107-137
398. Shivtiel, S., Kollet, O., Lapid, K., Schajnovitz, A., Goichberg, P., Kalinkovich, A., Shezen, E., Tesio, M., Netzer, N., Petit, I., Sharir, A., and Lapidot, T. (2008) CD45 regulates retention, motility, and numbers of hematopoietic progenitors, and affects osteoclast remodeling of metaphyseal trabecules. *The Journal of experimental medicine* **205**, 2381-2395
399. Mould, K. J., Barthel, L., Mohning, M. P., Thomas, S. M., McCubbrey, A. L., Danhorn, T., Leach, S. M., Fingerlin, T. E., O'Connor, B. P., Reisz, J. A., D'Alessandro, A., Bratton, D. L., Jakubzick, C. V., and Janssen, W. J. (2017) Cell Origin Dictates Programming of Resident versus Recruited Macrophages during Acute Lung Injury. *American journal of respiratory cell and molecular biology* **57**, 294-306
400. Cummins, E. P., Berra, E., Comerford, K. M., Ginouves, A., Fitzgerald, K. T., Seeballuck, F., Godson, C., Nielsen, J. E., Moynagh, P., Pouyssegur, J., and Taylor, C. T. (2006) Prolyl hydroxylase-1 negatively regulates I κ B kinase-beta, giving insight into hypoxia-induced NF κ B activity. *Proc Natl Acad Sci U S A* **103**, 18154-18159
401. Colgan, S. P., Furuta, G. T., and Taylor, C. T. (2020) Hypoxia and Innate Immunity: Keeping Up with the HIFsters. *Annual Review of Immunology* **38**, 341-363
402. Watts, E. R., and Walmsley, S. R. (2019) Inflammation and hypoxia: HIF and PHD isoform selectivity. *Trends in molecular medicine* **25**, 33-46
403. Palazon, A., Goldrath, A. W., Nizet, V., and Johnson, R. S. (2014) HIF transcription factors, inflammation, and immunity. *Immunity* **41**, 518-528
404. Imtiyaz, H. Z., and Simon, M. C. (2010) Hypoxia-inducible factors as essential regulators of inflammation. *Current topics in microbiology and immunology* **345**, 105-120

405. Agarwal, V., Bell, G. W., Nam, J.-W., and Bartel, D. P. (2015) Predicting effective microRNA target sites in mammalian mRNAs. *eLife* **4**, e05005
406. Rath, S., Sharma, R., Gupta, R., Ast, T., Chan, C., Durham, T. J., Goodman, R. P., Grabarek, Z., Haas, M. E., Hung, W. H. W., Joshi, P. R., Jourdain, A. A., Kim, S. H., Kotrys, A. V., Lam, S. S., McCoy, J. G., Meisel, J. D., Miranda, M., Panda, A., Patgiri, A., Rogers, R., Sadre, S., Shah, H., Skinner, O. S., To, T. L., Walker, M. A., Wang, H., Ward, P. S., Wengrod, J., Yuan, C. C., Calvo, S. E., and Mootha, V. K. (2021) MitoCarta3.0: an updated mitochondrial proteome now with sub-organelle localization and pathway annotations. *Nucleic Acids Res* **49**, D1541-d1547
407. Pitceathly, R. D. S., and Taanman, J. W. (2018) NDUFA4 (Renamed COXFA4) Is a Cytochrome-c Oxidase Subunit. *Trends Endocrinol Metab* **29**, 452-454
408. Balsa, E., Marco, R., Perales-Clemente, E., Szklarczyk, R., Calvo, E., Landázuri, Manuel O., and Enríquez, José A. (2012) NDUFA4 Is a Subunit of Complex IV of the Mammalian Electron Transport Chain. *Cell Metabolism* **16**, 378-386
409. Marongiu, L., Gornati, L., Artuso, I., Zanoni, I., and Granucci, F. (2019) Below the surface: The inner lives of TLR4 and TLR9. *Journal of Leukocyte Biology* **106**, 147-160
410. Pålsson-McDermott, E. M., and O'Neill, L. A. J. (2004) Signal transduction by the lipopolysaccharide receptor, Toll-like receptor-4. *Immunology* **113**, 153-162
411. Van den Bossche, J., O'Neill, L. A., and Menon, D. (2017) Macrophage Immunometabolism: Where Are We (Going)? *Trends in Immunology* **38**, 395-406
412. Russell, D. G., Huang, L., and VanderVen, B. C. (2019) Immunometabolism at the interface between macrophages and pathogens. *Nature Reviews Immunology* **19**, 291-304
413. Palmieri, E. M., Gonzalez-Cotto, M., Baseler, W. A., Davies, L. C., Ghesquière, B., Maio, N., Rice, C. M., Rouault, T. A., Cassel, T., Higashi, R. M., Lane, A. N., Fan, T. W. M., Wink, D. A., and McVicar, D. W. (2020) Nitric oxide orchestrates metabolic rewiring

- in M1 macrophages by targeting aconitase 2 and pyruvate dehydrogenase. *Nature communications* **11**, 698
414. Mills, E. L., Kelly, B., Logan, A., Costa, A. S. H., Varma, M., Bryant, C. E., Tourlomousis, P., Däbritz, J. H. M., Gottlieb, E., Latorre, I., Corr, S. C., McManus, G., Ryan, D., Jacobs, H. T., Szibor, M., Xavier, R. J., Braun, T., Frezza, C., Murphy, M. P., and O'Neill, L. A. (2016) Succinate Dehydrogenase Supports Metabolic Repurposing of Mitochondria to Drive Inflammatory Macrophages. *Cell* **167**, 457-470.e413
415. Ip, W. K. E., Hoshi, N., Shouval, D. S., Snapper, S., and Medzhitov, R. (2017) Anti-inflammatory effect of IL-10 mediated by metabolic reprogramming of macrophages. *Science* **356**, 513-519
416. Meiser, J., Krämer, L., Sapcariu, S. C., Battello, N., Ghelfi, J., D'Herouel, A. F., Skupin, A., and Hiller, K. (2016) Pro-inflammatory Macrophages Sustain Pyruvate Oxidation through Pyruvate Dehydrogenase for the Synthesis of Itaconate and to Enable Cytokine Expression *. *Journal of Biological Chemistry* **291**, 3932-3946
417. Viola, A., Munari, F., Sánchez-Rodríguez, R., Scolaro, T., and Castegna, A. (2019) The Metabolic Signature of Macrophage Responses. *Frontiers in Immunology* **10**
418. Cervera, A. M., Bayley, J.-P., Devilee, P., and McCreath, K. J. (2009) Inhibition of succinate dehydrogenase dysregulates histone modification in mammalian cells. *Molecular Cancer* **8**, 89
419. Letouzé, E., Martinelli, C., Lorient, C., Burnichon, N., Abermil, N., Ottolenghi, C., Janin, M., Menara, M., Nguyen, An T., Benit, P., Buffet, A., Marcaillou, C., Bertherat, J., Amar, L., Rustin, P., De Reyniès, A., Gimenez-Roqueplo, A.-P., and Favier, J. (2013) SDH Mutations Establish a Hypermethylator Phenotype in Paraganglioma. *Cancer Cell* **23**, 739-752
420. Xiao, M., Yang, H., Xu, W., Ma, S., Lin, H., Zhu, H., Liu, L., Liu, Y., Yang, C., Xu, Y., Zhao, S., Ye, D., Xiong, Y., and Guan, K.-L. (2012) Inhibition of α -KG-dependent

- histone and DNA demethylases by fumarate and succinate that are accumulated in mutations of FH and SDH tumor suppressors. *Genes Dev* **26**, 1326-1338
421. Kruidenier, L., Chung, C.-w., Cheng, Z., Liddle, J., Che, K., Joberty, G., Bantscheff, M., Bountra, C., Bridges, A., Diallo, H., Eberhard, D., Hutchinson, S., Jones, E., Katso, R., Leveridge, M., Mander, P. K., Mosley, J., Ramirez-Molina, C., Rowland, P., Schofield, C. J., Sheppard, R. J., Smith, J. E., Swales, C., Tanner, R., Thomas, P., Tumber, A., Drewes, G., Oppermann, U., Patel, D. J., Lee, K., and Wilson, D. M. (2012) A selective jumonji H3K27 demethylase inhibitor modulates the proinflammatory macrophage response. *Nature* **488**, 404-408
422. De Santa, F., Totaro, M. G., Prosperini, E., Notarbartolo, S., Testa, G., and Natoli, G. (2007) The Histone H3 Lysine-27 Demethylase Jmjd3 Links Inflammation to Inhibition of Polycomb-Mediated Gene Silencing. *Cell* **130**, 1083-1094
423. Daskalaki, M. G., Tsatsanis, C., and Kampranis, S. C. (2018) Histone methylation and acetylation in macrophages as a mechanism for regulation of inflammatory responses. *Journal of Cellular Physiology* **233**, 6495-6507
424. Alam, M. M., and O'Neill, L. A. (2011) MicroRNAs and the resolution phase of inflammation in macrophages. *European Journal of Immunology* **41**, 2482-2485
425. Tahamtan, A., Teymoori-Rad, M., Nakstad, B., and Salimi, V. (2018) Anti-Inflammatory MicroRNAs and Their Potential for Inflammatory Diseases Treatment. *Frontiers in immunology* **9**, 1377-1377
426. Perry, M. M., Moschos, S. A., Williams, A. E., Shepherd, N. J., Larner-Svensson, H. M., and Lindsay, M. A. (2008) Rapid changes in microRNA-146a expression negatively regulate the IL-1 β -induced inflammatory response in human lung alveolar epithelial cells. *The Journal of Immunology* **180**, 5689-5698
427. Bhaumik, D., Scott, G. K., Schokrpur, S., Patil, C. K., Orjalo, A. V., Rodier, F., Lithgow, G. J., and Campisi, J. (2009) MicroRNAs miR-146a/b negatively modulate the senescence-associated inflammatory mediators IL-6 and IL-8. *Aging* **1**, 402

428. Jones, S., Watkins, G., Le Good, N., Roberts, S., Murphy, C., Brockbank, S., Needham, M., Read, S., and Newham, P. (2009) The identification of differentially expressed microRNA in osteoarthritic tissue that modulate the production of TNF- α and MMP13. *Osteoarthritis and cartilage* **17**, 464-472
429. Nahid, M. A., Pauley, K. M., Satoh, M., and Chan, E. K. (2009) miR-146a is critical for endotoxin-induced tolerance. *Journal of Biological Chemistry* **284**, 34590-34599
430. Chassin, C., Kocur, M., Pott, J., Duerr, C. U., Gütle, D., Lotz, M., and Hornef, M. W. (2010) miR-146a mediates protective innate immune tolerance in the neonate intestine. *Cell host & microbe* **8**, 358-368
431. Recchiuti, A., Krishnamoorthy, S., Fredman, G., Chiang, N., and Serhan, C. N. (2011) MicroRNAs in resolution of acute inflammation: identification of novel resolvin DI-miRNA circuits. *The FASEB Journal* **25**, 544-560
432. Taganov, K. D., Boldin, M. P., Chang, K.-J., and Baltimore, D. (2006) NF- κ B-dependent induction of microRNA miR-146, an inhibitor targeted to signaling proteins of innate immune responses. *Proceedings of the National Academy of Sciences* **103**, 12481-12486
433. Sheedy, F. J., Palsson-McDermott, E., Hennessy, E. J., Martin, C., O'Leary, J. J., Ruan, Q., Johnson, D. S., Chen, Y., and O'Neill, L. A. J. (2010) Negative regulation of TLR4 via targeting of the proinflammatory tumor suppressor PDCD4 by the microRNA miR-21. *Nature Immunology* **11**, 141-147
434. Xu, G., Zhang, Z., Xing, Y., Wei, J., Ge, Z., Liu, X., Zhang, Y., and Huang, X. (2014) MicroRNA-149 negatively regulates tlr-triggered inflammatory response in macrophages by targeting myd88. *Journal of cellular biochemistry* **115**, 919-927
435. Vlacil, A.-K., Vollmeister, E., Bertrams, W., Schoesser, F., Oberoi, R., Schuett, J., Schuett, H., Huehn, S., Bedenbender, K., Schmeck, B. T., Schieffer, B., and Grote, K. (2020) Identification of microRNAs involved in NOD-dependent induction of pro-inflammatory genes in pulmonary endothelial cells. *PLoS One* **15**, e0228764

436. Li, X., Pritykin, Y., Concepcion, C. P., Lu, Y., La Rocca, G., Zhang, M., King, B., Cook, P. J., Au, Y. W., Popow, O., Paulo, J. A., Otis, H. G., Mastroleo, C., Ogradowski, P., Schreiner, R., Haigis, K. M., Betel, D., Leslie, C. S., and Ventura, A. (2020) High-Resolution In Vivo Identification of miRNA Targets by Halo-Enhanced Ago2 Pull-Down. *Molecular cell* **79**, 167-179.e111
437. Chen, S., Yang, J., Wei, Y., and Wei, X. (2020) Epigenetic regulation of macrophages: from homeostasis maintenance to host defense. *Cellular & Molecular Immunology* **17**, 36-49
438. Martínez-Reyes, I., and Chandel, N. S. (2020) Mitochondrial TCA cycle metabolites control physiology and disease. *Nature communications* **11**, 102
439. De Santa, F., Narang, V., Yap, Z. H., Tusi, B. K., Burgold, T., Austenaa, L., Bucci, G., Caganova, M., Notarbartolo, S., and Casola, S. (2009) Jmjd3 contributes to the control of gene expression in LPS-activated macrophages. *The EMBO journal* **28**, 3341-3352
440. Yan, Q., Sun, L., Zhu, Z., Wang, L., Li, S., and Richard, D. Y. (2014) Jmjd3-mediated epigenetic regulation of inflammatory cytokine gene expression in serum amyloid A-stimulated macrophages. *Cellular signalling* **26**, 1783-1791
441. Liu, P.-S., Wang, H., Li, X., Chao, T., Teav, T., Christen, S., Di Conza, G., Cheng, W.-C., Chou, C.-H., Vavakova, M., Muret, C., Debackere, K., Mazzone, M., Huang, H.-D., Fendt, S.-M., Ivanisevic, J., and Ho, P.-C. (2017) α -ketoglutarate orchestrates macrophage activation through metabolic and epigenetic reprogramming. *Nature Immunology* **18**, 985-994
442. Xiao, M., Yang, H., Xu, W., Ma, S., Lin, H., Zhu, H., Liu, L., Liu, Y., Yang, C., Xu, Y., Zhao, S., Ye, D., Xiong, Y., and Guan, K.-L. (2015) Corrigendum: inhibition of α -KG-dependent histone and DNA demethylases by fumarate and succinate that are accumulated in mutations of FH and SDH tumor suppressors. *Genes Dev* **29**, 887-887

443. Weinmann, A. S., Mitchell, D. M., Sanjabi, S., Bradley, M. N., Hoffmann, A., Liou, H.-C., and Smale, S. T. (2001) Nucleosome remodeling at the IL-12 p40 promoter is a TLR-dependent, Rel-independent event. *Nature immunology* **2**, 51-57
444. Weinmann, A. S., Plevy, S. E., and Smale, S. T. (1999) Rapid and selective remodeling of a positioned nucleosome during the induction of IL-12 p40 transcription. *Immunity* **11**, 665-675
445. Tannahill, G. M., Curtis, A. M., Adamik, J., Palsson-McDermott, E. M., McGettrick, A. F., Goel, G., Frezza, C., Bernard, N. J., Kelly, B., Foley, N. H., Zheng, L., Gardet, A., Tong, Z., Jany, S. S., Corr, S. C., Haneklaus, M., Caffrey, B. E., Pierce, K., Walmsley, S., Beasley, F. C., Cummins, E., Nizet, V., Whyte, M., Taylor, C. T., Lin, H., Masters, S. L., Gottlieb, E., Kelly, V. P., Clish, C., Auron, P. E., Xavier, R. J., and O'Neill, L. A. (2013) Succinate is an inflammatory signal that induces IL-1 β through HIF-1 α . *Nature* **496**, 238-242
446. Lampropoulou, V., Sergushichev, A., Bambouskova, M., Nair, S., Vincent, E. E., Loginicheva, E., Cervantes-Barragan, L., Ma, X., Huang, S. C., Griss, T., Weinheimer, C. J., Khader, S., Randolph, G. J., Pearce, E. J., Jones, R. G., Diwan, A., Diamond, M. S., and Artyomov, M. N. (2016) Itaconate Links Inhibition of Succinate Dehydrogenase with Macrophage Metabolic Remodeling and Regulation of Inflammation. *Cell Metab* **24**, 158-166
447. Krzak, G., Willis, C. M., Smith, J. A., Pluchino, S., and Peruzzotti-Jametti, L. (2021) Succinate Receptor 1: An Emerging Regulator of Myeloid Cell Function in Inflammation. *Trends in Immunology* **42**, 45-58
448. Harber, K. J., de Goede, K. E., Verberk, S. G. S., Meinster, E., de Vries, H. E., van Weeghel, M., de Winther, M. P. J., and Van den Bossche, J. (2020) Succinate Is an Inflammation-Induced Immunoregulatory Metabolite in Macrophages. *Metabolites* **10**
449. Keiran, N., Ceperuelo-Mallafré, V., Calvo, E., Hernández-Alvarez, M. I., Ejarque, M., Núñez-Roa, C., Horrillo, D., Maymó-Masip, E., Rodríguez, M. M., Fradera, R., de la

- Rosa, J. V., Jorba, R., Megia, A., Zorzano, A., Medina-Gómez, G., Serena, C., Castrillo, A., Vendrell, J., and Fernández-Veledo, S. (2019) SUCNR1 controls an anti-inflammatory program in macrophages to regulate the metabolic response to obesity. *Nat Immunol* **20**, 581-592
450. D'Alessio, F. R., Craig, J. M., Singer, B. D., Files, D. C., Mock, J. R., Garibaldi, B. T., Fallica, J., Tripathi, A., Mandke, P., Gans, J. H., Limjunyawong, N., Sidhaye, V. K., Heller, N. M., Mitzner, W., King, L. S., and Aggarwal, N. R. (2016) Enhanced resolution of experimental ARDS through IL-4-mediated lung macrophage reprogramming. *American Journal of Physiology-Lung Cellular and Molecular Physiology* **310**, L733-L746
451. Lu, H.-L., Huang, X.-Y., Luo, Y.-F., Tan, W.-P., Chen, P.-F., and Guo, Y.-B. (2018) Activation of M1 macrophages plays a critical role in the initiation of acute lung injury. *Bioscience Reports* **38**
452. Zhao, M., Fernandez, L. G., Doctor, A., Sharma, A. K., Zarbock, A., Tribble, C. G., Kron, I. L., and Laubach, V. E. (2006) Alveolar macrophage activation is a key initiation signal for acute lung ischemia-reperfusion injury. *American Journal of Physiology-Lung Cellular and Molecular Physiology* **291**, L1018-L1026
453. Cramer, T., Yamanishi, Y., Clausen, B. E., Förster, I., Pawlinski, R., Mackman, N., Haase, V. H., Jaenisch, R., Corr, M., Nizet, V., Firestein, G. S., Gerber, H. P., Ferrara, N., and Johnson, R. S. (2003) HIF-1 α is essential for myeloid cell-mediated inflammation. *Cell* **112**, 645-657
454. Matak, P., Heinis, M., Mathieu, J. R., Corriden, R., Cuvellier, S., Delga, S., Mounier, R., Rouquette, A., Raymond, J., Lamarque, D., Emile, J. F., Nizet, V., Touati, E., and Peyssonnaud, C. (2015) Myeloid HIF-1 is protective in Helicobacter pylori-mediated gastritis. *Journal of immunology (Baltimore, Md. : 1950)* **194**, 3259-3266
455. Lin, N., Shay, J. E. S., Xie, H., Lee, D. S. M., Skuli, N., Tang, Q., Zhou, Z., Azzam, A., Meng, H., Wang, H., FitzGerald, G. A., and Simon, M. C. (2018) Myeloid Cell Hypoxia-

- Inducible Factors Promote Resolution of Inflammation in Experimental Colitis. *Frontiers in Immunology* **9**
456. Berg, N. K., Li, J., Kim, B., Mills, T., Pei, G., Zhao, Z., Li, X., Zhang, X., Ruan, W., Eltzschig, H. K., and Yuan, X. (2021) Hypoxia-inducible factor-dependent induction of myeloid-derived netrin-1 attenuates natural killer cell infiltration during endotoxin-induced lung injury. *The FASEB Journal* **35**, e21334
 457. Abram, C. L., Roberge, G. L., Hu, Y., and Lowell, C. A. (2014) Comparative analysis of the efficiency and specificity of myeloid-Cre deleting strains using ROSA-EYFP reporter mice. *J Immunol Methods* **408**, 89-100
 458. Shi, J., Hua, L., Harmer, D., Li, P., and Ren, G. (2018) Cre Driver Mice Targeting Macrophages. *Methods Mol Biol* **1784**, 263-275
 459. McCubbrey, A. L., Barthel, L., Mould, K. J., Mohning, M. P., Redente, E. F., and Janssen, W. J. (2016) Selective and inducible targeting of CD11b+ mononuclear phagocytes in the murine lung with hCD68-rtTA transgenic systems. *American Journal of Physiology-Lung Cellular and Molecular Physiology* **311**, L87-L100
 460. Thompson, B. T., Chambers, R. C., and Liu, K. D. (2017) Acute Respiratory Distress Syndrome. *N Engl J Med* **377**, 1904-1905
 461. Lee, L. K., Medzikovic, L., Eghbali, M., Eltzschig, H. K., and Yuan, X. (2020) The Role of MicroRNAs in Acute Respiratory Distress Syndrome and Sepsis, From Targets to Therapies: A Narrative Review. *Anesth Analg*
 462. Medzhitov, R. (2008) Origin and physiological roles of inflammation. *Nature* **454**, 428-435
 463. Shen, H., Kreisel, D., and Goldstein, D. R. (2013) Processes of sterile inflammation. *The Journal of Immunology* **191**, 2857-2863
 464. Millien, V. O., Lu, W., Mak, G., Yuan, X., Knight, J. M., Porter, P., Kheradmand, F., and Corry, D. B. (2014) Airway fibrinogenolysis and the initiation of allergic inflammation. *Annals of the American Thoracic Society* **11 Suppl 5**, S277-283

465. Hong, M. J., Gu, B. H., Madison, M. C., Landers, C., Tung, H. Y., Kim, M., Yuan, X., You, R., Machado, A. A., Gilbert, B. E., Soroosh, P., Elloso, M., Song, L., Chen, M., Corry, D. B., Diehl, G., and Kheradmand, F. (2018) Protective role of gammadelta T cells in cigarette smoke and influenza infection. *Mucosal Immunol* **11**, 894-908
466. Singer, M., Deutschman, C. S., Seymour, C. W., Shankar-Hari, M., Annane, D., Bauer, M., Bellomo, R., Bernard, G. R., Chiche, J.-D., and Coopersmith, C. M. (2016) The third international consensus definitions for sepsis and septic shock (Sepsis-3). *Jama* **315**, 801-810
467. Rabb, H., Griffin, M. D., McKay, D. B., Swaminathan, S., Pickkers, P., Rosner, M. H., Kellum, J. A., Ronco, C., and Acute Dialysis Quality Initiative Consensus, X. W. G. (2016) Inflammation in AKI: Current Understanding, Key Questions, and Knowledge Gaps. *Journal of the American Society of Nephrology : JASN* **27**, 371-379
468. Arslan, F., De Kleijn, D. P., and Pasterkamp, G. (2011) Innate immune signaling in cardiac ischemia. *Nature Reviews Cardiology* **8**, 292
469. Harari, O. A., and Liao, J. K. (2010) NF- κ B and innate immunity in ischemic stroke. *Annals of the New York Academy of Sciences* **1207**, 32
470. Zhai, Y., Busuttil, R. W., and Kupiec-Weglinski, J. W. (2011) Liver Ischemia and Reperfusion Injury: New Insights into Mechanisms of Innate—Adaptive Immune-Mediated Tissue Inflammation. *American Journal of Transplantation* **11**, 1563-1569
471. Eltzschig, H. K., Weissmuller, T., Mager, A., and Eckle, T. (2006) Nucleotide metabolism and cell-cell interactions. *Methods Mol Biol* **341**, 73-87
472. Bhavani, S., Yuan, X., You, R., Shan, M., Corry, D., and Kheradmand, F. (2015) Loss of Peripheral Tolerance in Emphysema. Phenotypes, Exacerbations, and Disease Progression. *Annals of the American Thoracic Society* **12 Suppl 2**, S164-168
473. Yuan, X., Chang, C. Y., You, R., Shan, M., Gu, B. H., Madison, M. C., Diehl, G., Perusich, S., Song, L. Z., Cornwell, L., Rossen, R. D., Wetsel, R., Kimal, R., Coarfa, C.,

- Eltzschig, H. K., Corry, D. B., and Kheradmand, F. (2019) Cigarette smoke-induced reduction of C1q promotes emphysema. *JCI Insight* **5**
474. Lu, W., You, R., Yuan, X., Yang, T., Samuel, E. L., Marcano, D. C., Sikkema, W. K., Tour, J. M., Rodriguez, A., Kheradmand, F., and Corry, D. B. (2015) The microRNA miR-22 inhibits the histone deacetylase HDAC4 to promote T(H)17 cell-dependent emphysema. *Nat Immunol* **16**, 1185-1194
475. Poth, J. M., Brodsky, K., Ehrentraut, H., Grenz, A., and Eltzschig, H. K. (2013) Transcriptional control of adenosine signaling by hypoxia-inducible transcription factors during ischemic or inflammatory disease. *J Mol Med (Berl)* **91**, 183-193
476. Shan, M., Yuan, X., Song, L. Z., Roberts, L., Zarinkamar, N., Seryshev, A., Zhang, Y., Hilsenbeck, S., Chang, S. H., Dong, C., Corry, D. B., and Kheradmand, F. (2012) Cigarette smoke induction of osteopontin (SPP1) mediates T(H)17 inflammation in human and experimental emphysema. *Sci Transl Med* **4**, 117ra119
477. Deaglio, S., Dwyer, K. M., Gao, W., Friedman, D., Usheva, A., Erat, A., Chen, J. F., Enjyoji, K., Linden, J., Oukka, M., Kuchroo, V. K., Strom, T. B., and Robson, S. C. (2007) Adenosine generation catalyzed by CD39 and CD73 expressed on regulatory T cells mediates immune suppression. *J Exp Med* **204**, 1257-1265
478. Eltzschig, H. K., Sitkovsky, M. V., and Robson, S. C. (2012) Purinergic signaling during inflammation. *N Engl J Med* **367**, 2322-2333
479. Hasko, G., and Cronstein, B. (2013) Regulation of inflammation by adenosine. *Front Immunol* **4**, 85
480. Afonina, I. S., Zhong, Z., Karin, M., and Beyaert, R. (2017) Limiting inflammation—the negative regulation of NF- κ B and the NLRP3 inflammasome. *Nature Immunology* **18**, 861-869
481. Serhan, C. N., Chiang, N., and Van Dyke, T. E. (2008) Resolving inflammation: dual anti-inflammatory and pro-resolution lipid mediators. *Nature Reviews Immunology* **8**, 349-361

482. Serhan, C. N. (2014) Pro-resolving lipid mediators are leads for resolution physiology. *Nature* **510**, 92-101
483. Colgan, S. P. (2020) Resolvins resolve to heal mucosal wounds. *Proc Natl Acad Sci U S A* **117**, 10621-10622
484. Kominsky, D. J., Keely, S., MacManus, C. F., Glover, L. E., Scully, M., Collins, C. B., Bowers, B. E., Campbell, E. L., and Colgan, S. P. (2011) An endogenously anti-inflammatory role for methylation in mucosal inflammation identified through metabolite profiling. *Journal of immunology (Baltimore, Md. : 1950)* **186**, 6505-6514
485. MacManus, C. F., Campbell, E. L., Keely, S., Burgess, A., Kominsky, D. J., and Colgan, S. P. (2011) Anti-inflammatory actions of adrenomedullin through fine tuning of HIF stabilization. *Faseb j* **25**, 1856-1864
486. Körner, A., Schlegel, M., Theurer, J., Frohnmeyer, H., Adolph, M., Heijink, M., Giera, M., Rosenberger, P., and Mirakaj, V. (2018) Resolution of inflammation and sepsis survival are improved by dietary Ω -3 fatty acids. *Cell death and differentiation* **25**, 421-431
487. Watanabe, S., Alexander, M., Misharin, A. V., and Budinger, G. R. S. (2019) The role of macrophages in the resolution of inflammation. *J Clin Invest* **129**, 2619-2628
488. Serhan, C. N., and Levy, B. D. (2018) Resolvins in inflammation: emergence of the pro-resolving superfamily of mediators. *J Clin Invest* **128**, 2657-2669
489. Krishnamoorthy, N., Abdulnour, R. E., Walker, K. H., Engstrom, B. D., and Levy, B. D. (2018) Specialized Proresolving Mediators in Innate and Adaptive Immune Responses in Airway Diseases. *Physiol Rev* **98**, 1335-1370
490. Sham, H. P., Walker, K. H., Abdulnour, R. E., Krishnamoorthy, N., Douda, D. N., Norris, P. C., Barkas, I., Benito-Figueroa, S., Colby, J. K., Serhan, C. N., and Levy, B. D. (2018) 15-epi-Lipoxin A4, Resolvin D2, and Resolvin D3 Induce NF-kappaB Regulators in Bacterial Pneumonia. *Journal of immunology (Baltimore, Md. : 1950)* **200**, 2757-2766

491. Duvall, M. G., Bruggemann, T. R., and Levy, B. D. (2017) Bronchoprotective mechanisms for specialized pro-resolving mediators in the resolution of lung inflammation. *Mol Aspects Med* **58**, 44-56
492. Abdulnour, R. E., Howrylak, J. A., Tavares, A. H., Doua, D. N., Henkels, K. M., Miller, T. E., Fredenburgh, L. E., Baron, R. M., Gomez-Cambronero, J., and Levy, B. D. (2018) Phospholipase D isoforms differentially regulate leukocyte responses to acute lung injury. *J Leukoc Biol* **103**, 919-932
493. Sugimoto, M. A., Sousa, L. P., Pinho, V., Perretti, M., and Teixeira, M. M. (2016) Resolution of Inflammation: What Controls Its Onset? *Front Immunol* **7**, 160
494. Nemeth, Z. H., Lutz, C. S., Csoka, B., Deitch, E. A., Leibovich, S. J., Gause, W. C., Tone, M., Pacher, P., Vizi, E. S., and Hasko, G. (2005) Adenosine augments IL-10 production by macrophages through an A2B receptor-mediated posttranscriptional mechanism. *Journal of immunology (Baltimore, Md. : 1950)* **175**, 8260-8270
495. Kolodkin, A. L., Matthes, D. J., and Goodman, C. S. (1993) The semaphorin genes encode a family of transmembrane and secreted growth cone guidance molecules. *Cell* **75**, 1389-1399
496. Serafini, T., Kennedy, T. E., Gaiko, M. J., Mirzayan, C., Jessell, T. M., and Tessier-Lavigne, M. (1994) The netrins define a family of axon outgrowth-promoting proteins homologous to *C. elegans* UNC-6. *Cell* **78**, 409-424
497. Varadarajan, S. G., Kong, J. H., Phan, K. D., Kao, T. J., Panaitof, S. C., Cardin, J., Eltzschig, H., Kania, A., Novitch, B. G., and Butler, S. J. (2017) Netrin1 Produced by Neural Progenitors, Not Floor Plate Cells, Is Required for Axon Guidance in the Spinal Cord. *Neuron* **94**, 790-799 e793
498. Brunet, I., Gordon, E., Han, J., Cristofaro, B., Broqueres-You, D., Liu, C., Bouvree, K., Zhang, J., del Toro, R., Mathivet, T., Larrivee, B., Jagu, J., Pibouin-Fragner, L., Pardanaud, L., Machado, M. J., Kennedy, T. E., Zhuang, Z., Simons, M., Levy, B. I.,

- Tessier-Lavigne, M., Grenz, A., Eltzschig, H., and Eichmann, A. (2014) Netrin-1 controls sympathetic arterial innervation. *J Clin Invest* **124**, 3230-3240
499. Mirakaj, V., and Rosenberger, P. (2017) Immunomodulatory Functions of Neuronal Guidance Proteins. *Trends in Immunology* **38**, 444-456
500. Shimizu, I., Yoshida, Y., Moriya, J., Nojima, A., Uemura, A., Kobayashi, Y., and Minamino, T. (2013) Semaphorin3E-induced inflammation contributes to insulin resistance in dietary obesity. *Cell metabolism* **18**, 491-504
501. Movassagh, H., Saati, A., Nandagopal, S., Mohammed, A., Tatari, N., Shan, L., Duke-Cohan, J. S., Fowke, K. R., Lin, F., and Gounni, A. S. (2017) Chemorepellent Semaphorin 3E negatively regulates neutrophil migration in vitro and in vivo. *The Journal of Immunology* **198**, 1023-1033
502. Mirakaj, V., Thix, C. A., Laucher, S., Mielke, C., Morote-Garcia, J. C., Schmit, M. A., Henes, J., Unertl, K. E., Köhler, D., and Rosenberger, P. (2010) Netrin-1 dampens pulmonary inflammation during acute lung injury. *American journal of respiratory and critical care medicine* **181**, 815-824
503. Rosenberger, P., Schwab, J. M., Mirakaj, V., Masekowsky, E., Mager, A., Morote-Garcia, J. C., Unertl, K., and Eltzschig, H. K. (2009) Hypoxia-inducible factor-dependent induction of netrin-1 dampens inflammation caused by hypoxia. *Nat Immunol* **10**, 195-202
504. van Gils, J. M., Derby, M. C., Fernandes, L. R., Ramkhelawon, B., Ray, T. D., Rayner, K. J., Parathath, S., Distel, E., Feig, J. L., Alvarez-Leite, J. I., Rayner, A. J., McDonald, T. O., O'Brien, K. D., Stuart, L. M., Fisher, E. A., Lacy-Hulbert, A., and Moore, K. J. (2012) The neuroimmune guidance cue netrin-1 promotes atherosclerosis by inhibiting the emigration of macrophages from plaques. *Nature Immunology* **13**, 136-143
505. Ly, N. P., Komatsuzaki, K., Fraser, I. P., Tseng, A. A., Prophan, P., Moore, K. J., and Kinane, T. B. (2005) Netrin-1 inhibits leukocyte migration in vitro and in vivo.

- Proceedings of the National Academy of Sciences of the United States of America* **102**, 14729-14734
506. Wu, J. Y., Feng, L., Park, H.-T., Havlioglu, N., Wen, L., Tang, H., Bacon, K. B., Jiang, Z.-h., Zhang, X.-c., and Rao, Y. (2001) The neuronal repellent Slit inhibits leukocyte chemotaxis induced by chemotactic factors. *Nature* **410**, 948-952
507. Aherne, C. M., Collins, C. B., and Eltzschig, H. K. (2013) Netrin-1 guides inflammatory cell migration to control mucosal immune responses during intestinal inflammation. *Tissue Barriers* **1**, e24957
508. Granja, T., Köhler, D., Mirakaj, V., Nelson, E., König, K., and Rosenberger, P. (2014) Crucial role of Plexin C1 for pulmonary inflammation and survival during lung injury. *Mucosal Immunol* **7**, 879-891
509. König, K., Granja, T., Eckle, V. S., Mirakaj, V., Köhler, D., Schlegel, M., and Rosenberger, P. (2016) Inhibition of Plexin C1 Protects Against Hepatic Ischemia-Reperfusion Injury. *Crit Care Med* **44**, e625-632
510. Köhler, D., Granja, T., Volz, J., Koeppen, M., Langer, H. F., Hansmann, G., Legchenko, E., Geisler, T., Bakchoul, T., Eggstein, C., Häberle, H. A., Nieswandt, B., and Rosenberger, P. (2020) Red blood cell-derived semaphorin 7A promotes thrombo-inflammation in myocardial ischemia-reperfusion injury through platelet GPIb. *Nature communications* **11**, 1315
511. Ly, N. P., Komatsuzaki, K., Fraser, I. P., Tseng, A. A., Prophan, P., Moore, K. J., and Kinane, T. B. (2005) Netrin-1 inhibits leukocyte migration in vitro and in vivo. *Proc Natl Acad Sci U S A* **102**, 14729-14734
512. Mirakaj, V., Gatidou, D., Pötzsch, C., König, K., and Rosenberger, P. (2011) Netrin-1 Signaling Dampens Inflammatory Peritonitis. *The Journal of Immunology* **186**, 549-555
513. van Gils, J. M., Derby, M. C., Fernandes, L. R., Ramkhelawon, B., Ray, T. D., Rayner, K. J., Parathath, S., Distel, E., Feig, J. L., Alvarez-Leite, J. I., Rayner, A. J., McDonald, T. O., O'Brien, K. D., Stuart, L. M., Fisher, E. A., Lacy-Hulbert, A., and Moore, K. J.

- (2012) The neuroimmune guidance cue netrin-1 promotes atherosclerosis by inhibiting the emigration of macrophages from plaques. *Nat Immunol* **13**, 136-143
514. Ranganathan, P. V., Jayakumar, C., Mohamed, R., Dong, Z., and Ramesh, G. (2013) Netrin-1 regulates the inflammatory response of neutrophils and macrophages, and suppresses ischemic acute kidney injury by inhibiting COX-2-mediated PGE2 production. *Kidney international* **83**, 1087-1098
515. Ranganathan, P. V., Jayakumar, C., and Ramesh, G. (2013) Netrin-1-treated macrophages protect the kidney against ischemia-reperfusion injury and suppress inflammation by inducing M2 polarization. *American Journal of Physiology-Renal Physiology* **304**, F948-F957
516. Schlegel, M., Köhler, D., Körner, A., Granja, T., Straub, A., Giera, M., and Mirakaj, V. (2016) The neuroimmune guidance cue netrin-1 controls resolution programs and promotes liver regeneration. *Hepatology* **63**, 1689-1705
517. Mirakaj, V., Dalli, J., Granja, T., Rosenberger, P., and Serhan, C. N. (2014) Vagus nerve controls resolution and pro-resolving mediators of inflammation. *Journal of Experimental Medicine* **211**, 1037-1048
518. Bin, J. M., Han, D., Lai Wing Sun, K., Croteau, L. P., Dumontier, E., Cloutier, J. F., Kania, A., and Kennedy, T. E. (2015) Complete Loss of Netrin-1 Results in Embryonic Lethality and Severe Axon Guidance Defects without Increased Neural Cell Death. *Cell reports* **12**, 1099-1106
519. Liao, Y., Wang, J., Jaehnig, E. J., Shi, Z., and Zhang, B. (2019) WebGestalt 2019: gene set analysis toolkit with revamped UIs and APIs. *Nucleic Acids Res* **47**, W199-W205
520. Mirakaj, V., Jennewein, C., König, K., Granja, T., and Rosenberger, P. (2012) The guidance receptor neogenin promotes pulmonary inflammation during lung injury. *The FASEB Journal* **26**, 1549-1558
521. Mirakaj, V., Brown, S., Laucher, S., Steinl, C., Klein, G., Köhler, D., Skutella, T., Meisel, C., Brommer, B., and Rosenberger, P. (2011) Repulsive guidance molecule-A (RGM-A)

- inhibits leukocyte migration and mitigates inflammation. *Proceedings of the National Academy of Sciences* **108**, 6555-6560
522. Kabir, K., Gelinas, J.-P., Chen, M., Chen, D., Zhang, D., Luo, X., Yang, J.-H., Carter, D., and Rabinovici, R. (2002) Characterization of a murine model of endotoxin-induced acute lung injury. *Shock* **17**, 300-303
523. Ngamsri, K.-C., Wagner, R., Vollmer, I., Stark, S., and Reutershan, J. (2010) Adenosine Receptor A1 Regulates Polymorphonuclear Cell Trafficking and Microvascular Permeability in Lipopolysaccharide-Induced Lung Injury. *The Journal of Immunology* **185**, 4374-4384
524. Schingnitz, U., Hartmann, K., Macmanus, C. F., Eckle, T., Zug, S., Colgan, S. P., and Eltzschig, H. K. (2010) Signaling through the A2B adenosine receptor dampens endotoxin-induced acute lung injury. *Journal of immunology (Baltimore, Md. : 1950)* **184**, 5271-5279
525. Ehrentraut, H., Westrich, J. A., Eltzschig, H. K., and Clambey, E. T. (2012) Adora2b adenosine receptor engagement enhances regulatory T cell abundance during endotoxin-induced pulmonary inflammation. *PLoS One* **7**, e32416
526. Cramer, T., Yamanishi, Y., Clausen, B. E., Förster, I., Pawlinski, R., Mackman, N., Haase, V. H., Jaenisch, R., Corr, M., Nizet, V., Firestein, G. S., Gerber, H. P., Ferrara, N., and Johnson, R. S. (2003) HIF-1alpha is essential for myeloid cell-mediated inflammation. *Cell* **112**, 645-657
527. Morrison, B. E., Park, S. J., Mooney, J. M., and Mehrad, B. (2003) Chemokine-mediated recruitment of NK cells is a critical host defense mechanism in invasive aspergillosis. *The Journal of clinical investigation* **112**, 1862-1870
528. Jiang, D., Liang, J., Hodge, J., Lu, B., Zhu, Z., Yu, S., Fan, J., Gao, Y., Yin, Z., Homer, R., Gerard, C., and Noble, P. W. (2004) Regulation of pulmonary fibrosis by chemokine receptor CXCR3. *The Journal of Clinical Investigation* **114**, 291-299

529. Carlin, L. E., Hemann, E. A., Zacharias, Z. R., Heusel, J. W., and Legge, K. L. (2018) Natural Killer Cell Recruitment to the Lung During Influenza A Virus Infection Is Dependent on CXCR3, CCR5, and Virus Exposure Dose. *Frontiers in Immunology* **9**
530. Maghazachi, A. A. (2010) Role of chemokines in the biology of natural killer cells. *Curr Top Microbiol Immunol* **341**, 37-58
531. Robertson, M. J. (2002) Role of chemokines in the biology of natural killer cells. *J Leukoc Biol* **71**, 173-183
532. Mutz, C., Mirakaj, V., Vagts, D. A., Westermann, P., Waibler, K., König, K., Iber, T., Nöldge-Schomburg, G., and Rosenberger, P. (2010) The neuronal guidance protein netrin-1 reduces alveolar inflammation in a porcine model of acute lung injury. *Crit Care* **14**, R189-R189
533. Ranganathan, P. V., Jayakumar, C., and Ramesh, G. (2013) Netrin-1-treated macrophages protect the kidney against ischemia-reperfusion injury and suppress inflammation by inducing M2 polarization. *Am J Physiol Renal Physiol* **304**, F948-957
534. Mediero, A., Wilder, T., Ramkhelawon, B., Moore, K. J., and Cronstein, B. N. (2016) Netrin-1 and its receptor Unc5b are novel targets for the treatment of inflammatory arthritis. *FASEB J* **30**, 3835-3844
535. Aherne, C. M., Collins, C. B., Masterson, J. C., Tizzano, M., Boyle, T. A., Westrich, J. A., Parnes, J. A., Furuta, G. T., Rivera-Nieves, J., and Eltzschig, H. K. (2012) Neuronal guidance molecule netrin-1 attenuates inflammatory cell trafficking during acute experimental colitis. *Gut* **61**, 695-705
536. Taylor, L., Brodermann, M. H., McCaffary, D., Iqbal, A. J., and Greaves, D. R. (2016) Netrin-1 Reduces Monocyte and Macrophage Chemotaxis towards the Complement Component C5a. *PLoS One* **11**, e0160685
537. Schingnitz, U., Hartmann, K., MacManus, C. F., Eckle, T., Zug, S., Colgan, S. P., and Eltzschig, H. K. (2010) Signaling through the A2B Adenosine Receptor Dampens Endotoxin-Induced Acute Lung Injury. *The Journal of Immunology* **184**, 5271-5279

538. Zhang, Y., Chen, P., Di, G., Qi, X., Zhou, Q., and Gao, H. (2018) Netrin-1 promotes diabetic corneal wound healing through molecular mechanisms mediated via the adenosine 2B receptor. *Sci Rep* **8**, 5994
539. Schlegel, M., Köhler, D., Körner, A., Granja, T., Straub, A., Giera, M., and Mirakaj, V. (2016) The neuroimmune guidance cue netrin-1 controls resolution programs and promotes liver regeneration. *Hepatology* **63**, 1689-1705
540. Ramkhelawon, B., Hennessy, E. J., Ménager, M., Ray, T. D., Sheedy, F. J., Hutchison, S., Wanschel, A., Oldebeken, S., Geoffrion, M., and Spiro, W. (2014) Netrin-1 promotes adipose tissue macrophage retention and insulin resistance in obesity. *Nature medicine* **20**, 377
541. Hadi, T., Boytard, L., Silvestro, M., Alebrahim, D., Jacob, S., Feinstein, J., Barone, K., Spiro, W., Hutchison, S., Simon, R., Rateri, D., Pinet, F., Fenyo, D., Adelman, M., Moore, K. J., Eltzschig, H. K., Daugherty, A., and Ramkhelawon, B. (2018) Macrophage-derived netrin-1 promotes abdominal aortic aneurysm formation by activating MMP3 in vascular smooth muscle cells. *Nature communications* **9**, 5022
542. Ramkhelawon, B., Yang, Y., van Gils, J. M., Hewing, B., Rayner, K. J., Parathath, S., Guo, L., Oldebeken, S., Feig, J. L., and Fisher, E. A. (2013) Hypoxia Induces Netrin-1 and Unc5b in Atherosclerotic Plaques.
543. Paradisi, A., Maise, C., Bernet, A., Coissieux, M. M., Maccarrone, M., Scoazec, J. Y., and Mehlen, P. (2008) NF-kappaB regulates netrin-1 expression and affects the conditional tumor suppressive activity of the netrin-1 receptors. *Gastroenterology* **135**, 1248-1257
544. Tadagavadi, R. K., Wang, W., and Ramesh, G. (2010) Netrin-1 regulates Th1/Th2/Th17 cytokine production and inflammation through UNC5B receptor and protects kidney against ischemia-reperfusion injury. *Journal of immunology (Baltimore, Md. : 1950)* **185**, 3750-3758

545. Koscsó, B., Csóka, B., Kókai, E., Németh, Z. H., Pacher, P., Virág, L., Leibovich, S. J., and Haskó, G. (2013) Adenosine augments IL-10-induced STAT3 signaling in M2c macrophages. *J Leukoc Biol* **94**, 1309-1315
546. Haskó, G., Csóka, B., Németh, Z. H., Vizi, E. S., and Pacher, P. (2009) A(2B) adenosine receptors in immunity and inflammation. *Trends Immunol* **30**, 263-270
547. König, K., Gatidou, D., Granja, T., Meier, J., Rosenberger, P., and Mirakaj, V. (2012) The Axonal Guidance Receptor Neogenin Promotes Acute Inflammation. *PLoS One* **7**, e32145
548. Schlegel, M., Körner, A., Kaussen, T., Knausberg, U., Gerber, C., Hansmann, G., Jónasdóttir, H. S., Giera, M., and Mirakaj, V. (2019) Inhibition of neogenin fosters resolution of inflammation and tissue regeneration. *The Journal of clinical investigation* **129**, 2165-2165
549. Beldi, G., Wu, Y., Banz, Y., Nowak, M., Miller, L., Enjyoji, K., Haschemi, A., Yegutkin, G. G., Candinas, D., Exley, M., and Robson, S. C. (2008) Natural killer T cell dysfunction in CD39-null mice protects against concanavalin A-induced hepatitis. *Hepatology* **48**, 841-852
550. Victorino, F., Sojka, D. K., Brodsky, K. S., McNamee, E. N., Masterson, J. C., Homann, D., Yokoyama, W. M., Eltzschig, H. K., and Clambey, E. T. (2015) Tissue-Resident NK Cells Mediate Ischemic Kidney Injury and Are Not Depleted by Anti-Asialo-GM1 Antibody. *Journal of immunology (Baltimore, Md. : 1950)* **195**, 4973-4985
551. Hoegl, S., Ehrentraut, H., Brodsky, K. S., Victorino, F., Golden-Mason, L., Eltzschig, H. K., and McNamee, E. N. (2017) NK cells regulate CXCR2+ neutrophil recruitment during acute lung injury. *Journal of leukocyte biology* **101**, 471-480
552. Okamoto, M., Kato, S., Oizumi, K., Kinoshita, M., Inoue, Y., Hoshino, K., Akira, S., McKenzie, A. N., Young, H. A., and Hoshino, T. (2002) Interleukin 18 (IL-18) in synergy with IL-2 induces lethal lung injury in mice: a potential role for cytokines, chemokines,

- and natural killer cells in the pathogenesis of interstitial pneumonia. *Blood* **99**, 1289-1298
553. Abdul-Careem, M. F., Mian, M. F., Yue, G., Gillgrass, A., Chenoweth, M. J., Barra, N. G., Chew, M. V., Chan, T., Al-Garawi, A. A., Jordana, M., and Ashkar, A. A. (2012) Critical role of natural killer cells in lung immunopathology during influenza infection in mice. *J Infect Dis* **206**, 167-177
554. Li, F., Zhu, H., Sun, R., Wei, H., and Tian, Z. (2012) Natural Killer Cells Are Involved in Acute Lung Immune Injury Caused by Respiratory Syncytial Virus Infection. *Journal of Virology* **86**, 2251-2258
555. Wang, J., Li, F., Sun, R., Gao, X., Wei, H., and Tian, Z. (2014) *Klebsiella pneumoniae* alleviates influenza-induced acute lung injury via limiting NK cell expansion. *Journal of immunology (Baltimore, Md. : 1950)* **193**, 1133-1141
556. Shimasaki, N., Jain, A., and Campana, D. (2020) NK cells for cancer immunotherapy. *Nat Rev Drug Discov* **19**, 200-218
557. Giancchetti, E., Delfino, D. V., and Fierabracci, A. (2018) NK cells in autoimmune diseases: Linking innate and adaptive immune responses. *Autoimmun Rev* **17**, 142-154
558. Hammer, Q., Ruckert, T., and Romagnani, C. (2018) Natural killer cell specificity for viral infections. *Nat Immunol* **19**, 800-808
559. Rupaimoole, R., and Slack, F. J. (2017) MicroRNA therapeutics: towards a new era for the management of cancer and other diseases. *Nature Reviews Drug Discovery* **16**, 203-222
560. Chakraborty, C., Sharma, A. R., Sharma, G., Doss, C. G. P., and Lee, S.-S. (2017) Therapeutic miRNA and siRNA: Moving from Bench to Clinic as Next Generation Medicine. *Molecular Therapy - Nucleic Acids* **8**, 132-143
561. Zhang, L., Liao, Y., and Tang, L. (2019) MicroRNA-34 family: a potential tumor suppressor and therapeutic candidate in cancer. *Journal of Experimental & Clinical Cancer Research* **38**, 53

562. Okada, N., Lin, C.-P., Ribeiro, M. C., Biton, A., Lai, G., He, X., Bu, P., Vogel, H., Jablons, D. M., Keller, A. C., Wilkinson, J. E., He, B., Speed, T. P., and He, L. (2014) A positive feedback between p53 and miR-34 miRNAs mediates tumor suppression. *Genes Dev* **28**, 438-450
563. Bouchie, A. (2013) First microRNA mimic enters clinic. Nature Publishing Group
564. Chakraborty, C., Sharma, A. R., Sharma, G., and Lee, S.-S. (2021) Therapeutic advances of miRNAs: A preclinical and clinical update. *Journal of Advanced Research* **28**, 127-138
565. Layne, K., Ferro, A., and Passacquale, G. (2015) Netrin-1 as a novel therapeutic target in cardiovascular disease: to activate or inhibit? *Cardiovascular Research* **107**, 410-419
566. Bruikman, C. S., Vreeken, D., Hoogeveen, R. M., Bom, M. J., Danad, I., Pinto-Sietsma, S.-J., van Zonneveld, A. J., Knaapen, P., Hovingh, G. K., and Stroes, E. S. (2020) Netrin-1 and the grade of atherosclerosis are inversely correlated in humans. *Arteriosclerosis, thrombosis, and vascular biology* **40**, 462-472
567. Liu, C., Ke, X., Wang, Y., Feng, X., Li, Q., Zhang, Y., Zhu, J., and Li, Q. (2016) The level of netrin-1 is decreased in newly diagnosed type 2 diabetes mellitus patients. *BMC endocrine disorders* **16**, 1-5
568. Guo, D., Zhu, Z., Zhong, C., Peng, H., Wang, A., Xu, T., Peng, Y., Xu, T., Chen, C.-S., and Li, Q. (2019) Increased serum netrin-1 is associated with improved prognosis of ischemic stroke: an observational study from CATIS. *Stroke* **50**, 845-852
569. Ramesh, G., Kwon, O., and Ahn, K. (2010) Netrin-1: a novel universal biomarker of human kidney injury. In *Transplantation proceedings* Vol. 42 pp. 1519-1522, Elsevier
570. Ke, T., Wu, Y., Li, L., Liu, Y., Yao, X., Zhang, J., Kong, D., and Li, C. (2014) Netrin-1 ameliorates myocardial infarction-induced myocardial injury: mechanisms of action in rats and diabetic mice. *Human gene therapy* **25**, 787-797

Vita

Nathaniel Karl Berg was born in San Diego County, California, the son of two United States Navy Dental Corps officers. After graduating from Bonita Vista High School in Chula Vista, California in 2009 he matriculated into the University of Michigan – Ann Arbor. He received a degree in Bachelors of Science and Engineering with a major in nuclear engineering and radiological sciences in December, 2013. For a year's time, he worked as a research assistant in the Department of Radiation Oncology at the University of Michigan. In July 2014 he matriculated into the MD/PhD program at The University of Texas MD Anderson Cancer Center UTHealth Graduate School of Biomedical Sciences and McGovern Medical School.

Permanent Address:

2222 Maroneal St., Unit 321

Houston, Texas, 77030